

Residual Stress Improvement by Means of Induction Heating

EPRI

EPRI NP-81-4-LD
Project T113-5
Research Report
March 1981

Keywords:

IHSI
Residual Stress
BWR Piping
Stress Corrosion
Welds
Pipe Remedies

Prepared by
Ishikawajima-Harima Heavy Industries Co., Ltd.
Japan

ELECTRIC POWER RESEARCH INSTITUTE

8212170111 821203
PDR ADOCK 05000277
P PDR

5212170111

Residual Stress Improvement by Means of Induction Heating

NP-81-4-LD
Research Project T113-5

Research Report, March 1981

Prepared by

ISHIKAWAJIMA-HARIMA HEAVY INDUSTRIES CO., LTD.
Japan

Edited by
Anthony Giannuzzi
Robert Vaile

Nuclear Power Division
Electric Power Research Institute

Published by

BWR Owners Group
and

Electric Power Research Institute
3412 Hillview Avenue
Palo Alto, California 94304

EPRI Project Manager

A. Giannuzzi
Nuclear Power Division

PREFACE

This report presents results of an extensive analytical and experimental study performed by Ishikawajima Harima Heavy Industries Co., Ltd. (IHI) in Japan to qualify and verify the Induction Heating Stress Improvement (IHSI) process for boiling water reactor piping. The program activity was funded entirely by IHI. The role played by the Electric Power Research Institute has been to provide for public release of this information.

The IHI activity described in this report has focused on providing a sound basis for anticipating residual stress improvement resulting from the application of IHSI; identifying essential and non-essential variables associated with the process; verifying the effectiveness of the process both analytically using finite element methods, and experimentally by means of residual stress measurements; and establishing process parameters from which procedure specifications for field implementation can be prepared. This document is extensive in scope and exhaustive in detail. The report will be invaluable as a reference document to be used by utilities, architect engineers, vendors and regulators in understanding and evaluating the IHSI process.

The main body of the report presents a summary of the work performed by IHI in the development and verification of the IHSI process. The appendices which follow report on the analytical and/or experimental detailed studies which justify the summary. A considerable editorial effort has been devoted to rephrasing the main body of the report and the appendices so as to clarify important features which otherwise might have been ambiguous as a result of language differences. These editorial changes have been approved by IHI. No attempt has been made to alter the technical content or the report structure. Where no ambiguity exists in the original document submitted to EPRI, the original translation was preserved. The figures in this report were prepared by IHI and are reprinted herein in the form in which they were received.

CONTENTS

<u>Section</u>	<u>Page</u>
1 INTRODUCTION	1-1
2 CONCEPT OF IHSI	2-1
3 TEST APPROACH AND TEST RESULTS	3-1
3.1 Preliminary Test	3-1
3.2 Parametric Studies for 4-Inch Pipe	3-1
3.3 Demonstration Mock-up Test for 12-Inch Pipes	3-2
3.4 Demonstration Mock-up Test for 24-Inch Pipes	3-2
3.5 Effect of Repeated IHSI Treatment	3-2
3.6 Relaxation Studies on IHSI	3-3
4 COMPUTER CALCULATIONS	4-1
4.1 Preliminary Studies	4-1
4.2 Effects of a Geometrical Transition	4-1
4.3 Parametric Studies	4-2
5 EVALUATION OF PARAMETERS	5-1
5.1 Temperature Difference	5-2
5.2 Temperature Distribution (Heating Duration)	5-6
5.3 Coil Width	5-11
5.4 Coil Setting Location	5-14
5.5 Maximum Heating Temperature	5-14
5.6 Frequency of the Electric Supply	5-18
5.7 Pipe Size	5-20
5.8 Cooling	5-22
5.9 Coil Input Power	5-23
5.10 Geometrical Configuration	5-25
5.11 Summary of Parameters	5-32

<u>Section</u>	<u>Page</u>
6 EVALUATION OF OTHER EFFECTS OF IHSI TREATMENT	6-1
6.1 Sensitization Effects	6-1
6.2 Mechanical Properties	6-1
7 FIELD APPLICATION	7-1
7.1 Estimate of Input Power	7-1
7.2 Trial Heating	7-2
7.3 Estimate of Pipe Inner Surface Temperature	7-6
7.4 Examples of Field Application of the IHSI Process	7-7
7.4.1 Preparation	7-13
7.4.2 Trial Heating	7-13
7.4.3 Actual Heating	7-13
7.4.4 Results and Evaluation	7-13
8 PIPES WITH SMALL PRECRACKS	8-1
8.1 Objective	8-1
8.2 Test Details and Test Results	8-1
8.3 Computer Calculations for Precracked Pipes	8-2
8.4 Evaluation	8-7
8.5 Conclusion	8-10
9 RELAXATION	9-1
9.1 Relaxation at Operating Temperatures	9-1
9.2 Relaxation Resulting From Applied Axial Stress	9-1
10 CONCLUSIONS	10-1

ILLUSTRATIONS

<u>Figure</u>	<u>Page</u>
2.1 Outline of Heating and Cooling Process	2-2
2.2 Stress-Strain Diagram	2-3
2.3 Concept of IHSI	2-5
2.4(a) Temperature History Curve (4-Inch Pipe)	2-6
2.4(b) Through Thickness Residual Stress Distribution 1 Sec. After Heating	2-7
2.5 Temperature and Residual Stress Distribution Along Pipe Axis	2-8
2.6 Residual Stress Distribution Through the Thickness	2-9
5.1 Effect of Temperature Difference Between Outer and Inner Surface on Residual Stress of 4-Inch Pipe	5-3
5.2 Effect of Temperature Difference (Theoretical Calculation)	5-4
5.3 σ_R - ΔT Relations (Inside Surface Residual Stress Presented as a Function of Through Thickness Temperature Gradient - Theory and Experiment)	5-5
5.4 Effect of Different Through Thickness Temperature Distributions on State-of-Stress	5-7
5.5 Temperature Distribution Through the Thickness at Different Heating Times	5-8
5.6 Effect of Heating Duration on Temperature Distribution (Fourier Number)	5-10
5.7 Resultant Stress Distribution with Step Temperature Change in Axial Direction	5-12
5.8 Effect of Coil Width on Inner Surface Residual Stress	5-13
5.9 Effect of Heating Coil Location on Inner Surface Residual Stress	5-15
5.10 Coil Setting Location Guidelines	5-16
5.11 T-T-SCC Diagram for 304 Stainless Steel in Oxygenated Water at 250°C (CBB Test, 20 ppm DO, 310 hr)	5-17
5.12 Effect of Current Frequency on Temperature Distribution and State-of-Stress	5-19
5.13 Effect of Frequency on Residual Stress	5-21
5.14 Effect of Cooling on Through Thickness Temperature Distribution	5-24

<u>Figure</u>		<u>Page</u>
5.15	Analytical Model for Temperature Distribution	5-27
5.16	Residual Stress Distribution for Gently Sloping Thickness Transition	5-28
5.17	Calculated Model and Temperature Distribution for Nozzle to Pipe Transition	5-29
5.18	Residual Stress Distribution for Nozzle to Pipe Thickness Transition	5-30
5.19	J-1 Residual Stress Distribution for Nozzle to Pipe Transition	5-31
5.20	Residual Stress Distribution for Pipe to Elbow Weld	5-33
5.21	Analytical Model for Pipe to End Cap Joint	5-34
5.22	Residual Stress Distribution for Pipe to End Cap Weld	5-35
6.1	Hardness Distribution in 12-Inch Pipe Weld Joint	6-4
7.1	Estimation of Coil Input Power	7-3
7.2	Estimation of Steady State Condition by Trial Heating	7-4
7.3	Temperature Difference Between Outer and Inner Surface of a Pipe	7-8
7.4(a)	Record of Field Application of Induction Heating Stress Improvement	7-9
7.4(b)	Record of Field Application of Induction Heating Stress Improvement	7-11
8.1	Propagation Behavior of Notch	8-3
8.2	Cracking Observation at Notch Tip (R-53)	8-4
8.3	Cracking Observation at Notch Tip (R-45)	8-5
8.4	Calculated Residual Stress Through the Thickness of 12-Inch Pipe With a Flaw	8-6
8.5	Calculated COD at Maximum Heating	8-8
8.6	Relation of COD and CTOD to Deflection in Three Point Bend Test	8-9
8.7	COD and Stress Distribution	8-11
9.1	Residual Stress Distribution Comparing Three Heat Treatments to an As IHSied Pipe	9-2
9.2	Residual Stress Analysis by Two Element Models	9-3
9.3	Load-Strain Curve of Welded 14-Inch Pipe (Experiment)	9-5

TABLES

<u>Table</u>		<u>Page</u>
5.1	Summary of Parameters for Optimized Effect of IHST	5-36
6.1	Mechanical Test Results 12-Inch Pipe Weld Joint	6-3

APPENDICES

<u>Appendix</u>	<u>Title</u>
A-1	Improvement of Residual Stress Pattern in Pipe by High Frequency Induction Heating -- Preliminary Tests
A-2	Improvement of Residual Stress Pattern in Pipe by HFIH (Second Report) -- Parametric Survey
A-3	Improvement of Residual Stress Pattern in Pipe by HFIH (Third Report) -- Demonstration Mock-Up Test (12-Inch Pipe) -- Basic Study for 12-Inch Pipe -- Computer Calculation by FEM
A-4	Improvement of Residual Stress Pattern in Pipe Weldment (Fourth Report) -- Pipe With Small Pre-Crack
A-5	Improvement of Residual Stress Pattern in Pipe Weldment (Fifth Report) -- Effect of IHSI Repetition
A-6	Relaxation Study on IHSI
A-7	Effect of Plastic Deformation by IHSI and Subsequent Heat Treatment Upon IGSCC Susceptibility of Type 304 Stainless Steel
A-8	Some Analytical Case Study of IHSI -- Effect of Geometrical Transition
A-9	Analytical Studies of Some IHSI Parameters -- Temperature Difference -- Coil Width -- Frequency

AppendixTitle

A-10	Residual Stress Improvement for 24-Inch Pipes
A-11	Estimate of Input Power for IHSI
A-12	Trial Heating Technique of IHSI
A-13	Estimate of Pipe ID Temperature During IHSI
A-14	Analytical Studies of IHSI for a Pipe With a Small Pre-flaw
A-15	Residual Stress Improvement by Means of Induction Heating (An Article From IHI Engineering Review, Vol. 11, No. 4)

Section 1

INTRODUCTION

Intergranular stress corrosion cracking (IGSCC) of austenitic stainless steel is believed to occur when three factors, material sensitization, stress, and environment exceed some threshold simultaneously. It is believed that weld residual stress is one of the most important components of the tensile stress which contributes to IGSCC. A new technique, Induction Heating Stress Improvement (IHSI) has been developed with the capability of lowering the residual tensile stress on the inner surface of a pipe in the heat-affected zone near a weld, the region susceptible to IGSCC. This new technique can be simply explained by the fact that compressive residual stress is induced by plastic flow on the inside surface caused by a large thermal stress resulting from a large temperature difference across the pipe thickness. This large stress is produced during induction heating of the pipe outside surface and simultaneous cooling of the inside surface of the pipe. During heating the pipe yields in tension on the inside surface and upon cooling of the outside surface, compressive strains are produced on the inside surface. Many basic experiments and full-sized mock-up tests on the actual austenitic stainless steel pipes, 4-inch, 10-inch, 12-inch, and 24-inch, and calculations using finite-element techniques have been conducted in order to determine appropriate heating conditions and verify the effectiveness of IHSI. As a result of these studies, the key parameters which have a significant effect on IHSI have been determined.

Based on the studies mentioned above, IHSI has been successfully applied to piping in several boiling water reactors in Japan, both operating and under construction, to mitigate the occurrence of IGSCC.

Recently, some additional experimental and analytical studies have been conducted which demonstrate that a small initial crack in a pipe will not propagate during IHSI and also that the residual stress is effectively improved in this case.

In this report, the test details and calculations are briefly described and the key parameters resulting from these investigations are discussed in some detail.

The test results and calculations for a pre-cracked pipe are also explained. The details of test conditions and calculation methods are explained in the attached appendices.

Section 2

CONCEPT OF IHSI

The objective of IHSI is to introduce a large temperature difference between the inner and outer surfaces of a pipe in order to produce sufficient thermal stress to induce some plastic flow and consequently to obtain a compressive residual stress at the inner surface of the pipe. The large temperature difference can be introduced by heating a pipe from the outside with an induction coil while cooling water is supplied simultaneously to the inner surface of the pipe. This process is shown schematically in Figure 2.1.

The mechanism for the stress improvement is, briefly:

When a linear temperature gradient is produced across the thickness of a long pipe, the thermal stress induced can be approximately written as follows:

$$\sigma = \frac{E\alpha \Delta T}{2(1-\nu)} \quad (1)$$

where σ : Thermal stress at each surface, both axial and circumferential
 α : Linear thermal expansion coefficient
 ΔT : Temperature difference between inner and outer surfaces
 E : Young's modulus
 ν : Poisson's ratio

When this thermal stress is below the yield stress (e.g., point 1 in Figure 2.2), the stress is relieved when the temperature difference is removed, and no residual stress is produced. However, if the thermal stress exceeds the yield stress (e.g., point 2 in Figure 2.2), the subsequent removal of the temperature difference changes the stress-strain condition from point 2 to point 3. Thus compressive residual stress is produced.

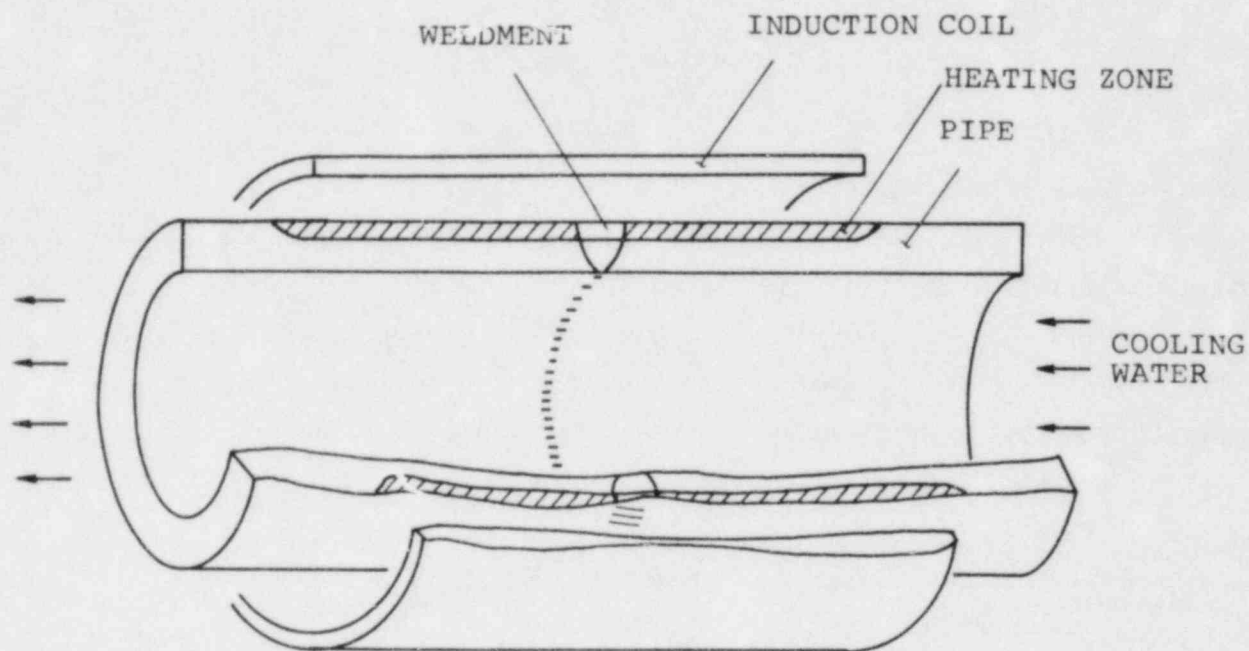


Fig. 2.1 OUTLINE OF HEATING AND COOLING PROCESS

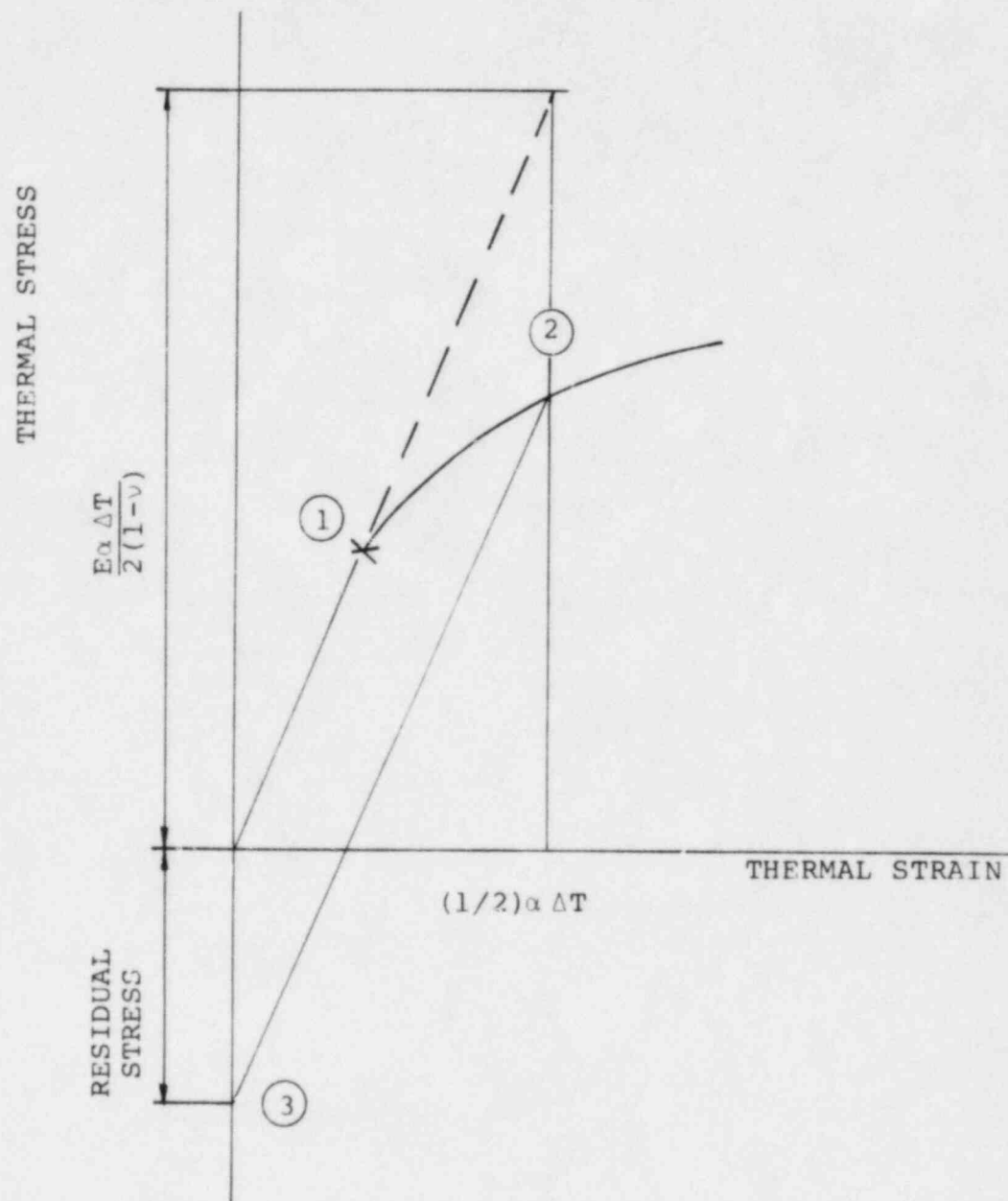


Fig. 2.2 STRESS-STRAIN DIAGRAM

Figure 2.3 illustrates the stress distribution, deformation and temperature distribution in the pipe element during heating and after treatment. As a plane-strain condition is always maintained through the thickness, each fiber on the inner surface is elastoplastically elongated to the equilibrium point during heating, therefore becoming longer than its original length. After the treatment, the fiber is compressed to approximately its original length (equilibrium position), thus producing compressive residual stress on the inner surface, and vice versa on the outer surface.

Figure 2.4(a) shows a calculated temperature history for a typical IHSI treatment and Figure 2.4(b) shows the stress distributions corresponding to some typical points in the temperature history.

Figure 2.5 shows the temperature and the residual stress distribution in the longitudinal direction of pipe which was induction heat treated by a coil of a finite length. The residual stresses on the inner surface of the pipe under the coil are compressive. Figure 2.6 shows the calculated residual stress distribution through the thickness at the coil center. The residual stresses remain compressive for approximately 60% of the pipe thickness.

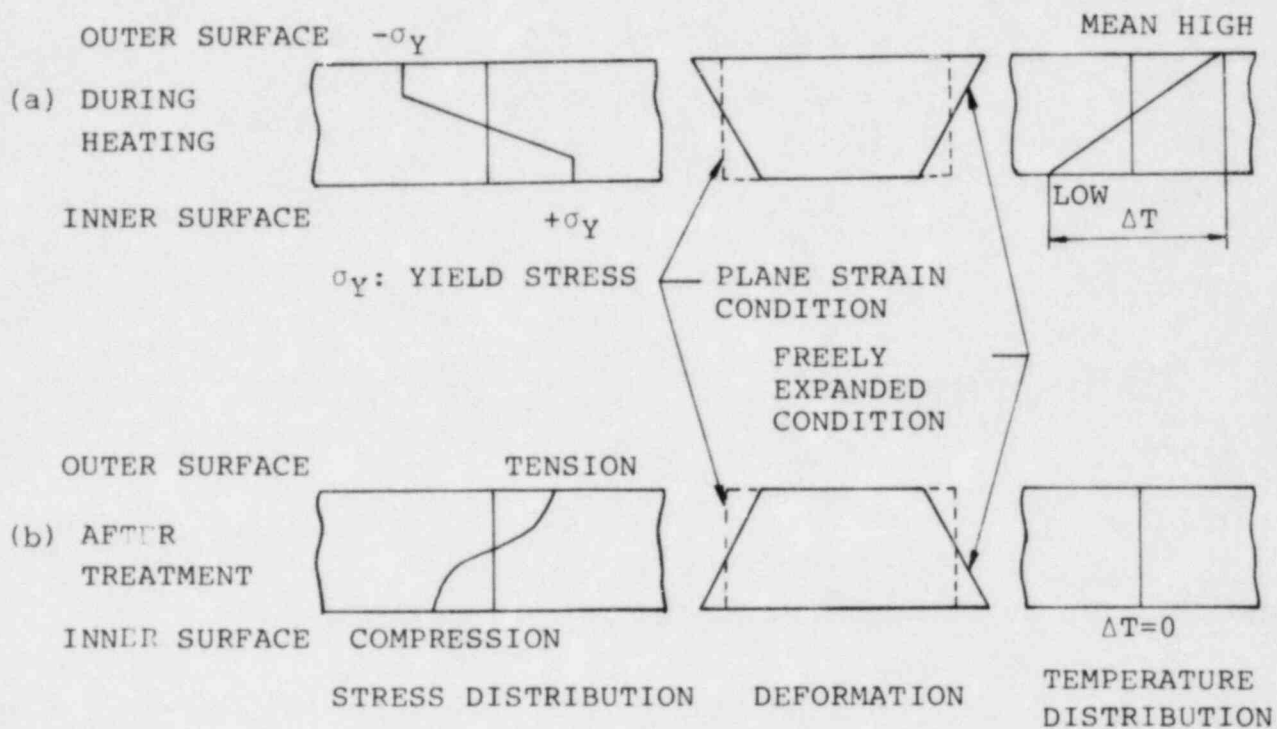


Fig. 2.3 CONCEPT OF IHSI

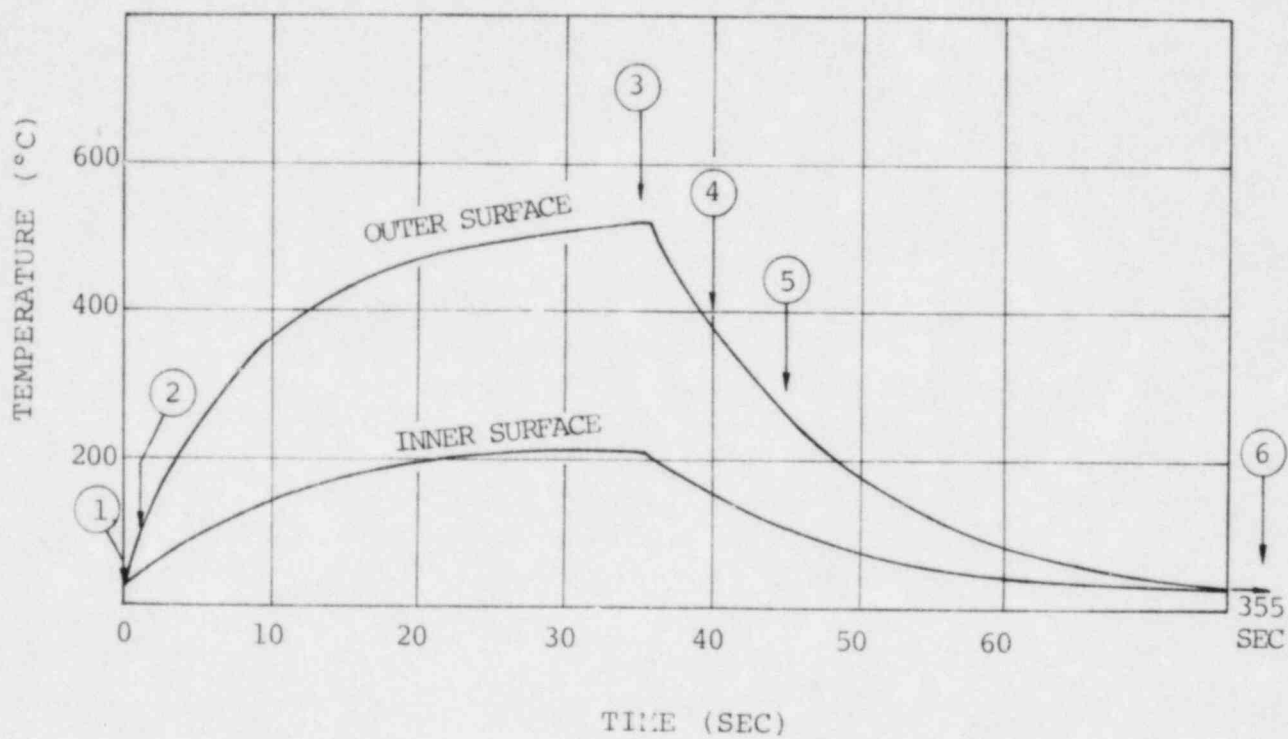


Fig. 2.4 (A) TEMPERATURE HISTORY CURVE (4 IN. PIPE)

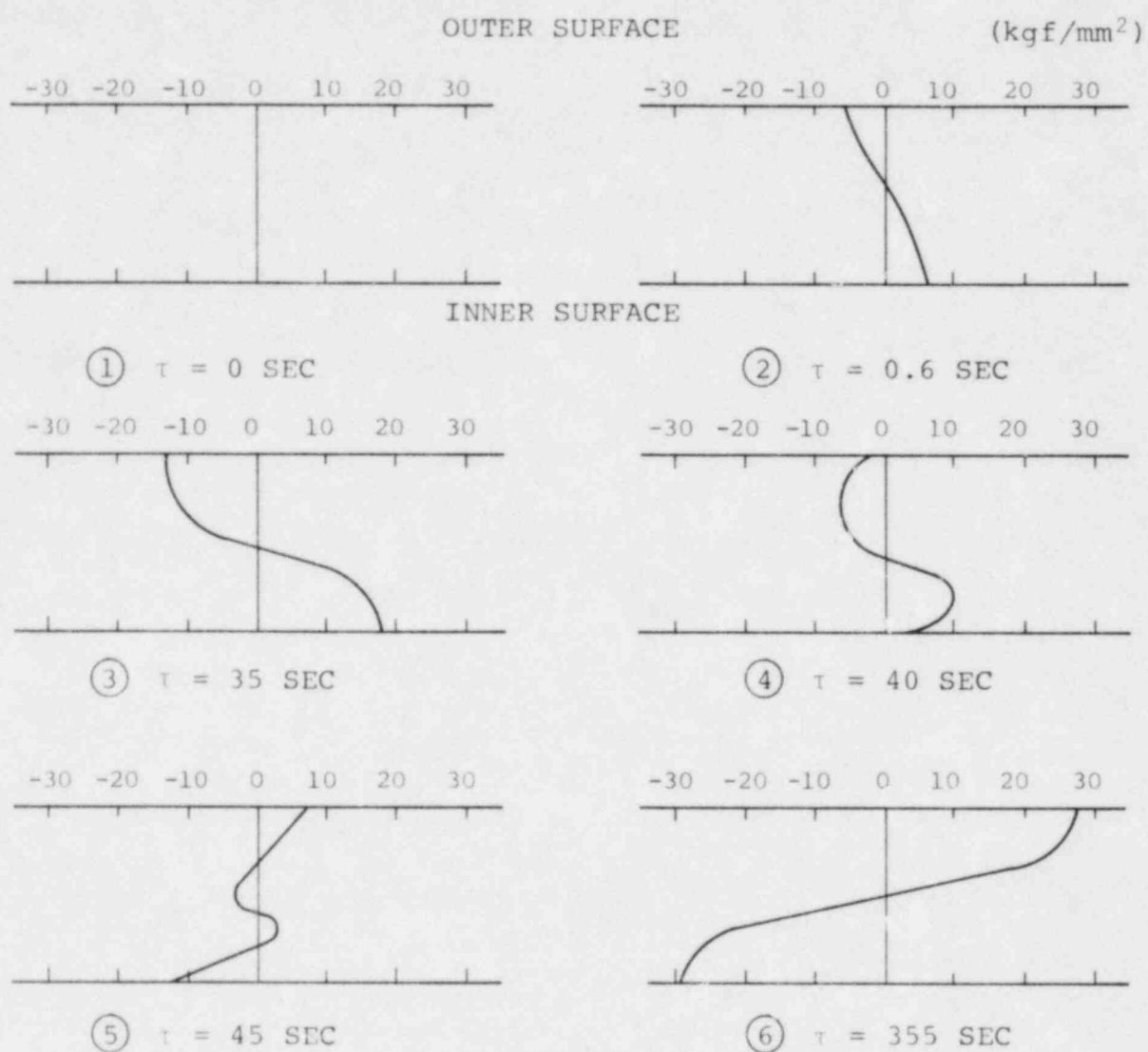


Fig. 2.4(b) THROUGH THICKNESS RESIDUAL STRESS DISTRIBUTION τ SEC. AFTER HEATING

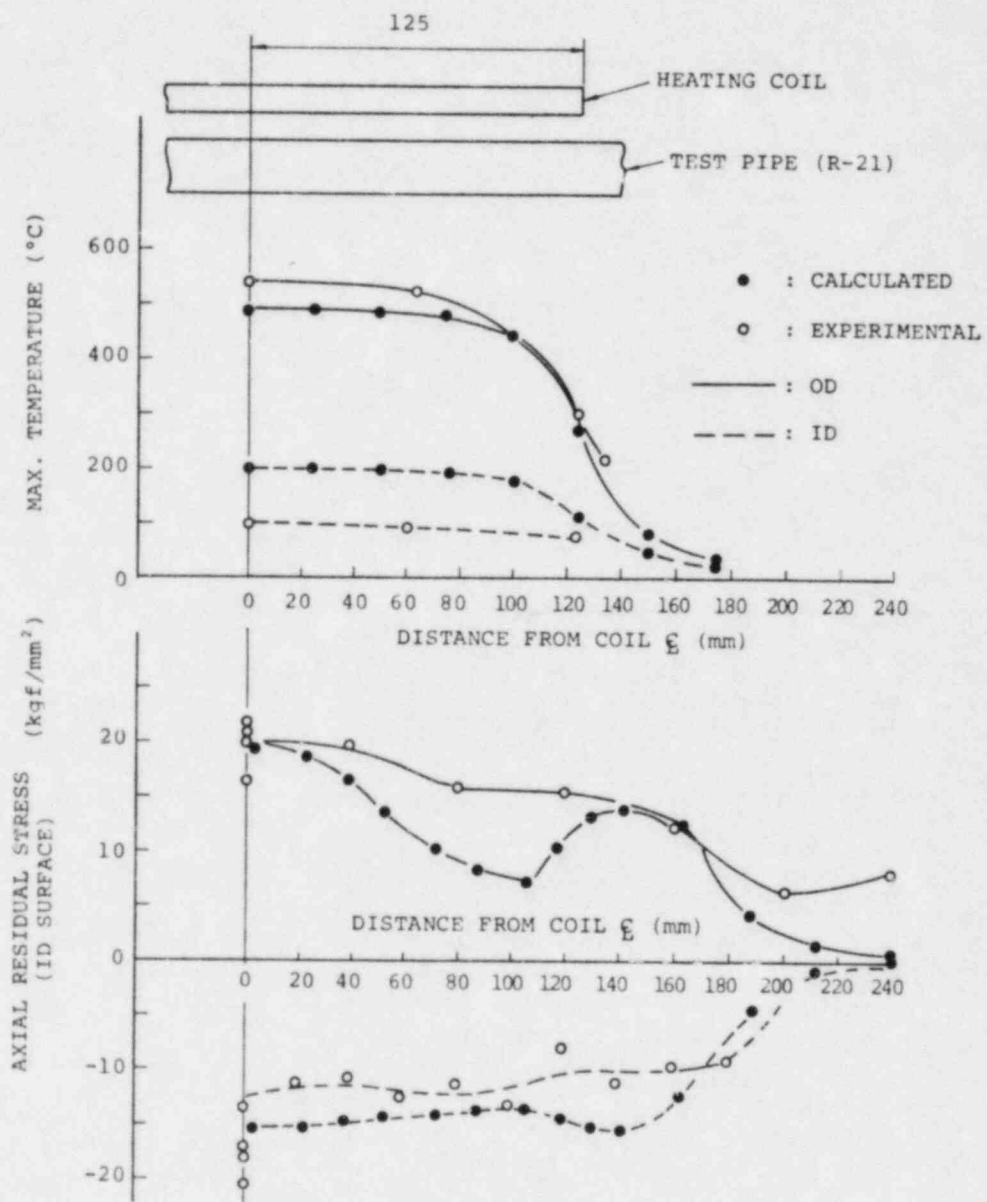


Fig. 2.5 TEMPERATURE AND RESIDUAL STRESS DISTRIBUTION ALONG PIPE AXIS

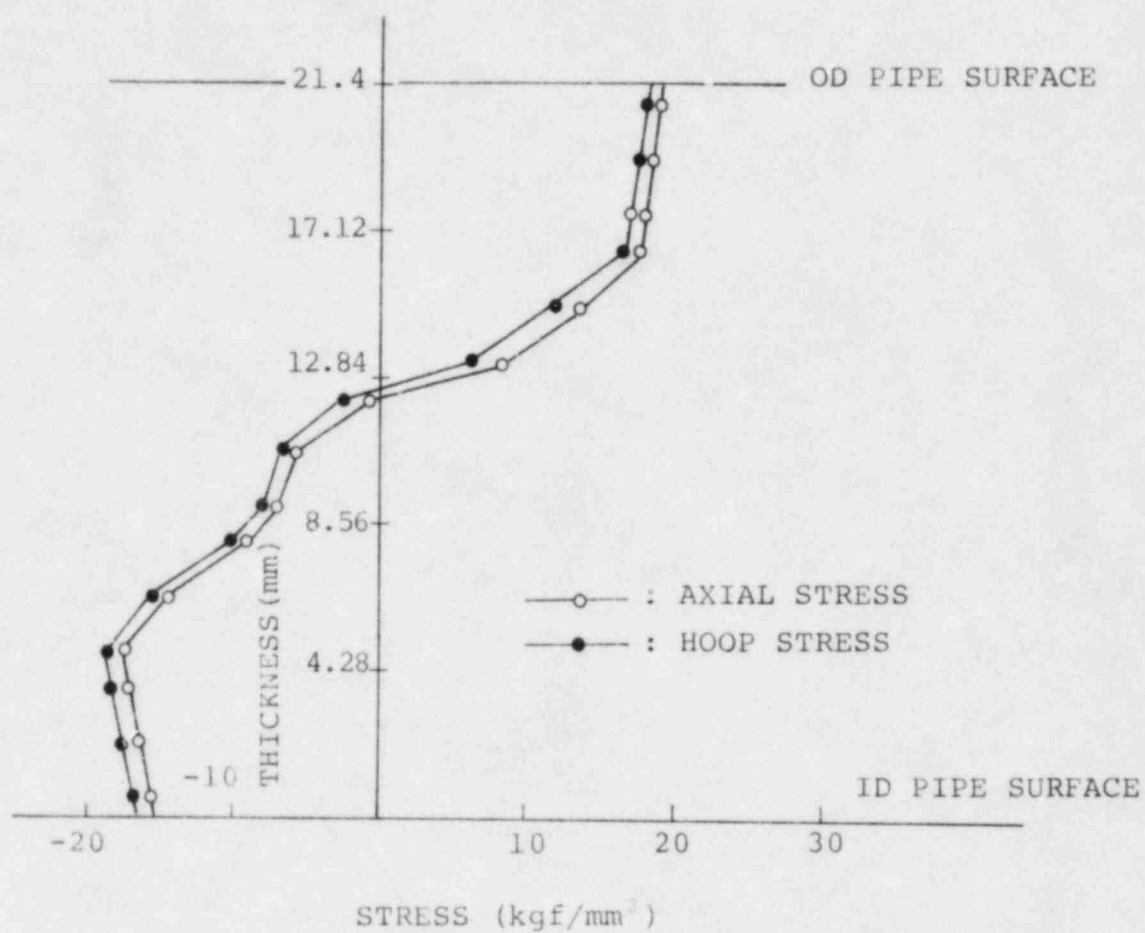


Fig. 2.6 RESIDUAL STRESS DISTRIBUTION THROUGH THE THICKNESS

Section 3

TEST APPROACH AND TEST RESULTS

Many tests were conducted to develop IHSI parameters and some of these have been previously reported.⁽¹⁾ In this section, all the tests and the test results, including what has not been reported previously are briefly explained. The detailed information is described in the appendices.

3.1 PRELIMINARY TEST

To evaluate the effectiveness of the IHSI process, two austenitic stainless steel pipes, each 4-inch Schedule 80, having one circumferential weld at the center of the pipe, were subjected to an IHSI treatment and the residual stresses were determined by conventional strain gage and cracking tests in boiling 42% $MgCl_2$ solution. It was shown from these data that IHSI produces a relatively large compressive stress, or at least less tensile stress, on the inside surface of the pipe throughout the weld heat affected zone. The details are presented in Appendix A-1.

3.2 PARAMETRIC STUDIES FOR 4-INCH PIPE

A parameter survey test was conducted to define improved heating and cooling conditions for the IHSI process. The primary variables considered were electric power frequency, heating time, temperature difference, and pipe size. The results showed that the temperature difference through the pipe thickness was important to the final state of residual stress, and that frequency and heating time were of less importance.

Reference: (1) Appendix A-15 Residual Stress Improvement by Means of Induction Heating.

The data for the 10-inch pipe suggested that large pipes require a longer heating coil to optimize the residual stress results. The details of these experiments are presented in the Appendix A-2.

3.3 DEMONSTRATION MOCK-UP TEST FOR 12-INCH PIPES

Prior to the field application of IHSI to 12-inch diameter recirculation primary loop riser piping in a boiling water reactor, a series of demonstration mock-up tests and some fundamental tests were conducted to determine the optimum heating conditions and to verify the validity of the IHSI process.

The results demonstrated that IHSI can be applied successfully not only to straight pipe but also to pipe-to-elbow joints and further, that no detrimental effect of this process on microstructure or mechanical properties occurs. The details of these tests are presented in Appendix A-3.

3.4 DEMONSTRATION MOCK-UP TEST FOR 24-INCH PIPES

Two 24-inch pipes, one with a thickness transition and the other just a straight pipe, were tested to demonstrate the validity of IHSI for larger pipes typical of the main recirculation loop piping in a boiling water reactor. The test results demonstrated that there were no difficulties in applying IHSI to larger pipe. The test details are presented in Appendix A-4. In addition to these tests, three full size mock-up tests were conducted in a joint utility-fabricator IHSI development program. The results of that program are presented elsewhere.

3.5 EFFECT OF REPEATED IHSI TREATMENT

It is desirable to make trial IHSI runs under laboratory conditions to determine the input power level and duration needed to produce the desired temperature regime in each size of pipe. From one set of such trial runs the effect of repeated IHSI treatment can be deduced. It appears that repeated IHSI treatment produces only slightly better residual stresses than a single treatment. The details are presented in Appendix A-5.

3.6 RELAXATION STUDIES ON IHSI

Relaxation behavior after IHSI was checked on 4-inch Schedule 80 pipes. Three pipes given an IHSI treatment were subjected to three different stress-relieving heat treatments (500°C x 24H, 400°C x 24H, 300°C x 24H) and the residual stress was measured. The results showed that no significant difference in residual stress was produced by the stress relaxation heat treatments of any of the pipes. The details of this investigation are presented in Appendix A-6.

Section 4

COMPUTER CALCULATIONS

4.1 PRELIMINARY STUDIES

Thermo-elastoplastic stress analyses were conducted for two finite-element models using the ANSYS computer code. One model was a smooth straight pipe to compute the stress distribution across the pipe wall and compare it with experimental data. The other was a pipe with a weld 60 mm from the coil end.

The material physical properties and the stress-strain curve were adjusted as a function of temperature, and a kinematic strain-hardening rule was applied to the model. The analysis produced a temperature distribution and residual stress along the pipe axis which compared closely with the experimental data. The calculated residual stress distribution through the pipe thickness indicated that for approximately 60% of the wall thickness, as measured from the inside surface, the residual stress was compressive following the IHSI treatment, assuming initial residual stress (before IHSI) of zero.

The results of the second analysis showed that the different mechanical properties of the weld metal, and the coil location, had no significant effect on the residual stresses.

The details of the computer calculations are presented in subsection B of Appendix A-3 of this report.

4.2 EFFECTS OF A GEOMETRICAL TRANSITION

Computer calculations were performed for different geometry pipe transitions using the finite-element code ITEPC-JI (a thermo-elastic-plastic stress analysis program developed by IHI). For this calculation, the physical properties and stress-strain relationships were varied with temperature and an isotropic-strain hardening rule was applied.

The calculated results showed that the geometric effects on residual stresses were not significant.

The details of the calculations are presented in Appendix A-8.

4.3 PARAMETRIC STUDIES

The effect of temperature difference, coil width and electric power frequency were studied by finite-element methods using the same program and the same mechanical and physical properties as described in paragraph 4.2.

The results of this study showed that temperature difference and coil width produced a significant effect on the residual stress distribution when they were smaller than the critical values and that frequency had no significant effect.

The details of the calculations are presented in Appendix A-9.

Section 5

EVALUATION OF PARAMETERS

The effectiveness of IHSI is influenced by many parameters; however, sufficient residual stress improvement is promised if the key parameters, which significantly affect the residual stresses, are properly controlled.

In this section, all relevant parameters are discussed from the following viewpoints:

1. Which are the key parameters?
2. In what range should they be controlled?

It can be readily observed from Equation (1) on page 2-1, that a thermal stress sufficient to cause plastic flow can be obtained for any material if the temperature difference is larger than $\frac{2(1-\nu)}{E\alpha} \sigma_Y$.

Therefore, temperature difference is one of the key parameters to be controlled in improving the residual stress distribution. It must be noted that Equation (1) is valid only for the case in which a sufficient length of pipe is uniformly heated for a sufficient time to make the temperature gradient through the thickness constant.

For these reasons, the heating coil length and temperature distribution across the thickness also become key parameters in the IHSI process.

These factors, which are the key parameters, and the controlling ranges of application are discussed in the following paragraphs.

5.1 TEMPERATURE DIFFERENCE

Thermal stress produced during heating is proportional to temperature difference (ΔT) across the pipe wall [Equation (1)]. Accordingly, it is expected that the plastic strain produced during heating and the resulting residual stresses will increase with increasing ΔT .

Figure 5.1 presents experimental results for 4-inch Schedule 80 pipes which were treated at different ΔT . Pipe R-15 produced a residual stress (σ_R) of -17 kg/mm^2 at $\Delta T = 322^\circ\text{C}$ and pipe R-17 produced -8 kg/mm^2 at $\Delta T = 132^\circ\text{C}$, which is in good agreement with the expected results. This $\sigma_R - \Delta T$ relationship is valid however only when residual stress is equal to or less than the yield strength of the pipe.

As illustrated in Figure 5.2, when the residual stress corresponds to a larger ΔT than $4\sigma_Y(1-\nu)/E\alpha$, yielding occurs at point 3a during cooling and the residual stress becomes $-\sigma_Y$, that is, the residual stress is always $-\sigma_Y$ even if $\Delta T > 4\sigma_Y(1-\nu)/E\alpha$.

$\sigma_R - \Delta T$ relations obtained experimentally and analytically are shown in Figure 5.3. In this figure, the abscissa describes ΔT normalized by $4\sigma_Y(1-\nu)/E\alpha$. Both curves indicate that the residual stress is almost constant if $\Delta T > 4\sigma_Y(1-\nu)/E\alpha$.

It may be concluded from the above discussion that the temperature difference should be larger than $4\sigma_Y(1-\nu)/E\alpha$ to obtain the maximum residual stress effect.

If one assumes the following material parameters for an austenitic stainless steel:

$\sigma_Y:$	25 kg/mm^2	$\nu:$	0.3
$E:$	$1.98 \times 10^4 \text{ kg/mm}^2$	$\alpha:$	$16.4 \times 10^{-6} \text{ mm/}^\circ\text{C}$

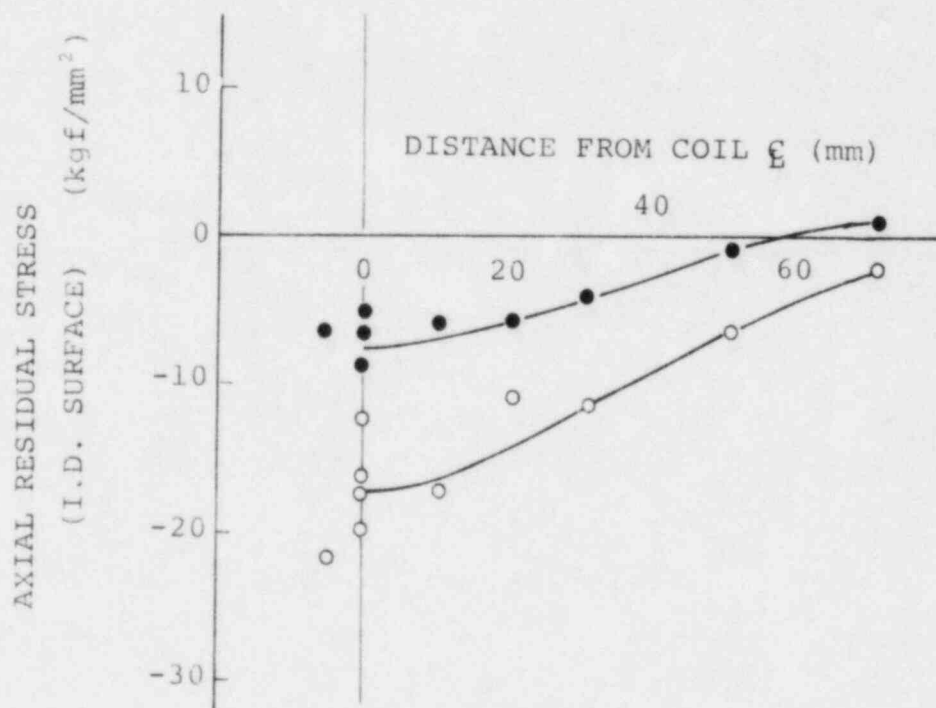
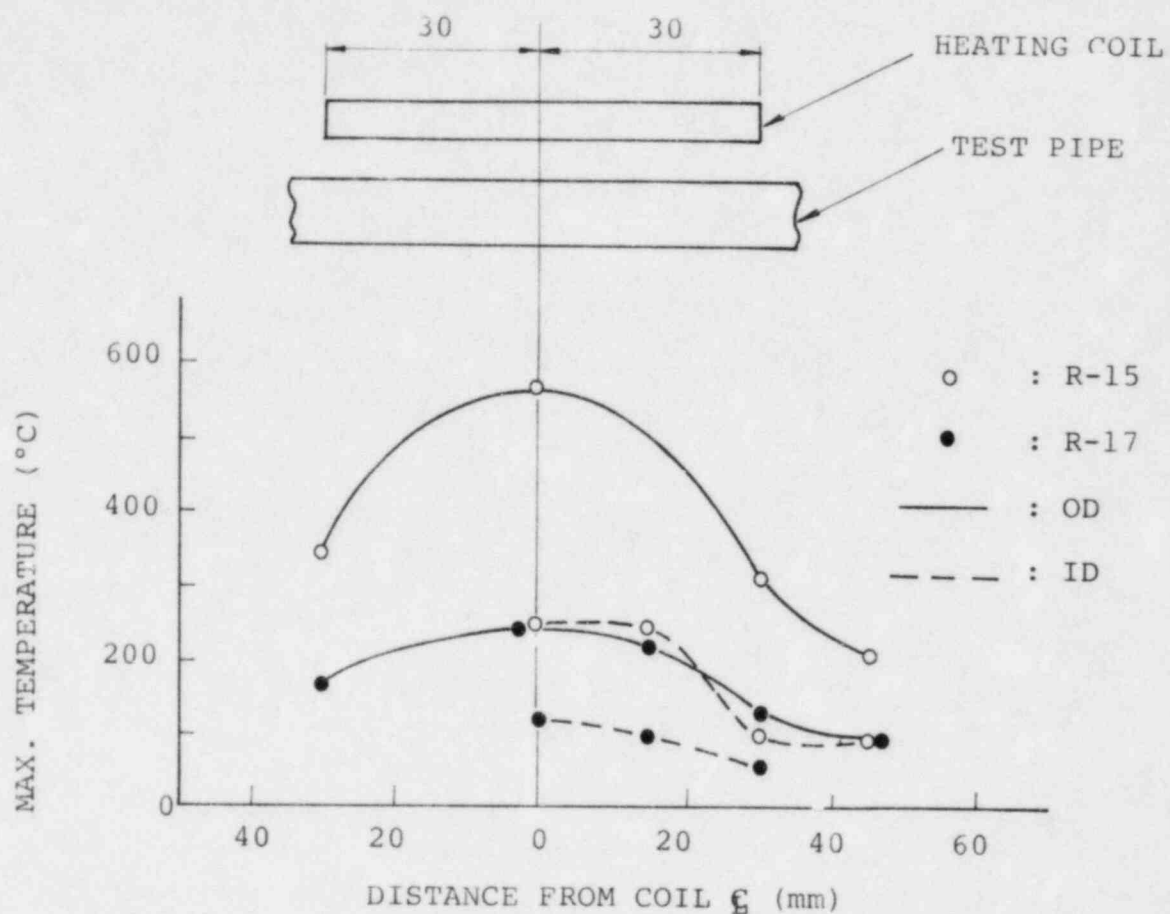


Fig. 5.1 EFFECT OF TEMPERATURE DIFFERENCE BETWEEN OUTER AND INNER SURFACE ON RESIDUAL STRESS OF 4 INCH PIPE

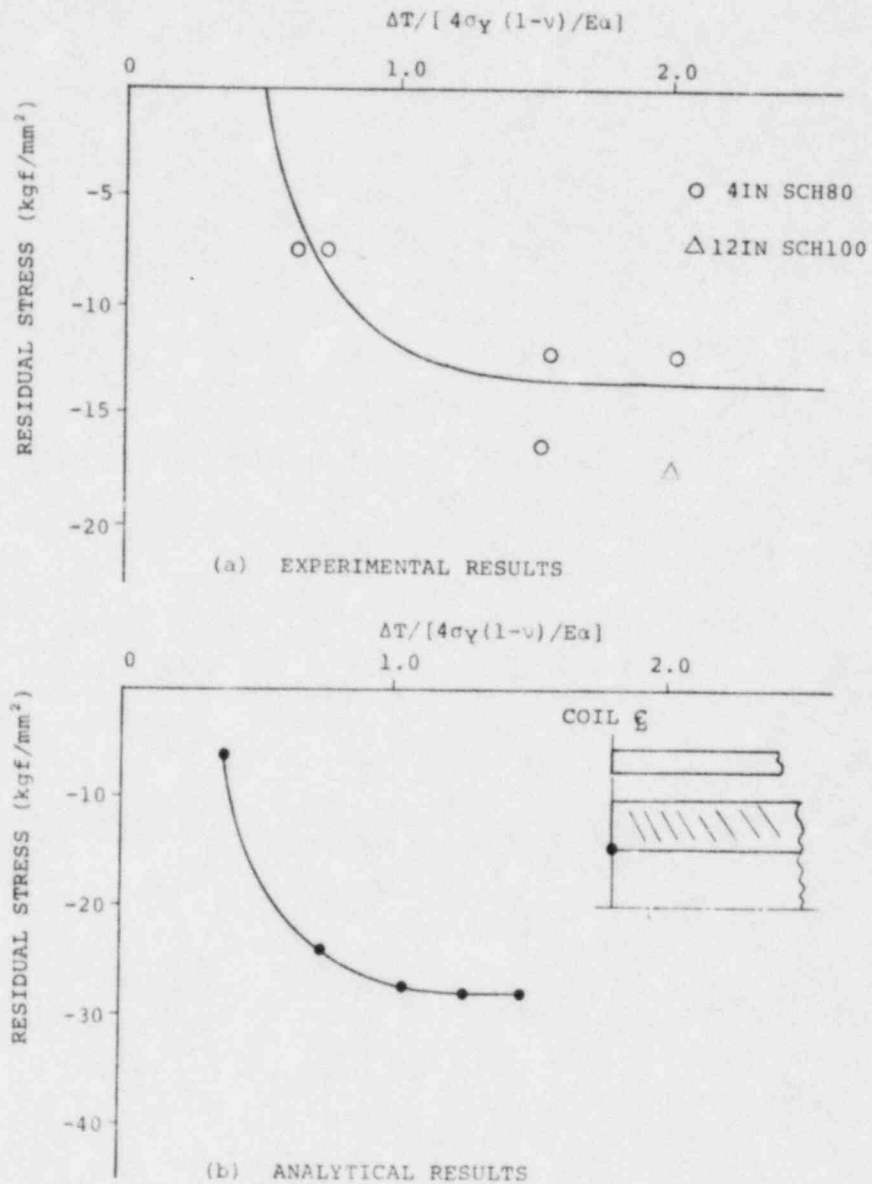


Fig. 5.3 σ_R - ΔT RELATIONS

(Inside Surface Residual Stress Presented as a Function of Through Thickness Temperature Gradient - Theory and Experiment).

the required minimum temperature difference (ΔT_{\min}) can be calculated as follows:

$$\Delta T_{\min} = \frac{4 \times 25 (1-0.3)}{1.98 \times 10^4 \times 16.4 \times 10^{-6}}$$
$$= 215.6^\circ\text{C}$$

This is the minimum temperature difference expected to produce the maximum residual stress.

Note: The material constants at 20°C were used for the above calculation because they give a larger ΔT than those at higher temperature.

5.2 TEMPERATURE DISTRIBUTION (HEATING DURATION)

Thermal stresses produced at the inner surface of a pipe depend on the temperature profile through the pipe thickness. As mentioned earlier, if the temperature gradient is linear, the thermal stresses are given by Equation (1). However, a temperature distribution similar to a thermal shock as shown in Figure 5.4(a) induces very small thermal stresses at pipe inner surface even if the same ΔT as that in Figure 2.4(b) is attained.

The temperature distribution in Figure 5.4(a) and (b) correspond to rapid heating and steady state heating respectively.

In order to obtain the steady state condition, the pipe should be heated for a sufficient time; thus, heating time becomes a key parameter.

In order to estimate the minimum required heating time, an idealized model as shown in Figure 5.5 may be considered. When an infinite plate, which has uniform

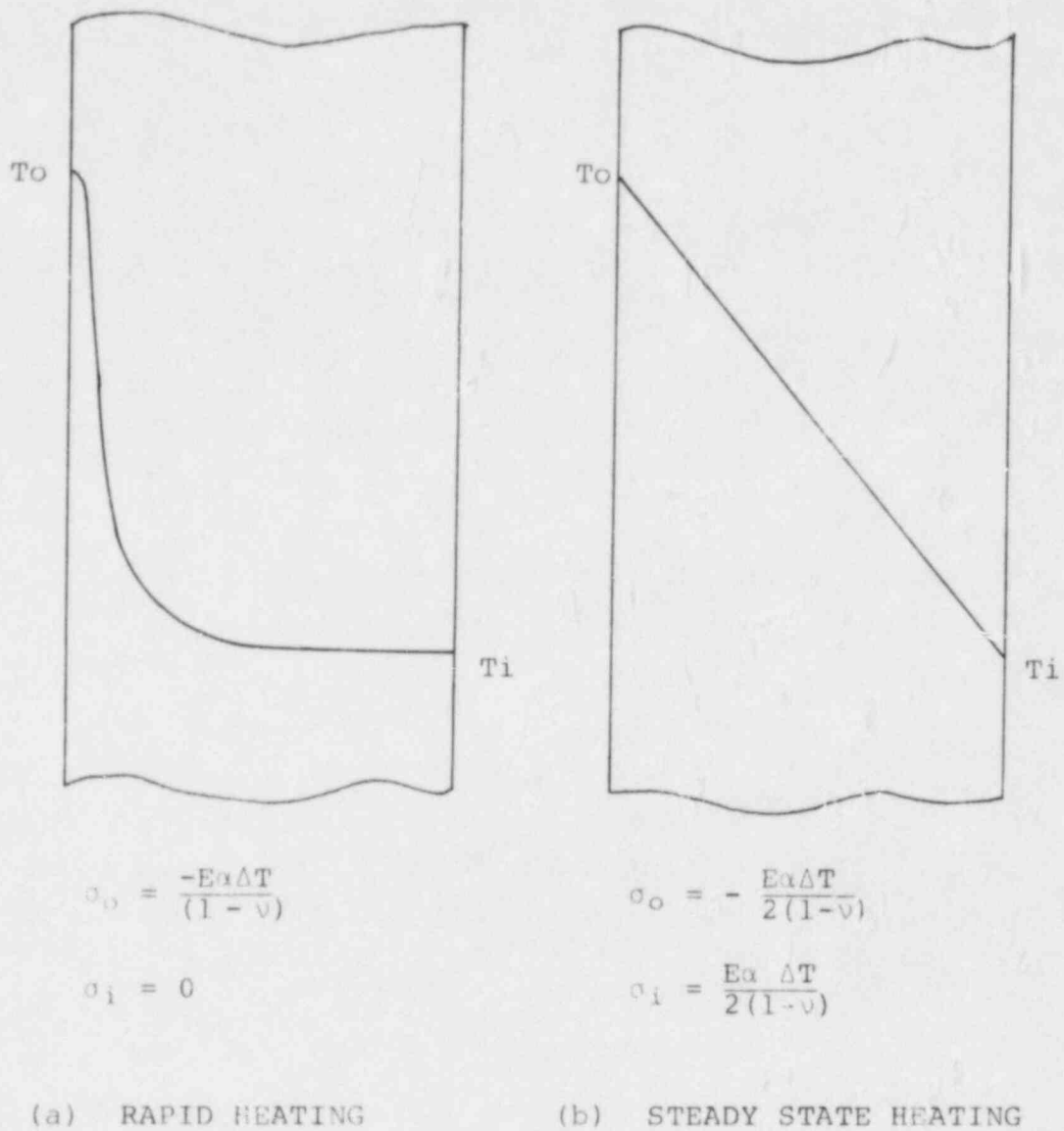
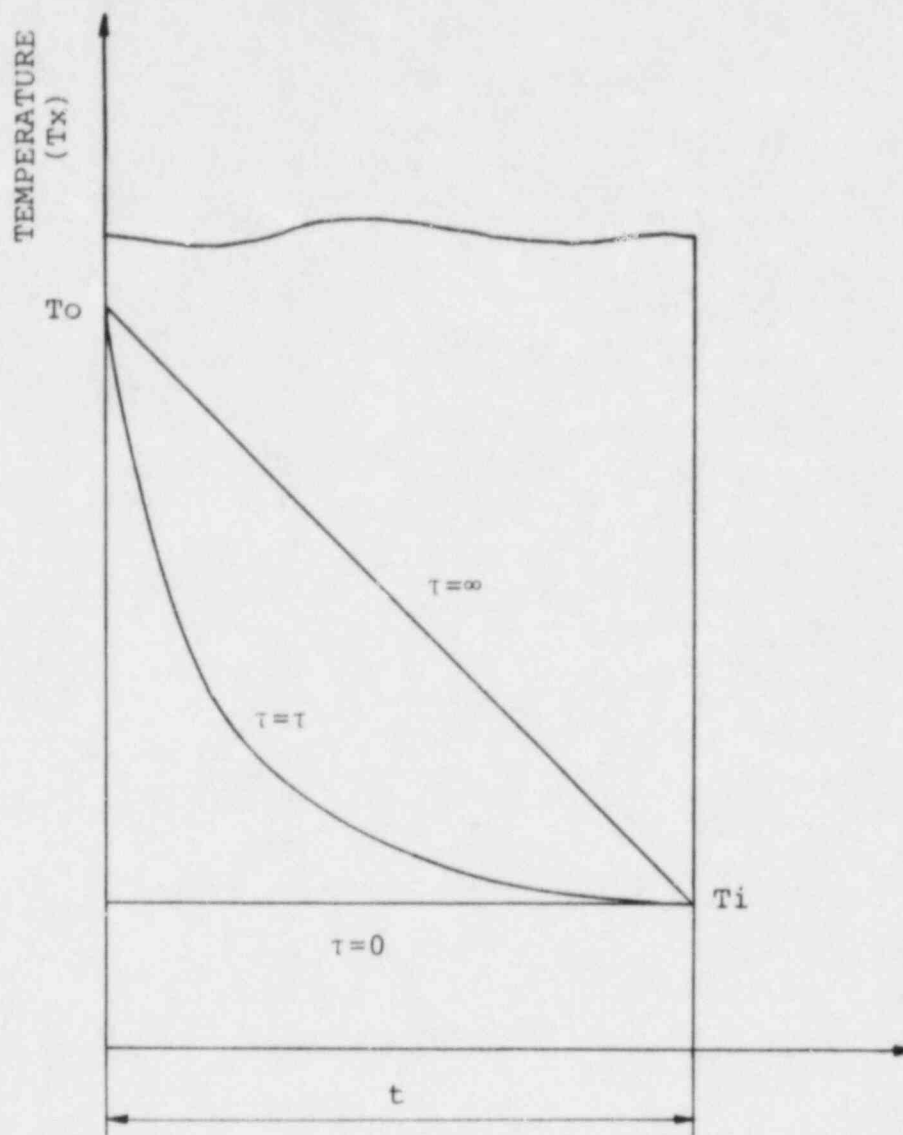


Fig. 5.4 EFFECT OF DIFFERENT THROUGH THICKNESS TEMPERATURE DISTRIBUTIONS ON STATE-OF-STRESS



$$T_x = (T_o - T_i) \left[\frac{x}{t} - \frac{2}{\pi} \sum_{n=1}^{\infty} \frac{(-1)^{n-1}}{n} e^{-(n\pi)^2 \frac{at}{t^2}} \times \sin \frac{n\pi x}{t} \right] + T_i$$

Fig. 5.5 TEMPERATURE DISTRIBUTION THROUGH THE THICKNESS
AT DIFFERENT HEATING TIMES

temperature T_i across the thickness, t , is suddenly heated to T_o on one surface, the temperature distribution across the thickness after an elapsed time of τ is given by the following equation.⁽¹⁾

$$T_x = \Delta T \left[\frac{x}{t} - \frac{2}{\pi} \sum_{n=1}^{\infty} \frac{(-1)^{n-1}}{n} e^{-(n\pi)^2 \frac{a\tau}{t^2}} \sin \frac{n\pi x}{t} \right] + T_i \quad (2)$$

T_o, T_i, T_x : temperature at $x = 0, x = t$ and $x = x$, respectively

a : Temperature diffusivity

n : Natural number $\Delta T = T_o - T_i$

It is obvious from Equation (2) that the second term in the parenthesis shows the variation from the steady state condition and that if the Fourier Number, $a\tau/t^2$, becomes large, the second term can be neglected; that is, $a\tau/t^2$ is the key parameter to obtain a steady state temperature distribution. In Figure 5.6, the calculated temperatures at mid-thickness during IHST are plotted against Fourier Number. The calculations were made on 12-inch, 20-inch and 28-inch pipes which were heated from the outer surface using an induction coil. For all cases the temperature $(T_{1/2} - T_i)/(T_o - T_i)$ becomes approximately constant when $a\tau/t^2 \geq 0.7$.

Based upon the above discussion, the heating time τ should be controlled so that the Fourier Number becomes larger than 0.7.

For example, given the following thermal diffusivity and pipe thickness:

$$a: 0.016 \text{ m}^2/\text{h} \quad t: 0.04 \text{ m (28-inch pipe)}$$

the required minimum heating duration can be calculated as follows:

$$\begin{aligned} \tau &= 0.7 \frac{(0.04)^2}{0.016} = 0.07 \text{ hr.} \\ &= 252 \text{ sec.} \end{aligned}$$

Reference: (1) Y. Katsutoh "Theory of Heat Conduction," Kyoritsu, Japan, p.45 (1956).

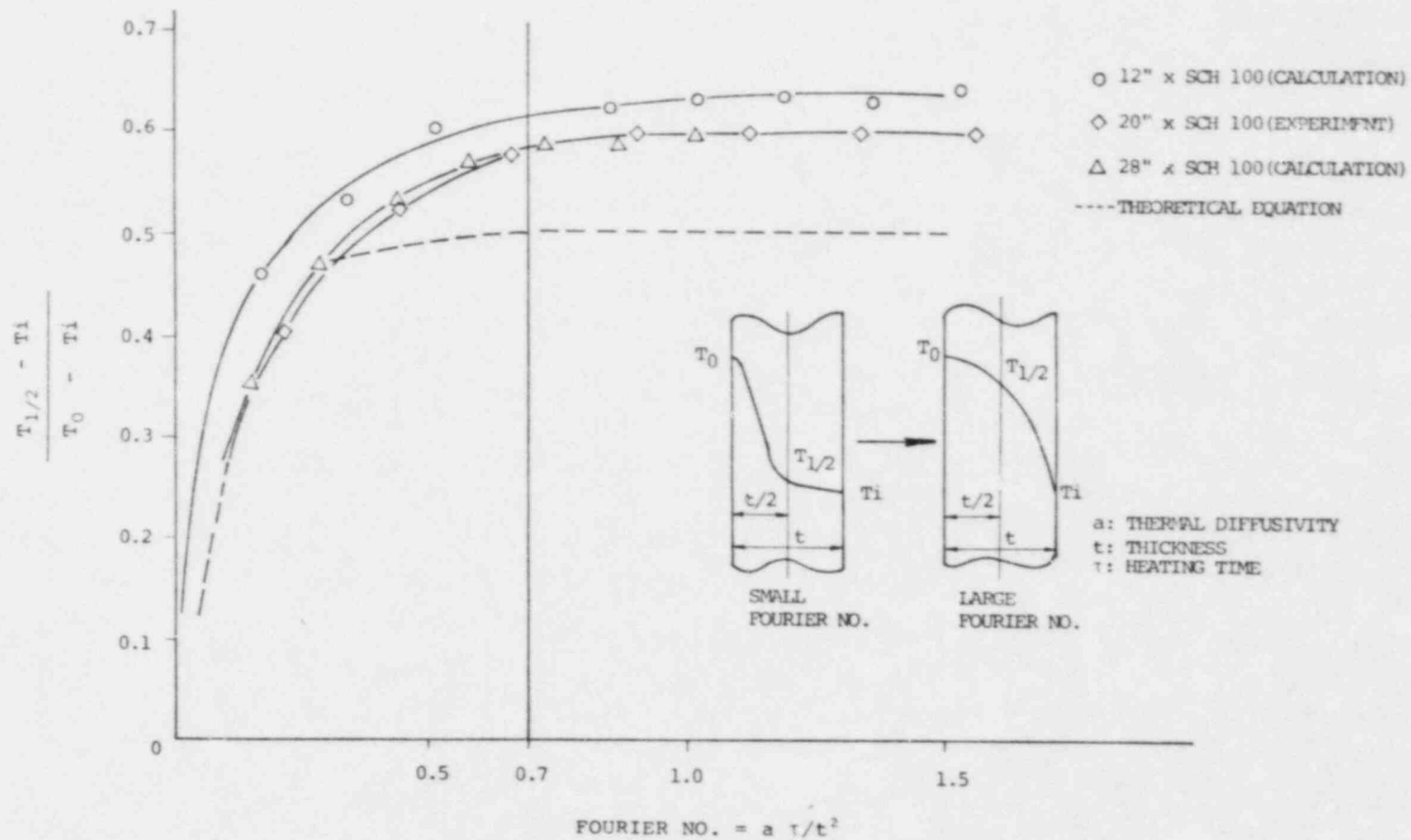


Fig. 5.6 EFFECT OF HEATING DURATION ON TEMPERATURE DISTRIBUTION

5.3 COIL WIDTH

Since the pipe is heated by a coil of finite width, a temperature difference in the axial direction occurs near the coil end. This situation is schematically illustrated in Figure 5.7. The effects of a step temperature change in the axial direction can be approximately expressed as the effect obtained when pipes with radii differing by ΔR are connected together by a shear force (Q). The effect of the shearing force can be expressed using elastic analysis as follows:

$$\begin{aligned} M_Q &= -D \frac{d^2 w}{dx^2} \\ &= \frac{Q}{\beta} e^{-\beta x} \sin \beta x \end{aligned} \quad (3)$$

where

$$\beta = \frac{4}{\sqrt{R^2 t^2}} \frac{3(1-\nu)}{2} = 1.285 \cdot \frac{1}{\sqrt{Rt}}$$

M_Q reaches a maximum at $\beta x = 0.8$ ($x = 0.623\sqrt{Rt}$) and exponentially decreases as x increases.

M_Q acts to cancel the thermal stress due to the temperature difference across the pipe thickness.

Therefore, the coil width should be great enough so that the effect of one coil end is not superimposed on the other. As a result, coil width becomes a key parameter and if it is larger than $3\sqrt{Rt}$, the maximum effect of Q is not increased by the effects of the other end. Since the above discussion is based on elastic analysis, a series of experiments and elastic-plastic analysis by finite element methods were performed to investigate this effect in more detail. The results of this study, presented in Figure 5.8, are consistent with the above discussion; namely, if the coil width is greater than $3\sqrt{Rt}$, the residual stresses obtained are approximately constant.

As an example, if the following parameters for pipe radius and thickness are given,

$$t = 40 \text{ mm} \quad R = 356 \text{ mm (28-inch pipe)}$$

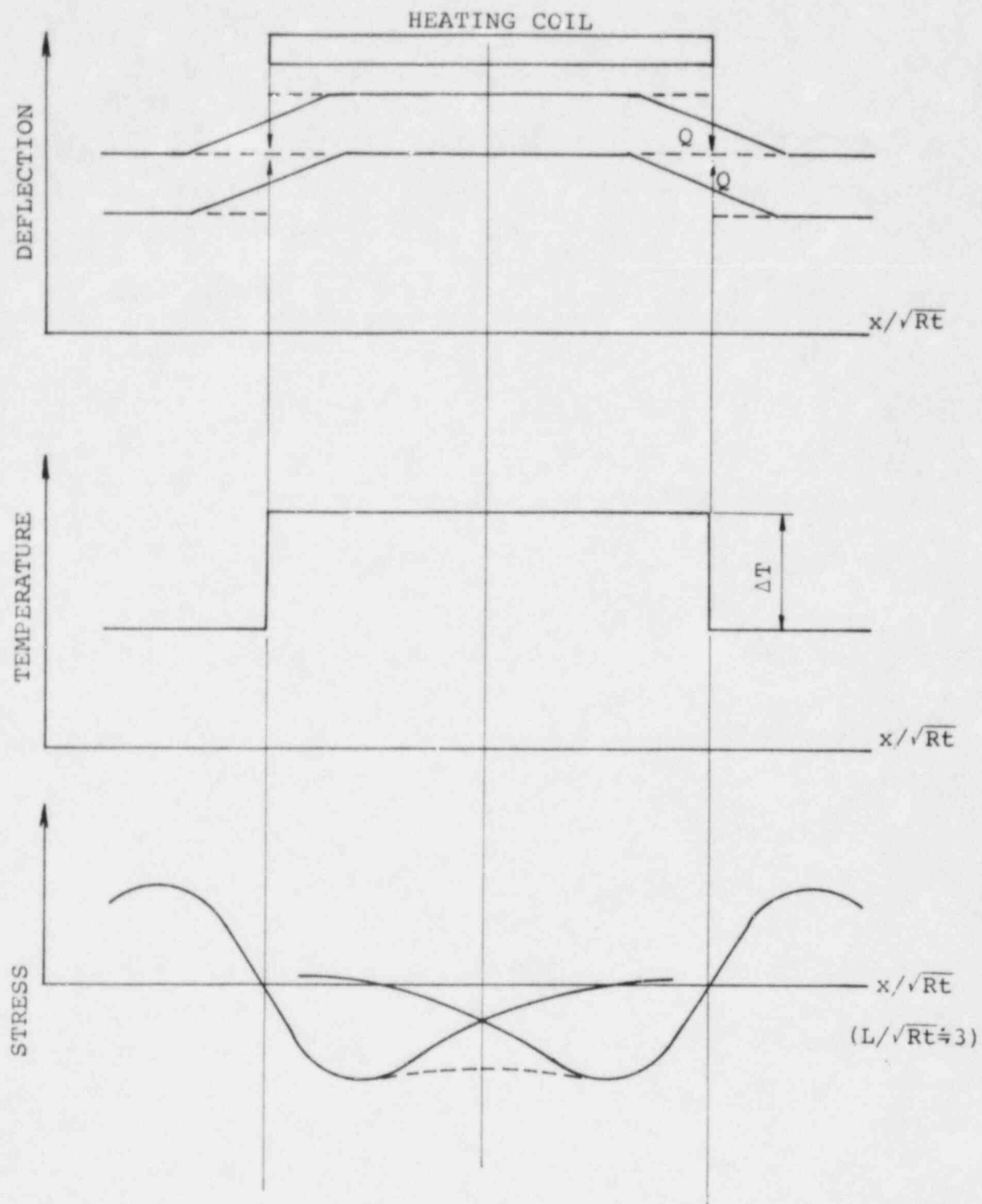


Fig. 5.7 RESULTANT STRESS DISTRIBUTION WITH STEP TEMPERATURE CHANGE IN AXIAL DIRECTION

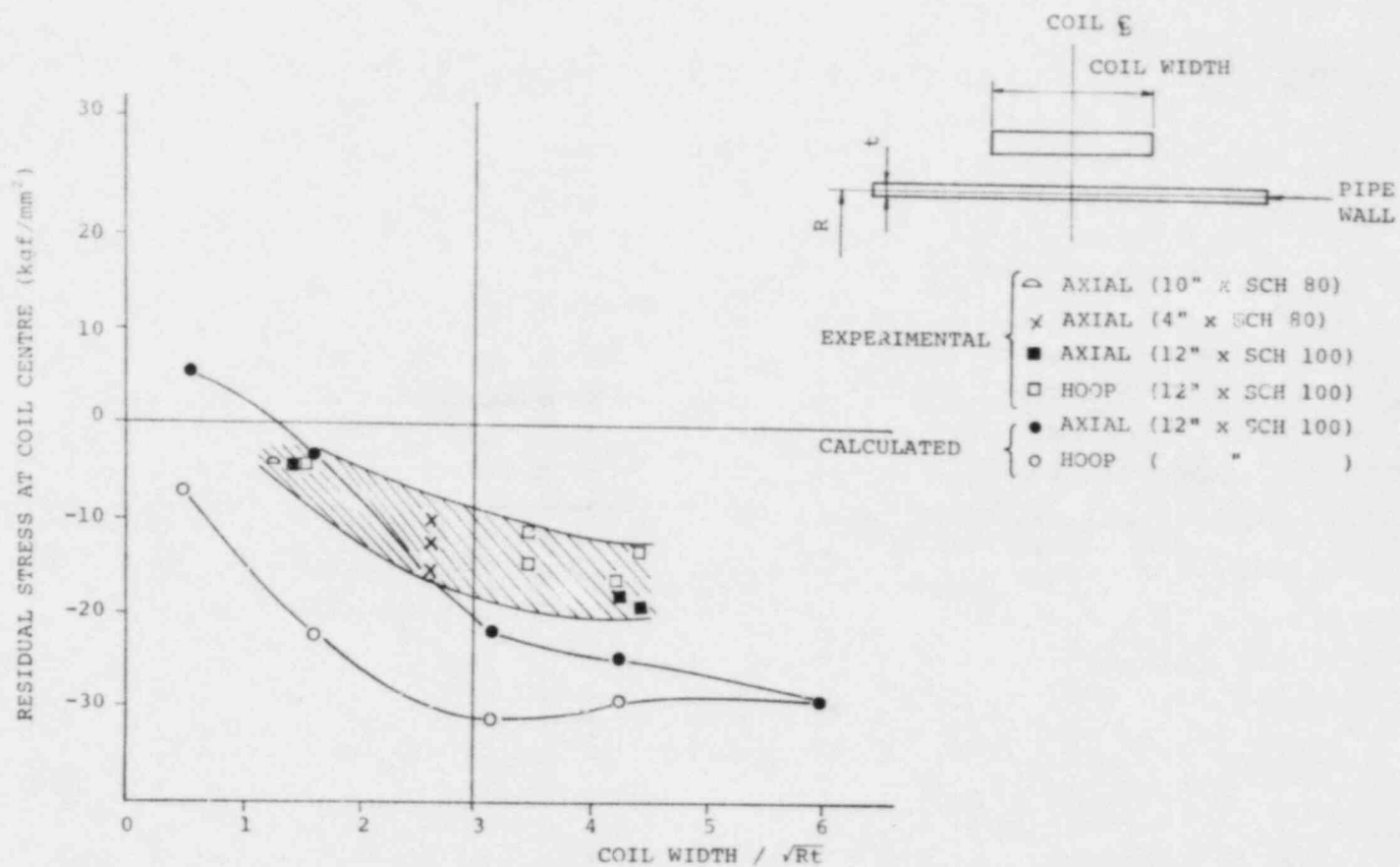


Fig. 5.8 EFFECT OF COIL WIDTH ON INNER SURFACE RESIDUAL STRESS

then the minimum required coil width can be calculated as follows:

$$\begin{aligned} L &= 3\sqrt{Rt} &= 3\sqrt{356 \times 40} \\ &= 358 \text{ mm} \end{aligned}$$

5.4 COIL SETTING LOCATION

It is clear from Figures 2.5 and 5.9 that the residual stresses at all inner surfaces of pipe under a coil can be improved by IHSI. Therefore, if the weld heat affected zone (HAZ) is located within the area covered by the heating coil, residual stresses in the HAZ are expected to be improved.

The HAZ of a normal weld is generally within 15 mm (or $t/2$) from the weld center line (mid-plane) as illustrated in Figure 5.10. Therefore, the coil should be positioned so that the weld center is located at least 15 mm (or $t/2$) inside the coil end.

Note: In many cases, the weld center line should be located much further inside the coil to obtain a larger temperature difference across the pipe thickness.

5.5 MAXIMUM HEATING TEMPERATURE

In general, as the maximum temperature increases, the temperature difference, ΔT , across the pipe thickness becomes larger. The effect of ΔT , however has already been taken into account in paragraph 5.4. Therefore, maximum temperature is not a key parameter from this perspective but should be restricted so as not to deteriorate the pipe material properties.

For austenitic stainless steel, the maximum temperature should be determined so as not to sensitize the pipe material. Considering that the maximum heating time for IHSI is only a few minutes, it is clear from Figure 5.11 that the temperature of 550°C is sufficiently low for Type 304 stainless steel.

As a result, the temperature on pipe outside surface should be limited to less than 550°C.

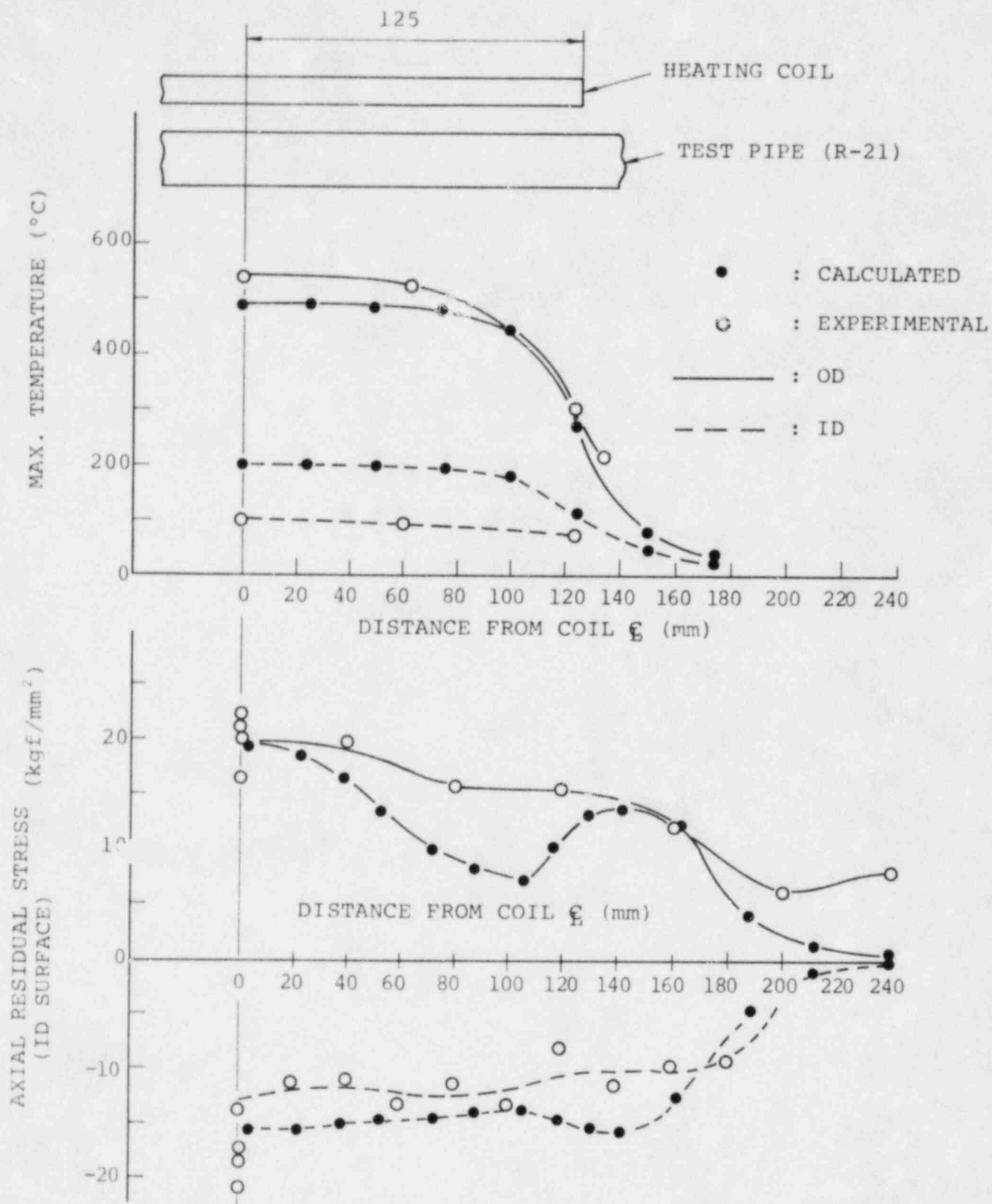


Fig. 5.9 EFFECT OF HEATING COIL LOCATION ON INNER SURFACE RESIDUAL STRESS

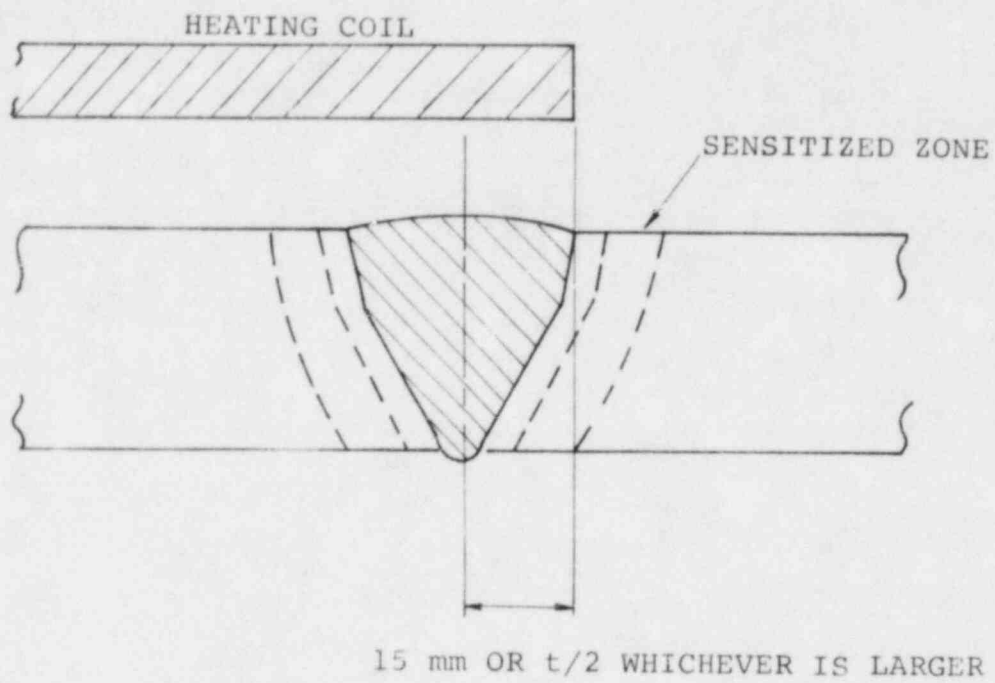


Fig. 5.10 COIL SETTING LOCATION GUIDELINES

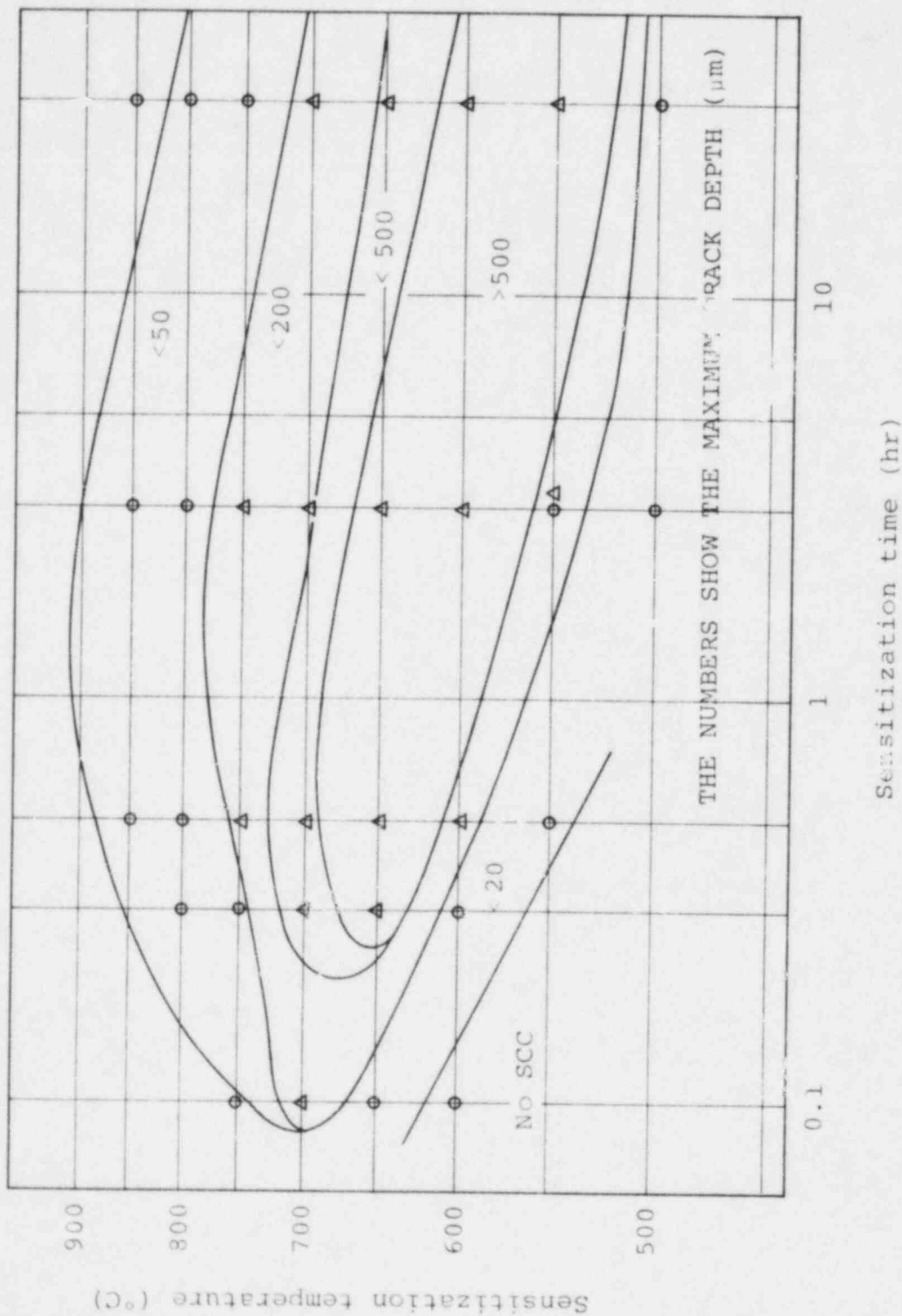


Fig. 5.11 T-T-SCC diagram for 304 stainless steel in oxygenated
(1)
water at 250°C (CBB test, 20 ppm DO, 310 hr)

Reference : M. Akashi, T. Kawamoto, Boshoku-Gijutsu, 27,165 (1978)

5.6 FREQUENCY OF THE ELECTRIC SUPPLY

The heating depth, S , (current penetration depth) for the induction heating process is given in Equation (4).

$$S = \frac{1}{2\pi} \sqrt{\frac{\rho}{\mu f \times 10^{-9}}} \quad (\text{cm}) \quad (4)$$

where μ : Specific magnetic permeability
 f : Frequency (Hz)
 ρ : Specific resistance ($\Omega \cdot \text{cm}$)

The temperature profile through the pipe thickness resulting from induction heating is given by the following equation.⁽¹⁾

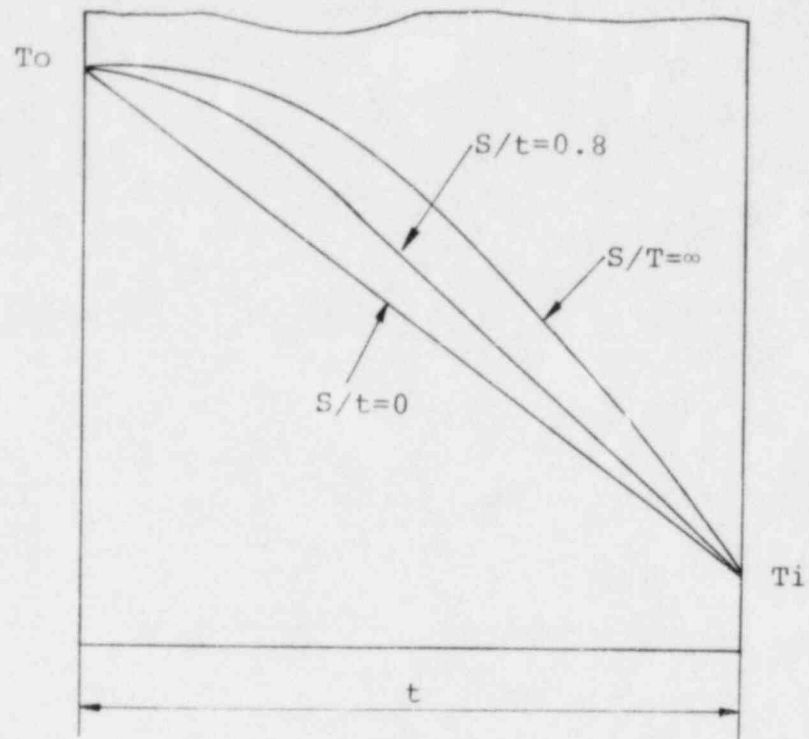
$$T_x = T_o - \frac{W_o S^2}{4\lambda_p} \left(-1 + \frac{2}{S}x + e^{-2x/S} \right) \quad (5)$$

where T_x , T_o : Temperature at position x and at outer surface respectively.
 λ_p : Thermal conductivity of pipe
 W_o : Heating density at outer surface
 x : Distance from outer surface

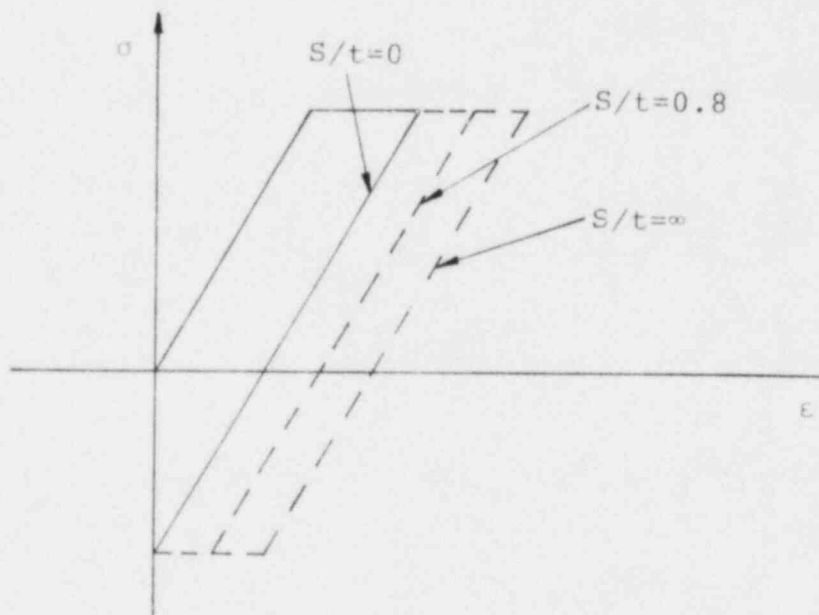
Equations (4) and (5) show that the temperature profile across the pipe thickness depends on frequency, f , and the profile changes from linear to a convex (parabolic) shape as the frequency changes from ∞ to 0. This situation is illustrated in Figure 5.12. For the parabolic temperature distribution, the thermal stress on the inner surface of a pipe is given by Equation (6)

$$\sigma = \frac{2E\alpha\Delta T}{3(1-\nu)} \quad (6)$$

Reference: (1) Appendix A-15 Residual Stress Improvement by Means of Induction Heating.



(a) TEMPERATURE DISTRIBUTION



(b) STRESS STRAIN RELATION FOR VARIOUS TEMPERATURE DISTRIBUTION

Fig. 5.12 EFFECT OF CURRENT FREQUENCY ON TEMPERATURE DISTRIBUTION AND STATE-OF-STRESS

Comparing Equations (6) with (1) demonstrates that a very low frequency (parabolic temperature distribution) provides a thermal stress which is 33.3% higher on the inside surface than the linear temperature distribution. Therefore the parabolic temperature distribution seems to improve residual stress more than the linear distribution. Since the minimum required temperature difference was determined based on a linear temperature distribution, it is expected that the residual stresses induced by a parabolic temperature distribution will be similar to that provided by a linear temperature distribution. This effect is illustrated in Figure 5.12.

In order to verify this expected result, elasto-plastic calculations for various S/t were performed using finite-element techniques. The results of these calculations are presented in Figure 5.13. As mentioned above, no significant difference in residual stress is observed in the range S/t from 0 to ∞ .

Therefore, it can be concluded that large S/t produces some additional margin in temperature difference but this margin is not converted to additional residual stress improvement when compared to small S/t as long as the minimum required temperature difference is maintained.

5.7 PIPE SIZE

Two parameters are important in pipe size evaluation, thickness, t , and diameter, d .

The effect of diameter has previously been considered in the discussion of coil width effects on residual stress.

The effect of thickness has also been accounted for in the prior discussion of coil width and heating time; and the effect of S/t was accounted for in the determination of the minimum temperature difference required to produce an optimized residual stress distribution.

Pipe size, therefore, need not be restricted as long as the coil width and heating time are properly controlled.

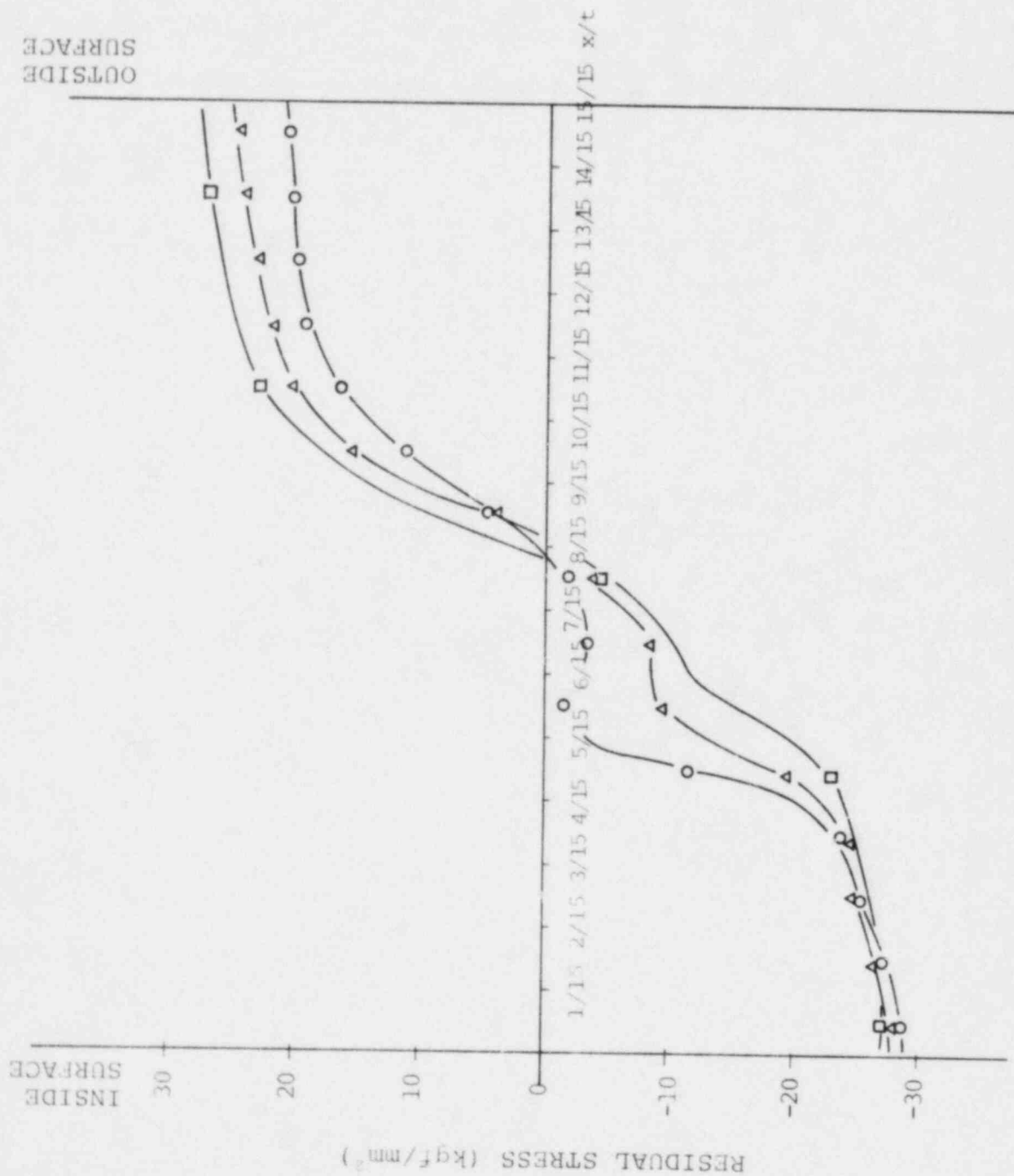


Fig. 5.13 EFFECT OF FREQUENCY ON RESIDUAL STRESS

5.8 COOLING

The through-thickness temperature difference resulting from the induction heat treatment process is easily derived by substituting t for x in Equation (5) and subtracting the value from T_o as presented below:

$$\Delta T = T_o - T_i = \frac{W_o S^2}{4\lambda_p} \left(-1 + \frac{2t}{S} + e^{-2t/S} \right) \quad (7)$$

One observes from Equation (7) that cooling variables do not affect the through-thickness temperature difference. Therefore, cooling variables are not key parameters.

It is necessary, however, to remove the heat produced by induction heating from the pipe inner surface in order to protect the pipe from overheating.

Heat convection from the pipe to the water is given by

$$q = hm (T_i - T_w) \quad (8)$$

where q : Heat flux at pipe inner surface
 hm : Mean heat transfer coefficient
 T_w : Water temperature

Consider the heat conduction in the pipe wall,

$$q = \lambda_p \frac{dT}{dx} \quad (9)$$

Differentiating equation (5) at $x = t$ and substituting Equation (9) into Equation (8), produces

$$T_i - T_w = \frac{W_o}{2hm} (1 - e^{-2t/S}) \quad (10)$$

where h_m is given by the Dittus - Boelter equation as,

$$h_m = 0.023 \frac{\lambda_w}{d^{0.2} v^{0.8}} \cdot P_r^{0.4} U_\infty^{0.8} \quad (11)$$

where λ_w : Thermal conductivity of water
 d : Inside diameter of pipe
 v : Coefficient of kinematic viscosity
 P_r : Prandtl Number
 U_∞ : Water flow rate

Temperature distributions across the thickness for various cooling conditions were calculated using Equations (5), (7), (10) and (11), and have been plotted in Figure 5.14. It can be easily understood that the temperature at outer and inner pipe surfaces are reduced as the cooling water flow rate is increased. In other words, higher water flow rate enlarges the allowance between T_o and the maximum temperature limit, maintaining the same temperature difference through the thickness.

5.9 COIL INPUT POWER

Coil input power is a function of

1. Heat generated per unit length: $\int_0^t W_o e^{-2x/S} dx$
2. Coil width: L
3. Pipe diameter: D
4. Efficiency: η

The coil input power can be represented functionally as follows:

$$P = f\left(\int_0^t W_o e^{-2x/S} dx, L, D, \eta\right) \quad (12)$$

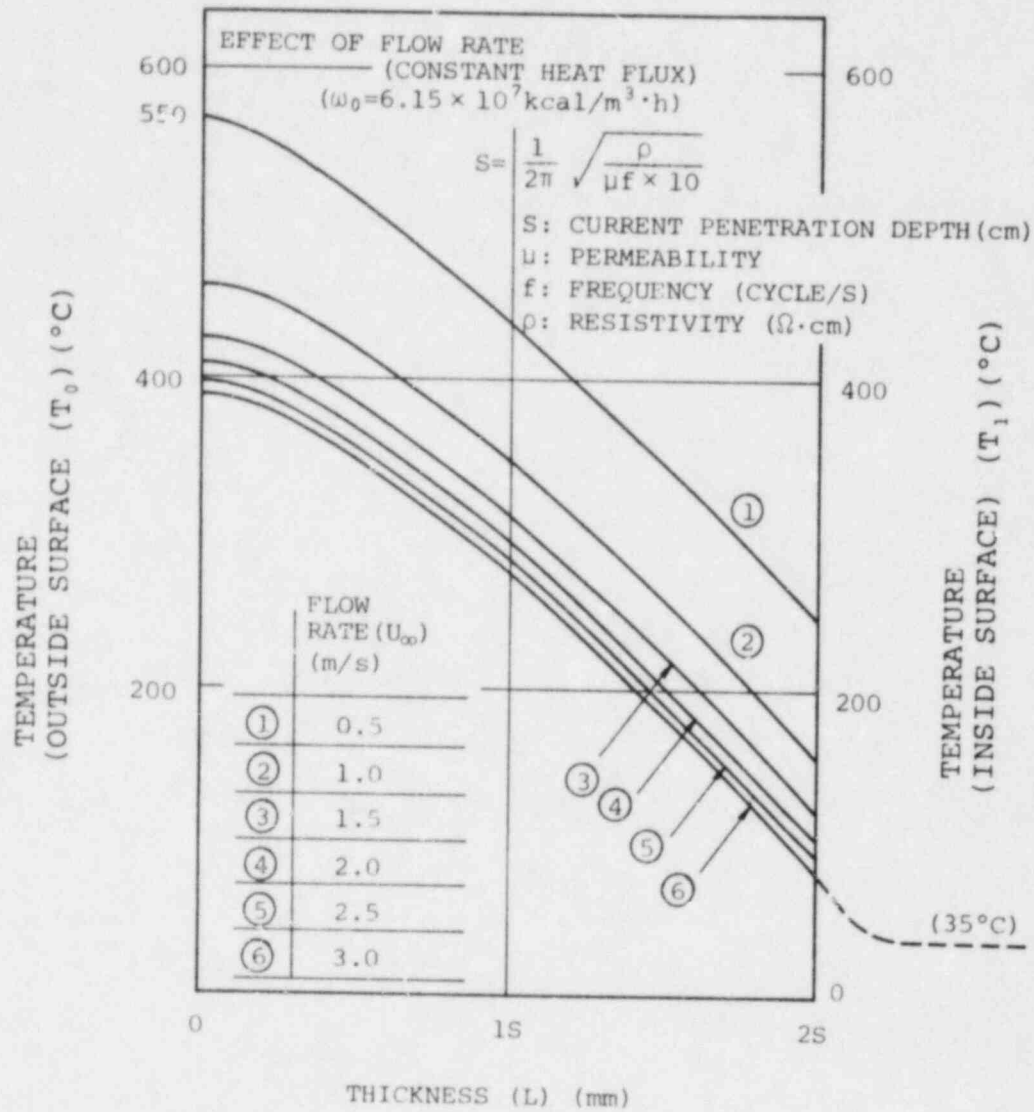


Fig. 5.14 EFFECT OF COOLING ON THROUGH THICKNESS TEMPERATURE DISTRIBUTION

The temperature difference between the pipe outer and inner surface is a function of

1. Heating density at the outer surface: W_o
2. Heating depth: S
3. Pipe thickness: t
4. Thermal conductivity: λ_p

as shown in Equation (7).

The temperature difference can be presented functionally as follows:

$$\Delta T = g(W_o, S, t, \lambda_p) \quad (13)$$

Comparing Equations (12) and (13), one observes that the coil input power: P and the temperature differences ΔT are not uniquely dependent upon the same parameters. That is ΔT can be changed by varying S , t , λ_p , L , D and η even if P is maintained at a constant value, and therefore, it is impossible to control ΔT by solely controlling P . Therefore to control ΔT one should measure ΔT directly.

After determining, S , t , λ_p , L , and D , we can, however estimate ΔT from coil input power P by assuming an appropriate η . This technique will be discussed later.

5.10 GEOMETRICAL CONFIGURATION

The previous discussions have been based on the induction heat treatment process applied to a uniform straight pipe.

In actual plants, however, there are many geometrical transitions in the vicinity of a weldment. Typical transitions include:

1. Counterbore for weld edge preparation
2. Nozzle-to-pipe transition
3. Pipe-to-elbow transition
4. Pipe-to-cap transition

In this paragraph, the effect of these transitions on the residual stresses produced by the IHSI process are discussed.

1. Counterbore for Weld Edge Preparation

The pipe end is usually counterbored to provide reasonable fit up for welding. As a result a thickness transition exists near the weld joint.

In order to investigate the effect of such a thickness transition, a representative model having a gently sloping transition was evaluated using finite-element techniques, as shown in Figure 5.15. The results of this evaluation are shown in Figure 5.16 and are compared to a smooth straight pipe. It is clear that the same amount of residual stress improvement is expected for the pipe having a gentle thickness transition as for a smooth pipe.

2. Nozzle-to-Pipe Transition

Since a nozzle has a thicker wall than the connecting pipe, there usually exists a steep thickness transition. This steep thickness transition effect was also evaluated analytically by finite-element methods. The finite-element model is shown in Figure 5.17 and the results are presented in Figure 5.18. All internal pipe surfaces under the coil exhibited an improvement in residual stress distribution resulting from the IHSI process.

This type of thickness transition in the 24-inch demonstration mock-up test joint, J-1 and the residual stresses measured following the IHSI treatment are plotted in Figure 5.19. The results demonstrate that the weld residual stresses on the pipe inner surface following an IHSI treatment are compressive in agreement with the calculated results.

It can be concluded from both the analysis and experiments that even a steep thickness transition has no significant effect on IHSI results.

3. Pipe-to-Elbow Transition

For this case, the heating coil will usually be placed so that the weld joint is located near the coil end in order to avoid interference of the coil with the elbow. But it is necessary that the heating coil covers a range of approximately $2t$ (t : thickness of elbow) from the weld center in order to obtain a sufficient temperature difference between the outside and inside surfaces of the elbow at this location.

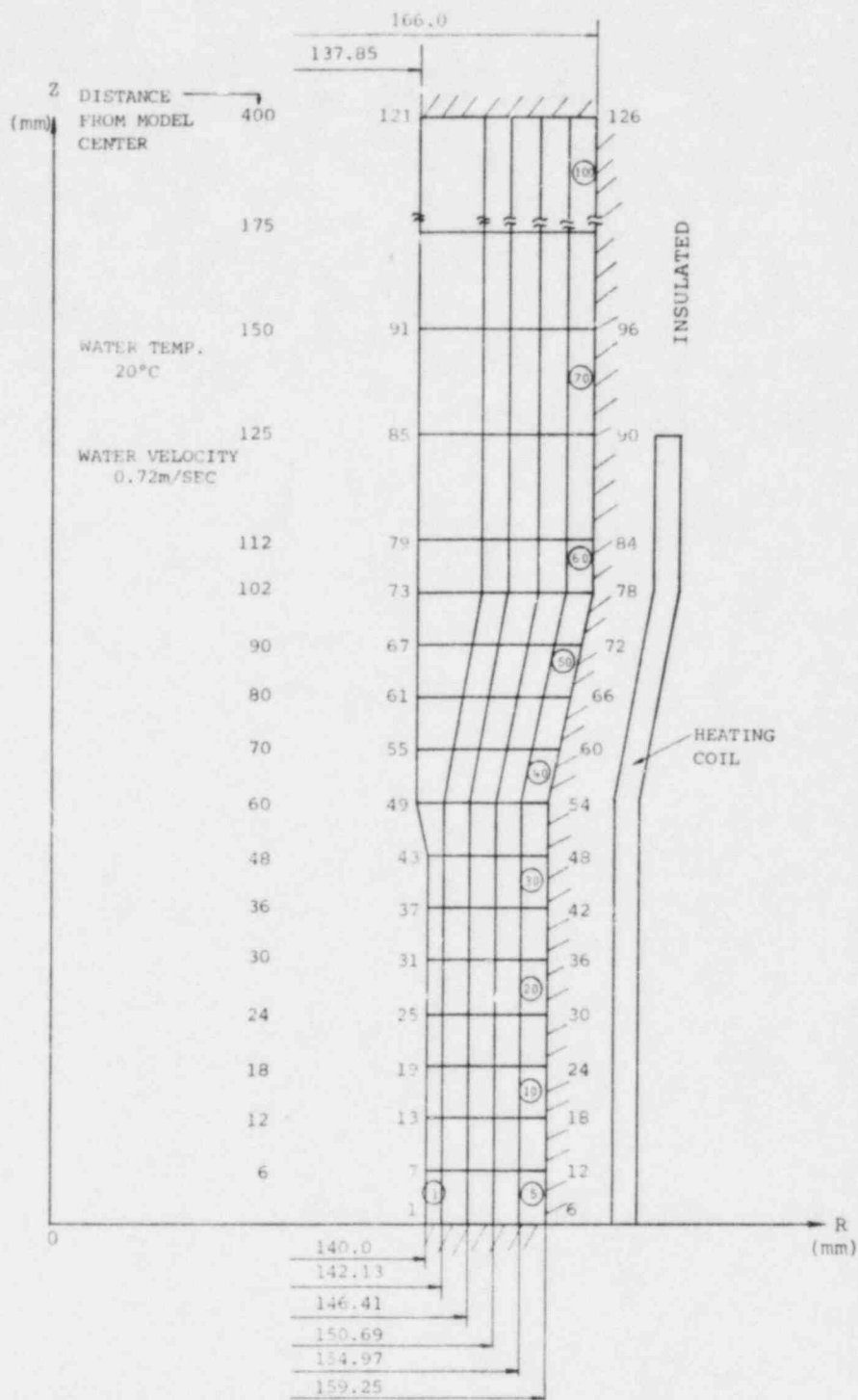


Fig. 5.15 ANALYTICAL MODEL FOR TEMPERATURE DISTRIBUTION

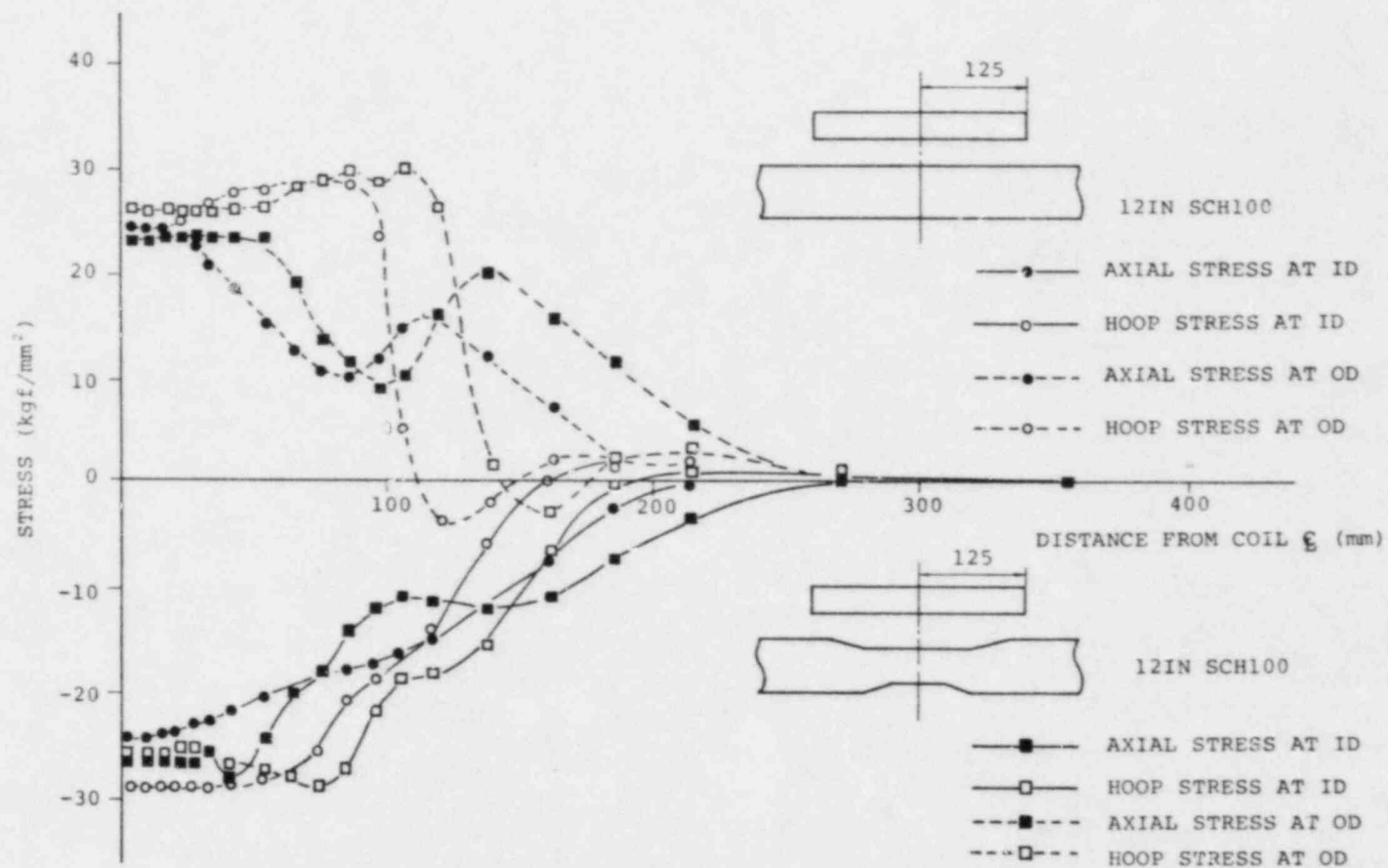


Fig. 5.16 RESIDUAL STRESS DISTRIBUTION FOR GENTLY SLOPING TRANSITION

Fig. 5.17 CALCULATED MODEL AND TEMPERATURE DISTRIBUTION FOR NOZZLE TO PIPE TRANSITION

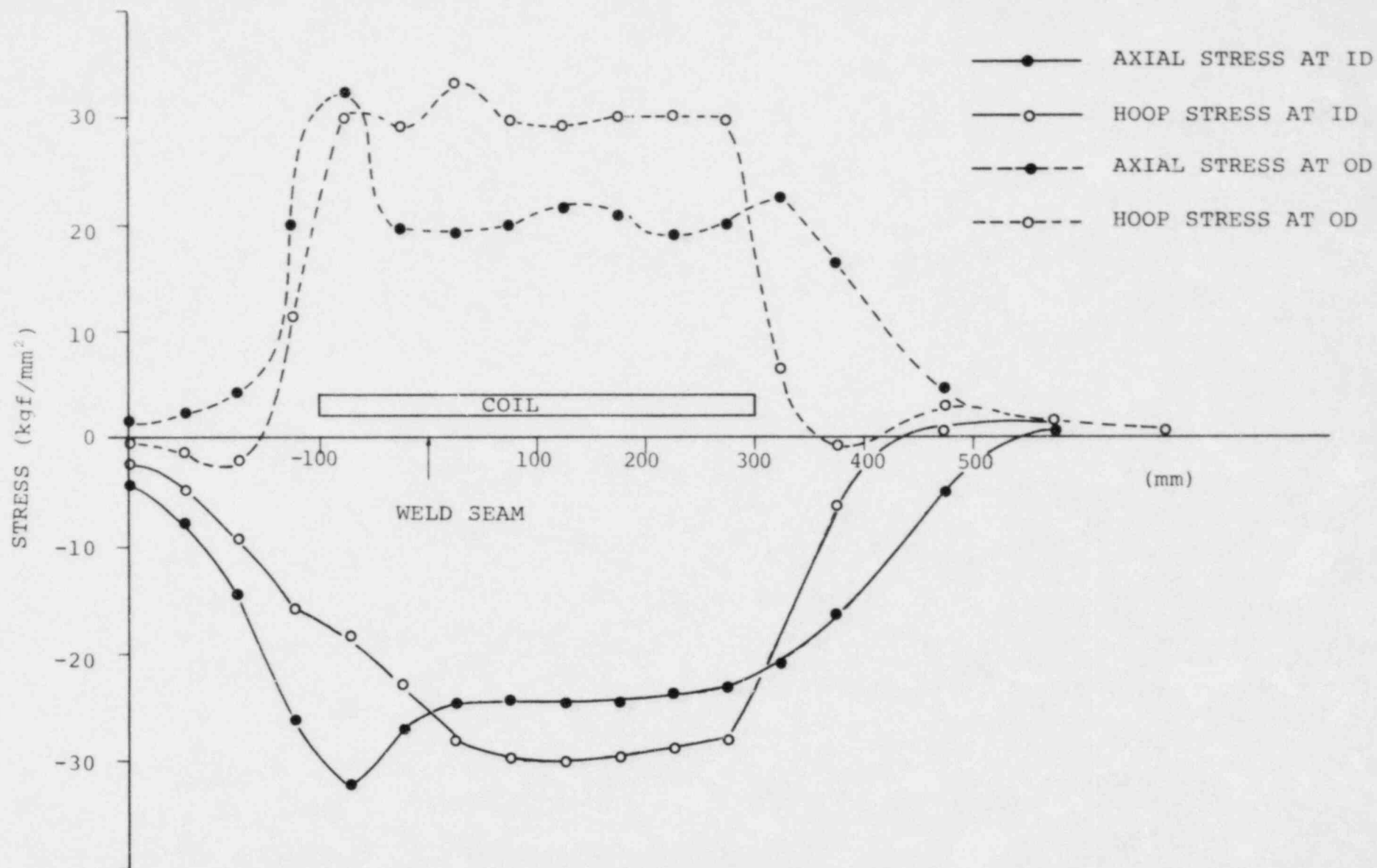


Fig. 5.18 RESIDUAL STRESS DISTRIBUTION FOR NOZZLE TO PIPE THICKNESS TRANSITION

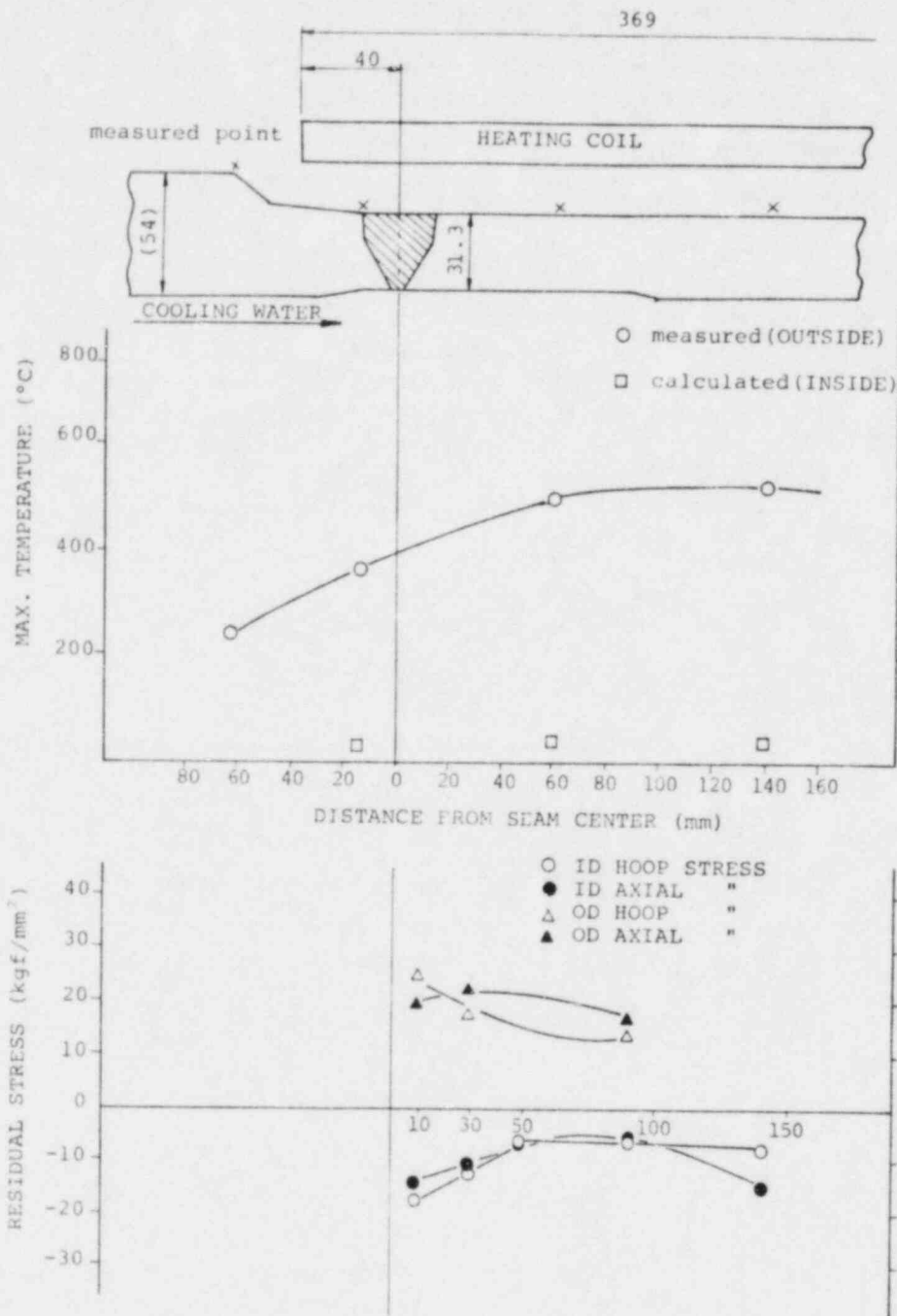


Fig. 5.19 J-1 RESIDUAL STRESS DISTRIBUTION FOR NOZZLE TO PIPE TRANSITION

The bend radius of the elbow is usually $1 \times D$ to $2 \times D$ or more, where D is the nominal pipe diameter. The thickness t is usually smaller than one tenth of D . Therefore, the heating area of $2t$ is much less than D . In this case, the assumption may be made that the heated area of the elbow is an extension of the mating pipe and that the same residual stress improvement can be expected. Figure 5.20 shows the experimental results for a pipe-to-elbow weld in a demonstration mock-up test. The residual stresses were reduced to less than 5 kg/mm^2 tension as expected.

4. Pipe-to-End-Cap

An end cap, usually hemispherical in configuration, is sometimes welded to a pipe. In order to evaluate the applicability of IHSI for a weld of this type, computer calculations were performed using finite-element techniques. The calculated model and the results are presented in Figures 5.21 and 5.22 respectively. It is anticipated, based on these modeling results that the residual stress of the pipe-to-cap weld can be improved.

5.11 SUMMARY OF PARAMETERS

The aforementioned discussions are summarized in Table 5.1 with the recommended controlling ranges. It is noteworthy to recall that the maximum effect of the residual stress improvement process is expected when the parameters are maintained within the recommended controlling range and that the IHSI effect does not disappear even if these parameters are below the specified value; but the effect may be reduced from the optimum value.

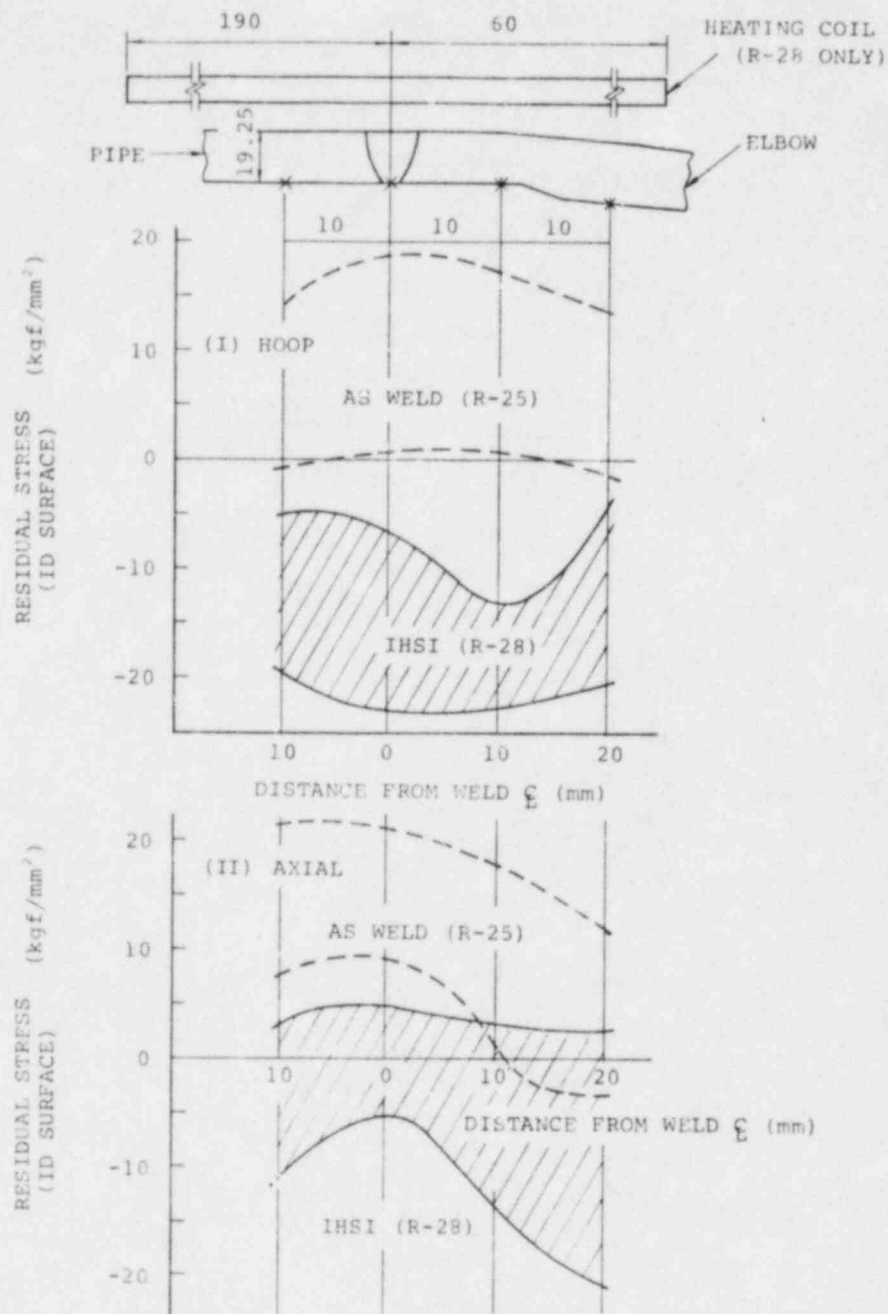


Fig. 5.20 RESIDUAL STRESS DISTRIBUTION FOR PIPE TO ELBOW WELD

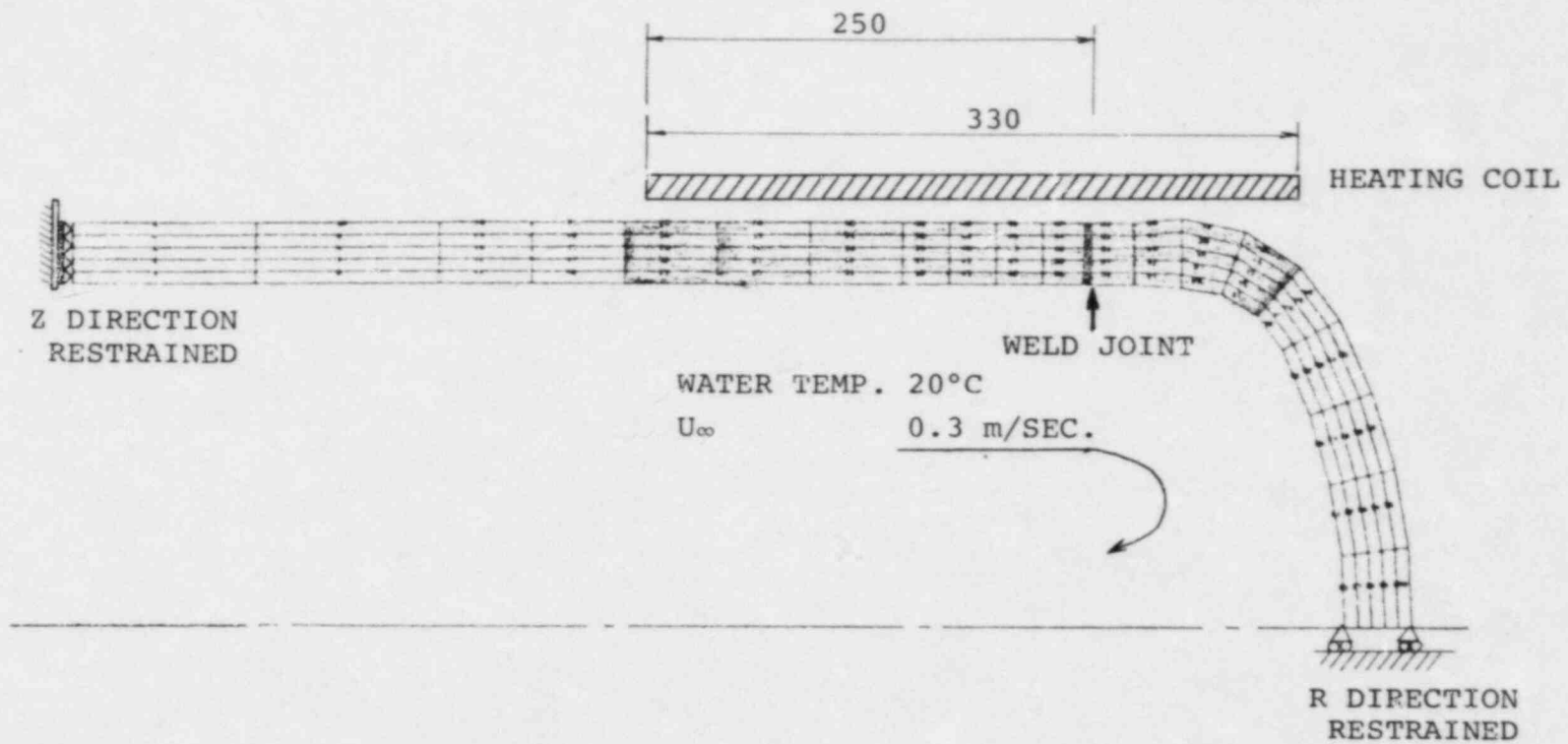


Fig. 5.21 ANALYTICAL MODEL FOR PIPE TO END CAP JOINT

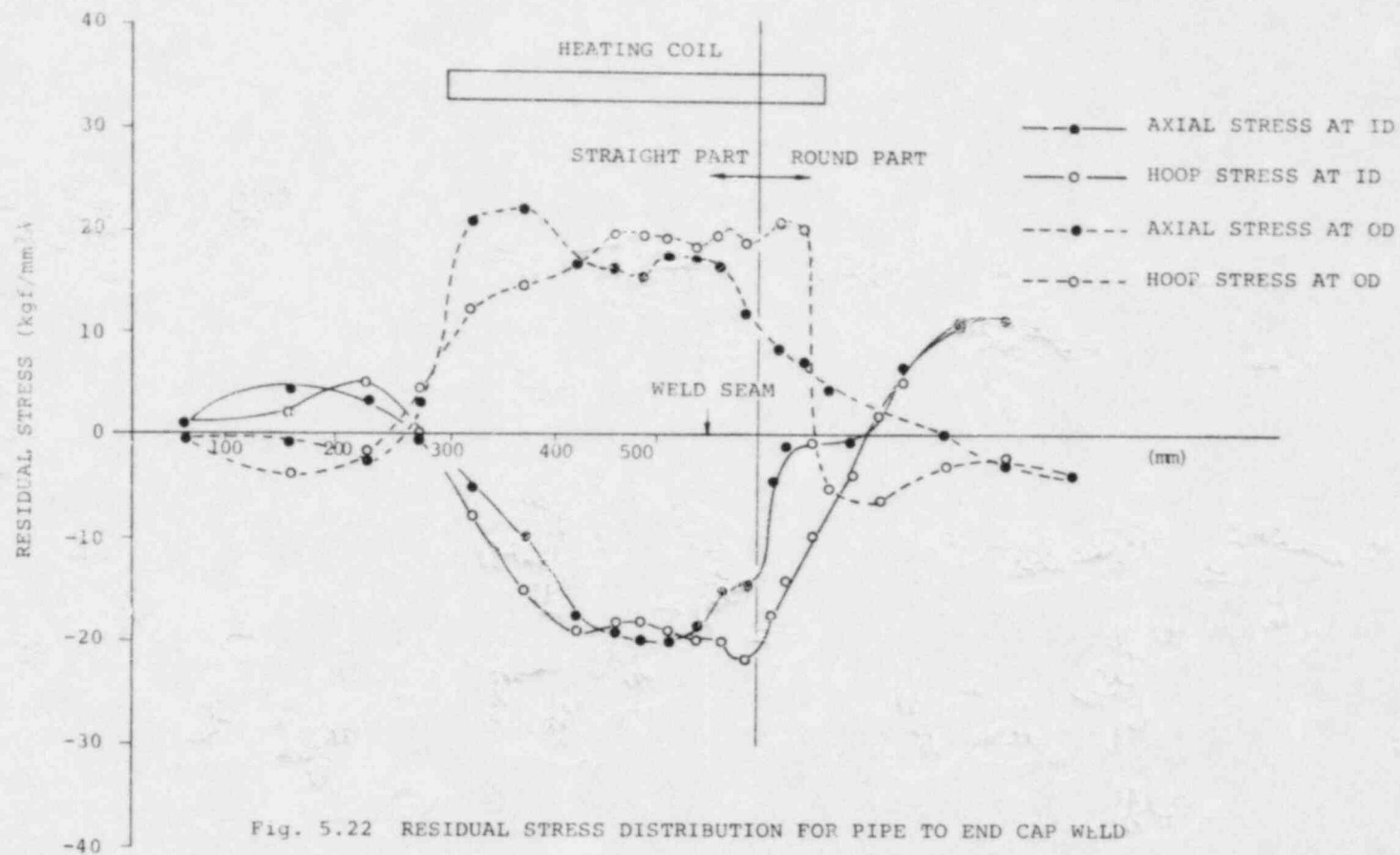


Fig. 5.22 RESIDUAL STRESS DISTRIBUTION FOR PIPE TO END CAP WELD

Table 5.1

SUMMARY OF PARAMETERS FOR OPTIMIZED EFFECT OF IHSI

<u>Number</u>	<u>Parameter</u>	<u>Controlling Range</u>	<u>Remarks</u>
1	Temperature Difference	$\Delta T > \frac{4\sigma_Y(1-\nu)}{E\alpha}$	
2	Heating Duration	$\tau > 0.7 \frac{t^2}{a}$	
3	Coil Width	$L > 3\sqrt{Rt}$	
4	Coil Location	$x > 15 \text{ mm or } \frac{t}{2}$	Whichever is greater
5	Maximum Temperature	$T_O < 550^\circ\text{C}$	
6	Frequency	-----	Control is not required
7	Pipe Size	-----	Automatically controlled by other parameters
8	Cooling	-----	To be sufficient to get enough ΔT
9	Coil Input Power	-----	To be sufficient to get enough ΔT
10	Geometrical Configuration	- - - -	

σ_Y : Material Yield Strength (kg/mm^2)

ν : Poisson's Ratio

E : Young's Modulus (kg/mm^2)

α : Thermal Expansion Coefficient ($\text{mm}/^\circ\text{C}$)

t : Wall Thickness of Pipe (mm)

R : Mean Radius of Pipe (mm)

a : Temperature Conductivity ($\text{mm}^2/\text{sec.}$)

x : Distance from Weld Center to Coil End (mm)

T_O : Pipe Outside Temperature ($^\circ\text{C}$)

Section 6

EVALUATION OF OTHER EFFECTS OF IHSI TREATMENT

In this section, other effects resulting from an IHSI treatment are discussed. The IHSI treatment is one of the heat treatments of pipe, so it is necessary to consider changes in metallurgical and mechanical properties resulting from the application of such a process.

6.1 SENSITIZATION EFFECTS

The pipe inner surface, which is the region of concern for IGSCC resistance, is continuously cooled by water during the IHSI process, so the temperature at the pipe inner surface will not rise above 100°C even in the extreme case. Because this temperature is lower than the reactor operating temperature, this temperature will produce no deleterious effect on the sensitization kinetics of the pipe inner surface. As for the pipe outer surface, the maximum temperature of the IHSI process is limited to less than 550°C as specified in paragraph 5.5. During the IHSI treatment, the heating time is limited to several minutes. Figure 5.11 presents a Time-Temperature - SCC diagram for Type 304 stainless steel obtained by CBB test⁽¹⁾ in 250°C water with 20 ppm dissolved oxygen for 310 hours. The data demonstrate that no SCC susceptibility results from this process. Consequently, sensitization is not expected to occur during the IHSI treatment.

6.2 MECHANICAL PROPERTIES

The IHSI treatment produces a small amount of plastic strain at the inner and outer pipe surfaces. In this section, the effect of that plastic strain is discussed. Since the maximum temperature at the outer surface is limited to less than 550°C and water is used as the cooling medium, the maximum temperature difference between the inner and outer surface will be no greater than 550°C.

Reference: (1) M. Axashi and T. Kawamoto, Boshoku - Gijutsu, 27, 165 (1978).

Thermal strains produced by such a ΔT can be approximated by using the following equation.

$$\begin{aligned}\epsilon_t &= 0.5 \alpha \Delta T \\ &= 0.5 \times 1.8 \times 10^{-5} \times 550 \\ &= 0.005\end{aligned}$$

No detrimental effects are expected from this plastic strain since this strain is very small compared with that produced in usual plastic work. An example of a mechanical test on a 12-inch pipe weld joint is presented in Table 6.1 and Figure 6.1. No significant differences were observed on the weld joint tension test, root bend test, side bend test and hardness when comparing the IHSI weld with the non-IHSI weld. Consequently, no detrimental mechanical property effects are anticipated when employing the IHSI process.

CONFIGURATION	JOINT NO.	IHSI	TEST ITEM				
			ULTIMATE STRENGTH (kgf/mm ²)	BEND TEST		MAX. HARDNESS (Hv=10kgf)	
				ROOT BEND TEST	SIDE BEND TEST	BASE METAL	DEPOSIT METAL
STRAIGHT PIPE + ELBOW	R-25	W/O	57.1 (MIN.)	W/O DEFECT	W/O DEFECT	198	213
			58.7 (MAX.)	W/O DEFECT	0.3 x 1*		
	R-28	WITH	57.7 (MIN.)	W/O DEFECT	W/O DEFECT	215	224
			59.7 (MAX.)	W/O DEFECT	W/O DEFECT		

* [WELD DEFECT SIZE (mm)] x NUMBER

Table 6.1 MECHANICAL TEST RESULTS 12-IN. PIPE WELD JOINT

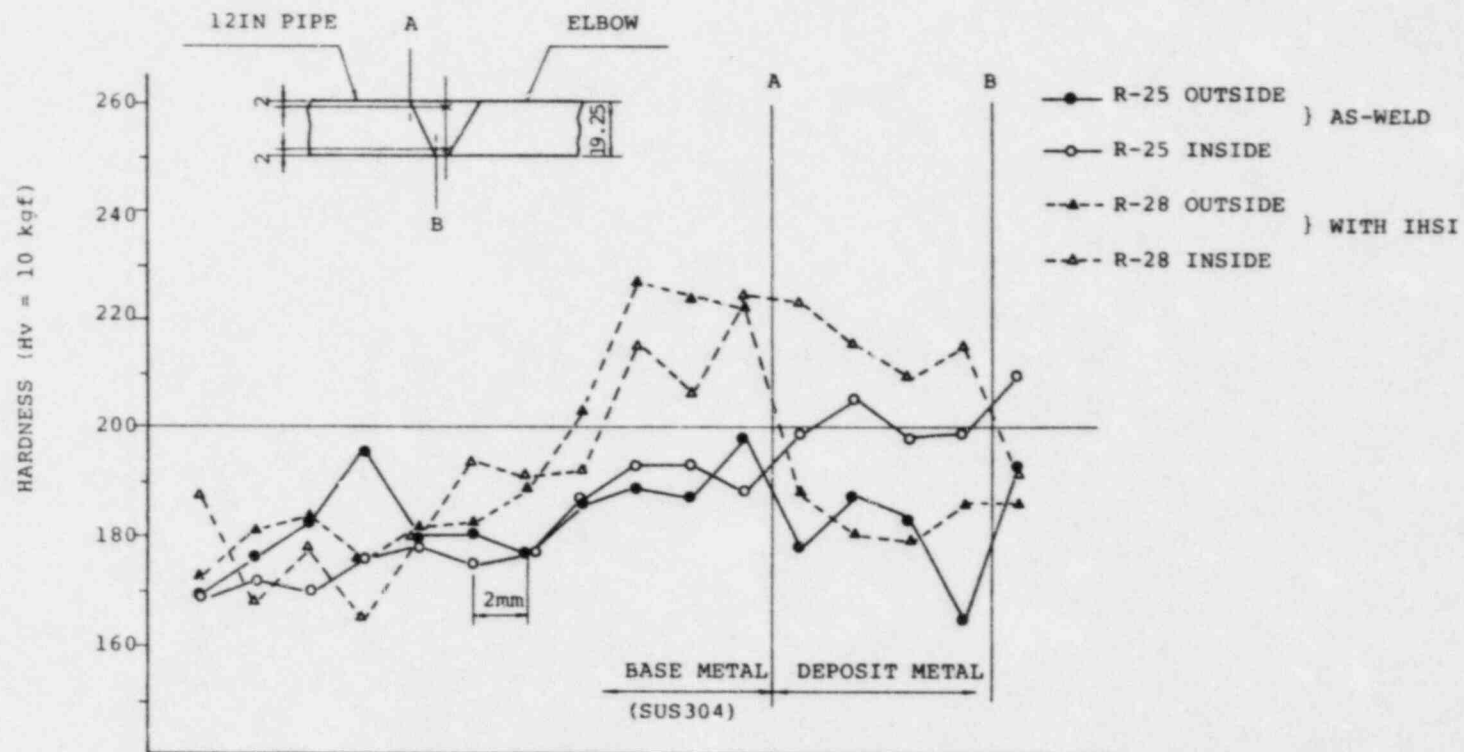


Fig. 6.1 HARDNESS DISTRIBUTION IN 12 IN PIPE WELD JOINT

Section 7

FIELD APPLICATION

When applying this process to the field, it is necessary for the confirmation of IHSI validity that key parameters are controlled within the specified range. Two key parameters, coil width and coil location, are verified prior to IHSI application. The other three key parameters are controlled during the IHSI process.

It is required to get a temperature difference greater than the minimum required while maintaining the maximum outer surface temperature not to exceed 550°C. The temperature difference between the outer and inner surface of a pipe and the maximum temperature of the pipe outer surface depend on the coil input power so we must choose a suitable input power. The required coil input power which is necessary to produce the required temperature difference is estimated initially. Trial heating is performed to confirm that the power produced is suitable.

Usually the temperature of the pipe surface cannot be measured directly. Consequently, an estimate of the temperature of the pipe inner surface is required. The method for performing that estimate follows.

7.1 ESTIMATE OF INPUT POWER

As mentioned above, the coil input power determines the time temperature relationship; when the input power is larger than required, the heating duration will be less than required since the outer surface temperature reaches 550°C too rapidly. When the input power is less than required, the temperature difference between inner and outer surface will be insufficient. So the optimum coil input power should be selected.

The required coil input power P_c is proportional to ΔT , D , L/t

where ΔT : Temperature difference
D: Pipe diameter
L: Coil width
t: Plate thickness

Test and calculation results relating the above parameters are shown in Figure 7.1. Required generator power P_g is obtained from the quantity P_c/η , where η is the efficiency which must be determined experimentally. For example, the required generator power P_g for heating of a 28-inch pipe is calculated as 340 KW as shown below.

$\Delta T = 400^\circ\text{C}$	$P_c = 290 \text{ kW}$ from Figure 7.1
$L = 450 \text{ mm}$	$P_g = 290/0.85 = 340 \text{ kW}$
$D = 707.7 \text{ mm}$	where, 0.85 is the value of the heat transfer
$t = 37 \text{ mm}$	efficiency

7.2 TRIAL HEATING

The coil input power is fixed after the trial heating. The trial heating is performed to verify that the coil input power determined from Figure 7.1 is proper. The trial heating is performed such that the maximum outside surface temperature is less than 280°C (operating temperature), therefore, minimizing material property effects. In Figure 7.2, an estimating method of long time heating condition from trial heating data is presented.

Since a sufficient width of the pipe outer surface is covered by the heating coil and the pipe inner surface is cooled by the flowing water, it is possible to predict the temperature by idealizing this situation as follows:

Assume an infinite length plate whose initial temperature is 0°C . When heat is introduced at one side which is under insulated conduction and the other side is maintained at 0°C , the temperature of the heated side after τ seconds will be given by the following equation.

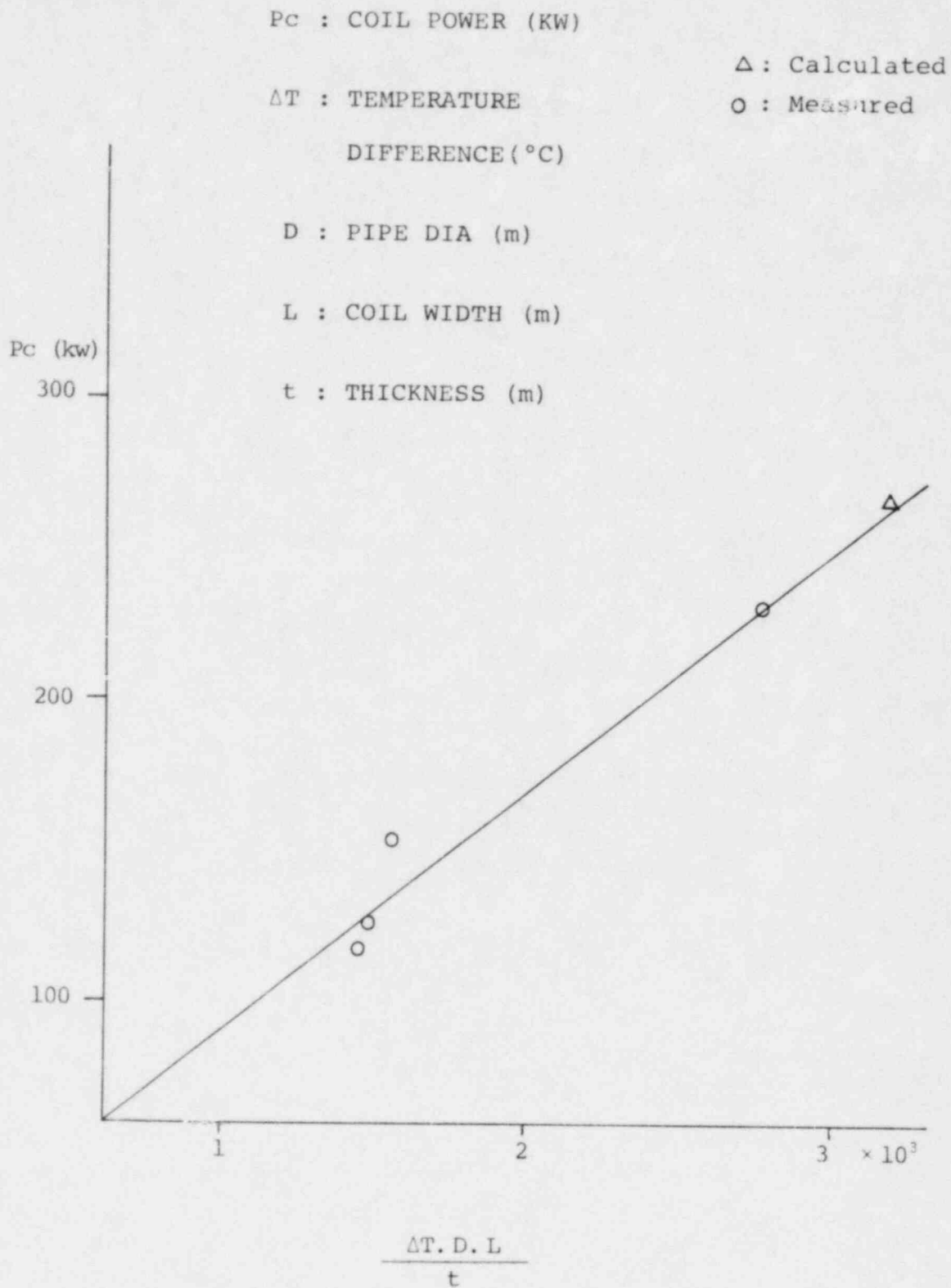


Fig. 7.1 ESTIMATION OF COIL INPUT POWER

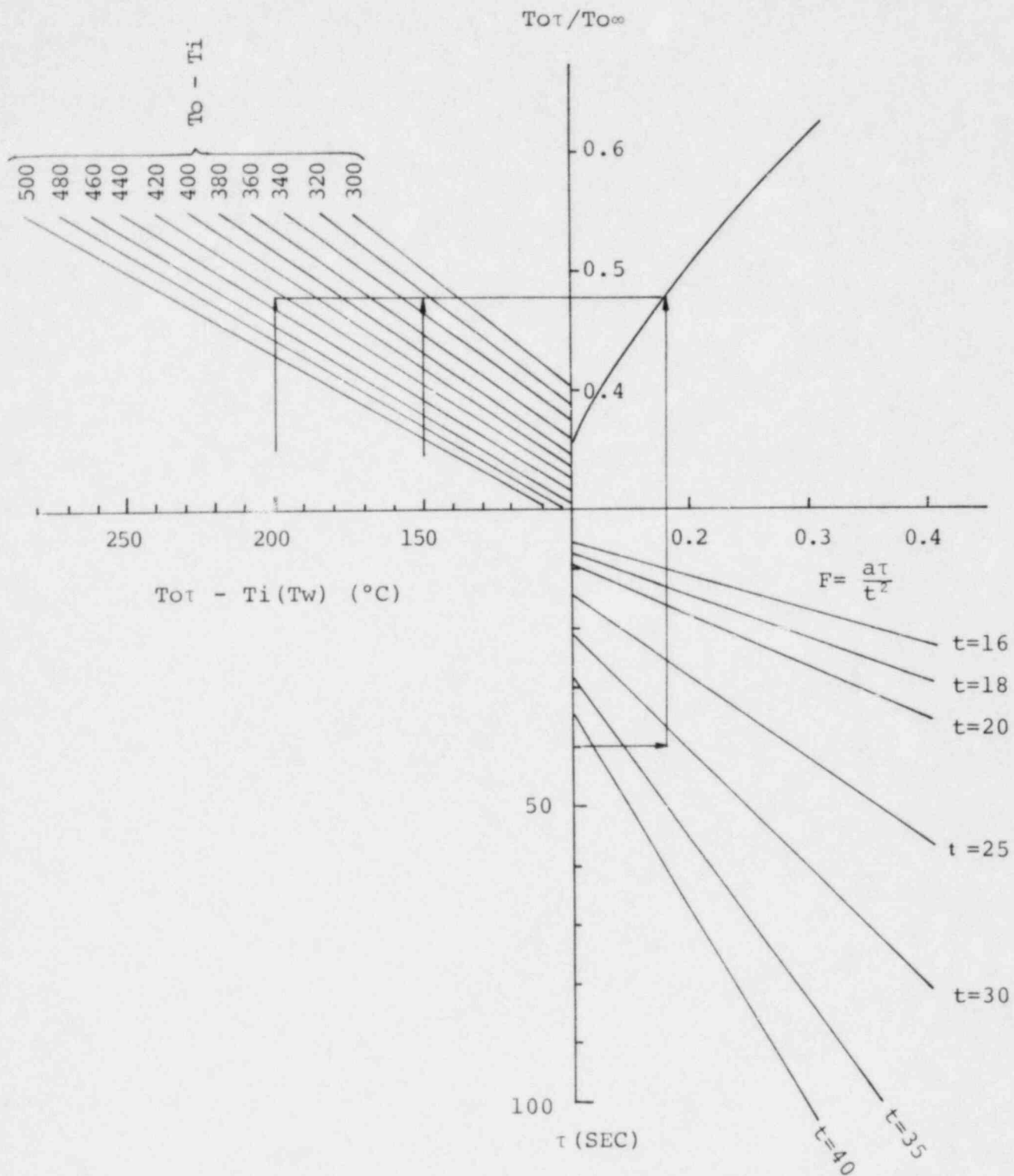


Fig. 7.2 ESTIMATION OF STEADY STATE CONDITION BY TRIAL HEATING

$$T = \frac{q}{\lambda_p} \frac{2}{t} \sum_{n=1}^{\infty} \frac{1}{\left(\frac{2n-1}{2}\right)^2 \pi^2 \frac{a}{t^2}} \times \left(1 - e^{-\left(\frac{2n-1}{2}\right)^2 \pi^2 \frac{a\tau}{t^2}}\right) \quad (14)$$

where T: Temperature
 q: Heat input
 λ_p : Thermal conductivity of the pipe
 a: Thermal diffusivity
 t: Plate thickness
 n: Natural number
 τ : Heating time

To make Equation (14) dimensionless, divide by the value of $T_{\tau=\infty}$ which is obtained from Equation (9) as $T_{\tau=\infty} = \frac{q \cdot t}{\lambda_p}$ at an infinite time following heating

$$g = \frac{T_{\tau=\tau}}{T_{\tau=\infty}} = \frac{2}{\pi} \sum_{n=1}^{\infty} \frac{1}{\left(\frac{2n-1}{2}\right)^2} \times \left(1 - e^{-\left(\frac{2n-1}{2}\right)^2 \pi^2 \frac{a\tau}{t^2}}\right) \quad (15)$$

The value g in Equation (15) has the meaning (Measured temperature of outer surface - Water temperature)/(Predicted maximum temperature of outer surface - Water temperature). Figure 7.2 presents the graph of g . The value g is plotted versus Fourier Number in quadrant A of Figure 7.2. The ordinate of quadrant B represents heating time of the trial heating. The lower abscissa of quadrant D represents the measured temperature of the outer surface minus the water temperature and the upper abscissa represents predicted maximum temperature of outer surface minus water temperature. An explanation of the use of Figure 7.2 is presented below. For a given set of experimentally determined trial heating parameters, locate in Figure 7.2 the measured value of τ on the ordinate of quadrant B. Move horizontally to the line for the plate or pipe thickness of interest. One may interpolate for intermediate values of the plate thickness. From this intersection point move vertically upwards to the line for g in quadrant A of Figure 7.2. From this intersection point move horizontally left to the measured value of the measured temperature of the outer surface minus the water temperature of the lower abscissa of quadrant D obtained in the trial experiment. The intersection point of this horizontal line with the family of curves representing the upper abscissa

of quadrant D produces the predicted maximum temperature of the outer surface minus the water temperature, thereby obtaining the predicted maximum temperature of the outer surface to be produced during the IHSI treatment.

7.3 ESTIMATE OF PIPE INNER SURFACE TEMPERATURE

The effect of IHSI is influenced strongly by the temperature difference between the outer and inner surfaces. When IHSI is applied at a reactor site, the temperature of the outer surface can be measured using thermocouples but the temperature of the inner surface cannot generally be measured. So it is necessary to predict the temperature difference exclusively from outer surface temperature data and cooling parameters. The estimation method for obtaining the temperature of the inner surface is explained as follows.

The temperature difference between the outer and inner surfaces is given by the following equation.⁽¹⁾

$$\begin{aligned}\Delta T_1 &= T_o - T_i \\ &= \frac{W_o S^2}{4\lambda_p} \left(-1 + \frac{2}{S} t + e^{-2t/S} \right)\end{aligned}\tag{14}$$

where W_o : Heating density on outer surface
 S : Heating depth
 λ_p : Thermal conductivity of the pipe
 t : Plate thickness

Reference: (1) Appendix A-13 Estimation of Pipe ID Temperature During IHSI.

The temperature difference between the outer surface and the water is given by the following equation.

$$\Delta T_2 = T_o - T_w$$

$$= \frac{W_o S}{2} \left\{ \frac{S}{2\lambda_p} \left(-1 + \frac{2t}{S} + e^{-2t/S} \right) + \frac{1}{hm} (1 + e^{-t/S}) \right\} \quad (15)$$

where hm : Heat transfer coefficient

From Equation (15), W_o is obtained and when obtained, W_o is substituted into Equation (14), and the temperature difference ($T_o - T_i$) is obtained. It is very difficult to do the above calculation at a reactor site. Figure 7.3 is presented to display graphically the above mentioned calculation, and is explained as follows.

Locate in Figure 7.3, the measured value of ($T_o - T_w$). Move horizontally to the line for the plate or pipe thickness. One may interpolate for intermediate values of plate thickness. From this intersection point move vertically upwards to the line for the value of plate thickness in the first quadrant. From this intersection, move horizontally left to the ordinate and read the value of ($T_o - T_i$).

7.4 EXAMPLES OF FIELD APPLICATION OF THE IHSI PROCESS

In the case of the field application, it is necessary to record and to evaluate the results. Four steps are required to obtain good results.

The first step is preparation. The second step is the trial heating to confirm the key parameters. The third step is the actual heating. The fourth step is evaluation of the results. Figure 7.4 shows some examples of the IHSI results for actual primary loop recirculation piping.

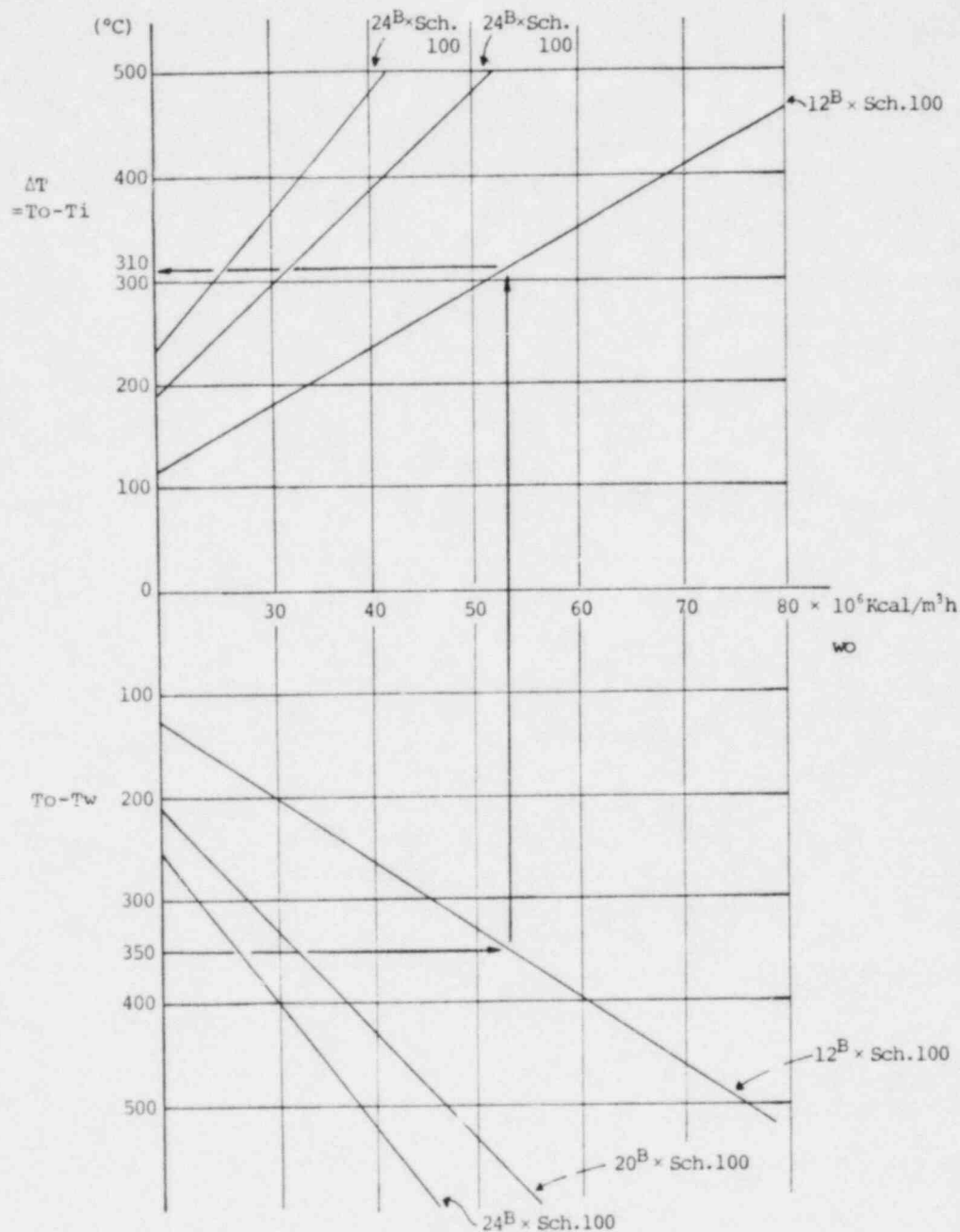


Fig. 7.3 TEMPERATURE DIFFERENCE BETWEEN OUTER AND INNER SURFACE OF A PIPE

OCT. 11, 1978

WELDING JOINT NO.		PLR - 6 - J	ESSENTIAL VARIABLES	REQUIRED	MEASURED
MATERIAL		SA376 SA240 TP304 + TP304 (PB + PB)	COIL WIDTH $L/\sqrt{RT} \geq 2.7$	$\geq 288\text{mm}$	290mm
TEMP. ON OUTER SURFACE		at ② 456°C	HEATING TIME $at/T^2 \geq 0.8$	$\geq 159\text{S}$	300S
ROOM TEMPERATURE		27 °C	DIF. OF TEMP. $\Delta T \geq \frac{4(1-\nu)}{E\alpha} \epsilon_y$	$\geq 203^\circ\text{C}$	343°C
COOLING WATER	TEMP.	36 °C	MAX. TEMP. ON OUTER SURFACE	$550^\circ\text{C} \geq$	483°C
	VELOCITY	1.18 m/s	LOCATION OF COIL $l \geq \text{MAX. } (T/2, 15\text{mm})$	$>15\text{mm}$	128mm

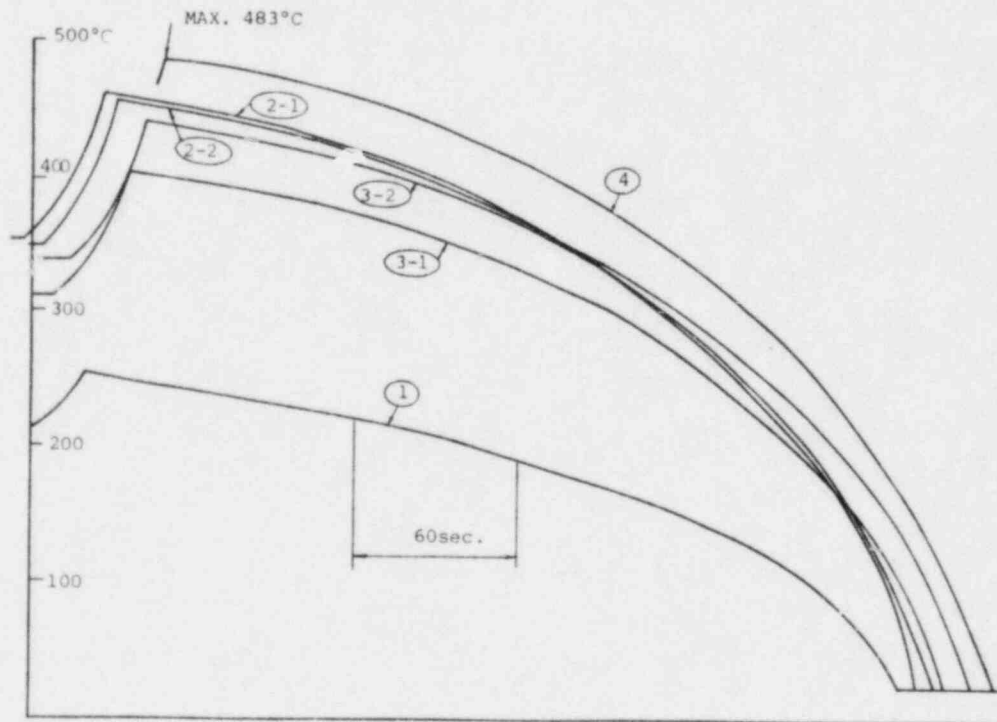
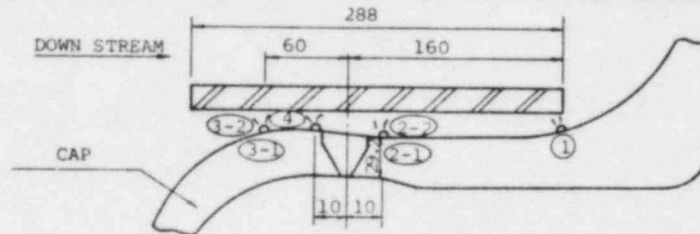


Fig. 7.4(a) Record of Field Application of Induction Heating Stress Improvement

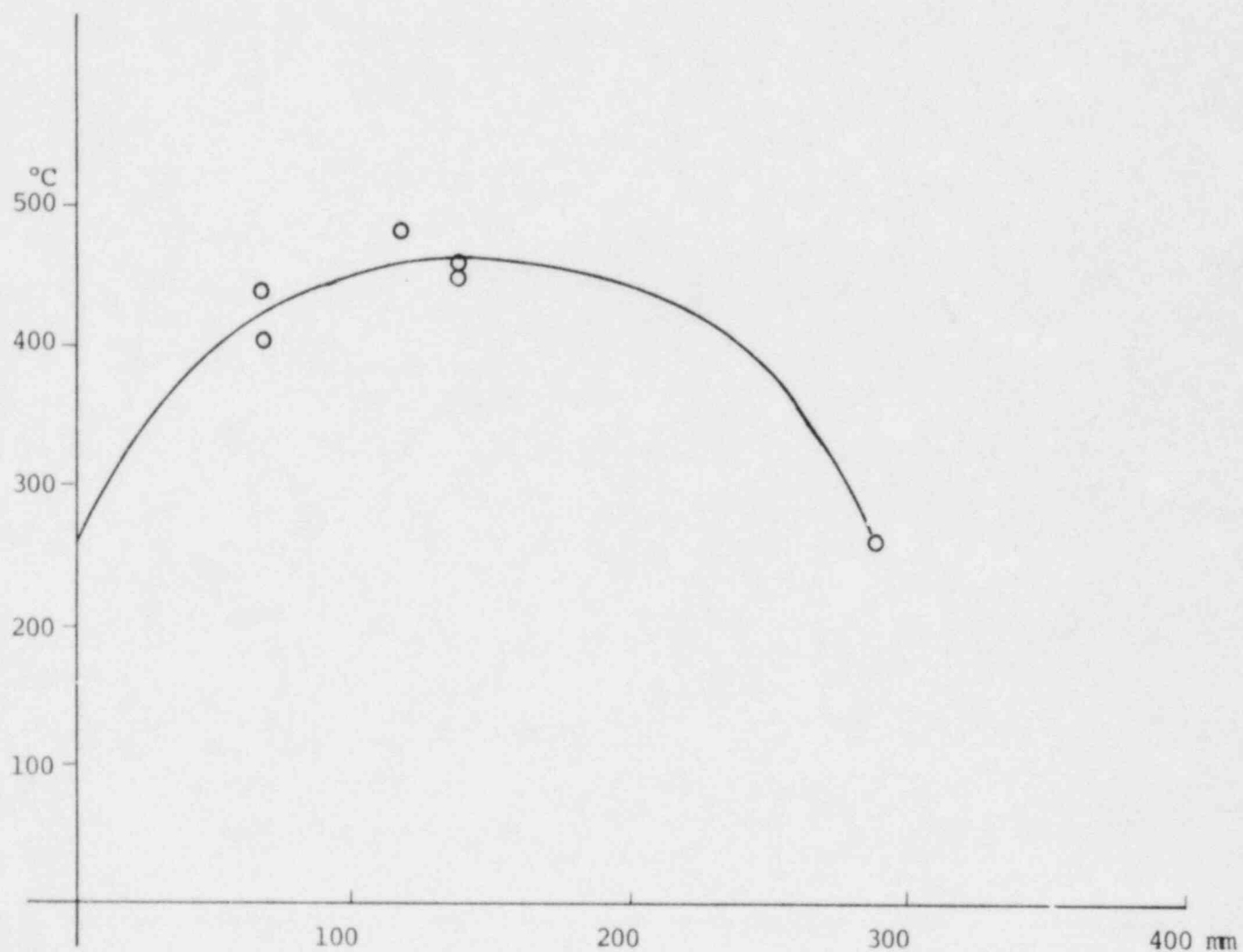
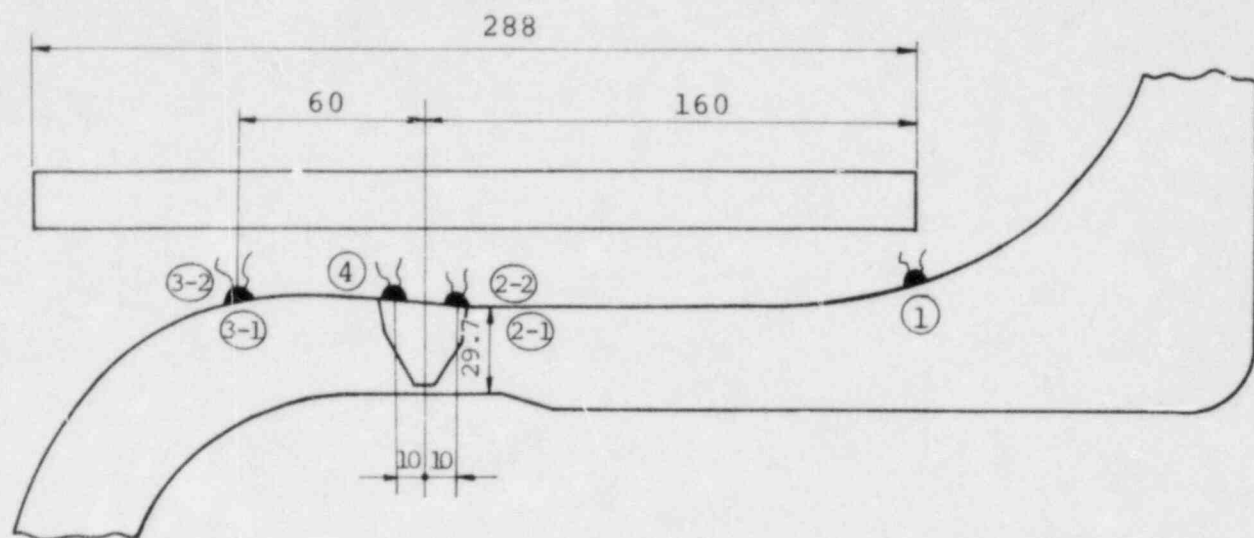


Fig. 7.4(a) (continued)

OCT. 10, 1978

WELDING JOINT NO.		PLR - 22 - B	ESSENTIAL VARIABLE	REQUIRED	MEASURED
MATERIAL		SA403 + SA376 WFW304 TP304 (PB + PB)	COIL WIDTH $L/\sqrt{RT} \geq 3.8$	$\geq 345\text{mm}$	380mm
TEMP. ON OUTER SURFACE		355 °C at (2-1)	HEATING TIME $at/T^2 \geq 0.8$	$\geq 146\text{S}$	243S
ROOM TEMPERATURE		25 °C	DIF. OF TEMP. $\Delta T \geq \frac{4(1-\nu)}{E\alpha}$	$\geq 227^\circ\text{C}$	288°C
COOLING WATER	TEMP.	37 °C	MAX. TEMP. ON OUTER SURFACE	$550^\circ\text{C} \geq$	542°C
	VELOCITY	3.27 m/s	LOCATION OF ℓ_{MAX} COIL $(T/2, 15\text{mm})$	$>15\text{mm}$	42mm

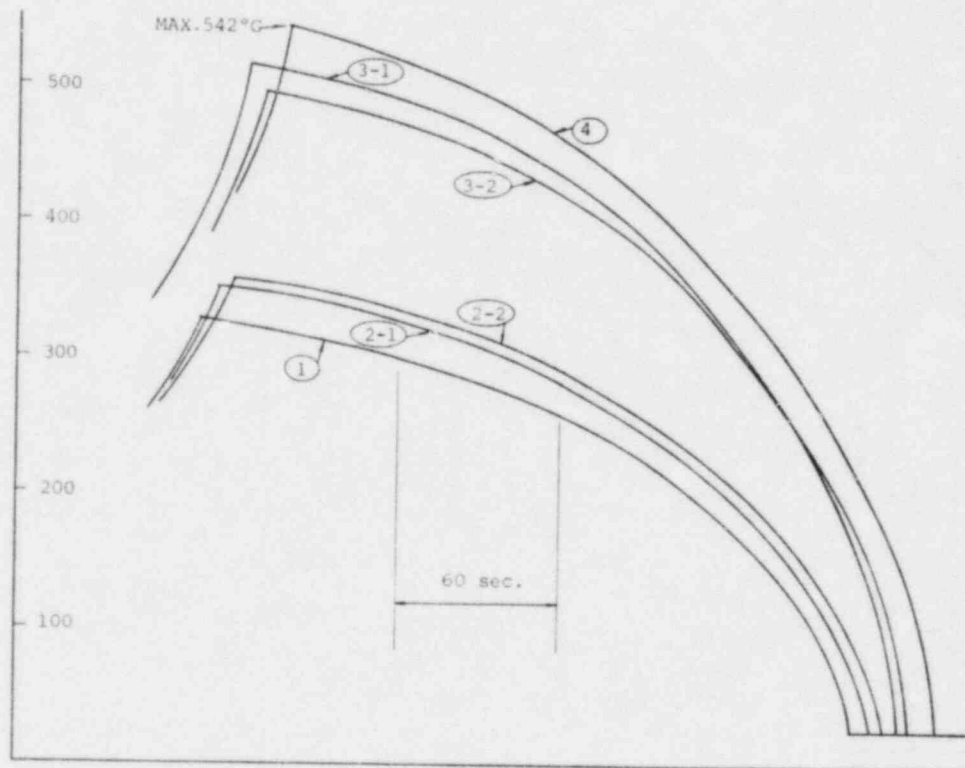
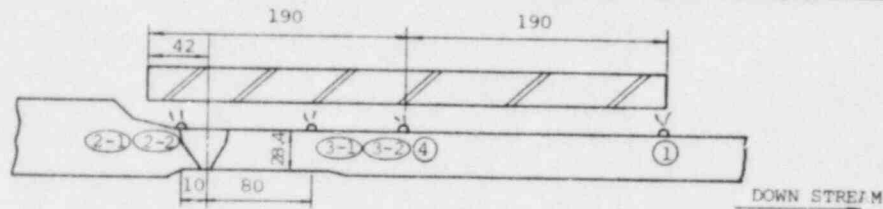


Fig. 7.4(b) Record of Field Application of Induction Heating Stress Improvement

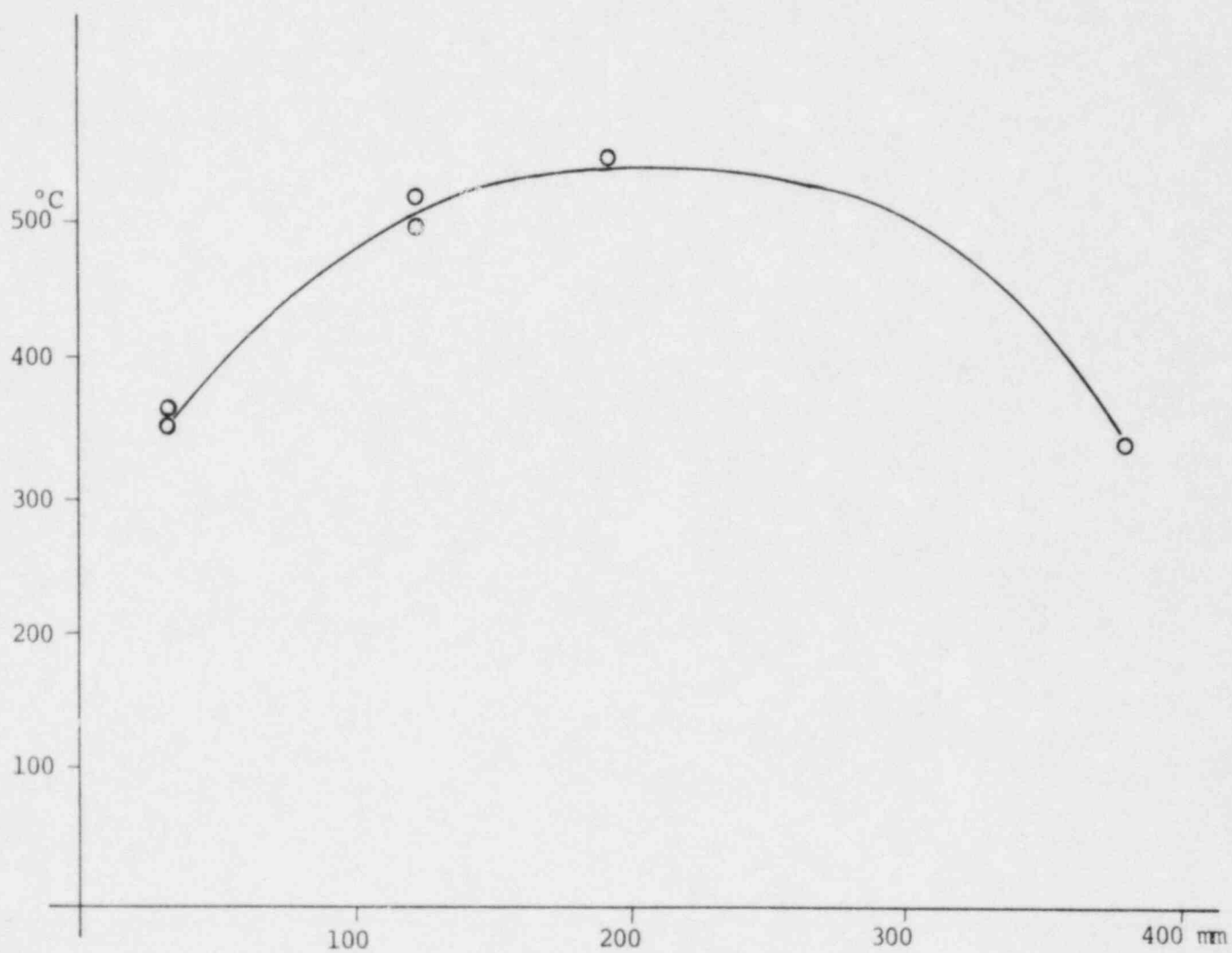
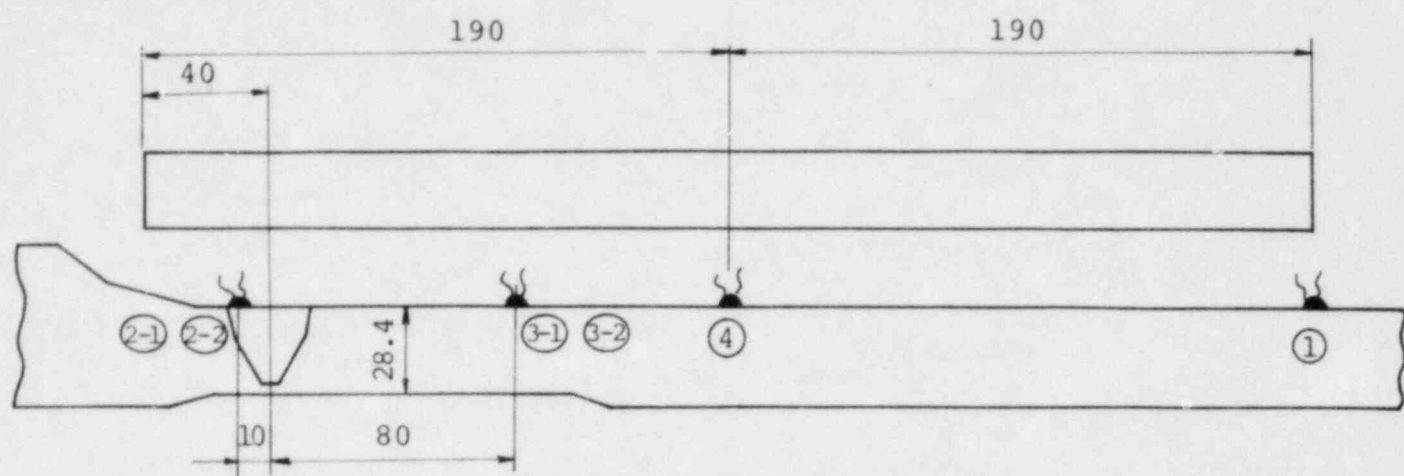


Fig. 7.4(b) (continued)

7.4.1 Preparation

Preparation is performed to check that the following items will be in the controlled range or have a suitable value.

1. Planning
 - a. Coil width
 - b. Power (equipment capacity)
2. Preparation for heating
 - a. Coil setting
 - b. Thermocouple location to check the outer surface temperature
 - c. Cooling condition (water temperature, water velocity)

7.4.2 Trial Heating

A trial heating is performed to check the following items below a maximum temperature of 280°C.

1. Suitability of power source
2. Adequate temperature difference in the controlled range
3. Heating duration in the controlled range

7.4.3 Actual Heating

After confirmation by the trial heating process, the actual IHSI heating to 550°C is performed.

7.4.4 Results and Evaluation

When the actual heating is performed, the results will have to be checked and evaluated. The following three key parameters are to be evaluated.

1. Heating duration
2. Temperature difference, which is calculated by estimating the inner surface temperature
3. Maximum temperature at outer surface and temperature distribution in the axial direction, which is made graphically to confirm that a good residual stress distribution is generated.

Section 8

PIPES WITH SMALL PRECRACKS

8.1 OBJECTIVE

When applying IHSI to an operating plant, there is concern that a small crack may be present which is undetectable by inservice inspection using ultrasonic examination techniques. In order to apply IHSI to an operating plant, it must be demonstrated that the residual stresses are improved and that detrimental effects are not produced by IHSI even in the presence of small flaws.

In this section, the effectiveness of IHSI is examined experimentally and analytically for the situation in which small indications may exist.

8.2 TEST DETAILS AND TEST RESULTS

A test was performed to confirm that the residual stress at the inner surface is improved by IHSI even if small cracks exist. Here we assume that a small indication is identical to a small crack. The test sequence is shown below.

1. 4-inch pipe is girth welded
2. Precrack formed by electron discharge machining
- 3a. IHSI treatment
- 3b. No treatment
- 4a. Immersion in boiling 42% $MgCl_2$ solution
- 4b. Immersion and dye penetrant examination

NOTE: The depth of the precrack was chosen as 25% of the wall thickness. This crack depth is nearly twice that of the calibration notch of the ultrasonic test standard specimen. This depth is large enough to be detected by the ultrasonic test, so this assumption appears to be very conservative.

Figure 8.1 presents the results of the $MgCl_2$ cracking test on the precracked pipe with and without IHSI. As shown in the figure no stress corrosion cracks were observed after the immersion of the test pipe into $MgCl_2$ solution after IHSI treatment, but many cracks were observed on the test pipe without IHSI.

Figure 8.1 also shows the stress corrosion cracks initiated at the artificial notch in the horizontal direction. Figure 8.2 and Figure 8.3 show the section of the artificial notch after the $MgCl_2$ test. The artificial notch was sectioned at the center of the notch length. No cracks were observed with IHSI, but several cracks have propagated in the depth direction at the notch tip of the test pipe without IHSI.

8.3 COMPUTER CALCULATIONS FOR PRECRACKED PIPES

Assuming the existence of a small crack at the inner surface of a pipe, finite-element method calculations using the program ITEMP II, IEPTC II were performed to investigate the inelastic behavior of the crack under transient loading during the IHSI treatment. The analytical model is shown below.

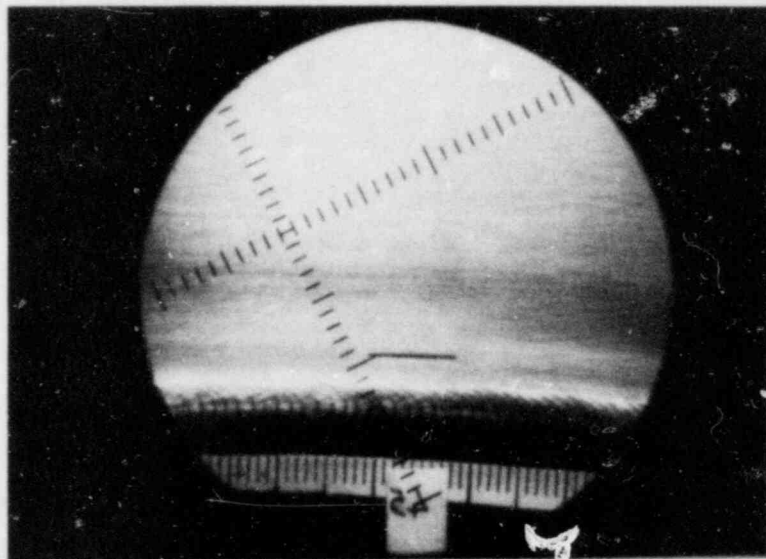
Case No.	Pipe Size		Crack Shape			Analytical Models
	Nominal Size	Outer Diameter (mm)	Thickness (mm)	Depth (mm)	Direction	
1	12-inch Sch. 100	318.5	19	1.4	Circumferential Crack	Axisymm.
2	"	"	"	2.4	"	"
3	"	"	"	4.2	"	"

In the above analyses, three different crack depths were selected. One was 2.4 mm (12.5% of pipe thickness) and another was about 1.2 mm and the third was about 4.8 mm. The 12.5% deep crack corresponds to the reference hole diameter of an ultrasonic test standard specimen.

Figure 8.4 presents the residual stress distribution for the axial stress near the tip of each crack following IHSI treatment. The residual stresses showed the minimum value near the crack tip and became gradually deeper as the crack depth increased.

(a) EDM

(EDM: ELECTRIC
DISCHARGE
MACHINING)



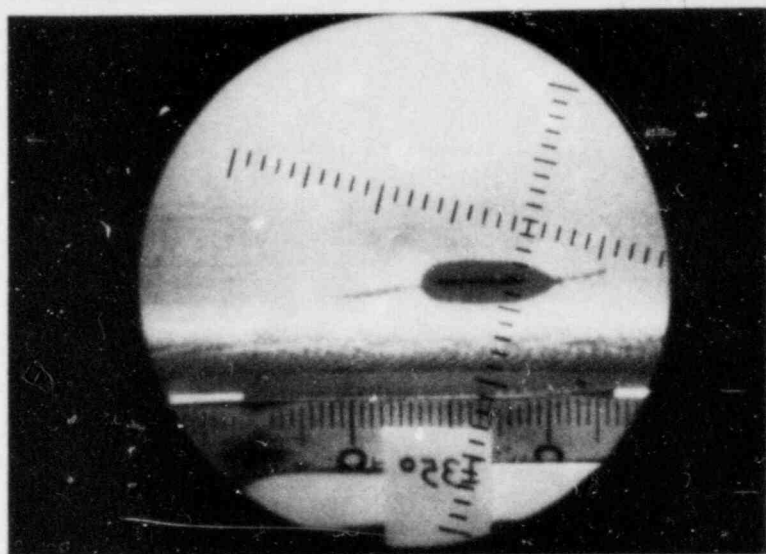
(b) EDM



MgCl₂



Propagation



(c) EDM



IHSI



MgCl₂



No Propagation

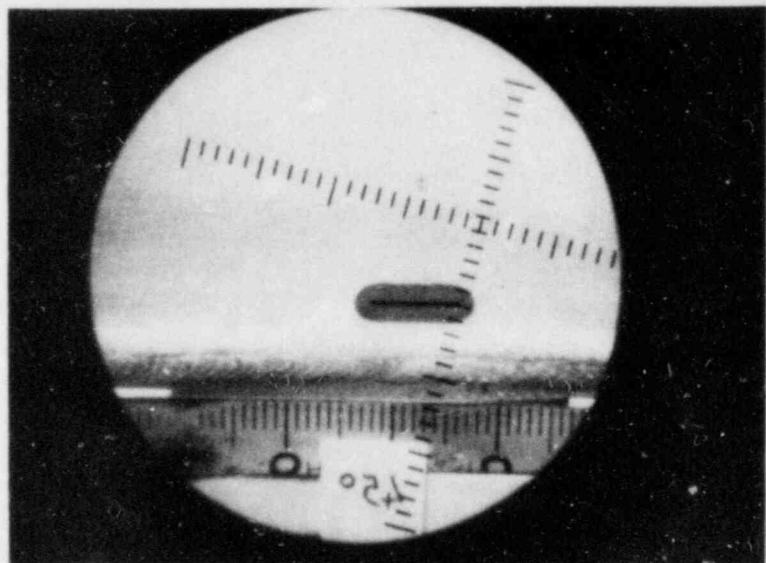
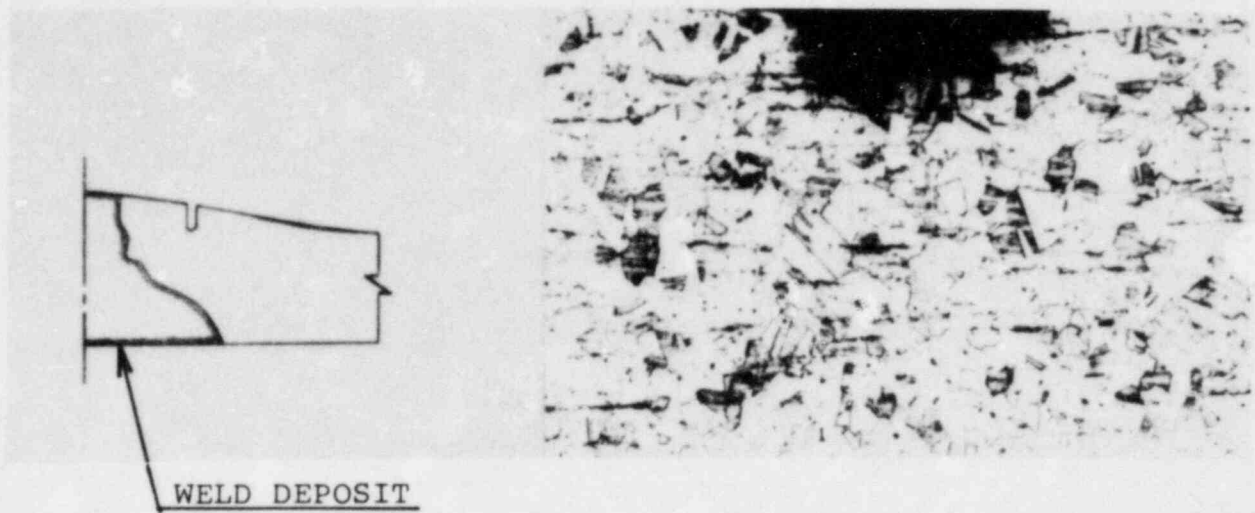
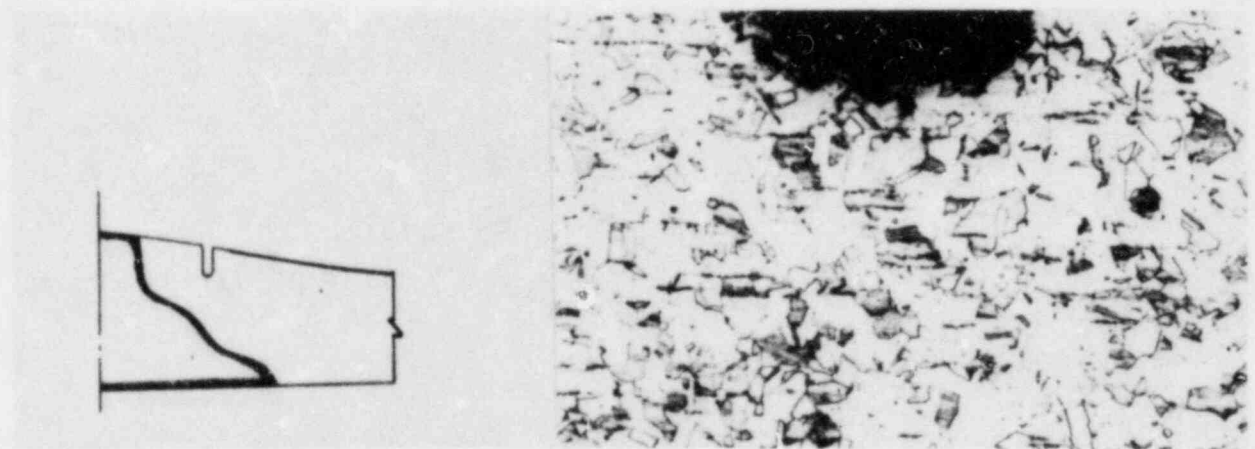


Fig. 8.1 Propagation Behavior of Notch



R-53 45°



R-53 225°

FIG. 8.2 CRACKING OBSERVATION AT NOTCH TIP (R-53)
MAG x 100

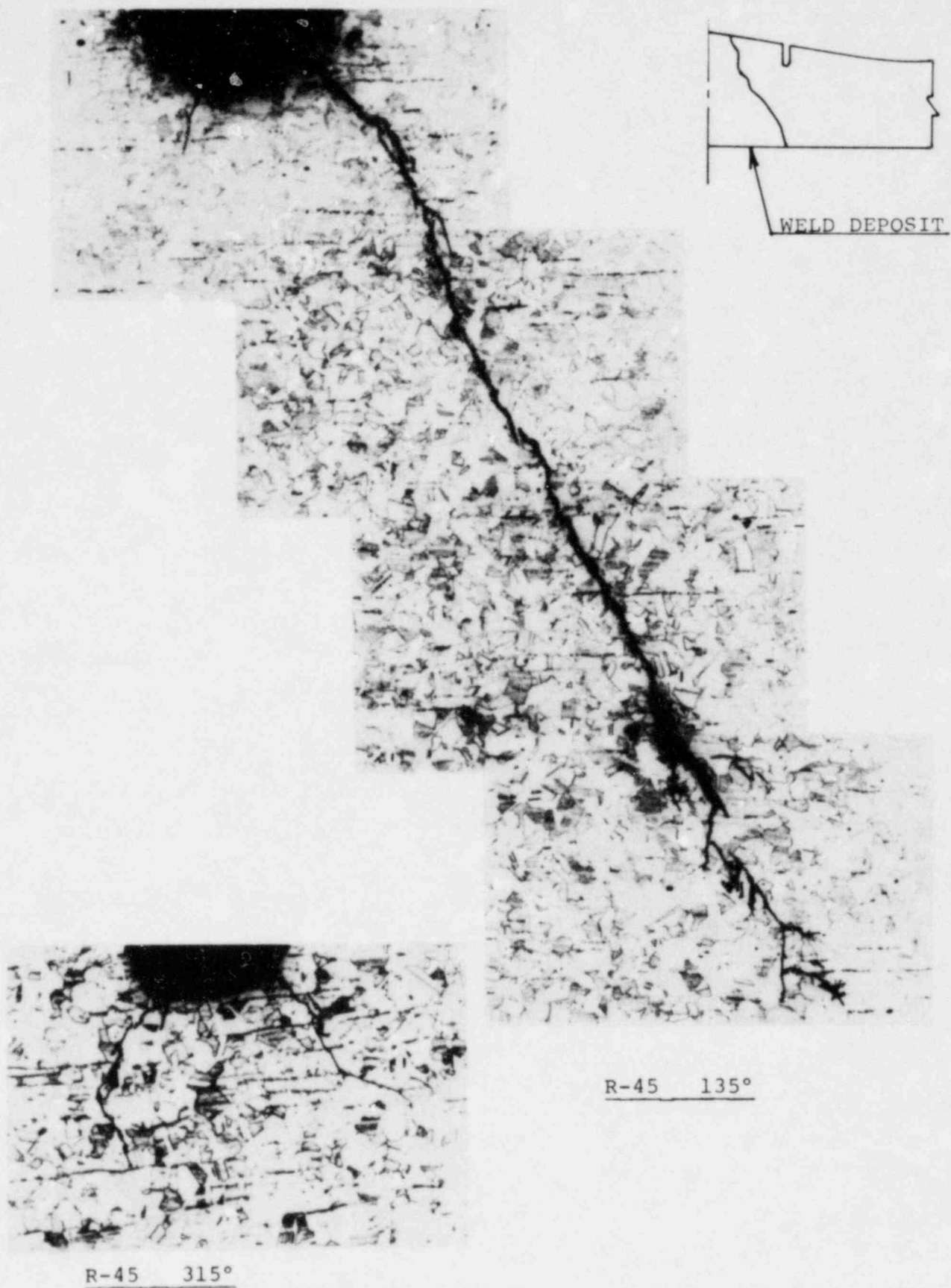


FIG. 8.3 CRACKING OBSERVATION AT NOTCH TIP (R-45)
MAG. x 100

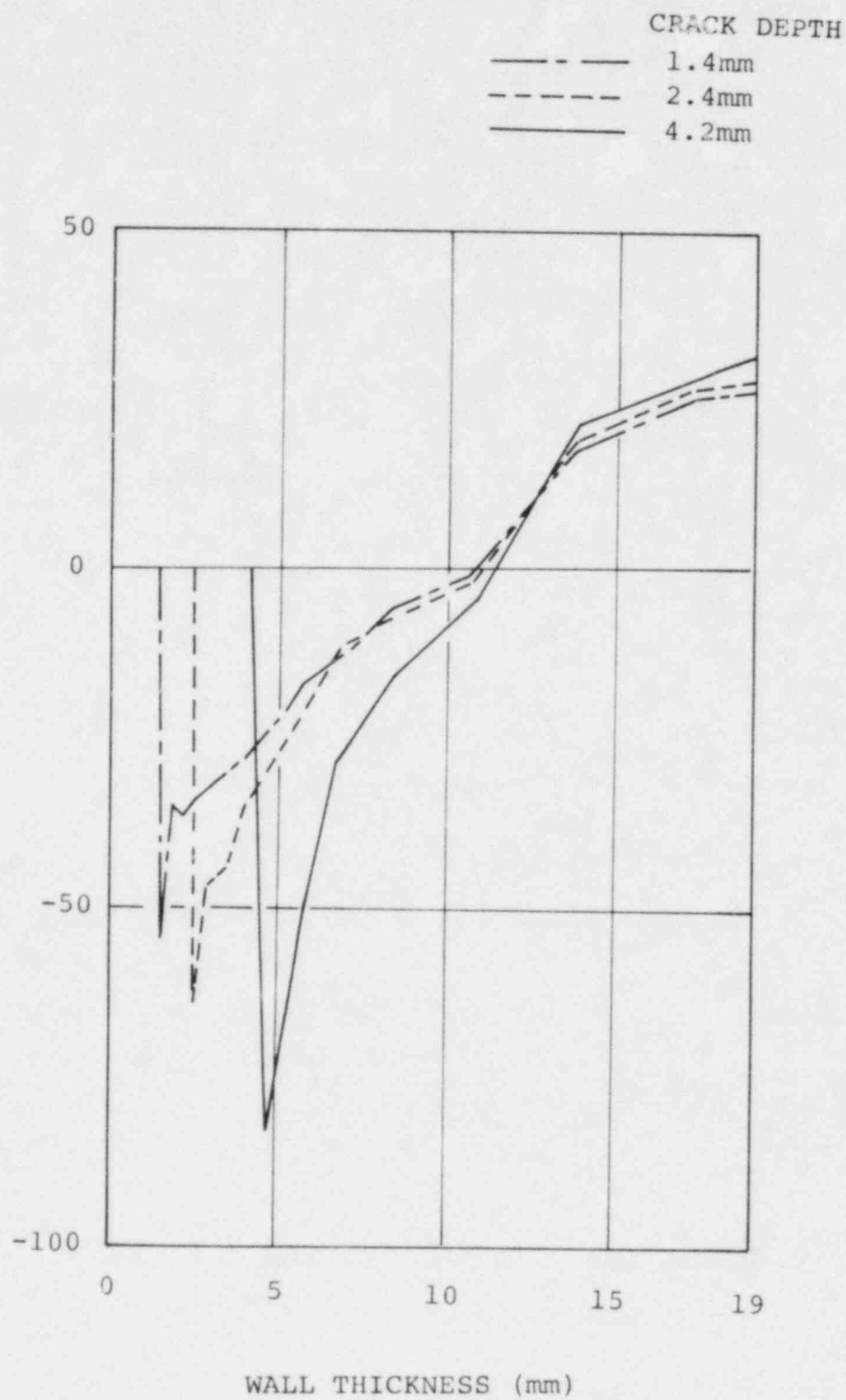


FIG. 8.4 CALCULATED RESIDUAL STRESS THROUGH THE THICKNESS OF 12 IN. PIPE WITH A FLAW

Figure 8.5 shows calculated COD (crack opening displacement) at the maximum heating condition during IHSI. As shown in the figure, the COD increases as the initial crack depth increases.

In order to maintain pipe integrity during IHSI for the pipe with an initial crack, it is necessary that crack extension does not occur. To determine the critical CTOD (crack tip opening displacement) for Type 304 stainless steel, a three point bend test was conducted. The test piece was 20 mm in height and 10 mm in width. The bending span was 80 mm. The crack depth was 2.4 mm and 4.8 mm. Figure 8.6 shows the relationship between COD, CTOD, and the deflection of the test piece. The observed CTODs are shown to be of similar value for the two crack sizes. The critical CTODs were about 1.22 mm and 1.30 mm for the crack depths of 2.4 mm and 4.8 mm respectively.

8.4 EVALUATION

The cracking test in 42% $MgCl_2$ solution and finite-element calculations showed that IHSI can improve the residual stresses at the crack tip as well as on the pipe inner surface even if there is an initial circumferential crack.

From the finite-element calculation, CTOD at maximum temperature during IHSI is about 30×10^{-3} mm for 2.4 mm crack depth. On the other hand, the critical CTOD is about 1.22 mm for 2.4 mm crack depth. From reference (1), the critical CTOD is about 3 mm. It is clear from the comparison of these CTODs that the safety factor is quite adequate.

In reference (2), an interesting calculation is described. The purpose of the calculation was to determine if with the presence of a small crack at the inner surface of a pipe, IHSI could be applied without detrimental effects and if under the operating conditions compressive residual stresses existed in the vicinity of the crack tip.

-
- References: (1) Mechanical Fracture Predictions for Sensitized Stainless Steel Piping with Circumferential Cracks, Section 4, EPRI NP-192 Sept. 1976.
- (2) G. Yagawa, et. al., EPAS Finite-Element Program for Analysis of Nonlinear Behavior of Nuclear Power Piping, 5th SMIRT, MblK, 1979.

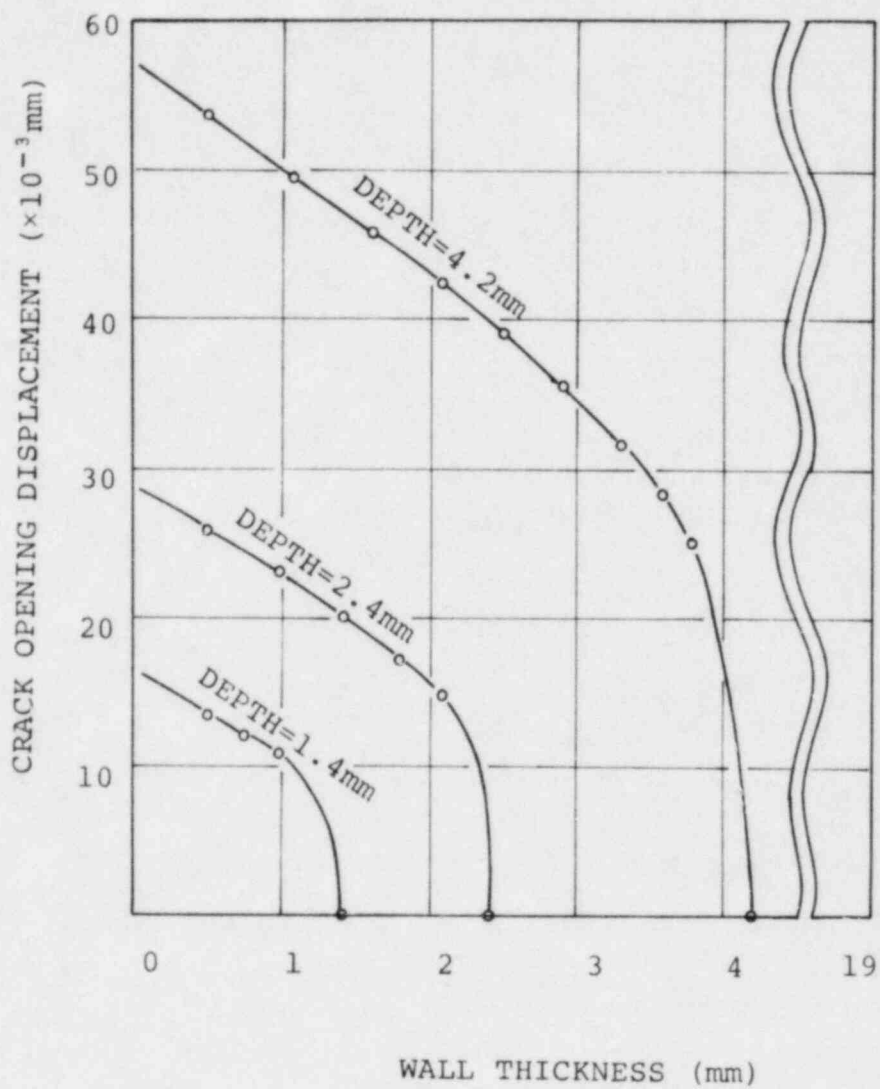


FIG. 8.5 CALCULATED COD AT MAXIMUM HEATING

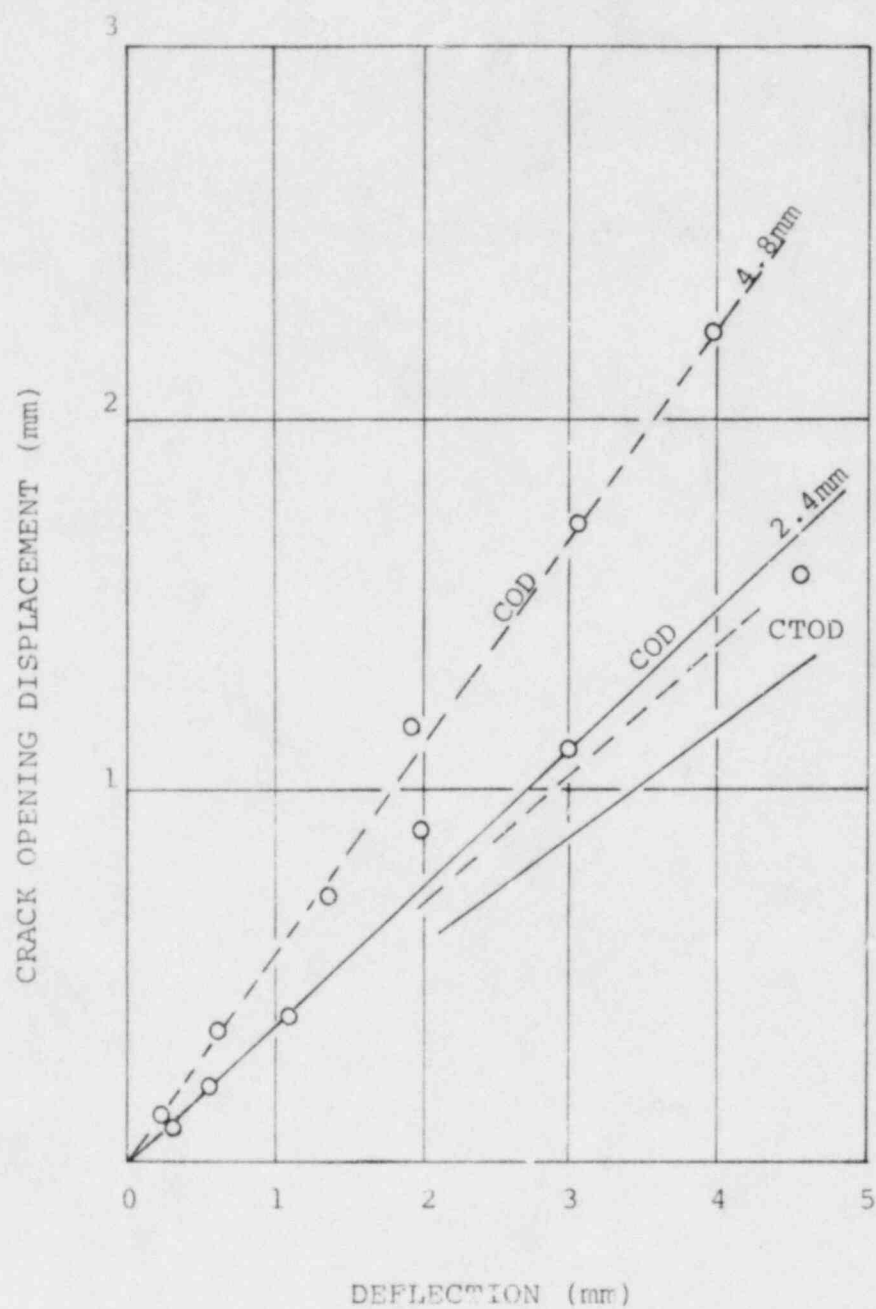


FIG. 8.6 RELATION OF COD AND CTOD TO DEFLECTION IN THREE POINT BEND TEST

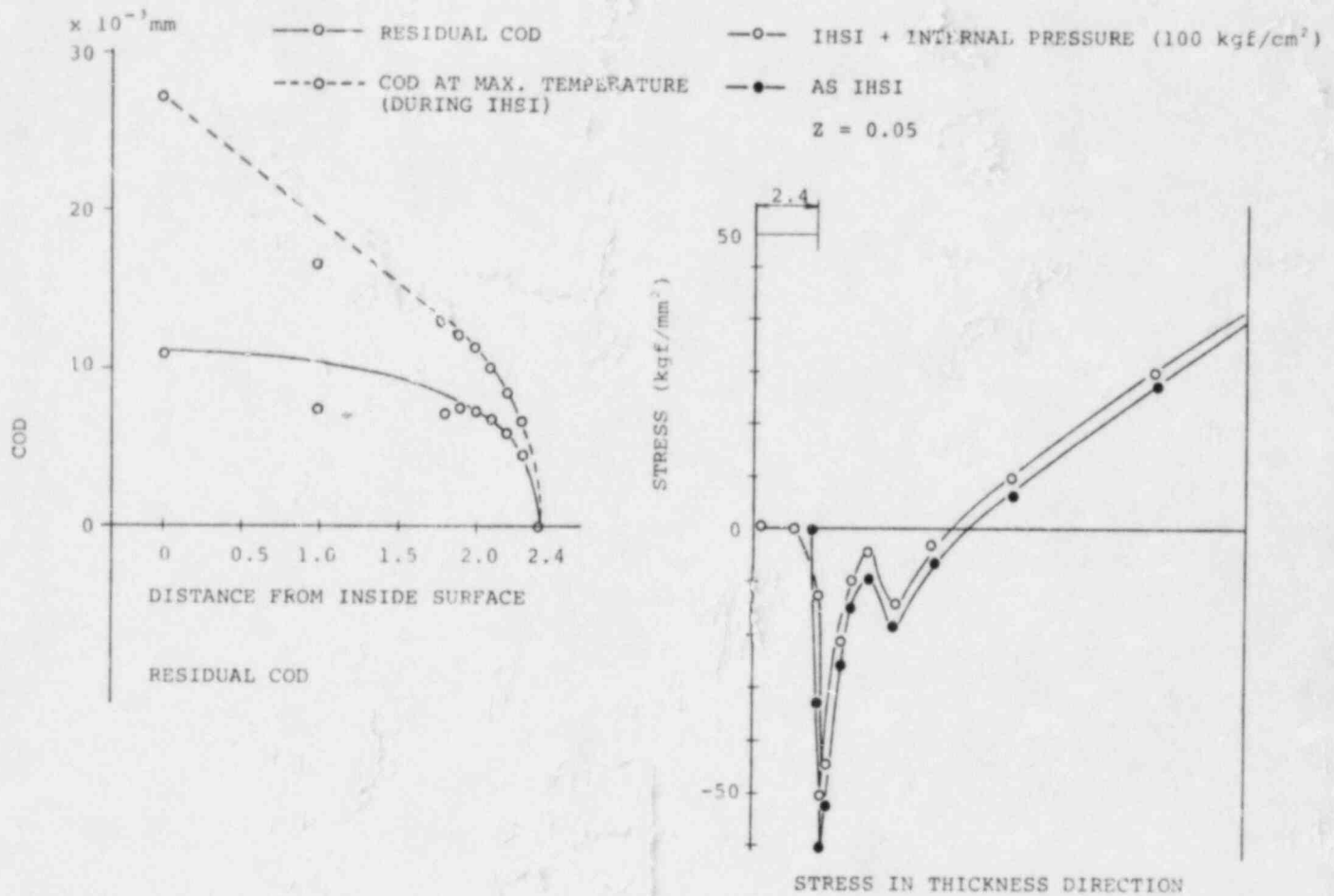


Fig. 8.7 COD AND STRESS DISTRIBUTION

Section 9

RELAXATION

9.1 RELAXATION AT OPERATING TEMPERATURES

There is concern that the residual stresses induced by IHSI may relax during long service at high temperature, but little data exist which can be used to estimate the relaxation behavior at temperatures near 300°C.

A test was conducted to determine the relaxation behavior of residual stresses due to heat treatments at 300°C, 400°C and 500°C for 24 hours following an IHSI treatment. Figure 9.1 shows the experimental results comparing these heat treatment conditions to an IHSI treated condition.

No apparent difference was observed among these data, showing that the residual stresses will not disappear or change due to service temperatures.

9.2 RELAXATION RESULTING FROM APPLIED AXIAL STRESS

It is well known that residual stresses are relieved by overstressing. This situation is illustrated for pipe after IHSI using the two-element model presented in Figure 9.2.

The pipe is assumed to be composed of two elements A and B which have tensile and compressive residual stress respectively. The stress and strain relationships of A and B are shown in Figure 9.2(b). Curve "C" shows the relationship of composite material (A + B).

When the pipe is strained to less than point 1 and then unloaded, the strain will recover entirely and no residual strain will remain. If the pipe, however, is strained beyond point 1, such as to point 2, the permanent strain ϵ remains after unloading. In this case the residual stress is relaxed to point 4. Using this diagram, the remaining residual stress after removing axial stress is plotted

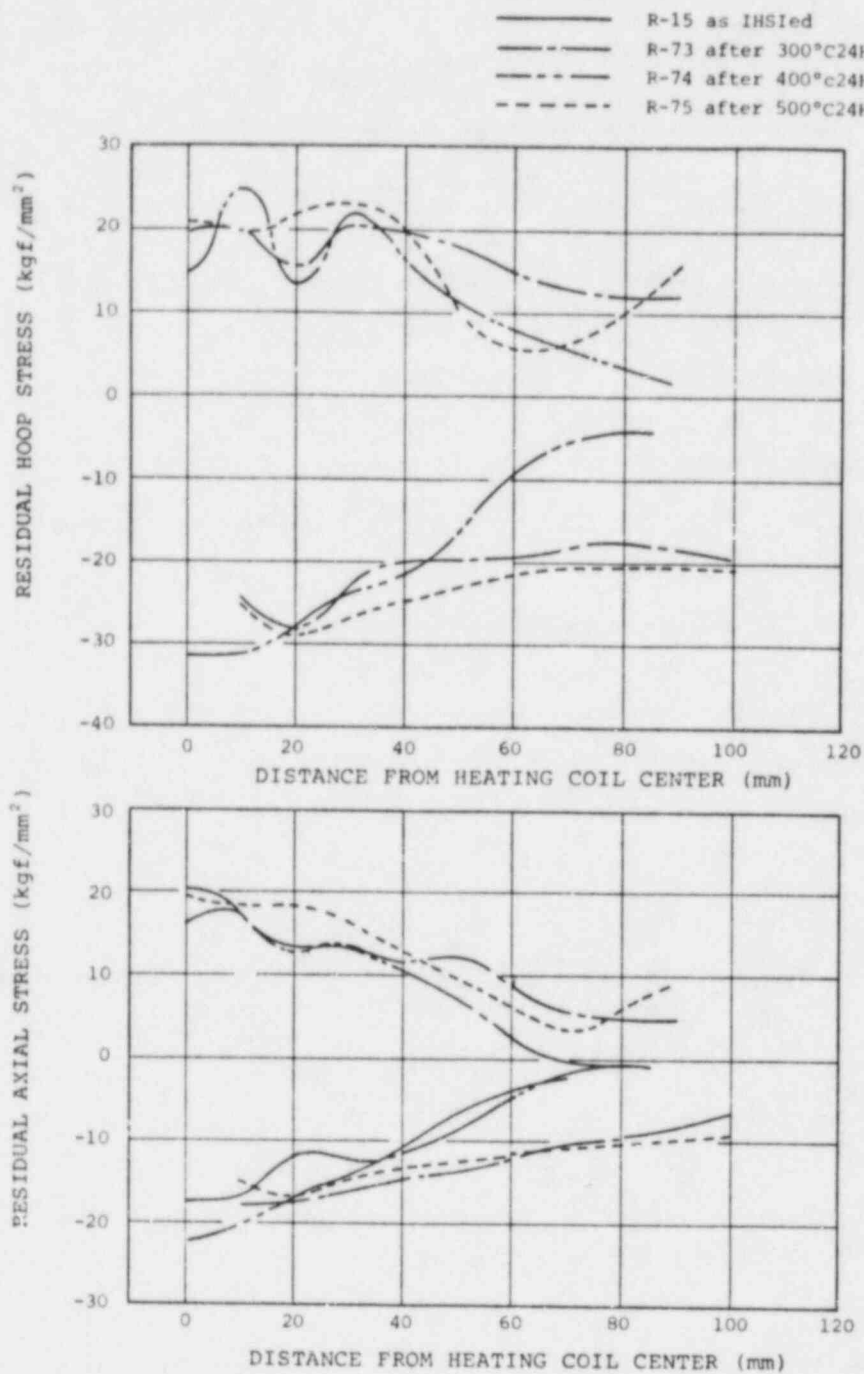
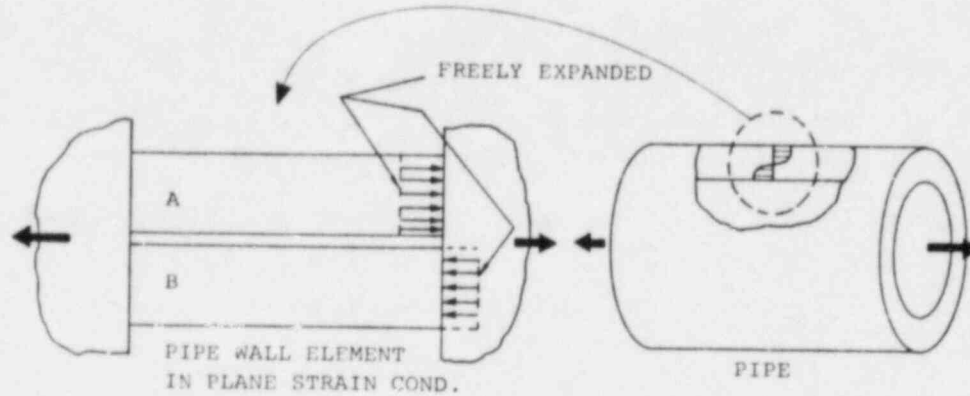
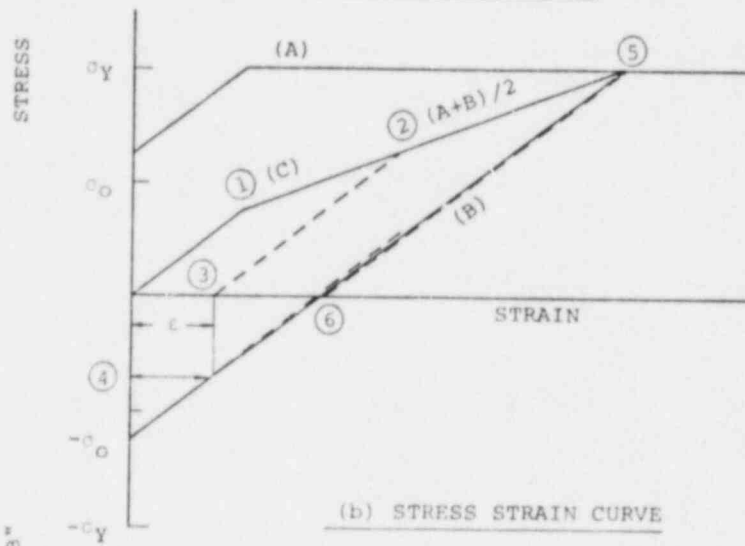


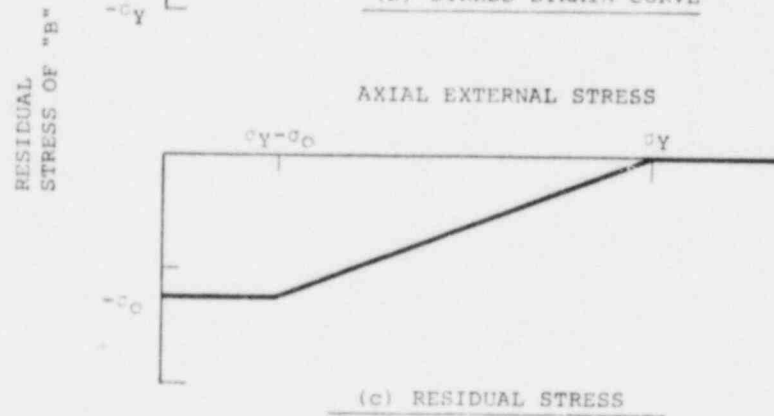
Fig. 9.1 Residual Stress Distribution Comparing Three Heat Treatment Conditions to an As IHSIed Pipe



(a) TWO ELEMENT MODEL



(b) STRESS STRAIN CURVE



(c) RESIDUAL STRESS

Fig. 9.2 RESIDUAL STRESS ANALYSIS BY TWO ELEMENT MODEL

versus axial stress in Figure 9.2(c). The results show that the residual stress is gradually reduced to zero as the external stress increases.

Figure 9.3 shows a load-strain relationship measured on the inside surface of a 14-inch, welded pipe at room temperature.⁽¹⁾ The area very close to the weld exhibited lower strain than the base metal; that is, the stress-strain behavior of the material near a girth weld was very different than that of the base metal. This suggests that stress relaxation of such a region near a weld will be different and possibly smaller than in the base material.

Testing to confirm the above mentioned hypothesis is now in progress.

Reference: (1) P198, JWES-AE-7807, Japan Welding Engineering Society, Nov. 1978.

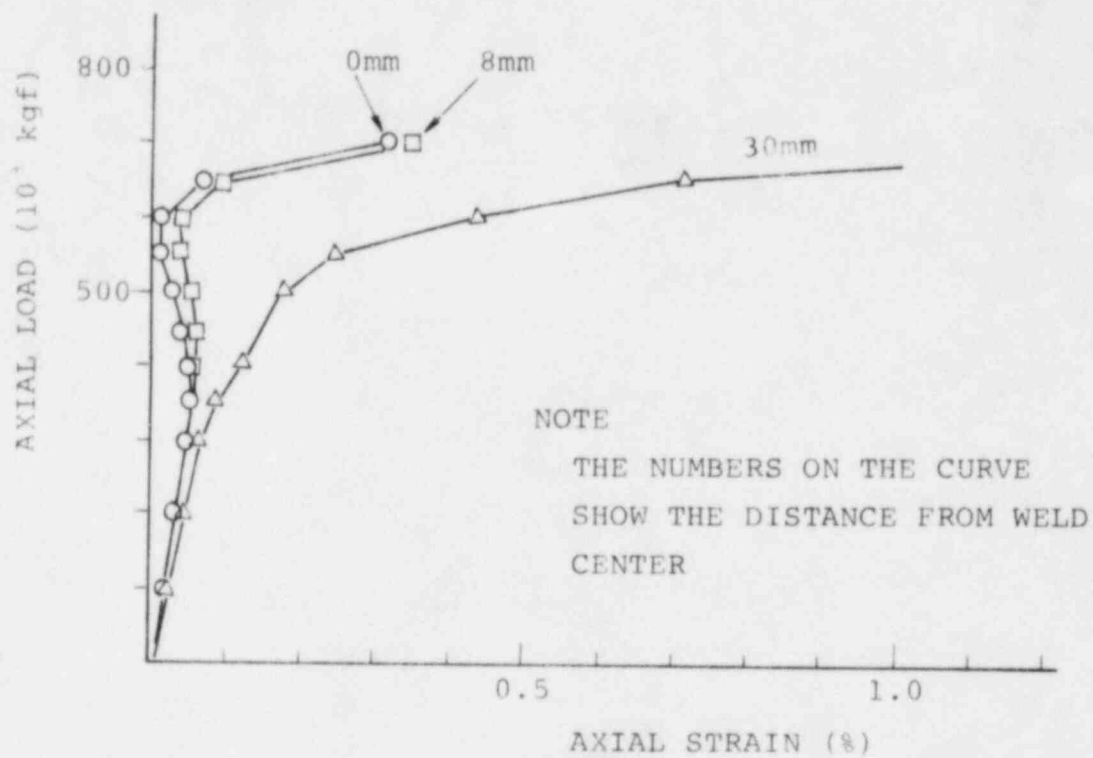


FIG. 9.3 LOAD-STRAIN CURVE OF WELDED 14 IN PIPE
(EXPERIMENT)

Section 10

CONCLUSIONS

Many basic experiments, full size mock-up tests and elastic-plastic finite element calculations were conducted to evaluate the IHSI process and the results lead to the following conclusions.

1. Key parameters which have significant effect on IHSI are:
 - a. Temperature difference between pipe outside and inside surfaces
 - b. Heating duration
 - c. Coil width
 - d. Coil location in relation to weld seam
 - e. Maximum heating temperature
2. A simple method to predict coil input power and pipe inside surface temperature was developed and has made IHSI a simple and reliable technique.
3. IHSI is valid not only for smooth pipes but also for pipes having preflaws which are not detected by NDE.
4. The beneficial residual stress effects of IHSI (imposed compressive residual stress) will not disappear during normal plant operation.

A - 1

IMPROVEMENT OF RESIDUAL STRESS PATTERN

IN PIPE BY HIGH FREQUENCY INDUCTION HEATING

- PRELIMINARY TESTS -

Summary

Preliminary studies to improve the residual stress pattern were performed using the High Frequency Induction Heating Technique.

Three 4B Schedule 80 SS pipes, each having one circumferential weld joint, were tested. The following preliminary results were obtained:

High tensile residual stresses in the inside surface of pipe weldment can be reduced by High Frequency Induction Heating.

1. Introduction

This paper presents experimental results for the High Frequency Induction Heating (HFIH) treatment of weld joints of 4B Schedule 80 austenitic stainless steel pipe. The parameters evaluated in this study include:

- (1) Max. temperature
- (2) residual stress

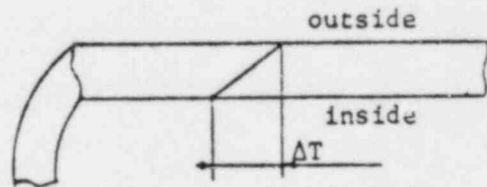
Post test metallography was performed on the induction heat treated samples.

The test matrix for this experiment is shown in Table -1.

2. Theoretical Considerations

A long circular pipe heated on its OD and cooled on ID will produce a radial temperature gradient and the maximum thermal elastic stress will be given by the following equation.

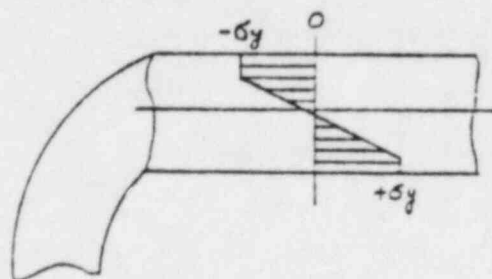
$$\sigma_{\max} = \frac{E\alpha \Delta T}{2(1-\nu)}$$



Where E ; Young's modulus
 α ; Coefficient of thermal expansion
 ΔT ; Temperature difference
 ν ; Poisson's ratio

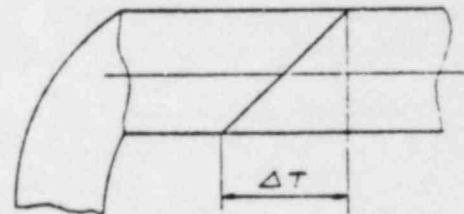
The stress is proportional to the temperature difference ΔT . When ΔT becomes greater than $2\sigma_y(1-\nu)/E\alpha$, σ_{\max} exceeds the yield strength and plastic flow will take place.

In this case, the axial stress is distributed as illustrated in the figure below.



σ_y ; Yield strength

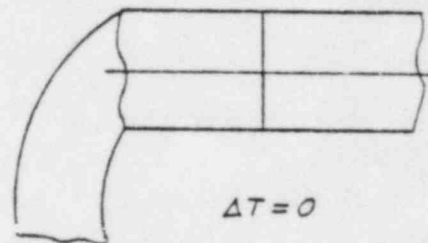
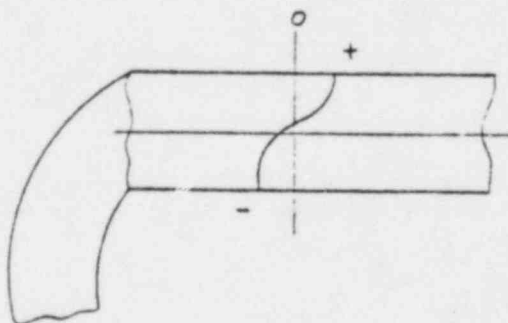
Stress distribution



$$\Delta T \frac{2\sigma_y(1 - \nu)}{E\alpha}$$

Temperature distribution

Terminating the heating and cooling process produces a uniform temperature distribution in the pipe. The thermal stress will be relieved, but some residual stresses will have been produced in the plastically deformed region of the pipe by the prior heating and cooling operation.



3. Experimental Approach

3.1 Material

Chemical composition and mechanical properties of Type 304 SS pipes are listed in Table-2.

3.2 Weld Edge Preparation

Joint geometry of the specimens is shown in Fig.-1.

3.3 Welding Conditions

Table-3 summarizes welding conditions and processes.

3.4 Thermocouples

Fig.-2 illustrates the location of the thermocouples on the pipe surface used to measure the temperature history during HFIH.

3.5 Heating and Cooling System

Equipment used for HFIH and cooling of the pipe inside surface are illustrated in Fig.-3.

3.6 Measurement of Heating and Cooling Cycles

Heating and cooling cycles were measured at the points shown in Fig.-2 and recorded using a pen recorder.

3.7 Measurement of Residual Stresses

The residual stress of pipes was measured by using strain gage and also checked by 42% boiling Magnesium Chloride Solution (MgCl_2).

3.8 Metallography

Each cross-section of the weld joint was etched in 10% oxalic acid solution and examined by conventional light microscopy.

4. Results and Discussions

4.1 Maximum temperature

The distribution of the maximum temperature produced by HFIH is plotted in Fig. -4.

4.2 Residual Stresses Profile and Crack Pattern

Fig.-5 and Fig.-6 present the effect of HFIH on the residual stress profile of 4B SS pipe inside surface.

High tensile residual stresses on the pipe surface are observed to be reduced by HFIH.

Photo No-1 and 2 show the cracking pattern of 4B SS pipe treated in 42% boiling $MgCl_2$ solution.

No cracking was observed on the ID of the pipe with HFIH while many cracks were observed on the ID of the pipe without HFIH.

4.3 Metallography

Photo No-3 shows the microstructure of the 4B SS pipe weld joints treated with HFIH.

No significant microstructural effects are observed since the maximum temperature is lower than 550°C.

5. Conclusion

Residual stresses at the inner surface of a 4B SS pipe can be improved by HFIH.

No significant microstructural effects are observed for the 4B SS pipe when HFIH is applied.

TABLE-1 HFIH^{*1} TEST MATRIX (PRELIMINARY TEST)

TP-No.	MT'L CERTIFICATE PIPE SIZE (MILL WORK NO.)	H.F.I.H. CONDITION *2 AFTER PIPE JOINT WELD			MAX. TEMP. IN BEAD CENTER (°C)			ITEM OF ANALYSIS			
		KW	A	V	OD	ID	ΔT (OD-ID)	*3 TTD	RESIDUAL STRESS		MICRO
									STRAIN GAGE	Mgcl ₂ AND MACRO	
R-1B	4B SCH.80 SUS304TP (TTC-5618)	72	155	540	540	168	372	○	/	○	/
R-2					536	170	366	○	○	/	○
R-3		42	120	400	340	88	252	○	○	/	○
R-4A		/	/	/	/	/	/	/	/	○	/

NOTE

- *1 WELDING CONDITIONS PRIOR TO H.F.I.H. ARE SHOWN IN TABLE-3.
- *2 DETAILS OF H.F.I.H. CONDITIONS ARE ILLUSTRATED IN TABLE-4.
- *3 TTD (TIME-TEMPERATURE-DISTANCE CURVE)

TABLE-2 CHEMICAL COMPOSITIONS AND MECHANICAL PROPERTIES OF BASE MATERIALS

MATERIAL	MILL WORK NO.	CHEMICAL COMPOSITION (Wt %)							MECHANICAL PROPERTIES		
		C	Si	Mn	P	S	Ni	Cr	Y.S ² (kg/mm ²)	T.S ² (kg/mm ²)	El (%)
4B SCH.80 SUS304TP	TTC5618	0.05	0.58	1.71	0.023	0.007	9.2	19	24	57	70

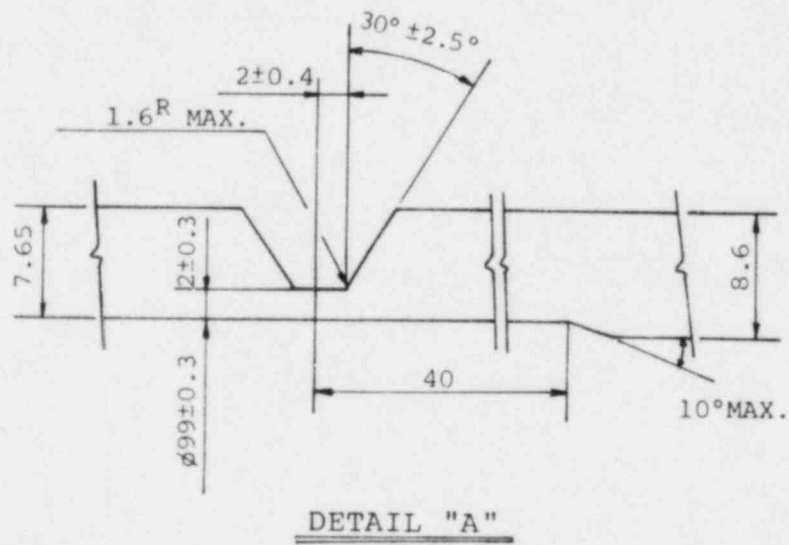
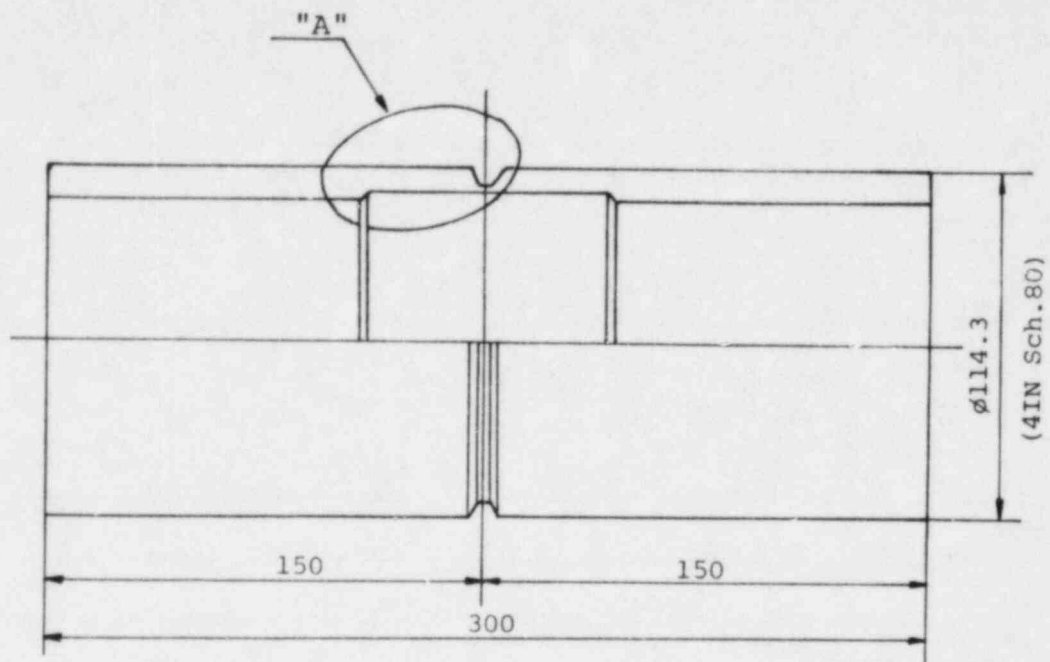


FIG-1 CONFIGURATION OF WELD PREPARATION

TABLE-3 WELDING CONDITION

TP-NO.	PROCESS	POSITION	HEAT INPUT (KJ/cm)	AVERAGE	COOLING METHOD
R-1B	GTAW (A)	1G	9.9 ~ 10.7 (1P ~ 3P) 21.6, 24.1 (4P, 5P)	10.2 22.9	NATURAL
R-2			9.9 ~ 10.9 (1P ~ 3P) 23, 23.7 (4P, 5P)	10.2 23.4	
R-3			9.7 ~ 11.3 (1P ~ 3P) 22.7, 23.6 (4P, 5P)	10.3 23.2	
R-4A			9.6 ~ 10.5 (1P ~ 3P) 23.5, 24.7 (4P, 5P)	10 24.1	

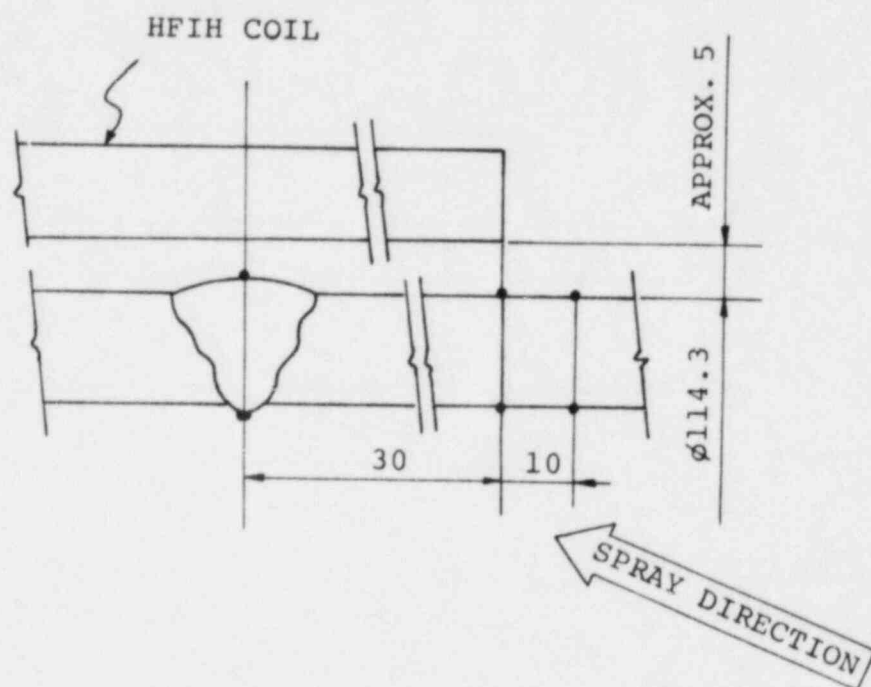


Fig. 2 LOCATION OF THERMOCOUPLES

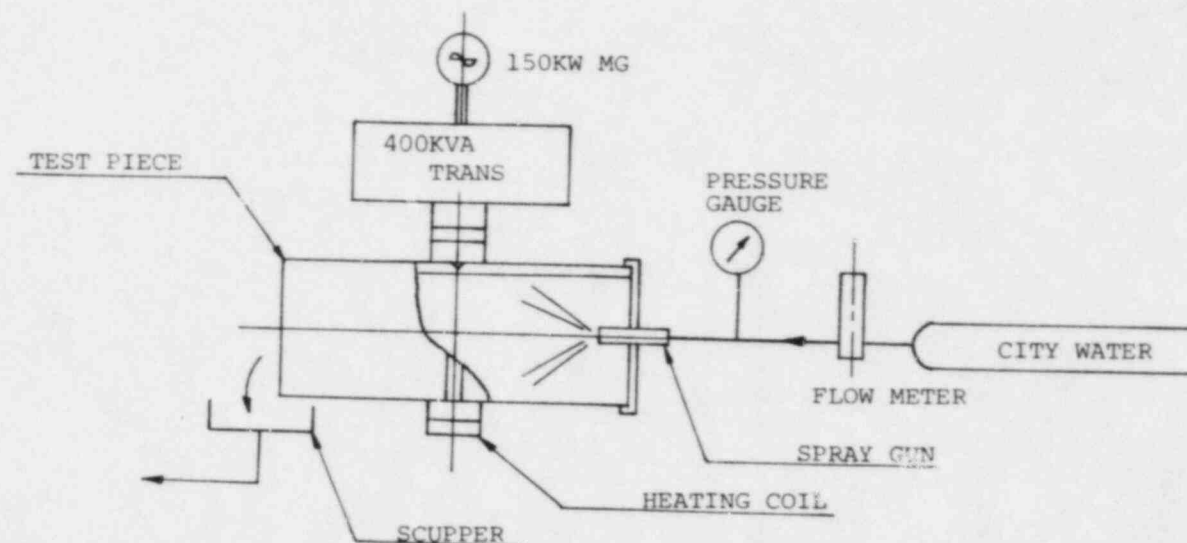


FIG-3 HEATING AND COOLING EQUIPMENTS

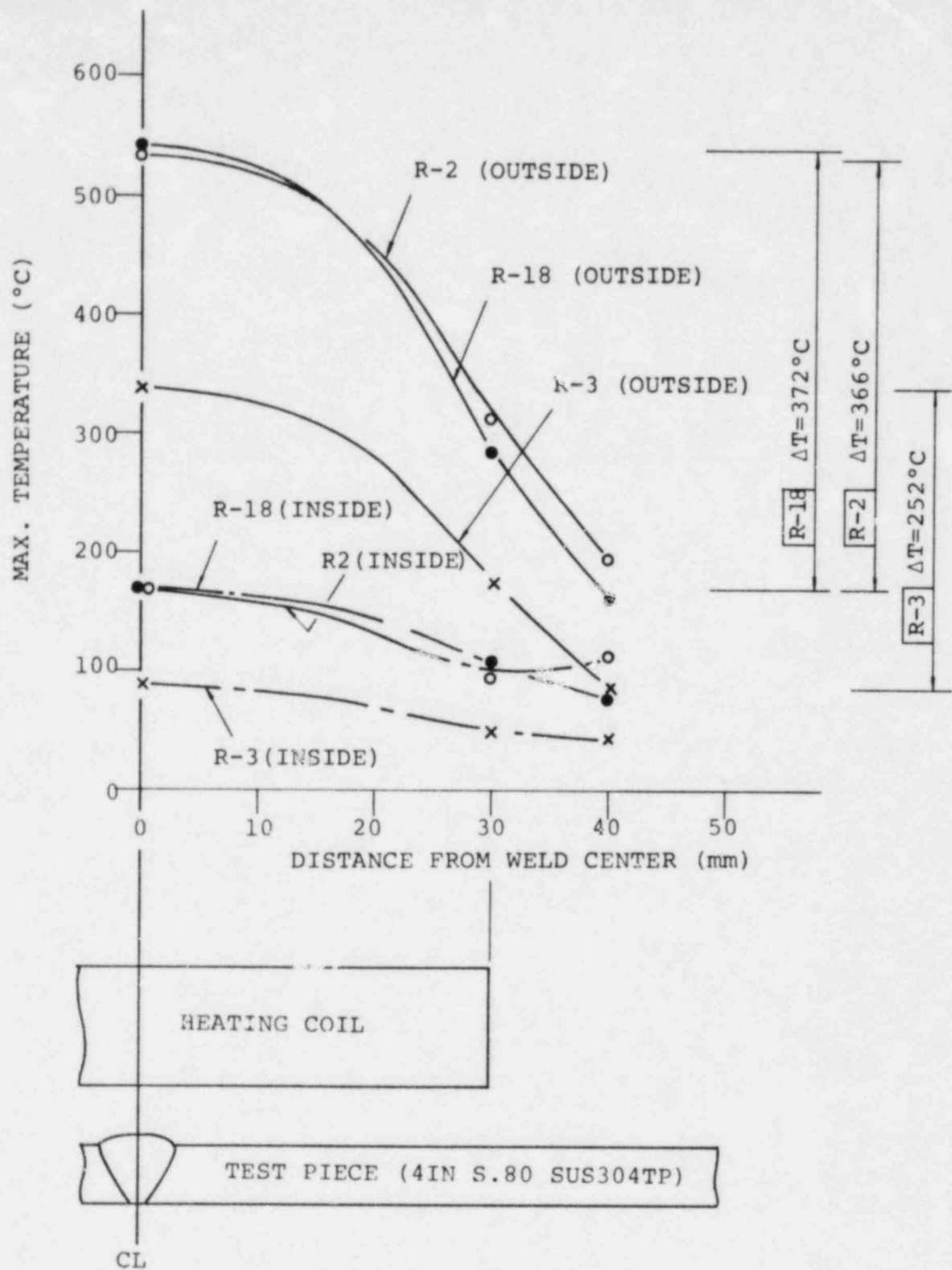


Fig. 4 Distribution of Maximum Temperature Produced by HFIH

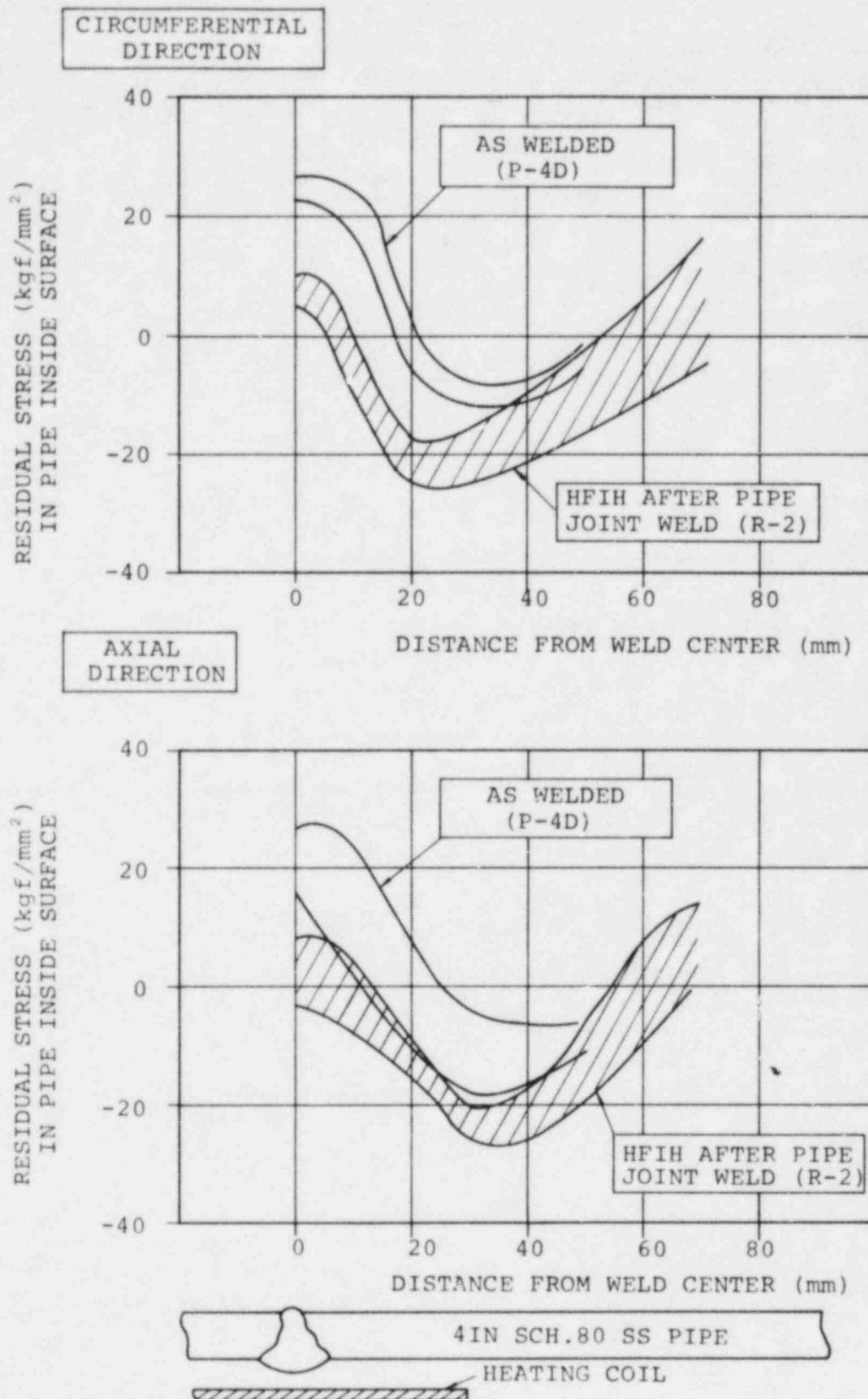


Fig. 5 EFFECT OF HFIH ON RESIDUAL STRESS OF 4IN SS PIPE

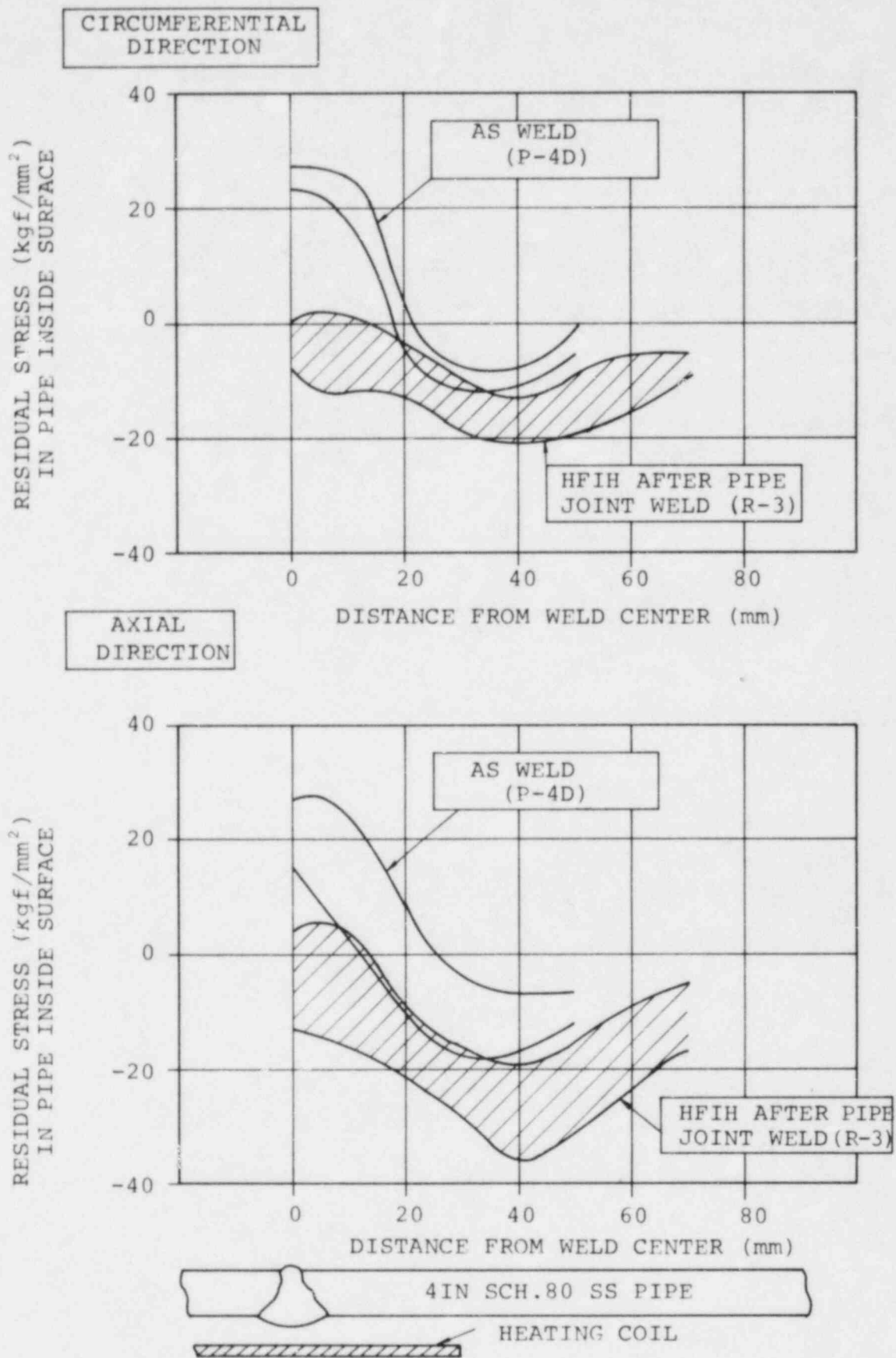


Fig. 6 EFFECT OF HFIH ON RESIDUAL STRESS OF 4IN SS PIPE

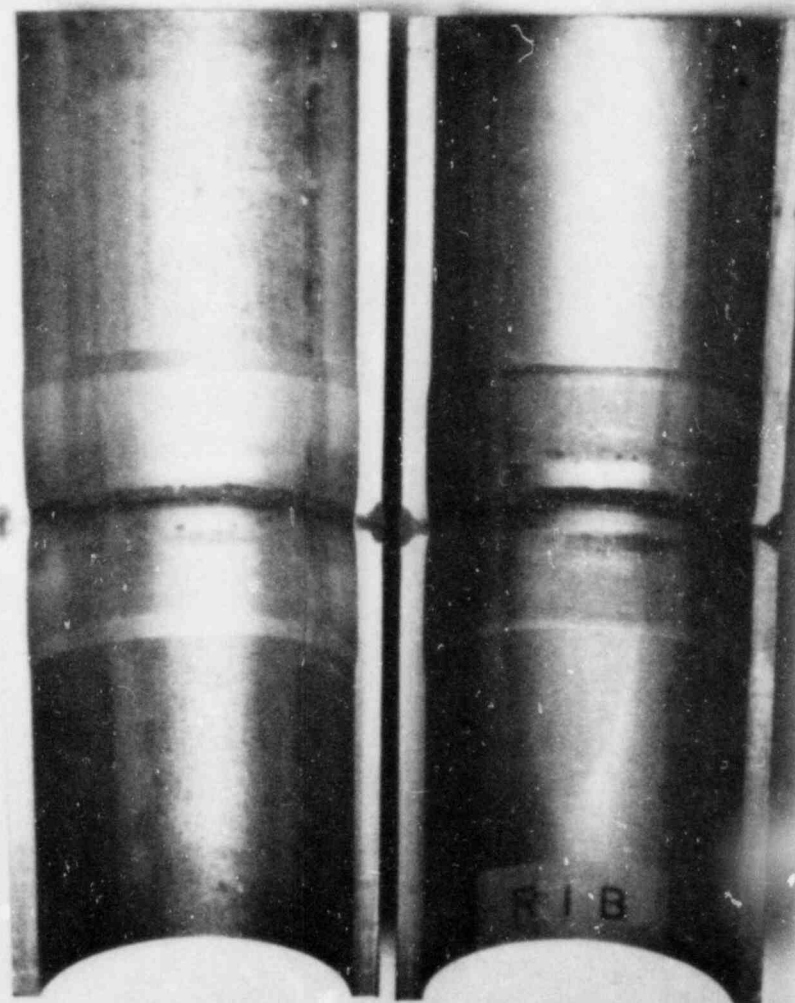
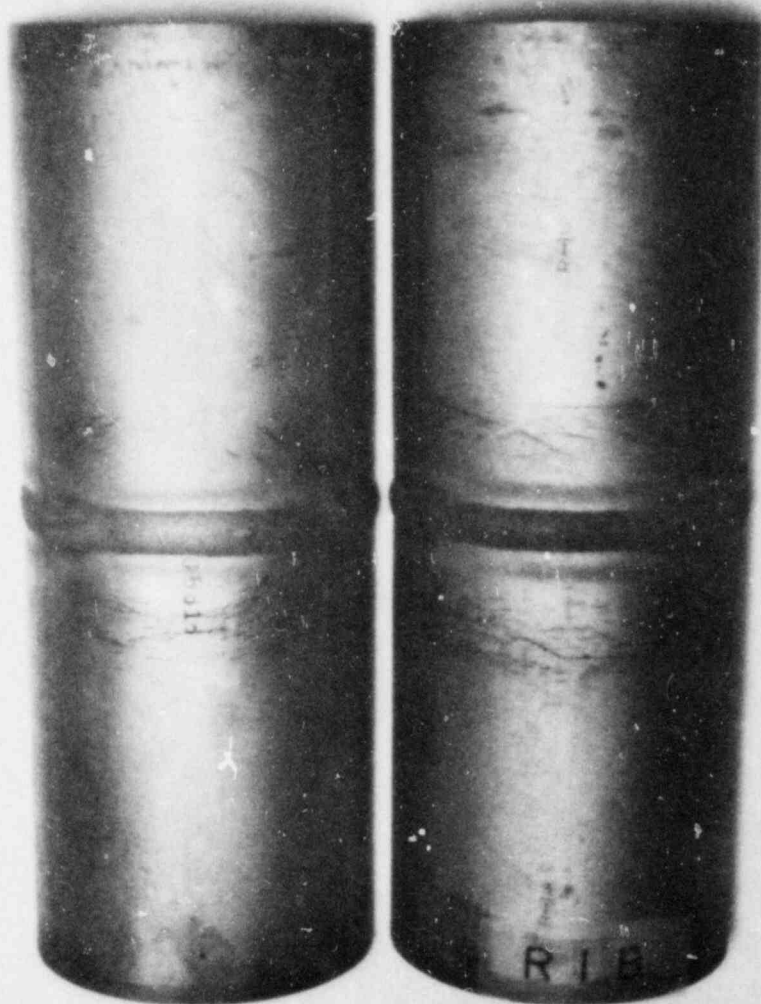


PHOTO-1 CRACK PATTERN OF 4 IN. SS PIPE WELD SPECIMEN (WITH HFIH)

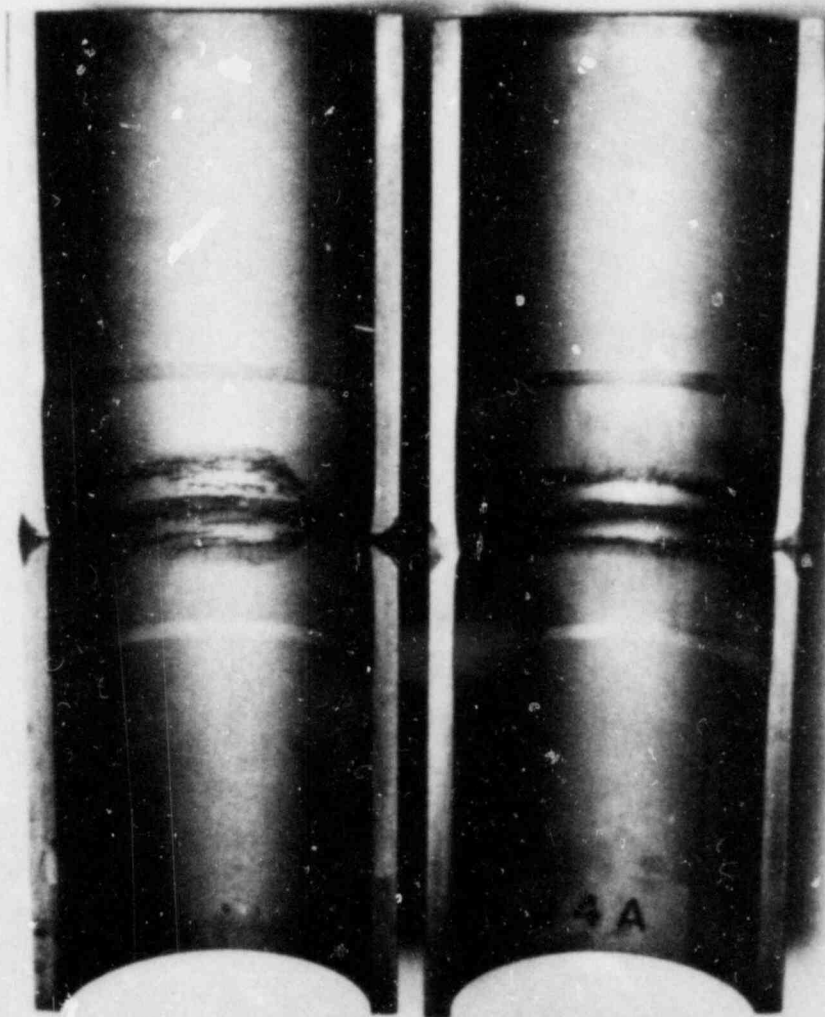
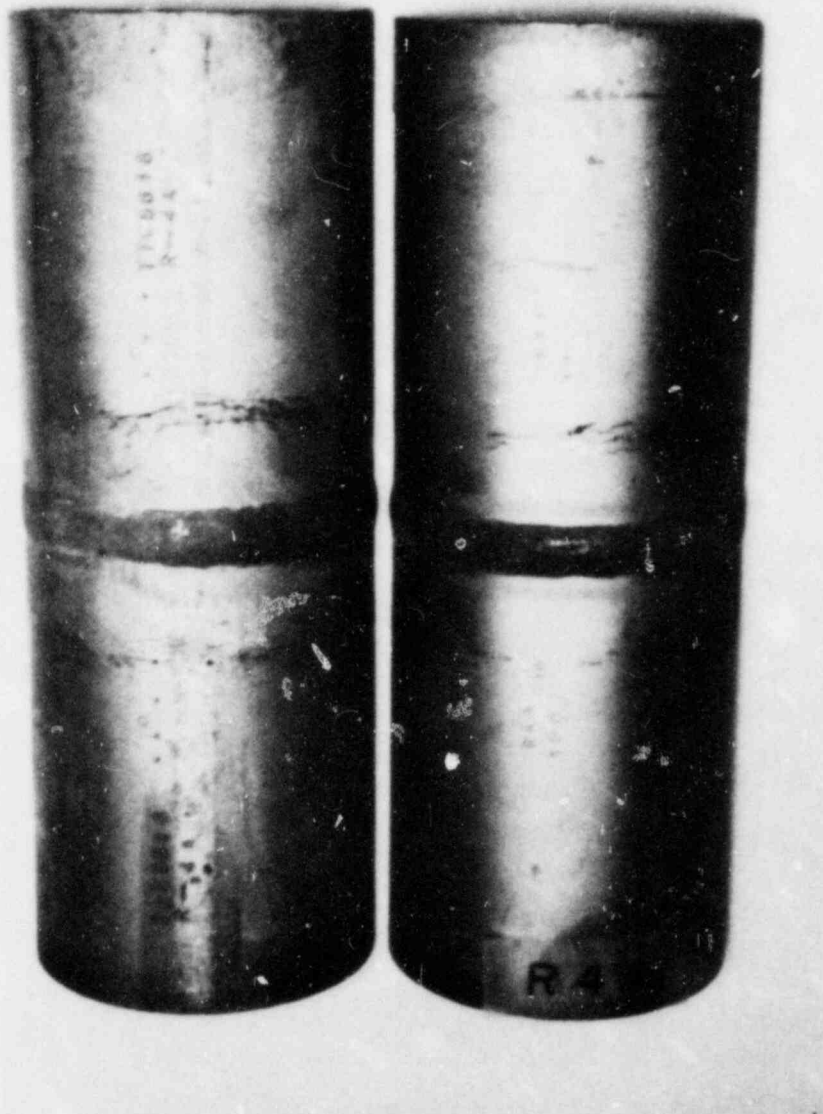


PHOTO-2 CRACK PATTERN OF 4 IN. SS PIPE WELD SPECIMEN (AS WELD)

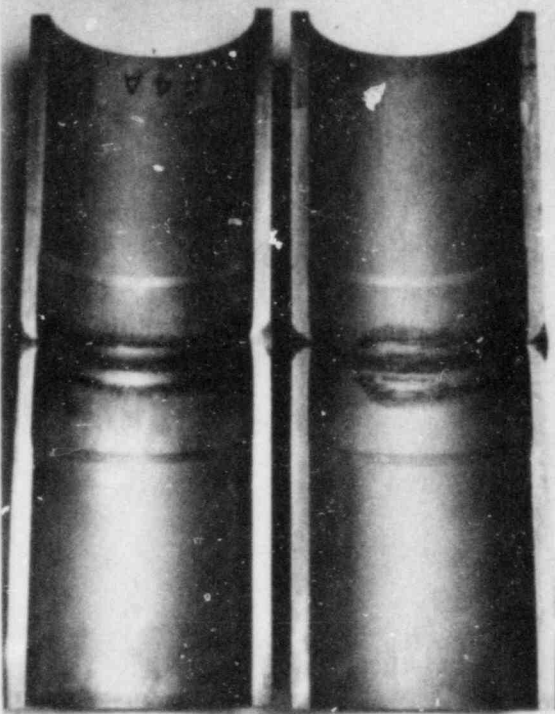
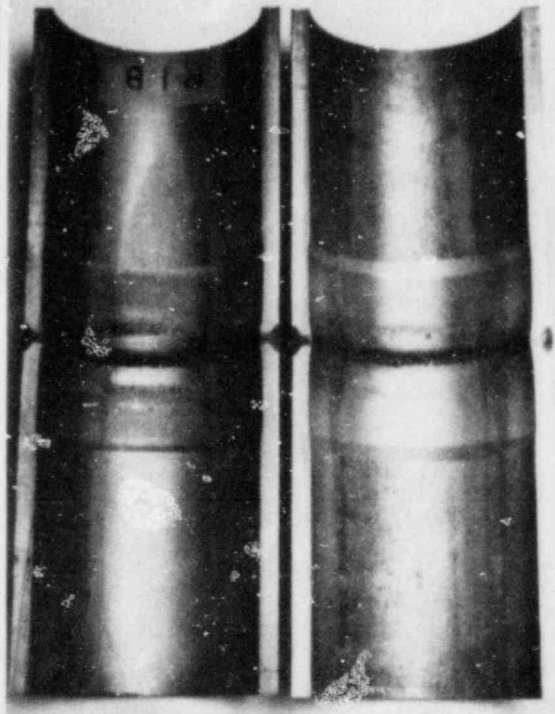
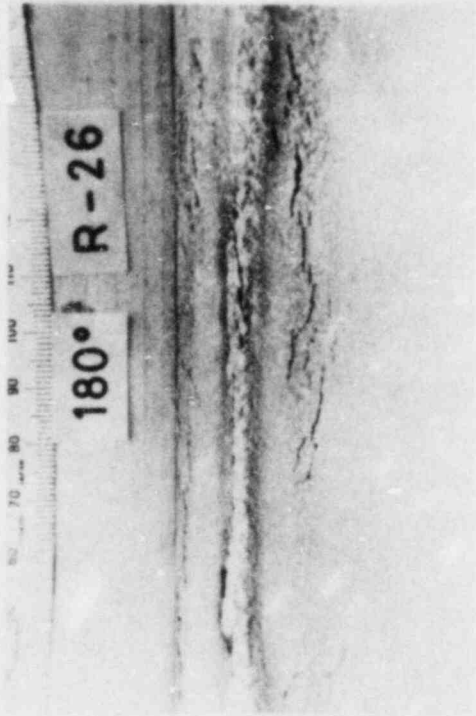
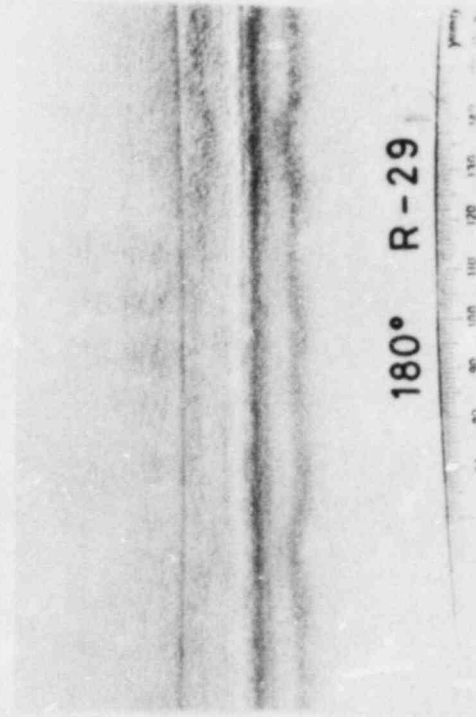
Item Type	As Weld	With HSI
(a) 4 IN test pipe		
(b) 12 IN test pipe		

PHOTO-3 MICRO STRUCTURE OF 4INSS PIPE IN HFIH AFTER JOINT WELDING
(X 500)

A - 2

IMPROVEMENT OF RESIDUAL STRESS PATTERN

IN PIPE BY HFIH (SECOND REPORT)

- PARAMETRIC SURVEY -

Summary

It was reported previously that the residual stress pattern of a pipe weld joint could be improved by high frequency induction heating and simultaneous water spray cooling on inside surface of the pipe.

This paper describes the results of a parametric survey to find a better heating and cooling condition for improvement of the residual stress pattern.

Many short pipes were treated with various heating and cooling conditions. The residual stresses were measured by the conventional strain gage method.

The main results are:

- (1) Frequency and heating time had no significant influence.
- (2) A larger through wall temperature difference produced a larger compressive stress.

1. Introduction

It was reported previously that the residual stress pattern of a weld joint in pipe could be improved by high frequency induction heating (HFIH) and water spray cooling.

The main objective of HFIH and water spray cooling is to obtain a large bending stress (beyond the yield strength) induced by the large temperature difference through the wall.

The bending stresses may be influenced by the many factors such as heating depth, heating time, heating temperature, temperature gradient in axial direction, etc. The influence of these factors has been investigated. This paper reports the results of the test mentioned above.

2. Experimental

2.1 Material

The chemical composition and the mechanical properties of the pipes used are shown in Table-1. The pipes were cut into short pieces and subjected to a stress relieving heat treatment ($900^{\circ}\text{C} \times 2\text{H}$).

2.2 Heating and Cooling

Heating was performed from the outside surface by HFIH using a single coil with various conditions as shown in Table-2.

The temperature on the inside and outside surfaces experienced during the treatment was measured by means of conventional A.C. thermocouples.

3. Results and Discussion

3.1 Heating Depth

In order to study the effect of heating depth, R-12 was heated using a frequency of 8.4 kHz while the others were heated using a frequency of 2 kHz.

The results are shown in Fig. 1. The inside surface temperature of R-12 was lower than that of R-15 because the heating depth of R-12 was shallower than that of R-15. There is, however, no significant difference in residual stress between R-12 and R-15. This results from the fact that the temperature difference through the wall of R-15 is sufficient to obtain the maximum effect.

3.2 Temperature Difference

R-13 was heated to a somewhat higher temperature and R-16 and 17 were heated to lower temperatures in order to study the effect of heating temperature (temperature difference) on residual stress.

Fig. 2 shows the results of the test. R-13 and R-15 have greater temperature differences resulting in more compressive stresses on the pipe ID than R-16 and R-17.

3.3 Heating Duration

R-14 was heated for a longer time than the others in order to investigate the effect of heating duration on residual stresses. The results are shown in Fig. 3 and no significant effect is observed.

3.4 Effect of Pipe Size

R-18 was prepared from 10B Schedule 80 pipe in order to investigate the effect of pipe size on residual stress.

The results are shown in Fig. 4. A greater temperature difference through wall was obtained on R-18, but smaller residual stresses were observed. The effect is explained as follows.

The temperature gradient in the axial direction is not favorable for this residual stress improvement, because it cancels the effect of the temperature difference in through thickness direction.

Generally, the effect of axisymmetric loading in a pipe can be neglected if the location of interest is remote from the loading point by a sufficient distance. This distance can be estimated as $(1.5 \sim 2.5) \sqrt{ah}$, where "a" is the mean radius and "h" is the wall thickness.

Therefore the region where the residual stress must be improved should be at least $1.5\sqrt{ah}$ away from the coil end, namely, a larger pipe should be heated using a wider coil.

4. Conclusion

The results obtained in this test have produced the following conclusions:

- (1) Heating depth and heating duration have no significant effect on the residual stresses in this test.
- (2) Larger temperature differences through wall are favorable to producing a larger compressive residual stress.
- (3) Heating a wider band of material will be required for larger pipe.

Reference

- (1) S. Timoshenko et al: "Theory of Plates and Shells," McGraw-Hill, (1959) pp. 469-471.

TABLE 1 CHEMICAL COMPOSITION AND MECHANICAL PROPERTIES

SPECIFIED VALUES PIPES	CHEMICAL COMPOSITION (%)							MECHANICAL PROPERTIES			REMARKS
	C max. .08	Si max. 1.00	Mn max. 2.00	P max. .040	S max. .030	Ni 8.00 11.00	Cr 18.00 20.00	$\sigma_{.2}$ *	σ_U *	EL (%) 35	
4B SCH 80 (TTC 4872)	.06	.59	1.75	.022	.006	9.40	18.60	28	62	65	R-12 to 18 R-20
10BSCH 80 (TTD 3543)	.06	.53	1.76	.018	.006	9.20	18.80	22	55	70	R-19

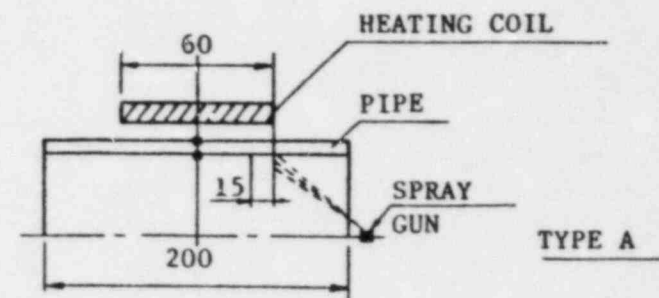
* STRESSES ARE IN Kg/mm^2

TABLE-2 HEATING CONDITION

TF NO.	HEATING METHOD (*1)	PIPE SIZE (INCH)	FREQUENCY (kHz)	HEATING DURATION (sec.)	MAX. TEM. (OUT) (°C)	MAX. TEM. (IN) (°C)	ΔT^{*2} (°C)
R-12	A	4	2	19	530	105	425
-13				16	676	250	426
-14				102	520	192	328
-15				21	562	240	322
-16				23	322	167	155
-17				25	247	115	132
-18		10		29	519	118	401

Notes: 1 Heating method are illustrated on the right.

2 ΔT is the temperature difference between outside and inside surfaces of pipe.



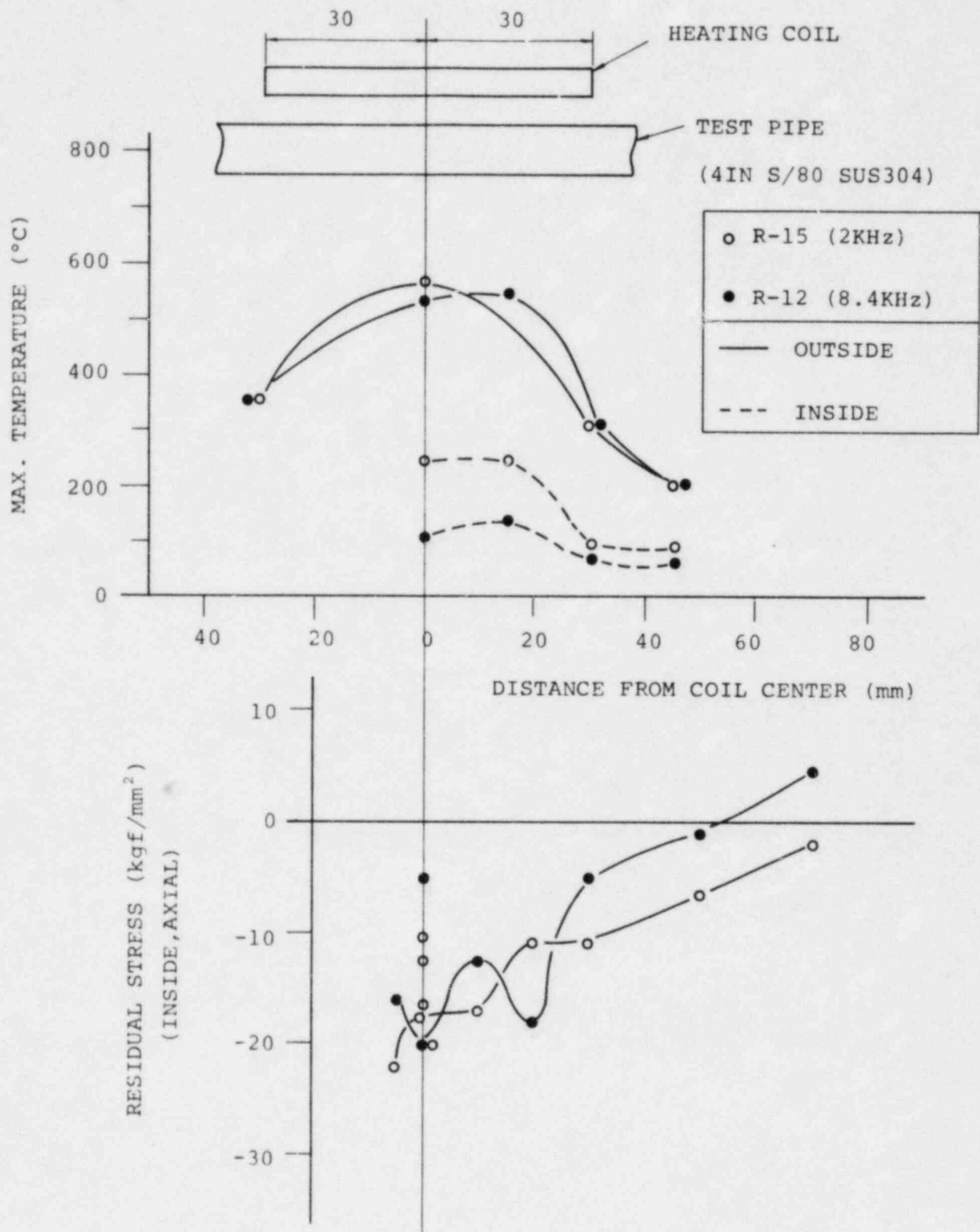


Fig. 1 EFFECT OF HEATING DEPTH ON INNER SURFACE RESIDUAL STRESSES

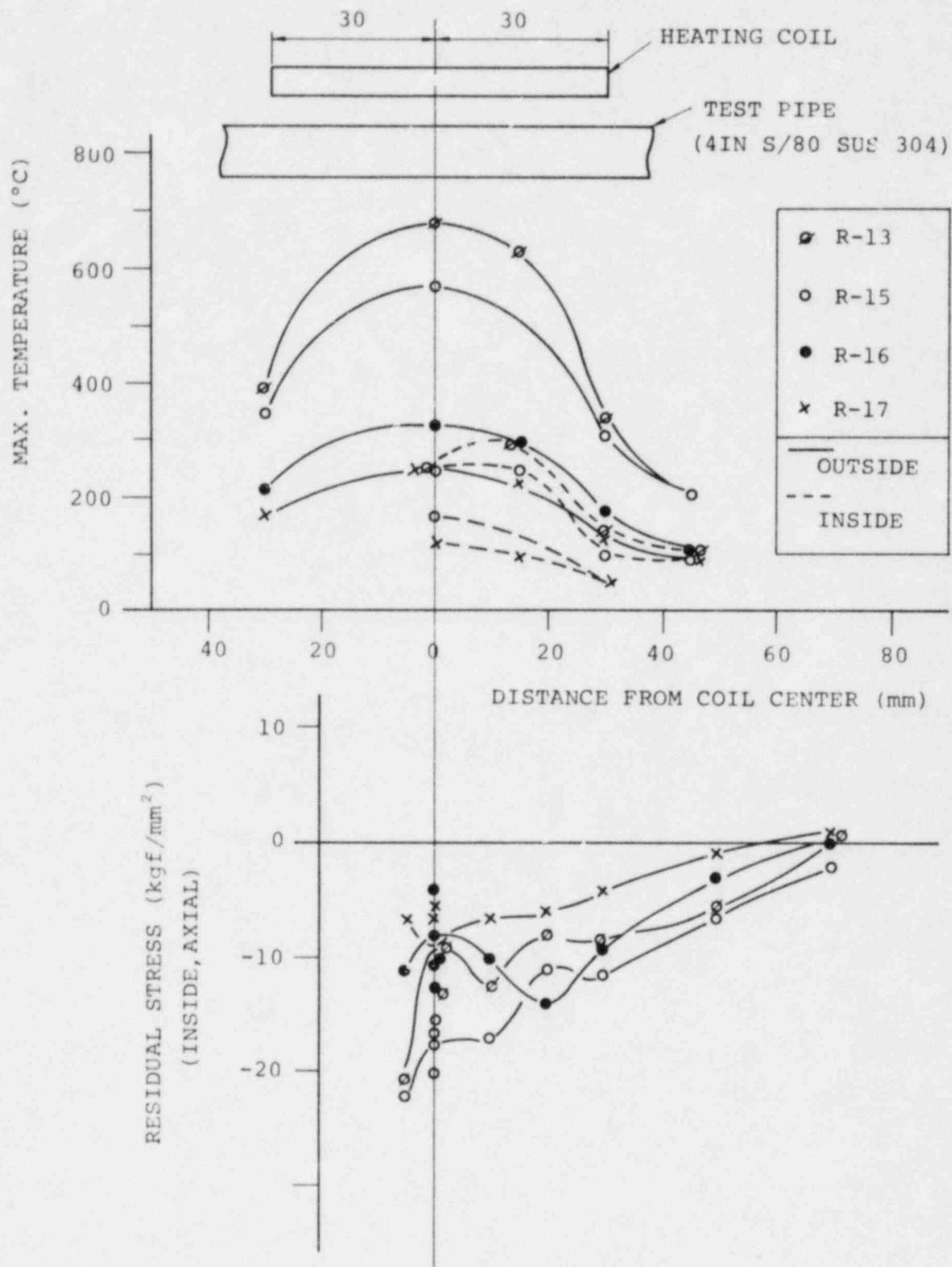


Fig. 2 EFFECT OF MAX. TEMPERATURE ON INNER SURFACE RESIDUAL STRESSES

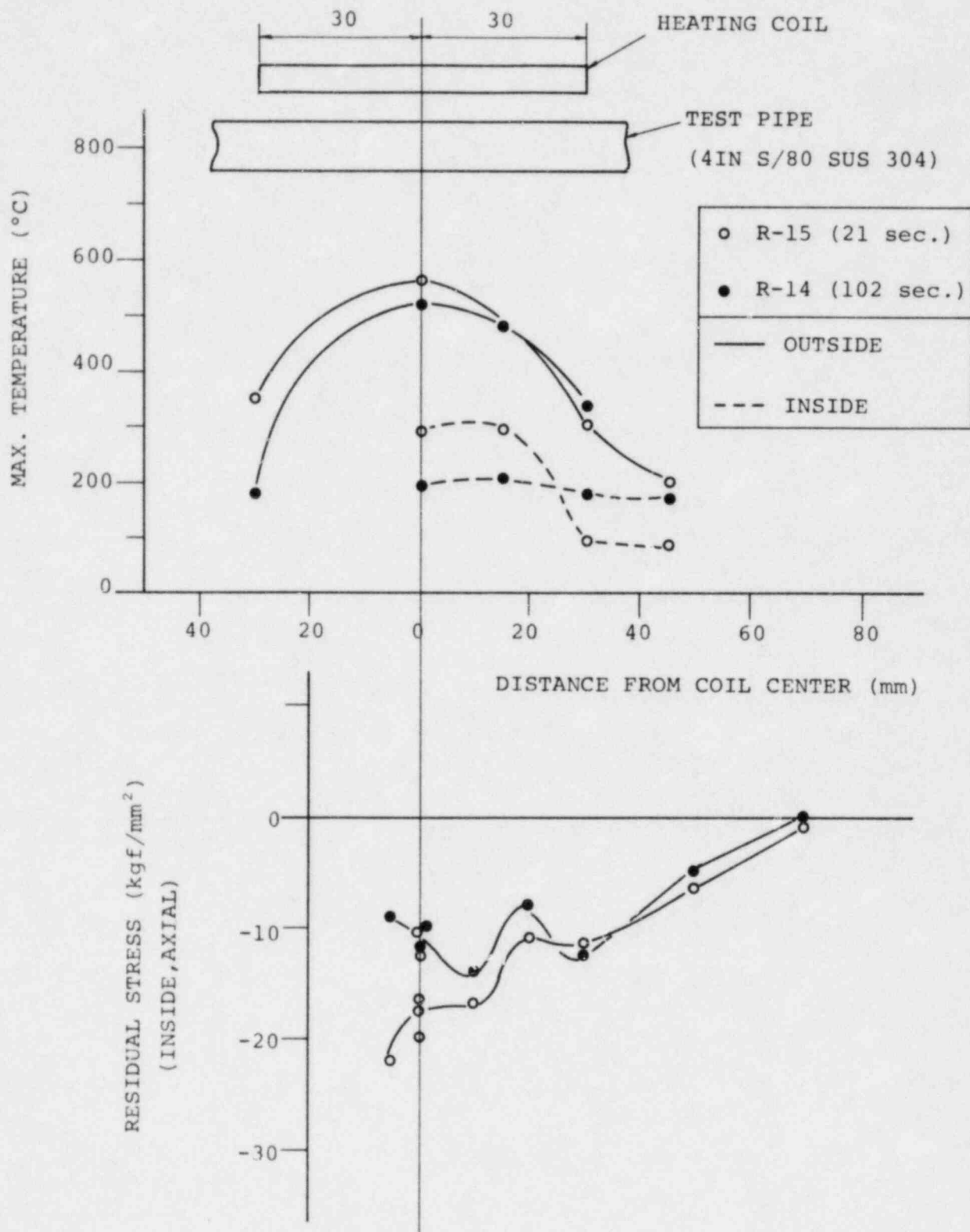


Fig. 3 EFFECT OF HEATING TIME ON INNER SURFACE
RESIDUAL STRESSES

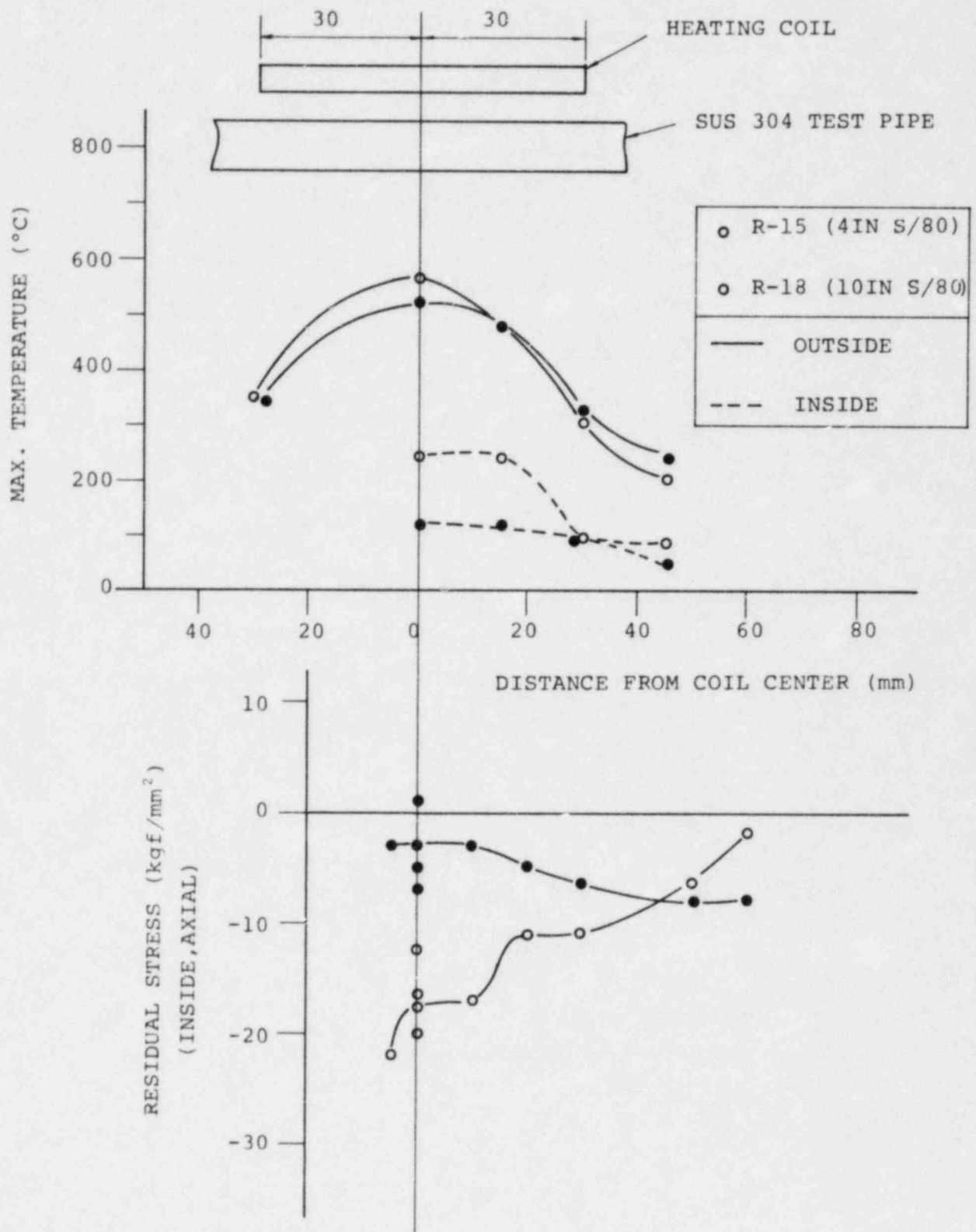


Fig. 4 EFFECT OF PIPE THICKNESS ON INNER SURFACE
RESIDUAL STRESSES

A- 3

IMPROVEMENT OF RESIDUAL STRESS PATTERN

IN PIPE BY HFIH

(3RD REPORT)

Summary

It has been reported previously that induction heating is very effective in improving the residual stress pattern on the inner surface of a welded pipe. A series of demonstration tests were conducted on 12 inch schedule 100 stainless steel pipes and elbows prior to the application of this process to an actual plant. The residual stresses with and without induction heating were measured by the conventional strain gage methods: Cracking tests in boiling 42% MgCl_2 solution were also conducted for this demonstration.

The main results were:

- (1) High tensile residual stresses were lowered or shifted to compression by HFtH.
- (2) No cracks were observed after the cracking test in MgCl_2 on the inside surface of the weld joints treated with induction heating. Conversely, many cracks were observed on the weld joints prepared without induction heating.

In addition, the effect of the heating coil width and cooling water rate was investigated using 12 inch pipe; also some calculations were conducted to study the residual stress distribution in through thickness direction and to check the effect of weld metal.

1. Introduction

It had been reported previously that induction heating is very effective in improving the residual stress pattern on the inner surface of a welded pipe. These data were based on tests conducted mainly with 4B Schedule 80 pipe.

It is necessary prior to application to larger pipes to show that induction heating produces satisfactory results on larger diameter pipe. Consequently, a series of basic survey and demonstration tests and numerical calculations were performed.

This paper describes primarily the results of the demonstration tests. Other results are described in subsection A, B, and C.

2. Experimental Procedure

2.1 Material

12B Schedule 100 austenitic stainless steel pipe and elbows were welded as shown in Fig. 1 to simulate the actual piping condition. The mechanical properties and chemical compositions are listed in Table-1.

2.2 Welding

The first three layers were welded by the GTAW process and the remainder by SMAW in the 5G (horizontally fixed) position to duplicate the field condition. The lower portions of the three joints, No - R - 26 and 28 were gauged and re-welded to simulate repair welds. The details are shown in Table-2.

2.3 Heating and Cooling Devices

The general arrangement of the heating and cooling devices and the test model are shown in Fig.-2.

The model was fabricated on a restraint frame to simulate the installed piping condition at the site.

The butt weld seam was located 60 mm from the coil edge to simulate a pipe to elbow configuration. The details of heating and cooling conditions are summarized in Table -3.

3. Results and Discussion

3.1 Temperature Distribution

The temperature distribution in the mid portion of the coil was very uniform if the pipe thickness was approximately uniform (see Fig. 3). Where there was a large thickness transition under the coil, the temperature varied with the thickness (see Fig. 6). This is easily understood by the following basic equation.

$$q = \lambda \cdot \frac{\theta_o - \theta_i}{t} \dots\dots\dots (1)$$

where, q :Heat flux

λ :Thermal conductivity

t :Wall thickness

θ_o, θ_i :Temperature at outside and inside surfaces respectively

In this case q and λ are nearly constant. Therefore $\theta_o - \theta_i$ is inversely proportional to t, that is, θ_o goes down and θ_i goes up as t becomes small. This behavior is also demonstrated in Table 3.

3.2 Residual Stresses

The residual stresses were measured using conventional strain gage techniques.

The results are presented in Fig. 4 to 6. The high tensile residual stresses in the as welded condition were lowered or shifted to compression by IHSI. The highest tensile residual stress after IHSI is approximately kg/mm^2 for R-27 and 28, but no tensile stresses were measured for R-30 which exhibited the largest temperature difference.

(a) Effect of repair weld

In order to evaluate the effect of repair welding, a simulated repair weld was performed in the interval between 157.5 and 202.5 degrees on two weldments, No R-26 and R-28. R-26 which had not been treated by HFIH was exposed to Magnesium chloride solution and developed many cracks near the repair weld since high tensile residual stresses were present (see Fig. 7). On the other hand, the residual stresses on R-28, which had been HFIH treated after repair welding was evaluated by conventional strain gage technique. The results are shown in Fig. 4. The residual stresses in the repaired portion of the pipe in the vicinity of the repair were not significantly different from the as welded and HFIH locations of the pipe.

These results indicate that although repair welds induce high tensile residual stresses to the pipe ID, the stresses are lowered and possibly shifted to compression by HFIH.

(b) Effects of restraint

The mock-up containing weldments R-24 through 27 was fixtured in a restraint frame simulating a worst case plant condition. R-24 and R-27

had the thinnest cross and consequently were the most severely constrained. The results of the HFIH treatment presented in Fig. 6 and 7 show that the residual stresses were effectively improved. One can approximate the restraint effect by utilizing the following simple model.

The free thermal expansion of pipe due to HFIH is

$$\delta = \alpha L(T_a - T_r)$$

where : Coefficient of linear thermal expansion

$$\alpha = 1.8 \times 10^{-5} \text{ mm/mm}^\circ\text{C}$$

L : Heating width = coil length = 250 mm

T_a : Average temperature across the thickness $\approx 350^\circ\text{C}$

T_r : Room temperature $\approx 20^\circ\text{C}$

Therefore

$$\begin{aligned}\delta &= 1.8 \times 10^{-5} \times 250 (350 - 20) \\ &= 1.49 \text{ mm}\end{aligned}$$

The axial force in the mock up induced by local heating is given by (see Fig. 13).

$$P = \frac{24}{5} \cdot \frac{EI}{l^3} \cdot \delta$$

where E : Young's modulus

I : Moment of inertia of section

l : Piping length (see Fig. 13)

and results in

$$\begin{aligned}P &= \frac{24}{5} \cdot \frac{2.1 \times 10^4 \times 2.171 \times 10^3}{(1.247 \times 10^3)^3} \times 1.49 \\ &= 1.68 \times 10^4 \text{ kg}\end{aligned}$$

The minimum cross sectional area (at R-24 and 27) is,

$$\begin{aligned} A &= \pi \cdot (318.5 - 15) \cdot 15 \\ &= 1.43 \times 10^4 \text{ mm}^2 \end{aligned}$$

The axial thrust stress induced during HFIR is

$$\sigma = \frac{P}{A} = 1.17 \text{ kg/mm}^2$$

This stress is very small compared to that introduced by the through wall temperature difference, that is, the restraint effect is negligible.

Generally, the pipe restraints (support) are located at such incremental distances that the thermal stresses produced normally are within allowable limits and, therefore, the restriction of any free end displacement due to local heating can produce only small stresses.

3.3 42% MgCl_2 Cracking Test

Cracking tests in boiling 42% MgCl_2 solution were conducted on pipes R-24, 26 and 29, and the results are shown in Fig. 7 and 8.

Many cracks were observed in the highly stresses areas, such as the outer surface or inner surface of the untreated joint but no cracks were observed on the inside surface of R-24 and 29, which had been treated by IHSI.

This observation indicates that the high tensile residual stresses on R-24 and 29 are reduced or changed to compression at points near the weld on the inside surface of the IHSIed pipes.

3.4 Mechanical Properties

Tensile, bending and hardness tests were conducted on R-25, 28, 30 and 33 to investigate the difference in mechanical properties between joints fabricated with and without IHSI.

These results are shown in Table 4, Fig. 9 and 10. The tensile strength after HFIH was a little bit (0.4 to 1.0 kg/mm²) larger than that before HFIH.

A small increase in hardness at the outer and inner surfaces was also observed in the HFIH treated pipes but no hardness differences were observed elsewhere. The results of these measurements are presented in Fig. 9 and 10. These results show that mechanical properties do not change except for a slight increase in tensile strength and hardness near pipe surfaces.

This observation results from the fact that the plastic strain induced by HFIH is 0.5% or less as presented below.

The maximum temperature of a pipe outside surface is monitored and controlled so that it doesn't exceed 550°C. The cooling water temperature is higher than 0°C. Therefore, the maximum temperature difference between the outer and inner surface of the pipe is less than 550°C.

Assuming a linear temperature distribution across the pipe thickness, the thermal strain at the inside surface ϵ_{th} is approximately given by

$$\begin{aligned}\epsilon_{th} &= \frac{1}{2} \alpha \cdot \Delta T \\ &= 0.5 \times 1.8 \times 10^{-5} (550-0) \\ &= 4.95 \times 10^{-3}\end{aligned}$$

Consequently, the maximum strain at inside pipe surface is about 0.5%. This strain level is too small to produce a substantial difference in mechanical properties.

3.5 Microstructure

The microstructure of the weld joints with and without IHFI were observed using a 10% oxalic acid etchant.

Figure 5 shows the microstructure of pipes R-25 and 28.

No significant differences were observed.

This observation results from the fact that the strain due to HFIF is not so large as to produce a big difference in microstructure.

4. Conclusion

A series of demonstration tests were conducted to demonstrate the validity of the HFIF process for 12 inch pipes. The following conclusions were obtained from these demonstration tests.

- (1) High tensile residual stresses were lowered or shifted to compression not only in 4 inch pipes but also in 12 inch pipes.
- (2) This observation was verified by the cracking tests in boiling 42% MgCl_2 solution.
- (3) The pipe restraint (restriction of free end displacement) produced no significant changes to the residual stress improvement process.
- (4) The repair welded portion of pipe subsequently HFIF treated demonstrated a significant improvement in residual stresses.
- (5) Little difference was observed in mechanical properties and microstructures between pipes which were treated and pipes which were not treated using the HFIF process.

Table 1 Chemical composition and Mechanical Properties

Heat No.	Chemical Composition %								Mechanical Properties			Remarks
	L or C	C max. 0.08	Si max. 1.00	Mn max. 2.00	P max. 0.040	S max. 0.030	Ni 8.00~ 11.00	Cr 18.00~ 20.00	Yield* Point 21 (kg/mm ²)	Tensile* Strength 53 (kg/mm ²)	Elongation 30 (%)	
D58412	L C	.06 .06	.56 .56	1.71 1.74	.022 .020	.006 .006	9.25 9.20	18.10 18.10	24	58	70	PIPE
D59218	L C	.05 .06	.55 .54	1.69 1.72	.023 .022	.005 .006	9.20 9.25	18.45 18.35	23	57	74	90° LONG ELBOW
49-281-3	L C	.03~ .033	.55 .54	1.75 1.79	.024 .024	.008 .013	9.77 9.15	18.88 18.86	26.1	54.5	67.5	SAFE END (FORGING)

* SPECIFIED VALUES SHOW MINIMUM.

TABLE 3 TEST MATRIX

JOINT NO.	*1 THICK	HEATING CONDITION								ANALYSES				
		WIRE DIAMETER	POWER	WIDTH OF COIL	HEATING DURA- TION	COOLING COND. VELOCITY	ENT/ EXIT (°C)	*2 T _o (°C)	*2 ΔT (T _o :T _i) (°C)	*3 TTD	*4 MgCl ₂	*5 S.G.	MECHA.	MICRO.
R-24	15	3	300	250	179	0.5	34.5 37	394	281	○	○	-	-	-
R-25	19.25									-	-	○	○	○
R-26	19.25									-	○	-	-	-
R-27	15	3	300	250	176	0.5	37 40	400	236	○	-	○	-	-
R-28	19.25	3	300	250	177	0.5	32 33	514	395	○	-	○	○	○
F-29	19.25	3	300	250	178	0.5	34 35	514	386	○	○	-	-	-
R-30	28.5	3	300	250	116	0.5	31 32	526	477	○	-	○	○	○
R-33	28.5									-	-	○	○	○

*1 WALL THICKNESS AT JOINT

*2 T_o AND T_i SHOW THE OUTSIDE AND
INSIDE TEMPERATURE RESPECTIVELY

*3 TTD: TIME TEMPERATURE DISTANCE CURVE

*4 MgCl₂: CRACKING TEST IN 42% BOILING MgCl₂ SOLUTION

*5 S.G: RESIDUAL STRESS MEASUREMENT BY STRAIN GAGE

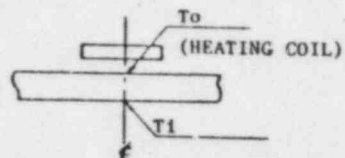


TABLE-4 MECHANICAL TEST RESULTS

MATERIAL	JOWT- No.	TEST ITEM IHSI	TENSILE STRENGTH (kg/mm ²)	BENDING TEST ^{*1}		HV MAX. (HV=10kg)	
				FACE	SIDE	BASE MTL.	WELD MTL.
PIPE (12BS/100) SUS304 + ELBOW (12BS/100) SUS304	R-25	NO	MIN. 57.1 MAX. 58.7	N.D. N.D.	N.D. 0.3x1	205	213
	R-28	YES	MIN. 57.7 MAX. 59.7	N.D. N.D.	N.D. N.D.	247	192
SAFE END + SAFE END (ASME SA182 F304)	R-33	NO	MIN. 55.5 MAX. 57.3	N.D. N.D.	1.0x1 N.D.	205	238
	R-30	YES	MIN. 55.9 MAX. 57.9	N.D. N.D.	N.D. N.D.	194	216

*1 N.D.: NO DEFECT

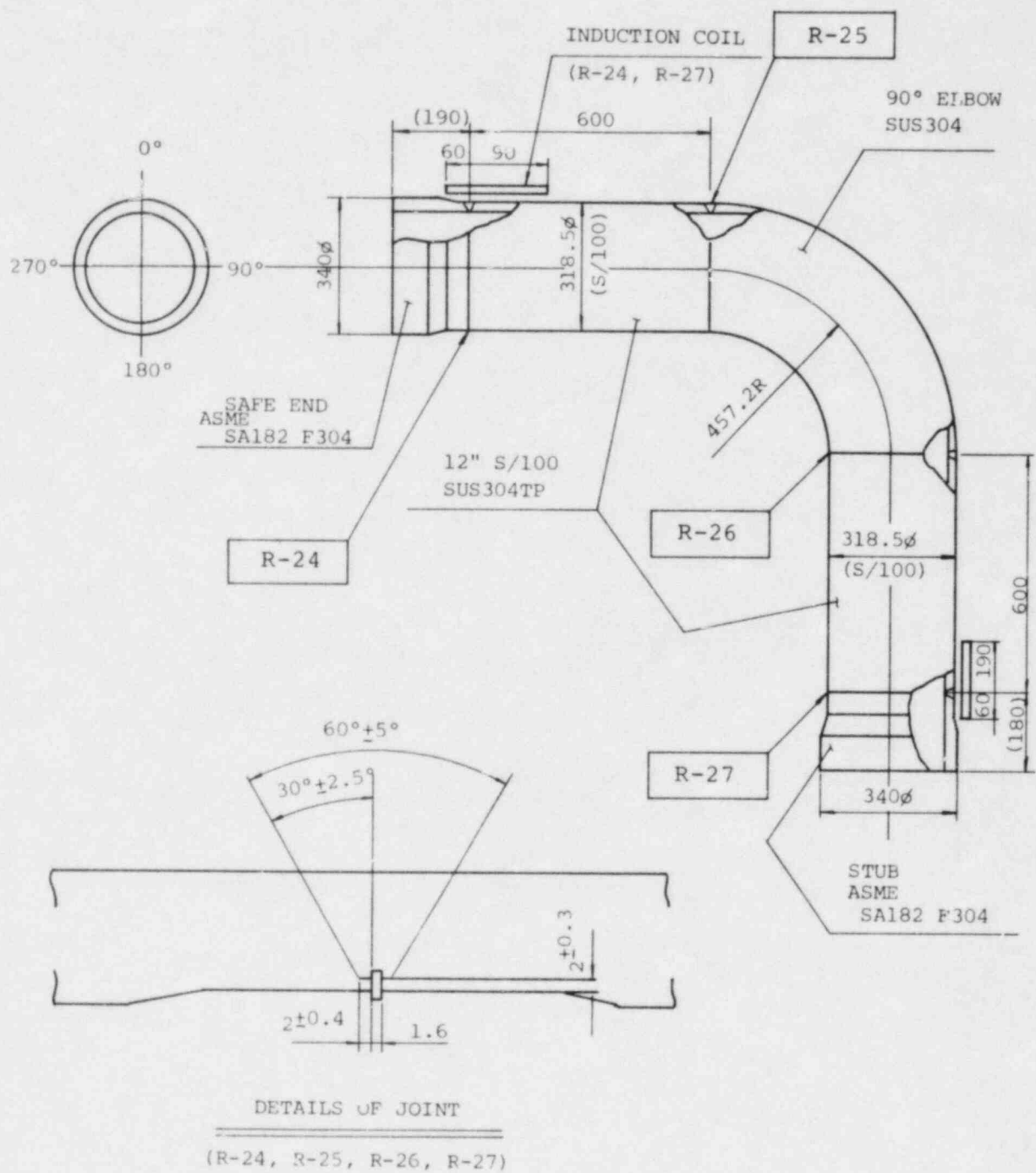


Fig. 1 MOCK UP FOR 12" PIPE DEMONSTRATION TESTS
(R-24, -25, -26, -27)

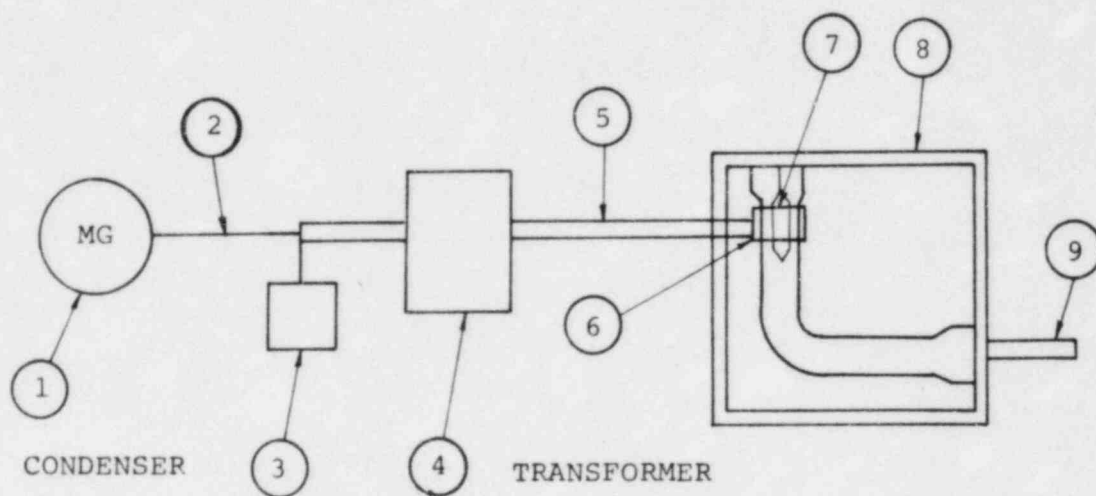


Fig. 2 INDUCTION HEATING DEVICE

MARK	NAME	FUNCTION	REMARKS
1	MOTOR GENE.	300 kW 3 kHz	
2	CABLE	50 m	
3	CONDENSER	8.9 μ F	
4	TRANSFORMER	1000 kVA	14:1
5	LEAD	180W \times 1000l	
6	INDUCTION COIL	250 W	
7	BAFFLE CYLINDER	PIPE 8"	STUB 600l ELBOW 550l
8	RESTRAINT FRAME		
9	FEED WATER PIPE	2"	

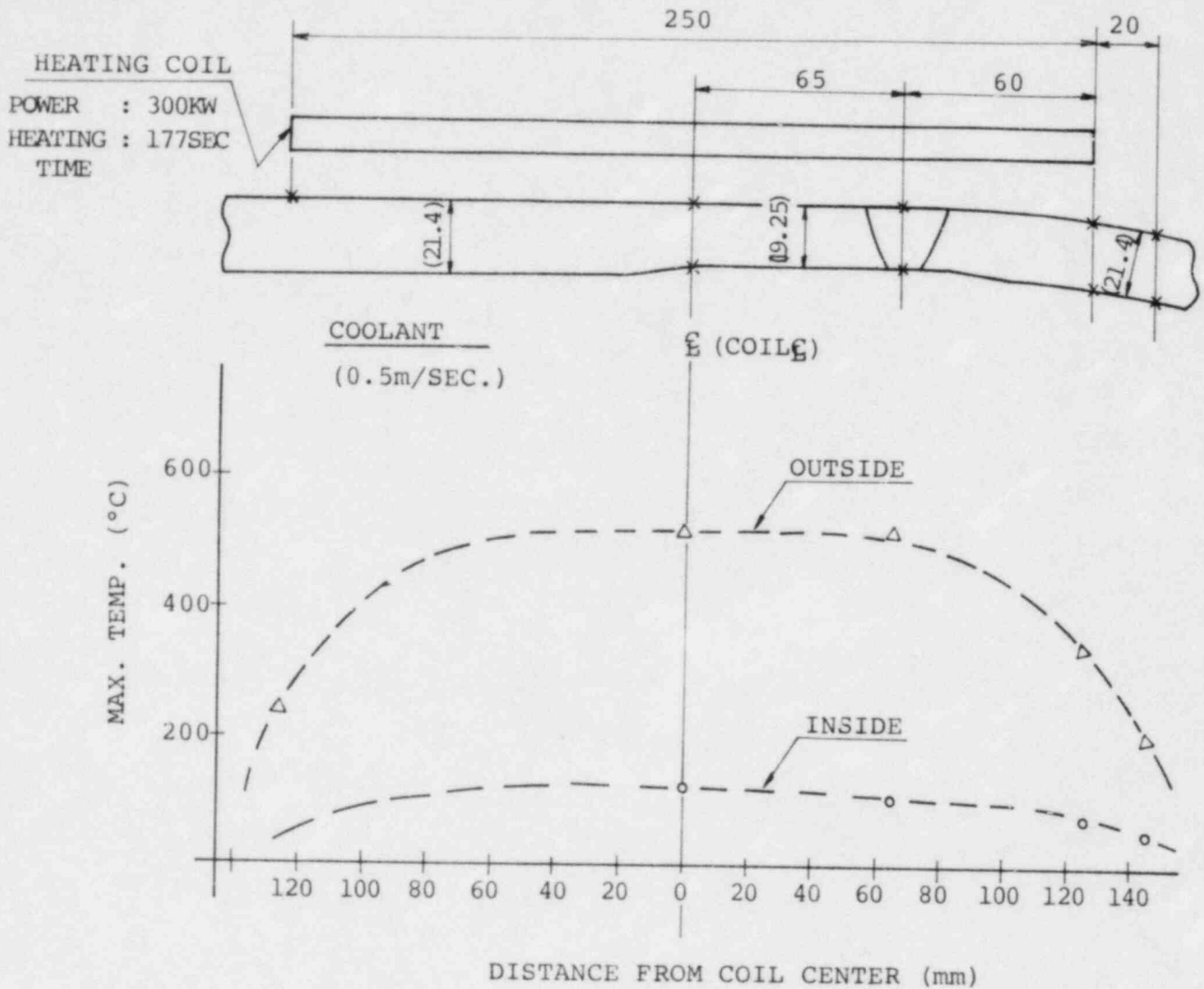


Fig. 3 TEMPERATURE DISTRIBUTION OF R-28, A PIPE TO ELBOW JOINT

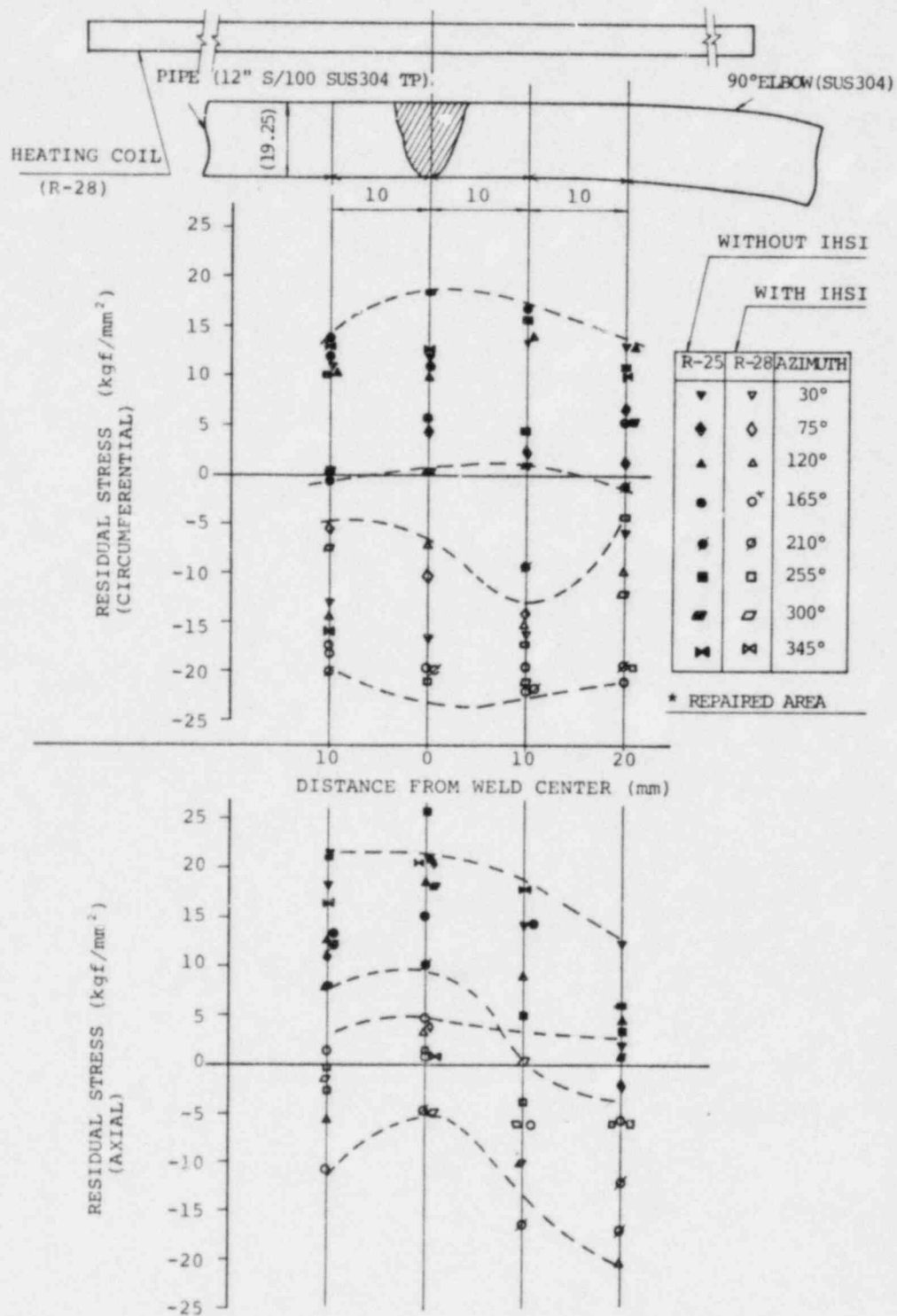


Fig. 4 RESIDUAL STRESS OF R-25 NAD R-28

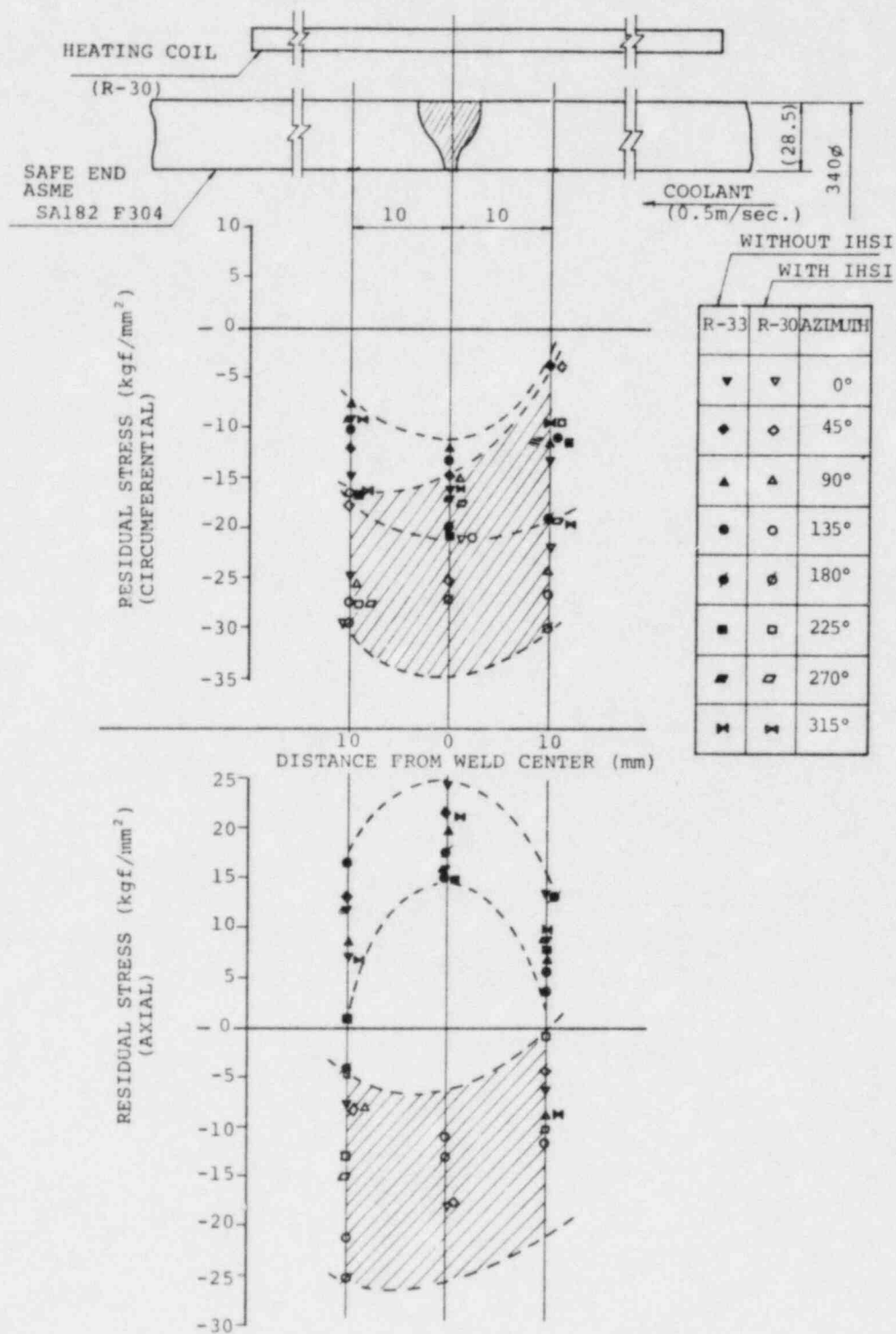


Fig. 5 RESIDUAL STRESS OF R-30 AND R-33

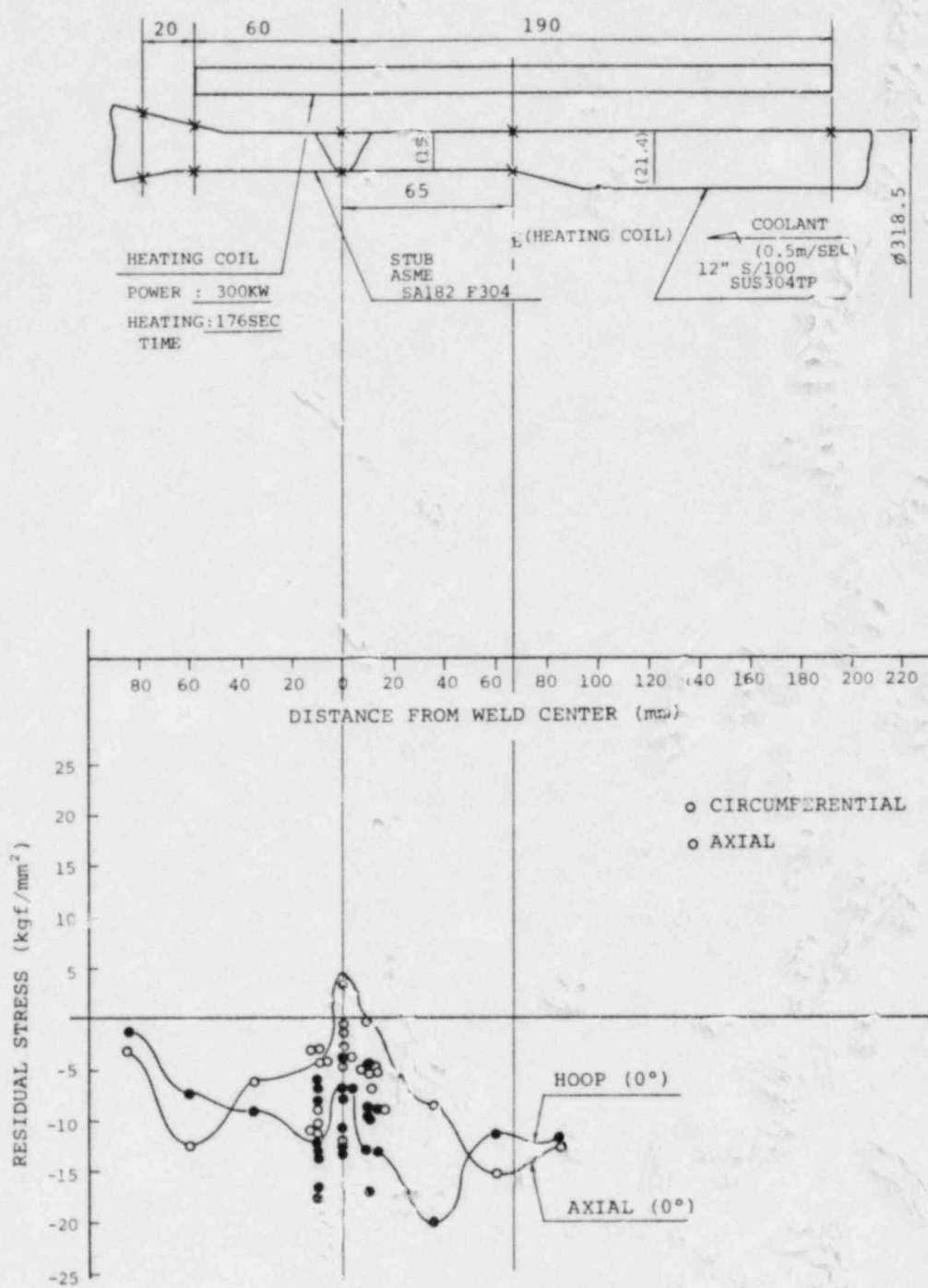
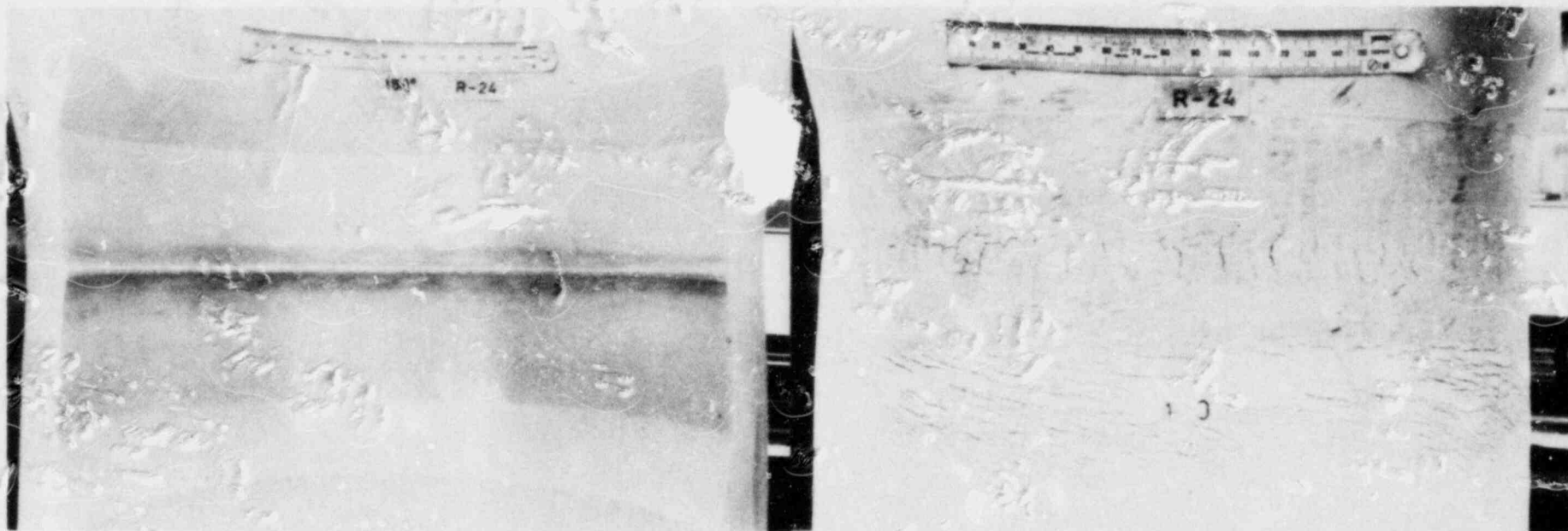


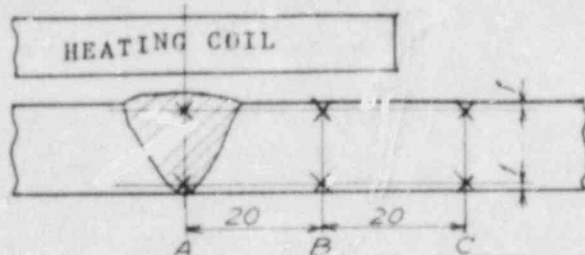
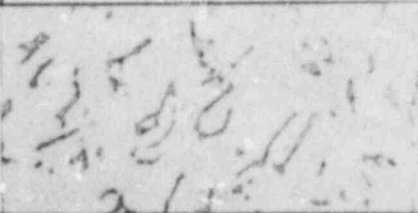

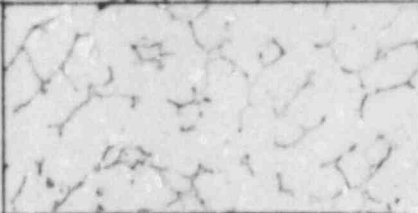
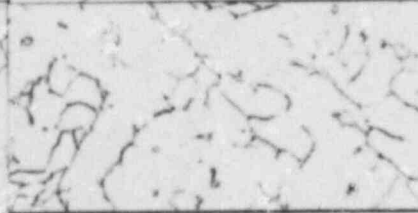
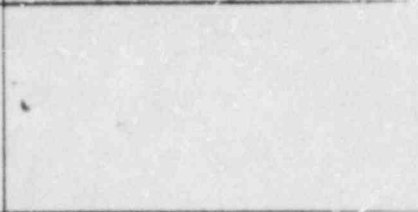
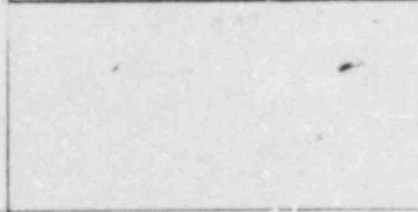
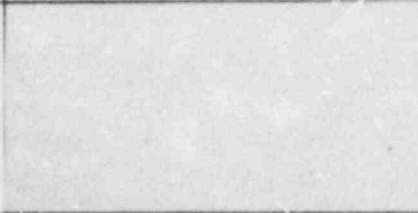



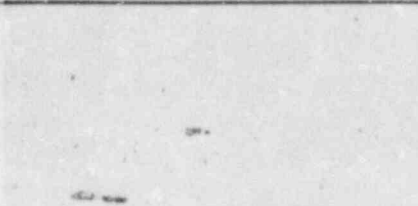
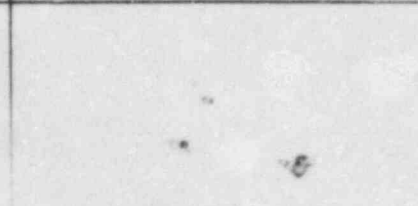
Fig. 6 RESIDUAL STRESS OF R-27



INSIDE SURFACE

OUTSIDE SURFACE

FIG. 7 CRACKING PATTERN OF R-24 AFTER IHSI (42% BOILING Mg Cl₂)

<div>HEATING COIL</div> 			
TP-NO.	R-2	R-3	
MAX. TEMP.	536 °C	340 °C	
A	ID		
	OD		
B	ID		
	OD		
C	ID		
	OD		

Note

* Max. temp. indicate in head center of pipe (outside surface)

Fig. 8 Crack pattern of inner surface of pipe joint after 42% MgCl₂ test (demonstration test)

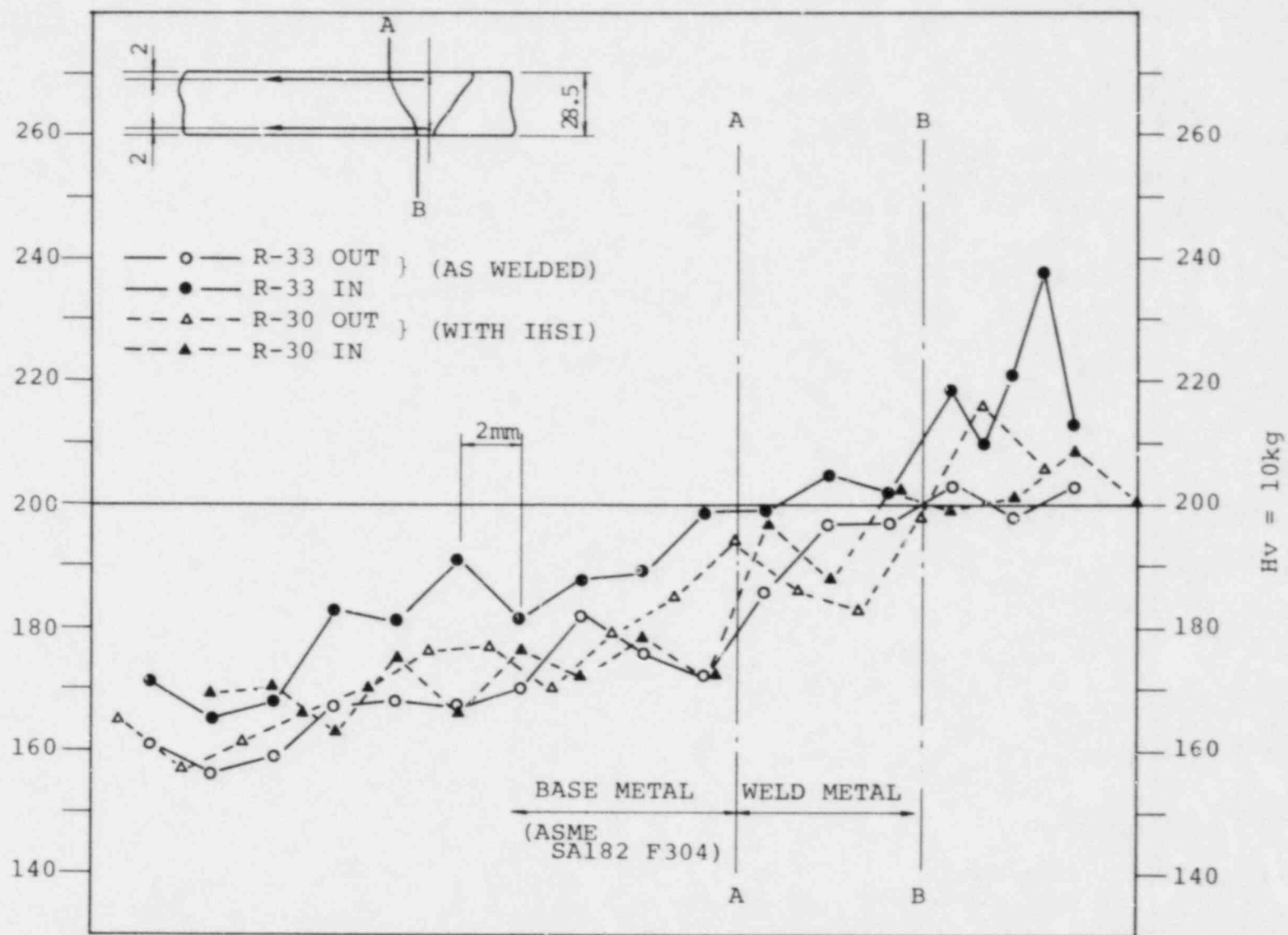


Fig. 9 HARDNESS TEST RESULT FOR R-30 AND R-33

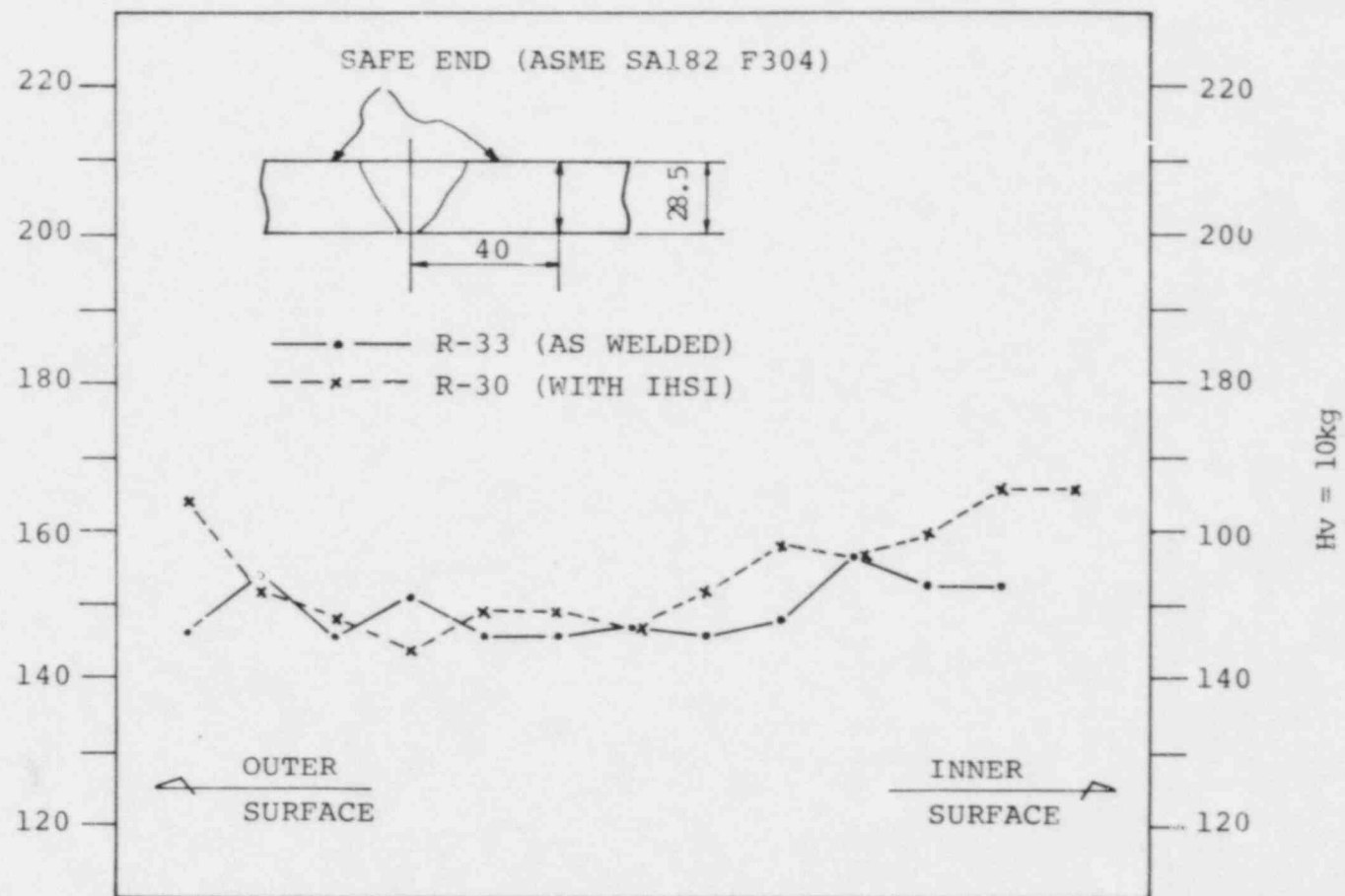


Fig. 10 THROUGH THICKNESS HARDNESS DISTRIBUTION FOR R-30 AND R-33

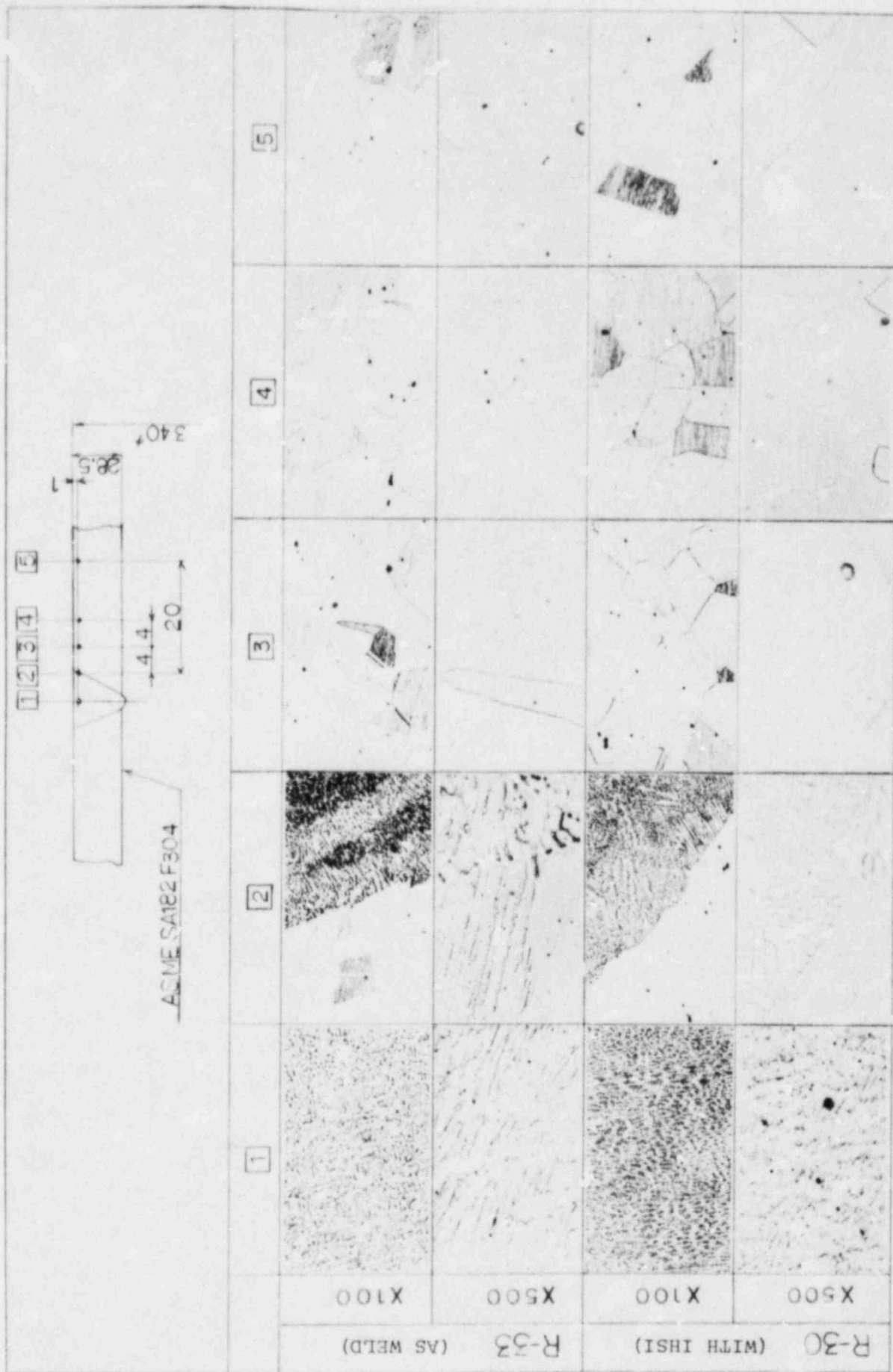
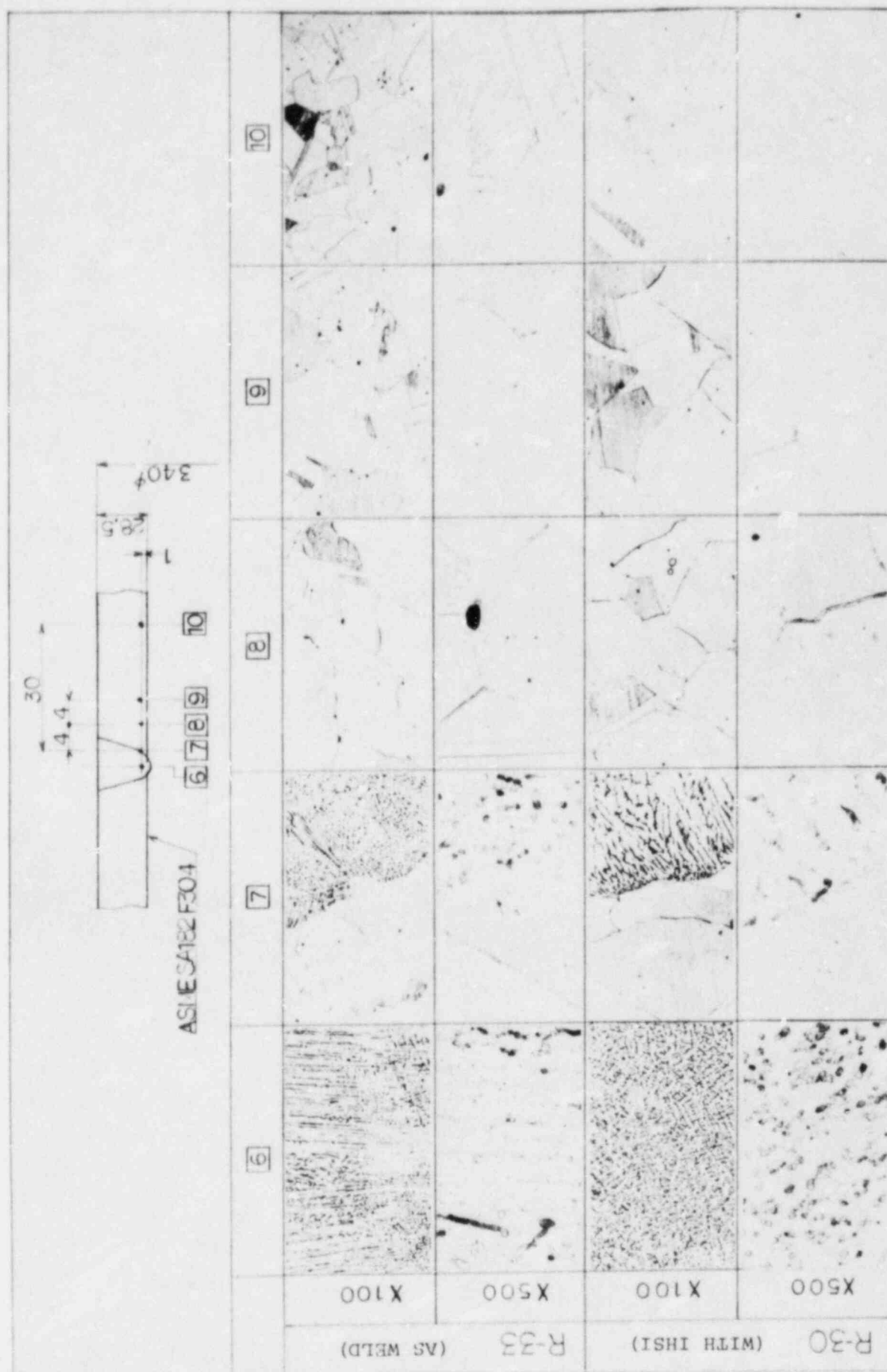
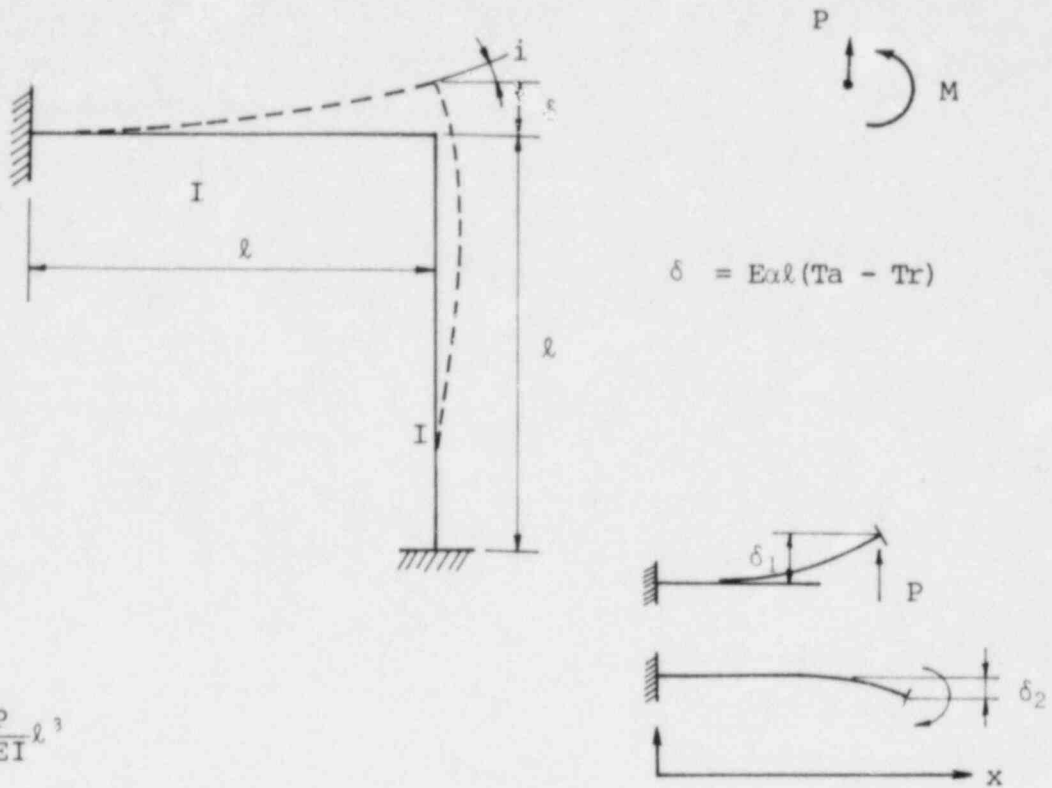


FIG. 11 R-30, R-33 MICRO STRUCTURE OF OUTSIDE SURFACE





$$\delta_1 = \frac{P}{3EI} l^3$$

$$\delta_2 = - \frac{M}{2EI} l^2$$

$$i = \frac{P}{2EI} l^2 - \frac{Ml}{EI} = \frac{Ml}{EI}$$

$$\frac{Pl^3}{3EI} - \frac{M}{2EI} l^2 = \delta$$

$$\frac{Pl^2}{2EI} = \frac{2Ml}{EI}$$

$$M = \frac{1}{4} Pl$$

$$\frac{Pl^3}{3EI} - \frac{1}{2EI} \frac{Pl^3}{4} = \delta$$

$$\frac{(8-3)Pl^3}{24EI} = \delta$$

$$\therefore P = \frac{24}{5} \frac{EI}{l^3} \cdot \delta$$

Fig. 13 FORCE INDUCED BY LOCAL HEATING

SUBSECTION A

BASIC SURVEY

The effects of cooling water flow rate and coil width on the residual stress distribution of an IHSI treated pipe were studied experimentally. The results of that study are presented below.

1. Material

SUS 304 (AISI TYPE 304), 12B Schedule 100 pipe was used in this study.

The mechanical properties for this material are shown in Table 1.

2. Stress Relief Treatment

All pipes were stress relieved for 2 hours at 900°C to relieve the pipe fabrication residual stresses.

3. Heating and Cooling Details

Heating and cooling details for these pipes are presented in Table A-1.

4. Results (Fig. A-1,2,3)

4.1 Effect of Flow Rate (R-21 and R-22)

(a) The temperatures on the inside and outside surfaces were reduced as the flow rate increased.

(b) No significant effect of flow rate on the residual stress was observed.

4.2 Effect of Coil Width (R-22 and R-23)

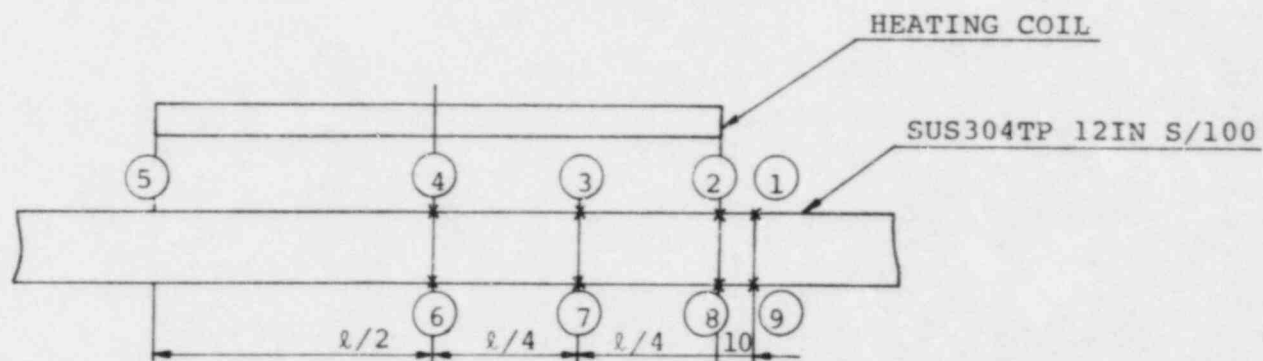
(a) The uniformly heated zone of pipe R-23 was smaller than pipe R-22 consistent with the differences in coil width.

(b) The stress improvement region became small as the coil width was reduced, but degree of stress improvement at the coil center did not change markedly.

TABLE A-1 HEATING PARAMETERS AND RESULT OF TEMPERATURE MEASUREMENTS

TP-No.	HEATING PARAMETERS								MAXIMUM TEMP. (°)										*1	Δ1
	FREQUENCY (kHz)	POWER (kW)	WIDTH OF COIL (mm)	HEATING DURATION (sec)	COOLING COND.			ROOM TEMP. (°C)	①	②	③	④	⑤	⑥	⑦	⑧	⑨	④-⑥		
					VELOCITY (m/sec)	ENT (°C)	EXIT (°C)													
R-21	3	300	250	180	0.72	21.5	22.5	22	220	311	526	537	334	102	98	81	-	435		
R-22	3	300	250	157	0.43	22.0	24.0	18	207	301	523	548	358	126	127	77	60	422		
R-23	1	250	200	125	0.43	22.0	24.0	18	199	293	535	558	387	122	122	67	34	436		

*1 The measured points are shown below.



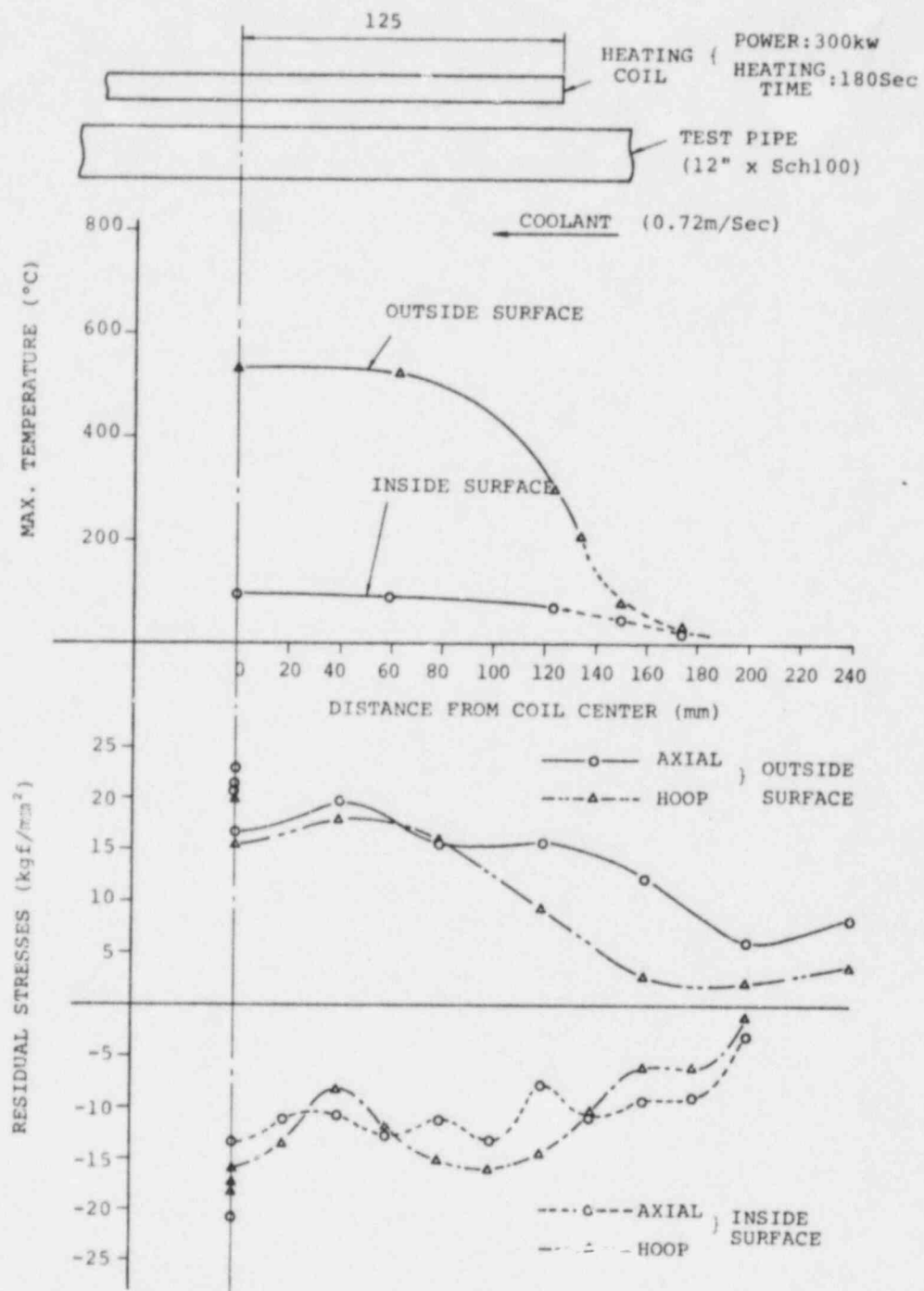


Fig. 2 A-1 MAXIMUM TEMPERATURE AND RESIDUAL STRESS DISTRIBUTION
FOR TEST PIPE

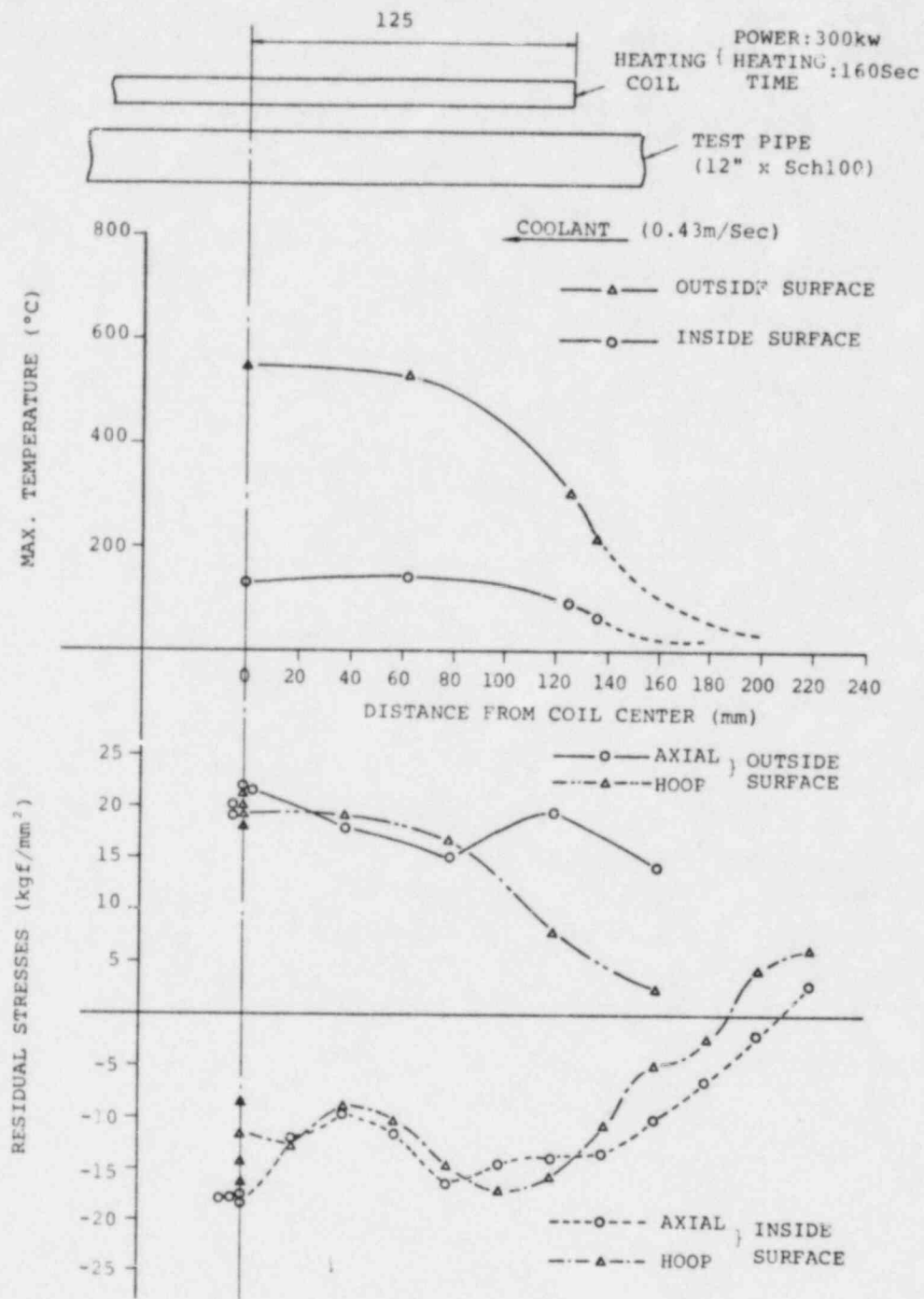


Fig. A-2 MAXIMUM TEMPERATURE AND RESIDUAL STRESS DISTRIBUTION
OF PIPE R-22

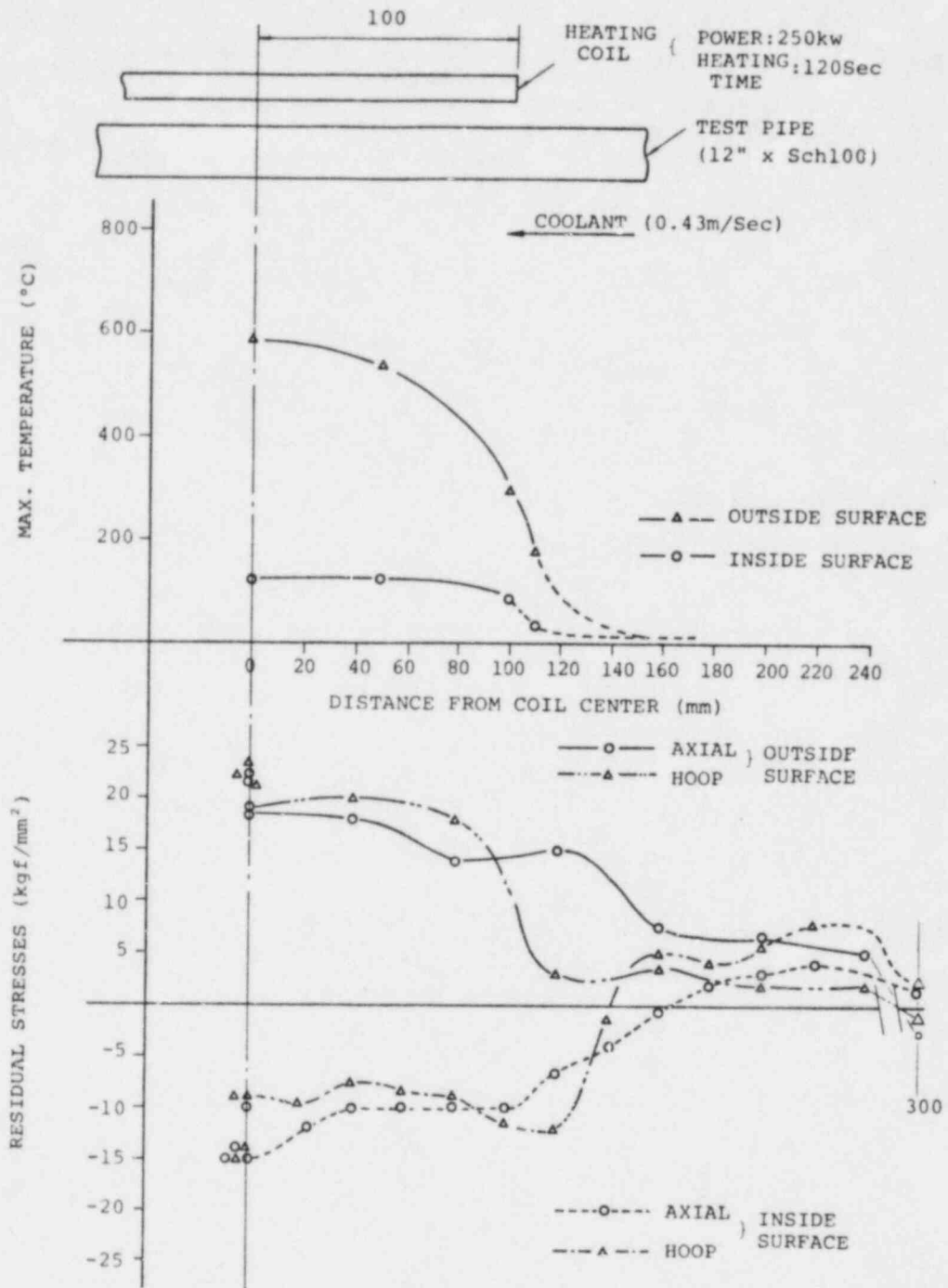


Fig. A-3 MAXIMUM TEMPERATURE AND RESIDUAL STRESS DISTRIBUTION
FOR TEST PIPE

SUBSECTION B

FINITE ELEMENT COMPUTER CALCULATIONS

Computer calculations were performed to obtain the through-thickness stress profile for the pipe and to evaluate the experimental results.

1. Finite Element Program Characteristics

Program name: ANSYS

Strain hardening rule: Kinetic strain hardening rule

2. Boundary Conditions and Calculated Models

Fig. B-1 Model for temperature calculation

Fig. B-2 Model for stress calculation

Fig. B-3 Finite element model

Fig. B-4 Heating pattern

Fig. B-5 Stress - strain relation at various temperature

Table B-1 Material properties

3. Results

3.1 Temperature Distribution (Fig. B-6,8)

(a) The calculated temperature distribution displayed a shape similar to the experimental results.

(b) The calculated temperature difference (ΔT) between the outside and inside surfaces was somewhat smaller than the experimental value.

3.2 Residual Stresses (Fig. B-6,7)

(a) Calculated residual stresses were very close to the experimental values.

(b) The stress improved area on inside surface was about 25 mm larger than the coil width.

(c) The depth in which the compressive stress remained was approximately 60% of the wall thickness.

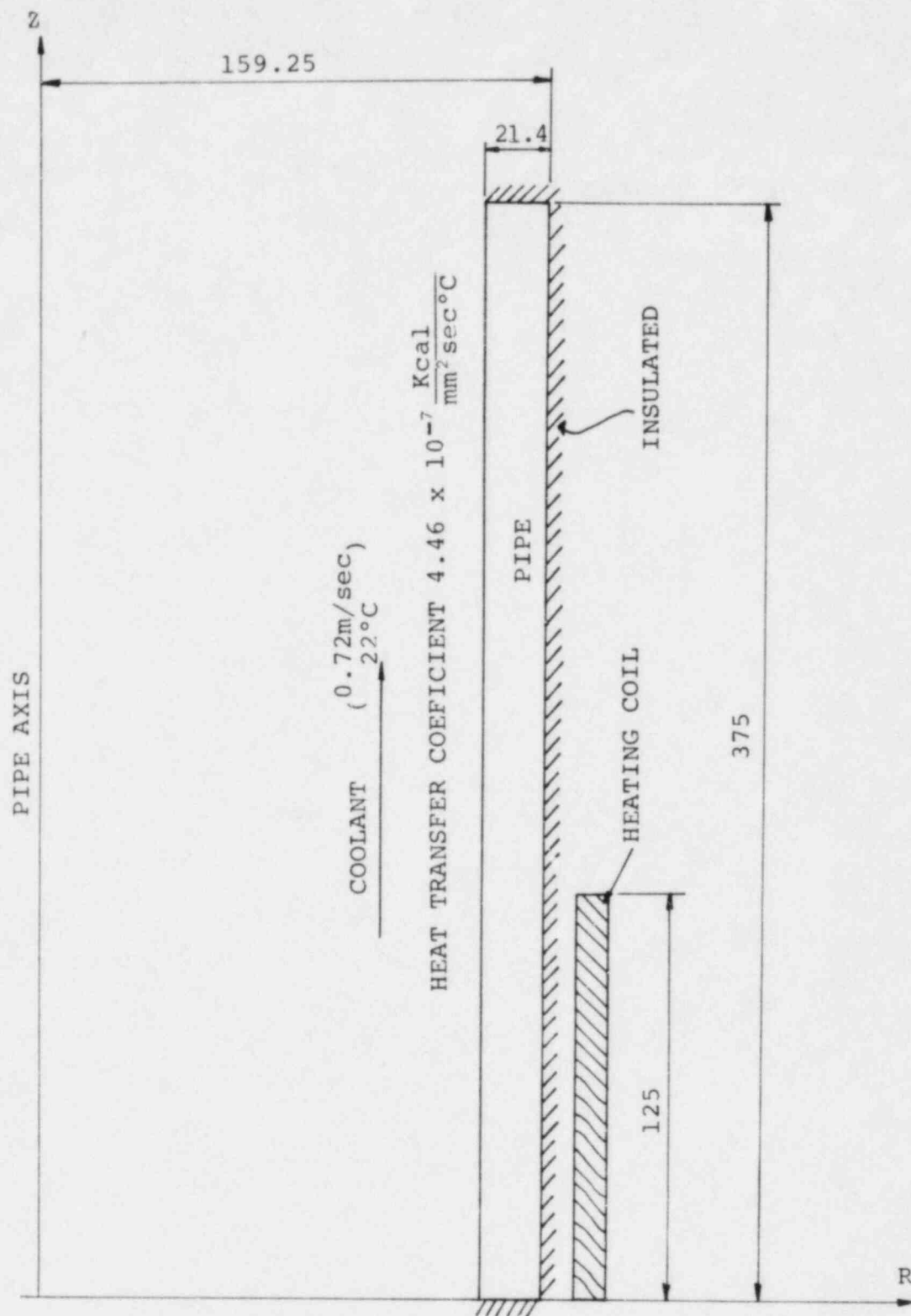


Fig. B-1 ANALYTICAL MODEL FOR HEAT TRANSFER

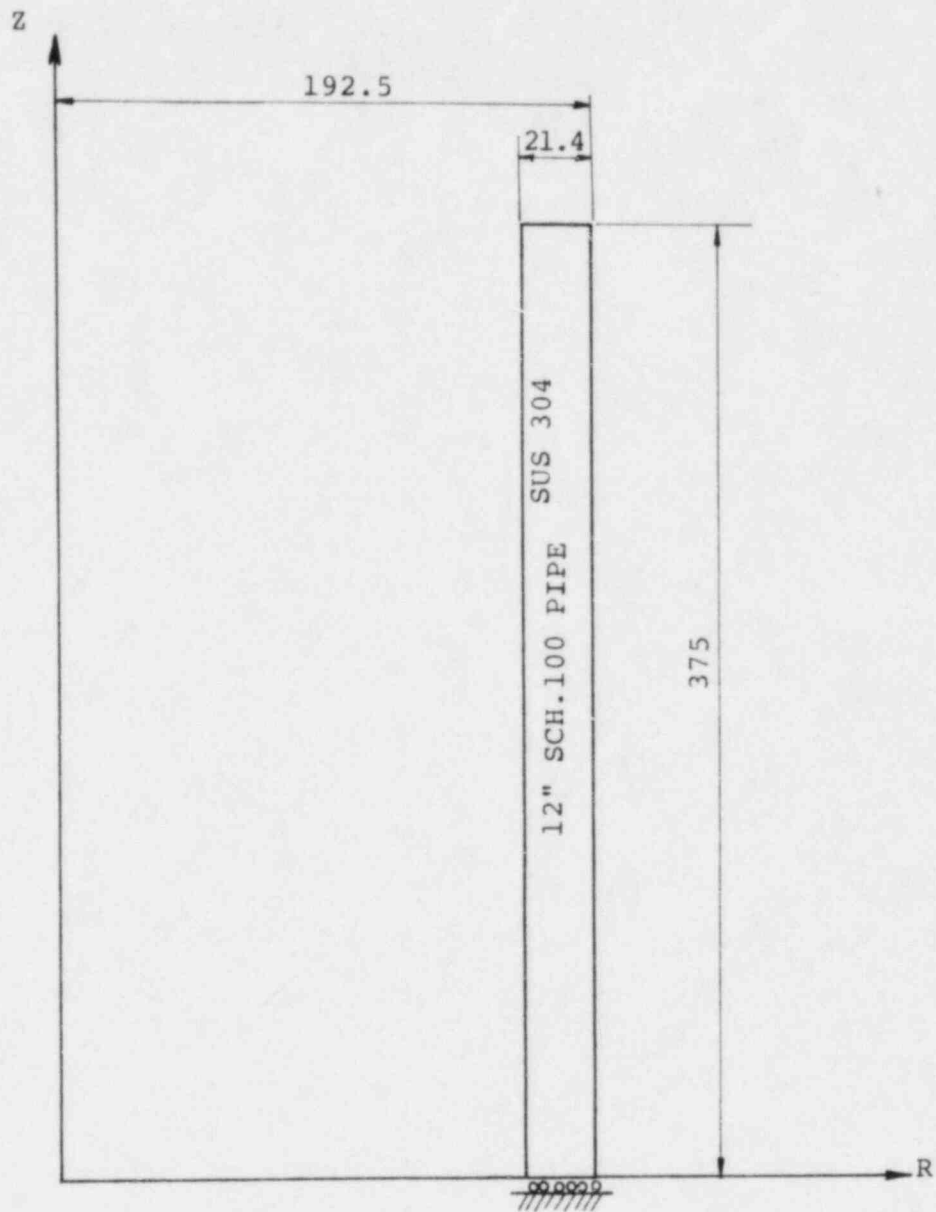


Fig. B-2 ANALYTICAL MODEL FOR STRESS

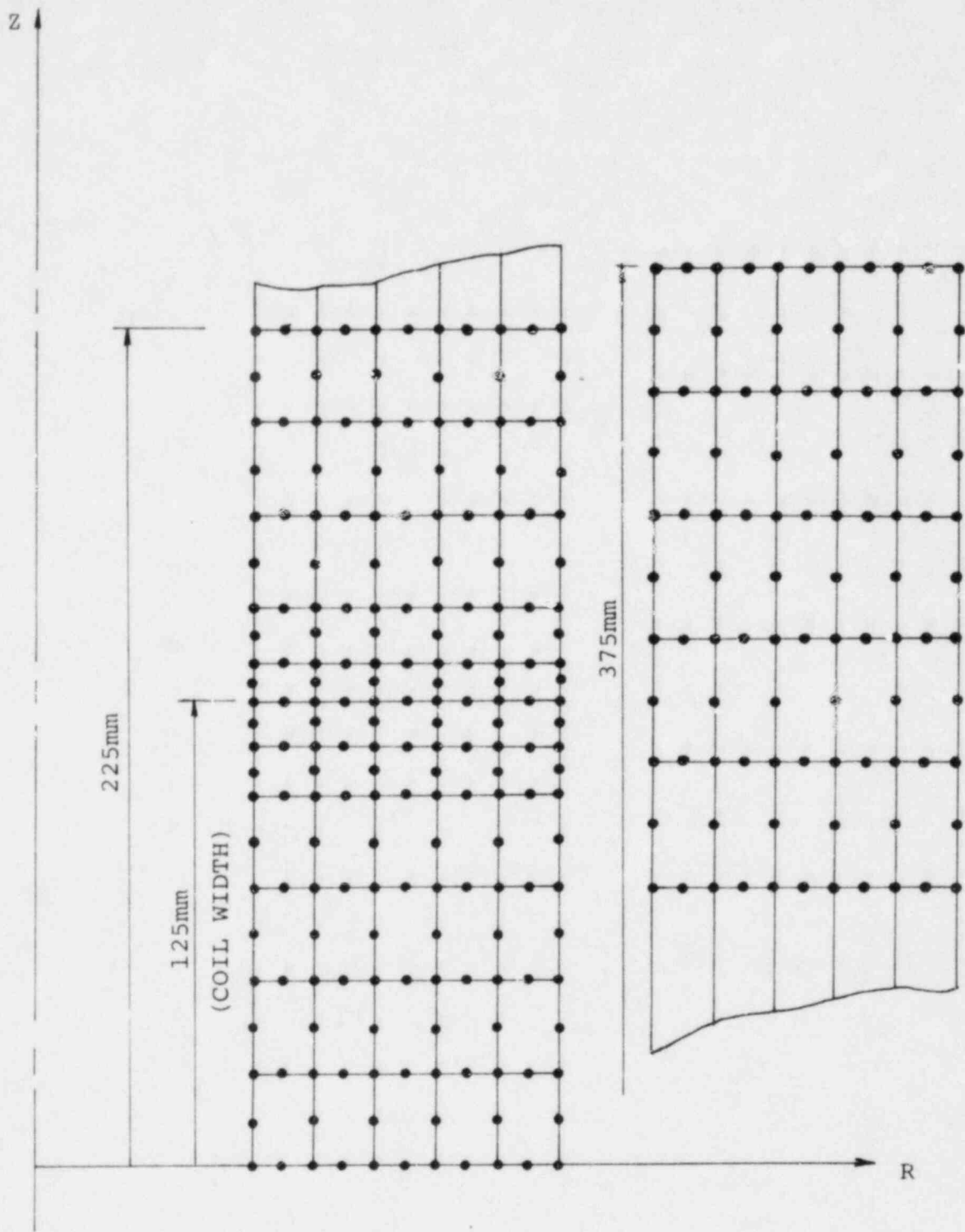


Fig. B-3 FEM MODEL

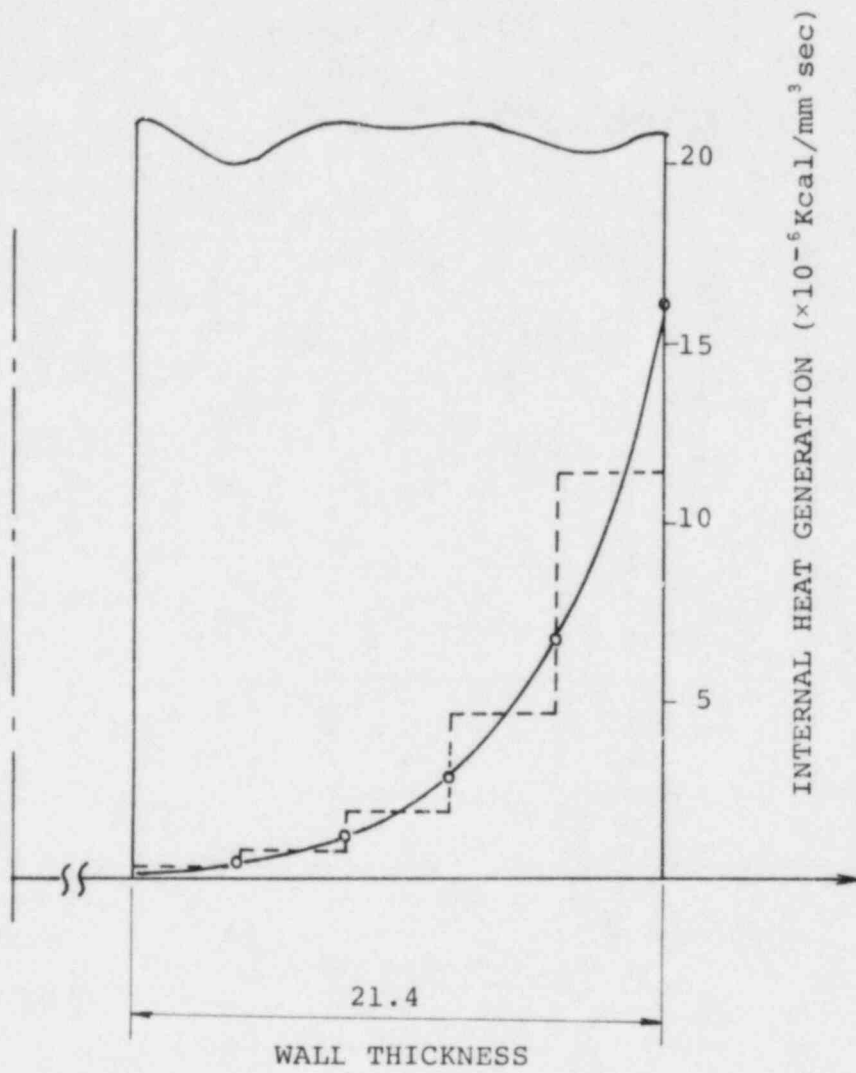


Fig. B-4 INTERNAL HEAT GENERATION

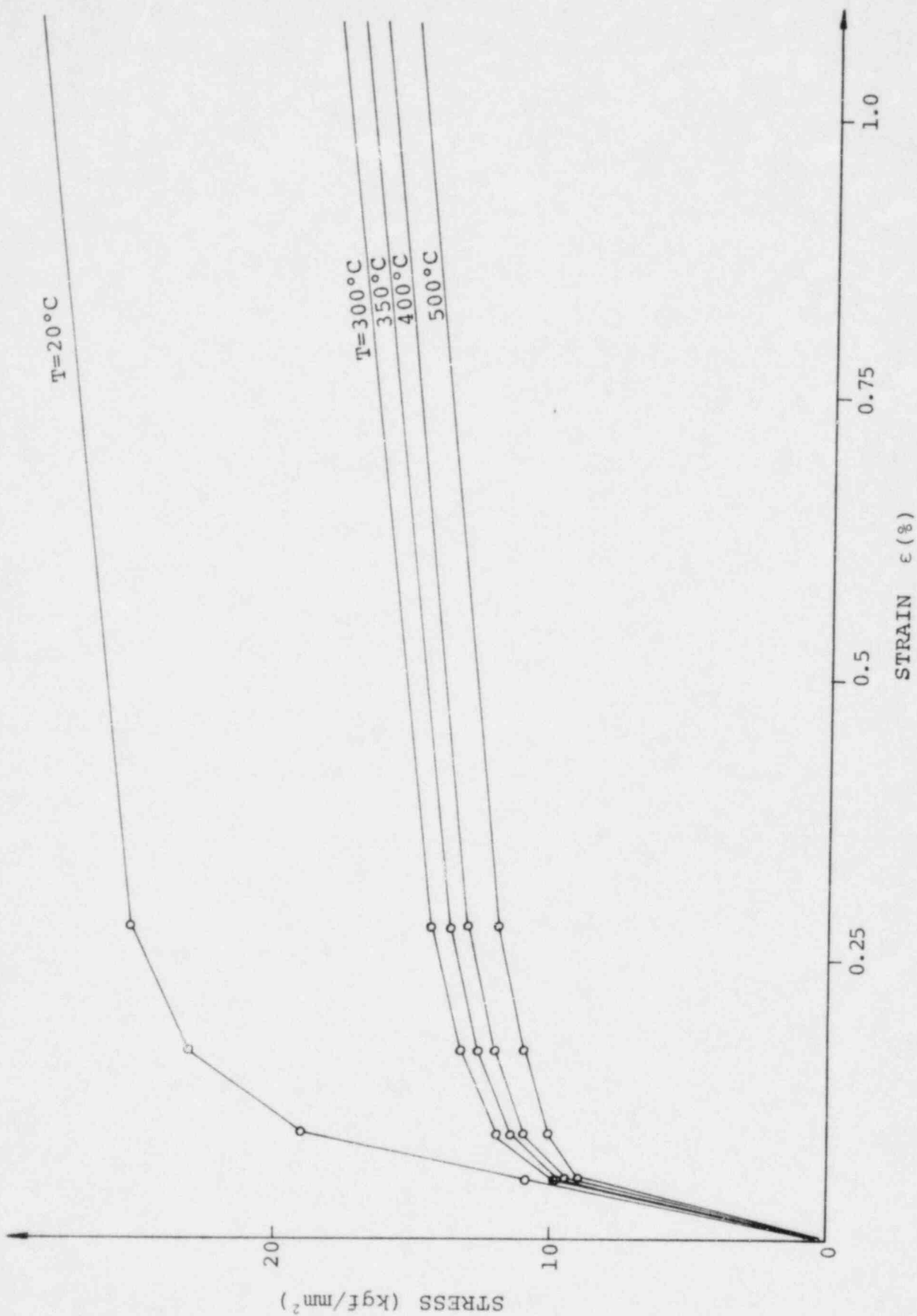


Fig. B-5 STRESS STRAIN CURVE AT TEMPERATURE

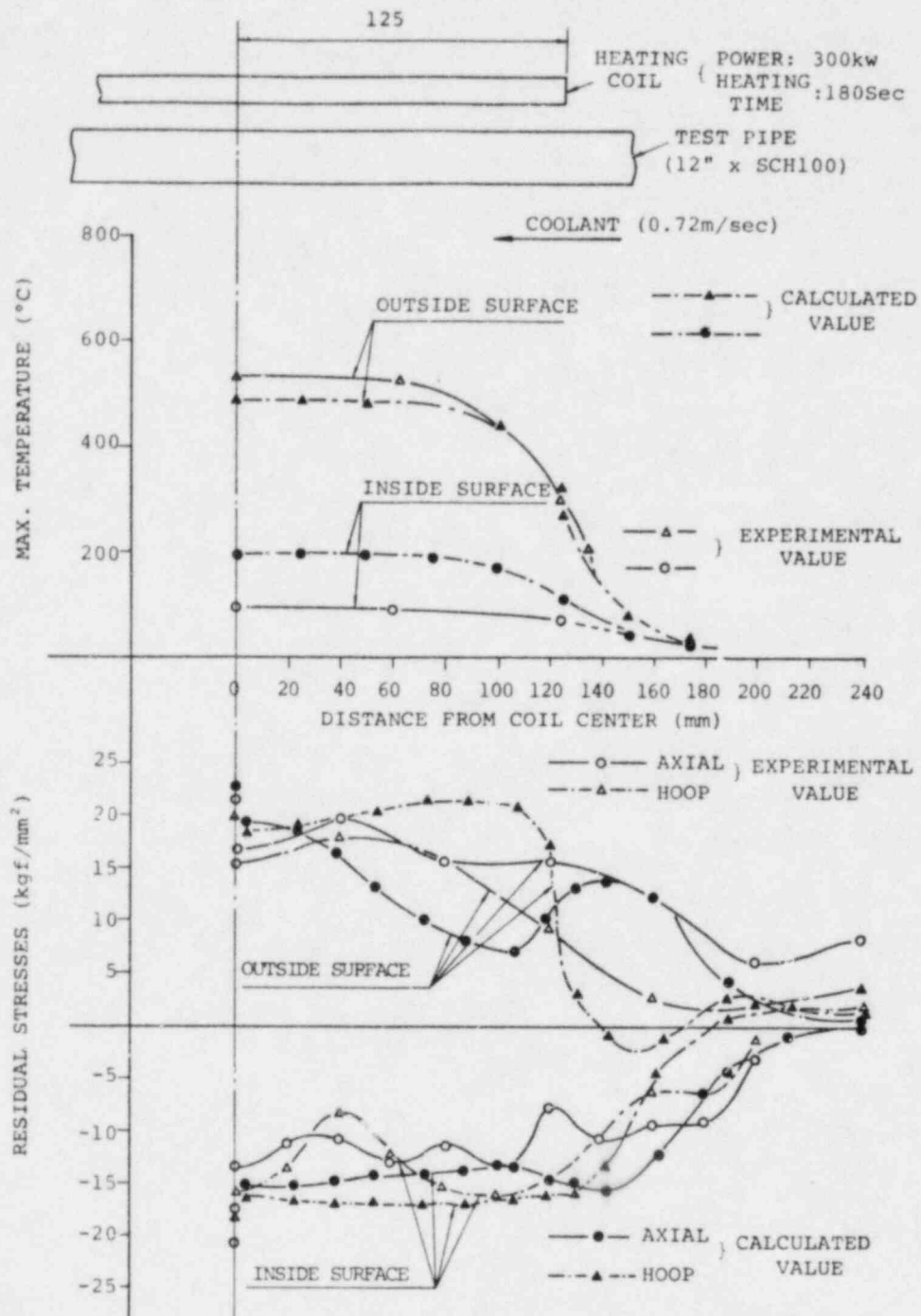
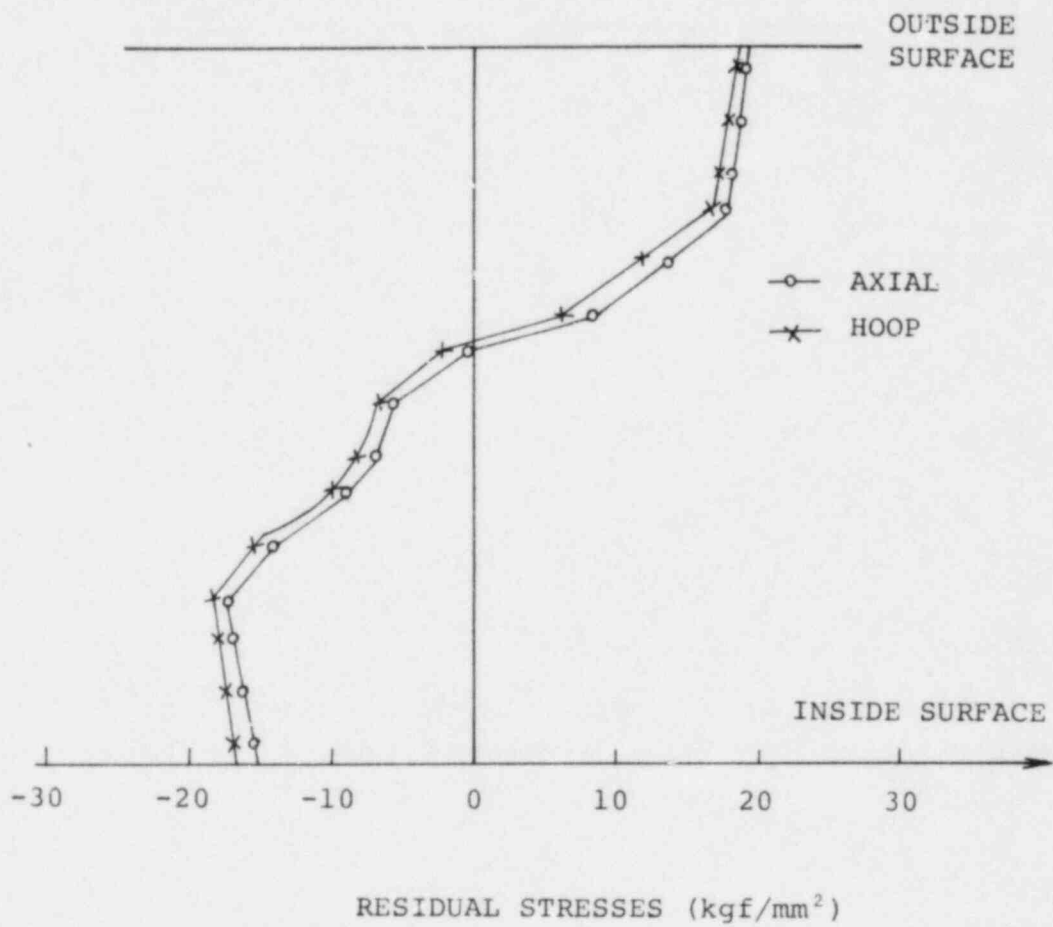


Fig. B-6 EXPERIMENTAL AND CALCULATED TEMPERATURE AND STRESSES
FOR PIPE R-21



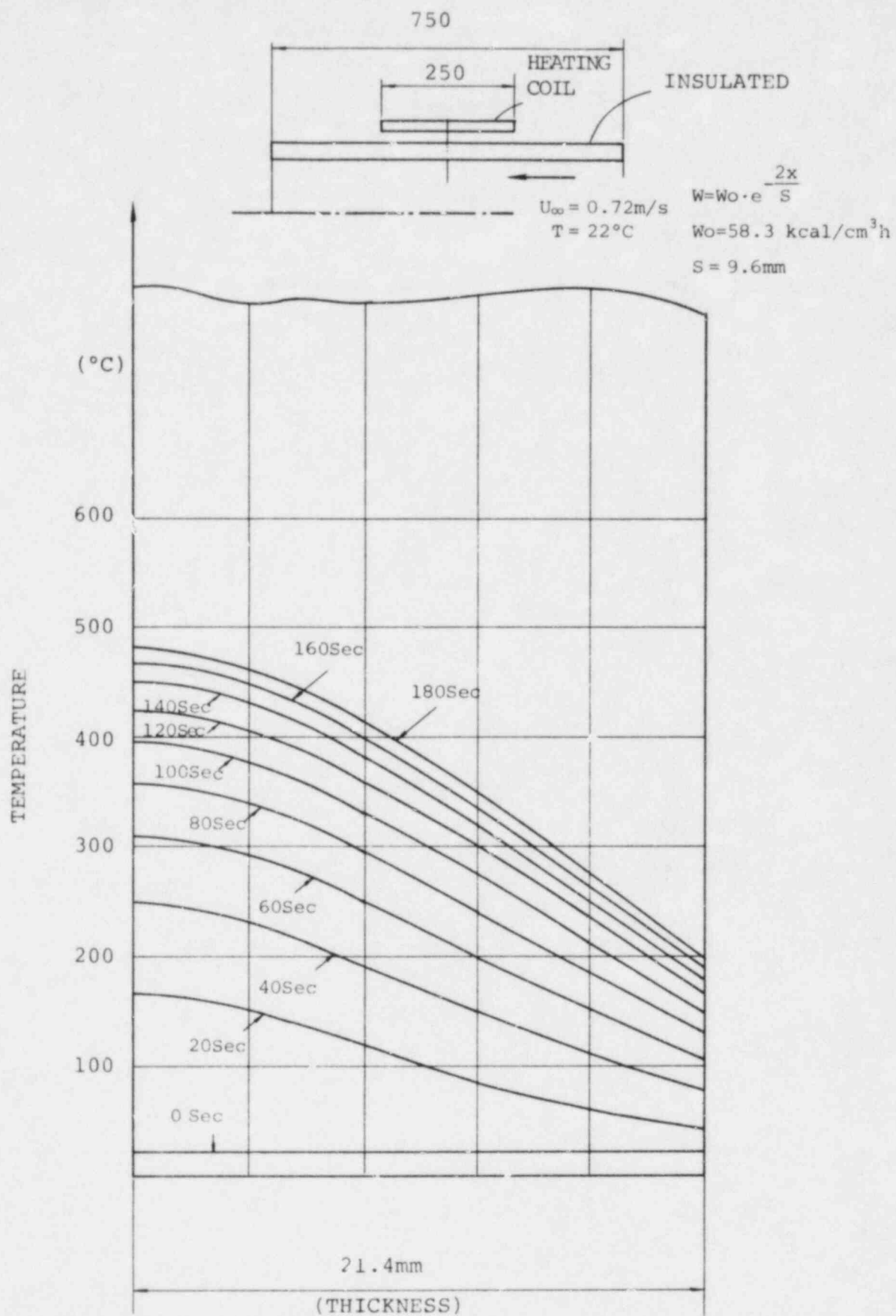


Fig. B-8 CALCULATED THROUGH-THICKNESS TEMPERATURE DISTRIBUTION

TABLE B-1. MATERIAL PROPERTIES USED IN FINITE ELEMENT MODEL

TEMPERATURE (°C)	THERMAL CONDUCTIVITY (Kcal/cm-s-°C)	SPECIFIC HEAT (Kcal/kg-°C)	THERMAL DIFFUSIVITY (cm ² /s)
20	34.7×10 ⁻⁶	0.107	
50	35.7	0.112	0.0390
100	37.2	0.117	0.0399
150	38.9	0.122	0.0409
200	40.5	0.125	0.0420
250	42.1	0.127	0.0432
300	43.7	0.130	0.0439
350	45.4	0.131	0.0447
400	47.0	0.132	0.0453
450	48.6	0.134	0.0462
500	50.3	0.135	0.0470
550	51.8	0.137	0.0478
600	53.5	0.139	0.0487
650	55.1	0.141	0.0497
700	56.7	0.143	0.0506
750	58.3	0.145	0.0514
800	59.9	0.148	0.0523

TEMPERATURE (°C)	YOUNG'S MODULUS (kg/cm ²)	POISSON'S RATIO	DENSITY (kg/cm ³)
20	1.98×10 ⁻⁶	0.260	8.03×10 ⁻³
50	1.97	0.264	8.02
100	1.95	0.270	8.00
150	1.91	0.274	7.97
200	1.88	0.278	7.95
250	1.84	0.281	7.93
300	1.79	0.284	7.90
350	1.76	0.288	7.88
400	1.72	0.292	7.86
450	1.67	0.296	7.83
500	1.63	0.300	7.81
550	1.58	0.304	7.79
600	1.53	0.308	7.77
650	1.47	0.314	7.74
700	1.41	0.318	7.72
750	1.36	0.320	7.70
800	1.31	0.324	7.67

TABLE B-1. - continued

TEMPERATURE (°C)	THERMAL EXPANSION (INSTANTANEOUS) (1/°C)	THERMAL EXPANSION (MEAN FROM R.T.) (1/°C)
20	16.4×10^{-6}	16.4×10^{-6}
50	16.7	16.6
100	17.1	16.8
150	17.5	17.1
200	17.9	17.3
250	18.3	17.4
300	18.6	17.6
350	19.0	17.8
400	19.3	18.0
450	19.8	18.2
500	20.2	18.4
550	20.5	18.6
600	20.9	18.7
650	21.3	18.9
700	21.6	19.0
750	22.0	19.1
800	22.4	19.2

SUBSECTION C

COMPUTER CALCULATION BY FEM (II)

Computer calculations were performed to investigate the effect of the weld deposit on residual stresses produced by the IHSI process.

1. Finite Element Program

Program name: ANSYS

Strain hardening rule: Kinetic strain hardening rule

2. Boundary Condition and Calculated Model

Fig. C-1 Model for temperature calculation

Fig. C-2 Model for stress calculation

Fig. C-3 Finite element model

Heating pattern: Fig. B-4

Material properties: Table B-1

The yield strength of the weld metal was assumed to be 140% of the base metal at every temperature.

3. Results

Fig. C-4,5,6 present the principal results

No significant change from Fig. B-6 and 7 in residual stress distribution was observed when the weld metal is added to the finite element model.

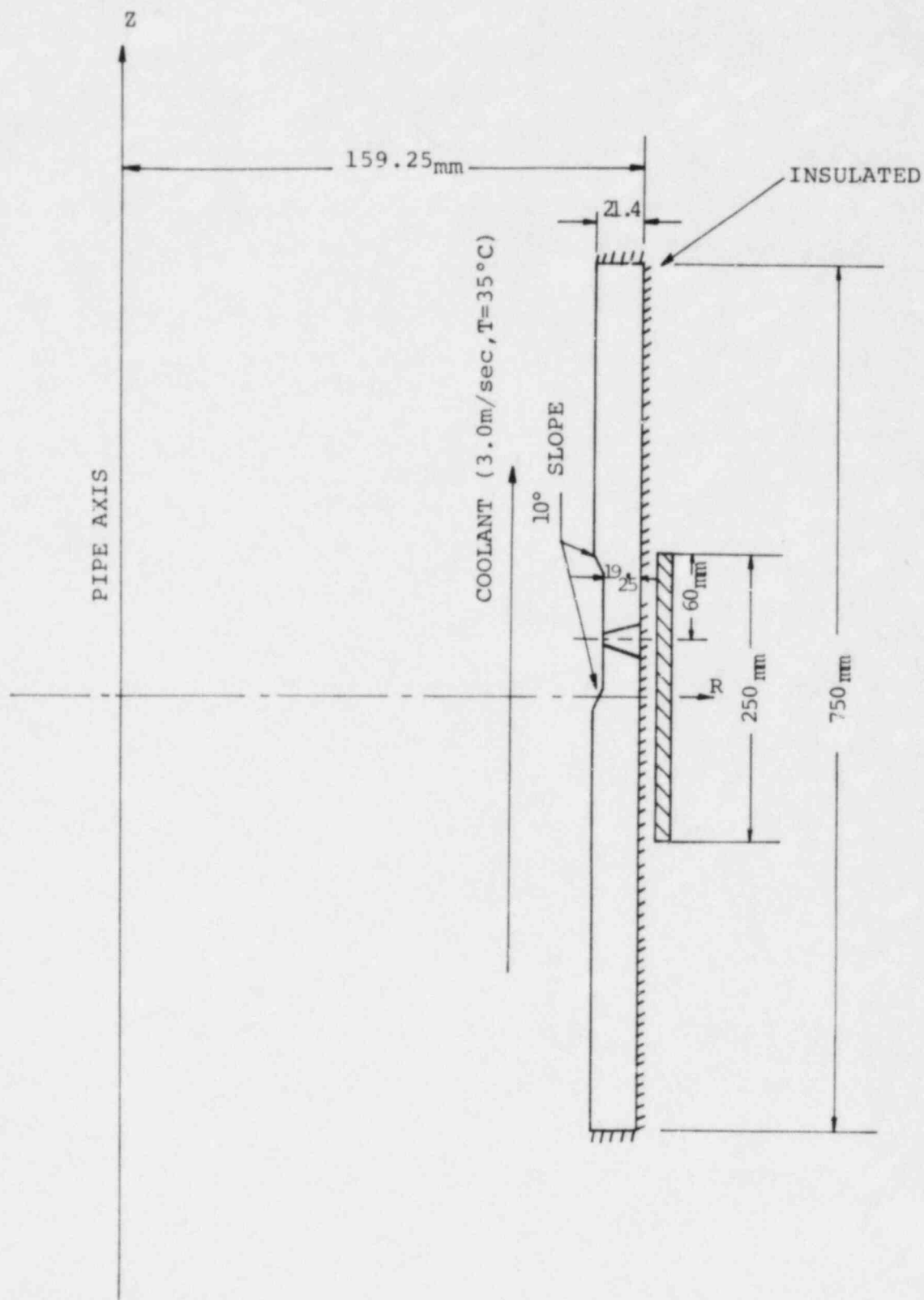


Fig. C-1 ANALITICAL MODEL FOR TEMPERATURE

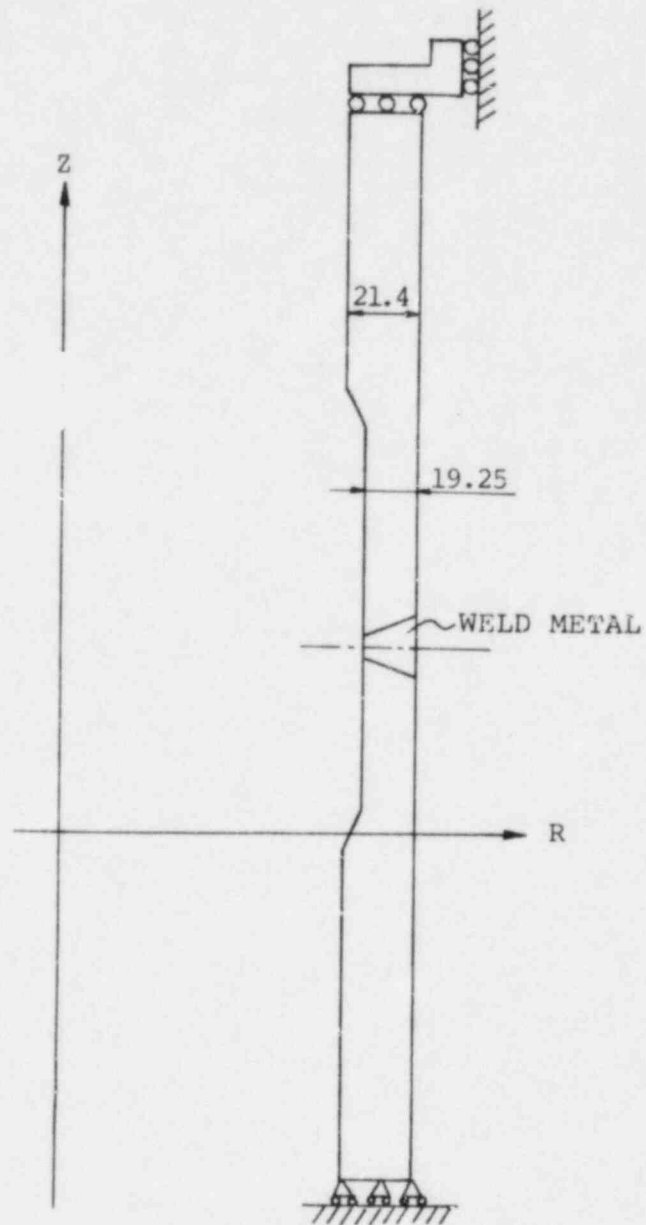


Fig. C-2 ANALYTICAL MODEL FOR STRESS

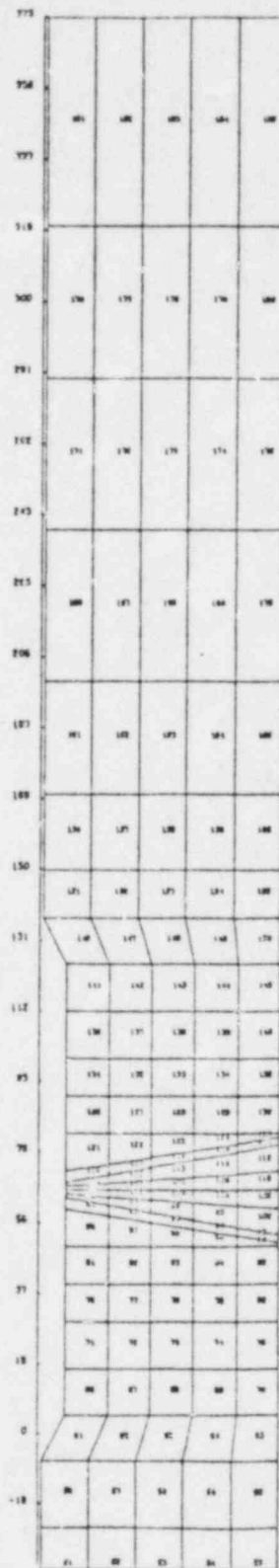


Fig. C-3
FEM MODEL

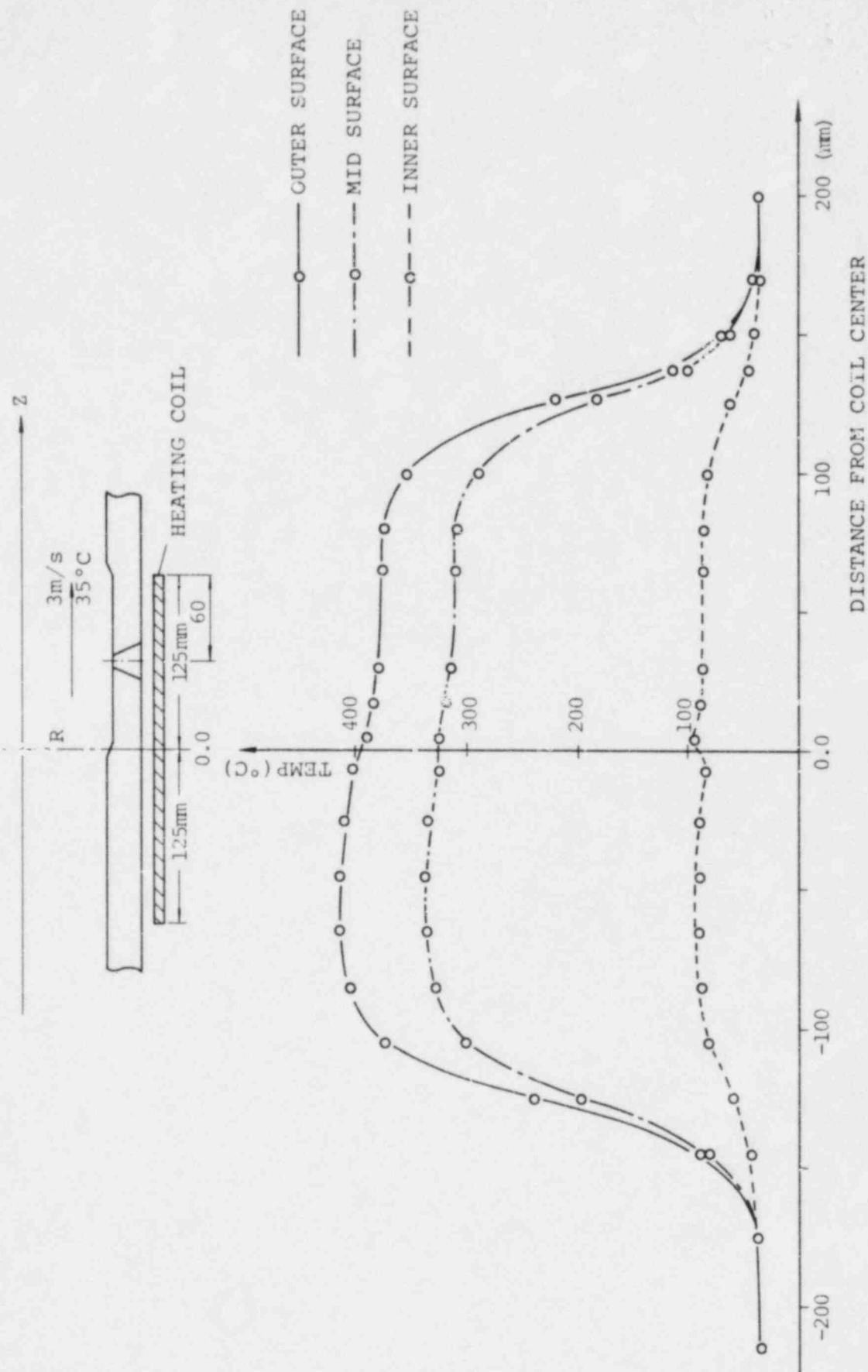


Fig. C-4 CALCULATED TEMPERATURE DISTRIBUTION

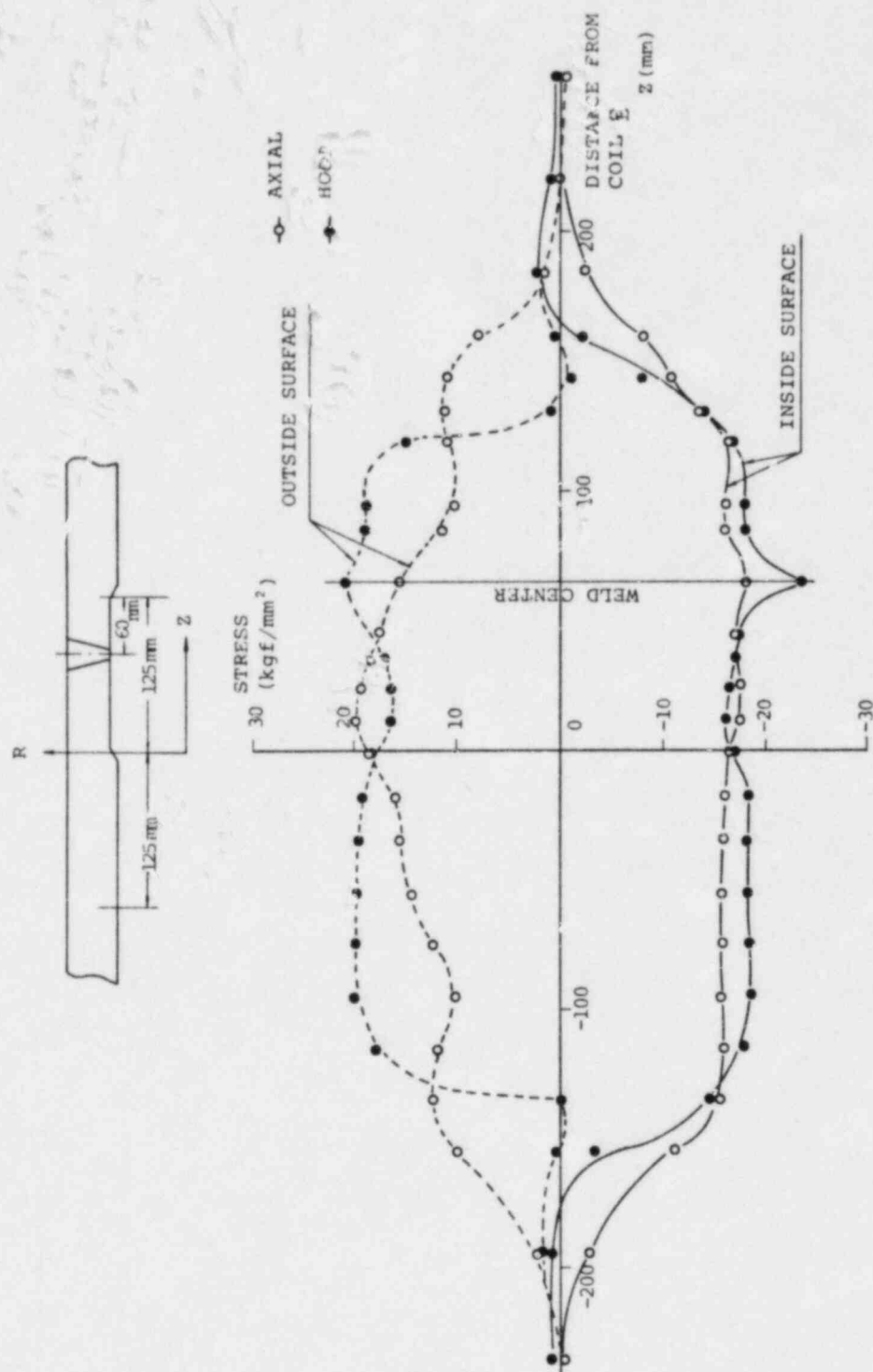


Fig. C-5 CALCULATED RESIDUAL STRESSES

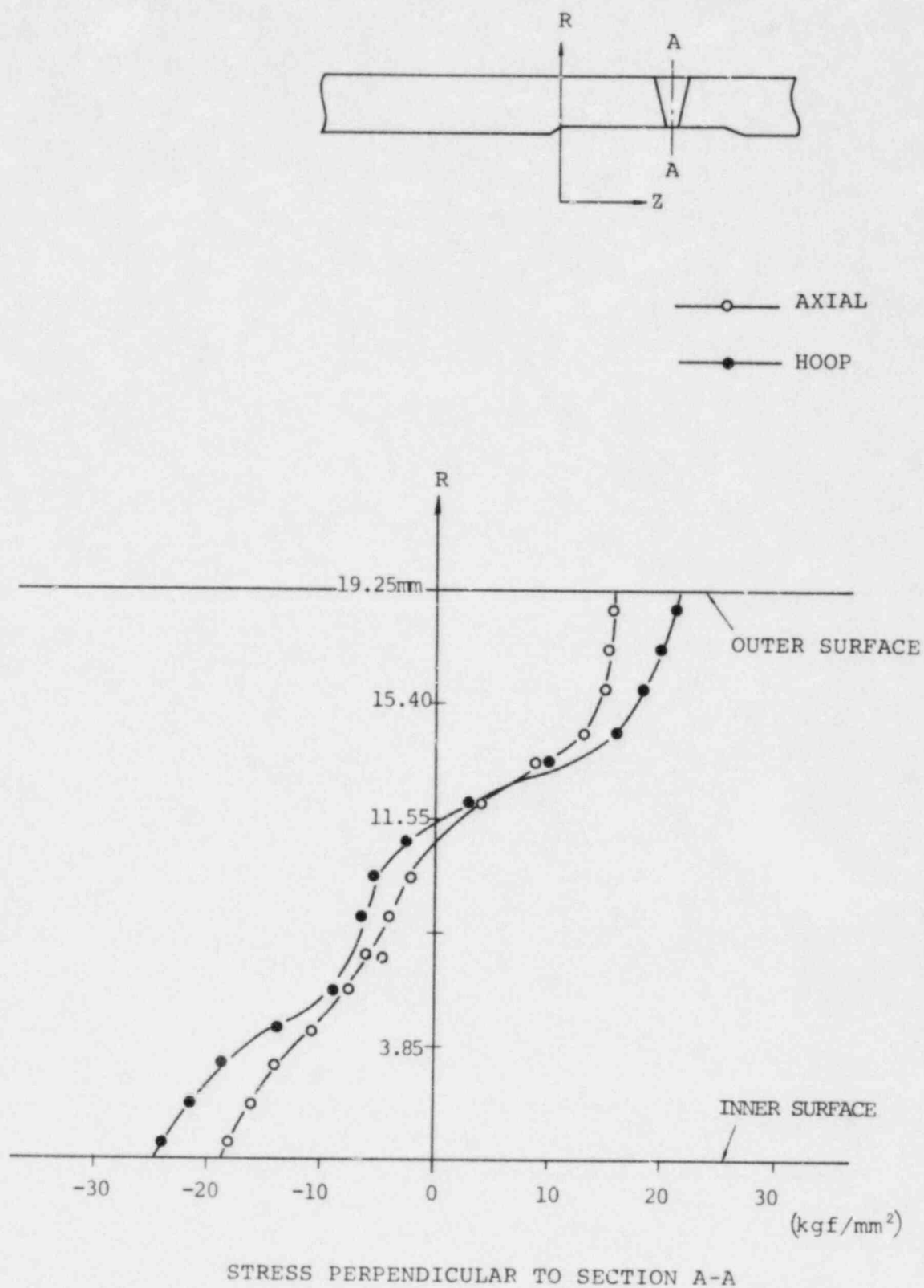


Fig. C-6 CALCULATED RESIDUAL STRESSES

A - 4

IMPROVEMENT OF RESIDUAL STRESS PATTERN

IN PIPE WELDMENT

(4TH REPORT)

SUMMARY

In order to verify the effectiveness of IHSI (Induction Heating Stress Improvement) in the presence of some crack like defects near the weld, a cracking test was conducted on two pipe weldments in boiling 42% magnesium chloride solution. Two small cracks were introduced by electric discharge machining on each pipe and one weldment was heat treated using IHSI prior to the MgCl_2 cracking test.

Liquid penetrant tests and microscope observation following the MgCl_2 exposure revealed that no crack had initiated on the artificial crack treated by IHSI. However, the untreated pipe exhibited some cracking.

1. Introduction

It had been previously reported that the residual stress pattern of a pipe weld joint can be altered by high frequency induction heating on the OD surface and simultaneous ID cooling. This treatment is named IHSI (Induction Heating Stress Improvement).

In the actual plant in service, some defects are anticipated to exist near the weldment and therefore it is one of the most important studies to verify the validity of IHSI in the presence of some defects.

In this study, IHSI was applied to a pipe weldment with notches machined by means of electric discharge.

This paper describes the results of the cracking test conducted on the notched pipes by exposing them to boiling 42 wt% MgCl_2 solution.

2. Experimental

(1) Material

The chemical composition and mechanical properties of 4B schedule 80 austenitic stainless steel used in the experiment are given in Table 1.

(2) Welding

Two test weldments were produced by automatic gas tungsten pulse-arc welding. Their welding conditions are given in Table 2.

(3) Notch Preparation

Two notches per one test pipe were prepared by electric discharge machining. Their dimension and location are given in Figure 1.

The depth of the notch was prepared to be about double the allowable planar surface indication of IWB in ASME Code Sect. XI, in Service Inspection that is $2 \times 12.5\%$ wall thickness. The aspect

ratio was made to be between 0.20 and 0.25.

(4) IHSI

IHSI was carried out on one test pipe under normal conditions and the temperature profile at maximum heating condition is given in Figure 2. No treatment was performed on the other pipe.

(5) Cracking Test

Both test pipes were immersed in boiling 42% MgCl_2 solution for 48 hours. After this treatment, their inner surface was observed by liquid penetrant examination. Micro-photographs near the notch tip were taken in order to check the existence of SCC in the direction of wall thickness.

3. Results and Discussion

Distribution of maximum heating temperature during IHSI is given in Figure 2. The significant temperature difference, $\Delta T = 2\sigma_Y (1 - \nu)/E\alpha$, was obtained in the range exceeding the width of the coil.

The results of liquid penetrant examinations are shown in Figure 3. Fig. 3(a) shows the notch by electric discharge machining. Fig. 3(b) and Fig. 3(c) show the results of liquid penetrant examination for pipes with IHSI and without IHSI, respectively. No cracks were observed on the inside surface of the pipe with IHSI while many cracks were found on those without IHSI. Fig. 4 and Fig. 5 show the results of the microphotographic examination near the notch tip. No SCC was observed at the notch tips in the pipe with IHSI, while significant cracking was found on those without IHSI.

It may be concluded that the effect of IHSI for a pipe weldment with cracks is significant for mitigation of SCC caused by welding residual stresses.

4. Conclusion

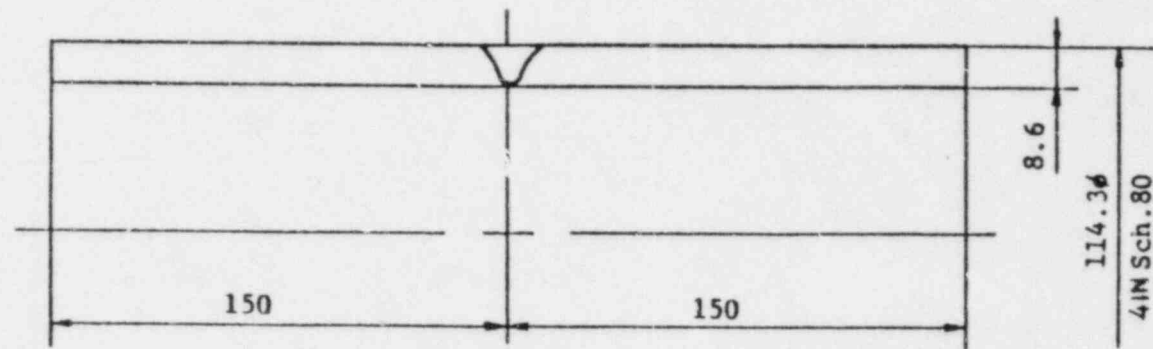
The results obtained in this study led to the following conclusions:

- (1) IHSI treatment can also improve the stress around the notch near the weldment.
- (2) The application of IHSI to a weldment with an existing crack is found to be significant in preventing IGSCC nucleation as well as propagation of an existing crack.

4^B Sch.80 SUS304 TP

Specified Charge No.	C	Si	Mn	S	Ni	Cr	Yield Point	Tensile Strength	Elongation
	max. 0.08	max. 1.00	max. 2.00	max. 0.030	max. 11.00	max. 20.00	21 (kg/mm ²)	53 (kg/mm ²)	35 (%)
TTC 3750	0.05	0.50	1.65	0.006	9.10	18.20	29	59	66

Table 1. Chemical Composition and Mechanical Properties of 4 inch Schedule 80 Pipe Used in This Evaluation.



	Welding Method	Position	Layer	Current (A)	Voltage (V)	Inter Pass Temp. (°C)	Heat Input (KJ/cm)	Welding Rod
R-53	Auto GTAW	1 G	1	60 ~ 150	7 ~ 10	≤ 70	9.9	
			2 ~ 3	60 ~ 170	8 ~ 10	≤ 70	6.1 ~ 9.1	Ø1.2 E308
R-54			4 ~ 5	180 ~ 230	10 ~ 11	≤ 70	15.4 ~ 19.9	

Table 2 Welding Condition

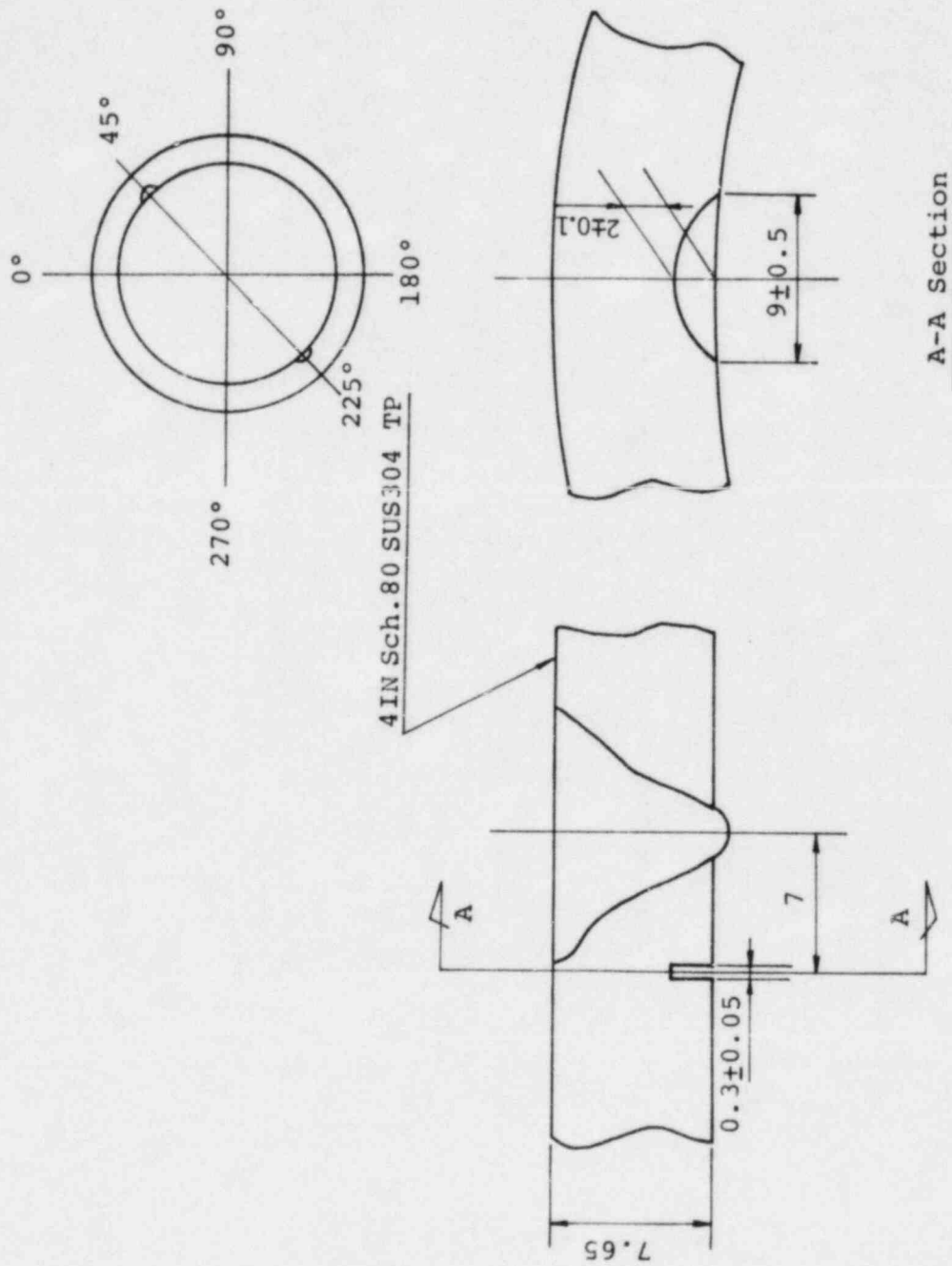


Fig. 1 Configuration of EDM Notches

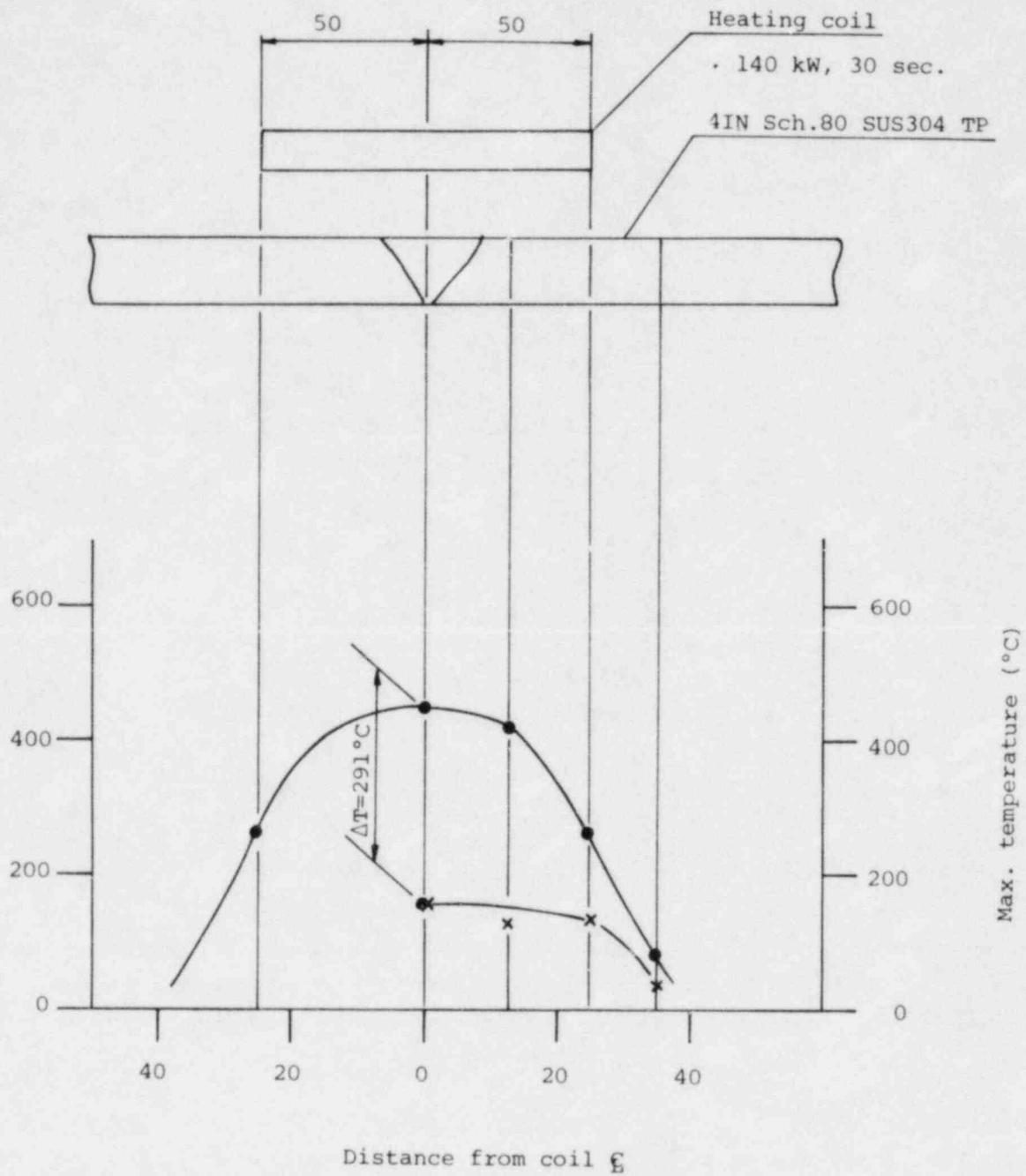
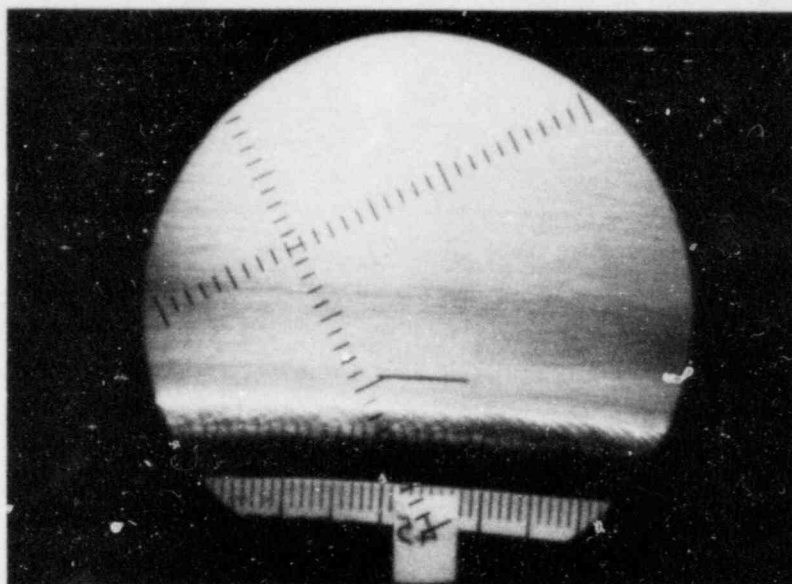


Fig. 2 TTD Curve (TP-No. R-53)

(a) EDM

(EDM: ELECTRIC
DISCHARGE
MACHINING)



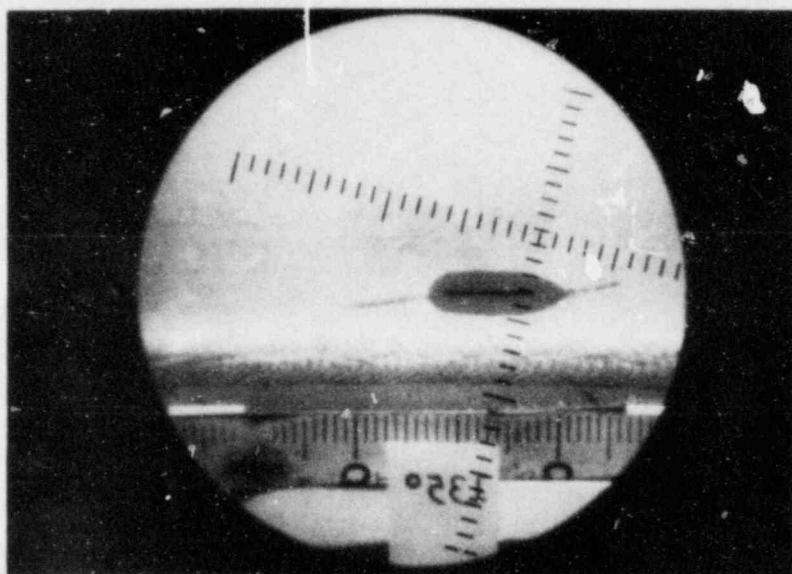
(b) EDM

↓

MgCl₂

↓

Propagation



(c) EDM

↓

IHSI

↓

MgCl₂

↓

No Propagation

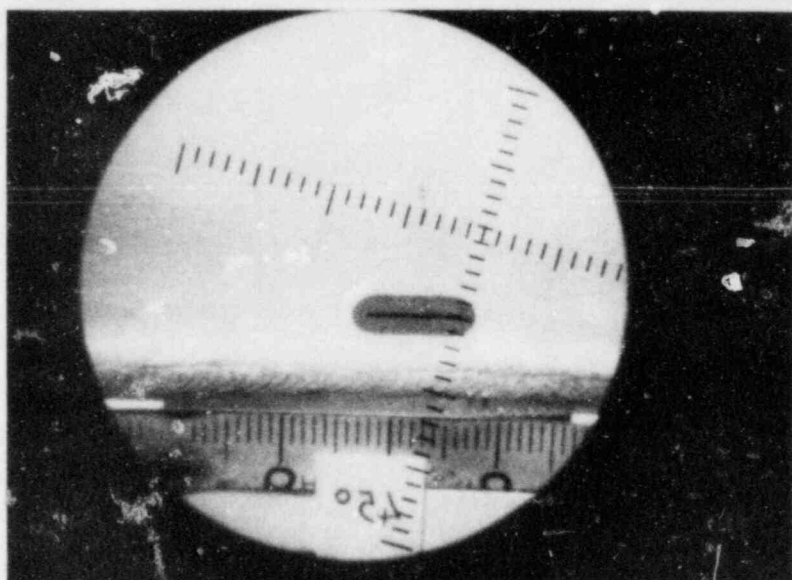


Fig. 3 Propagation Behavior of Notch

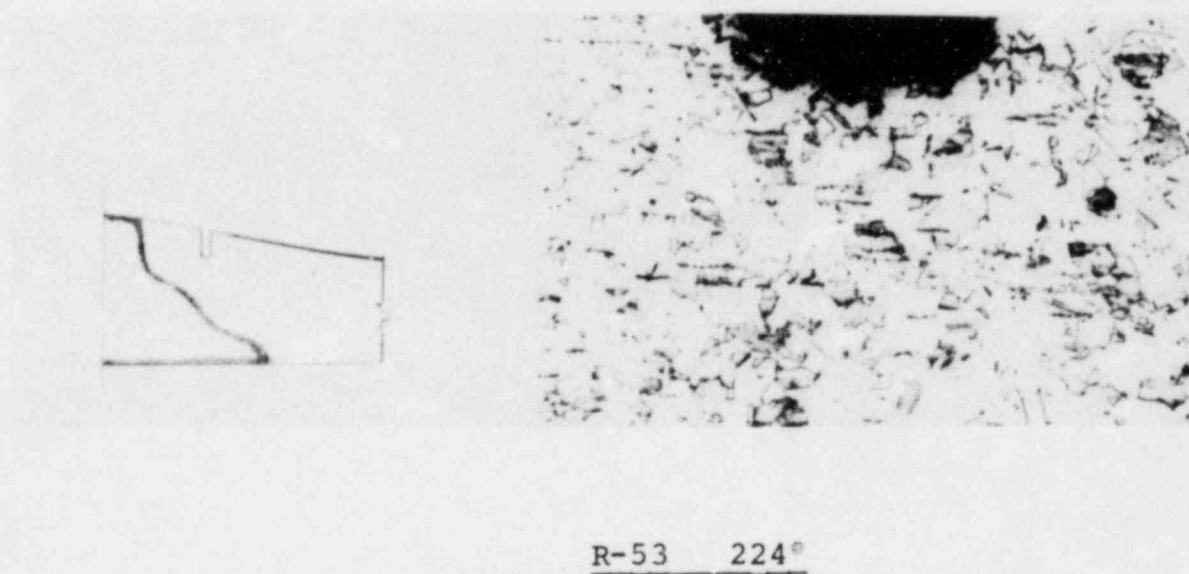
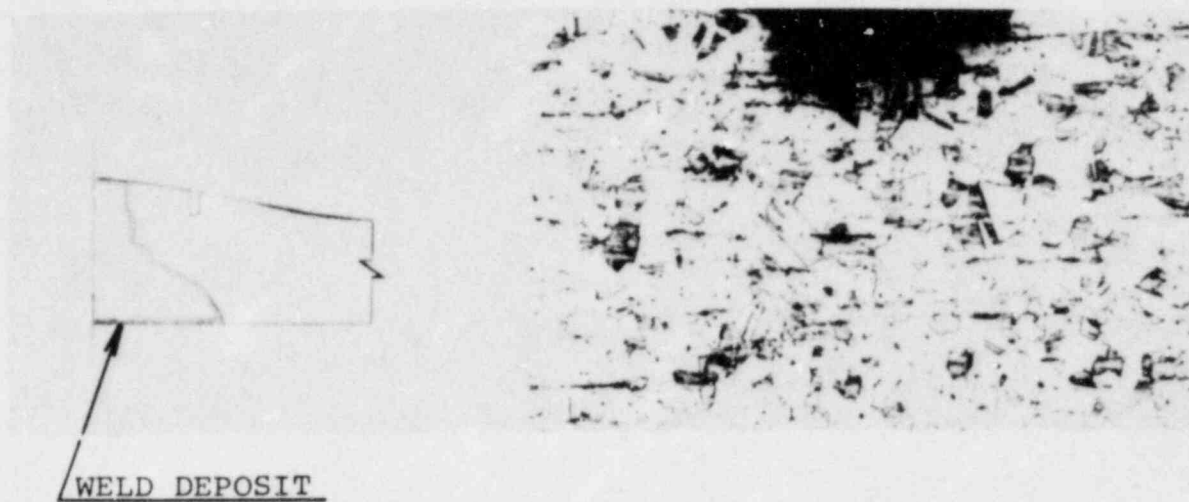


FIG. 4 CRACKING OBSERVATION AT NOTCH TIP (R-53)
MAG. X 100

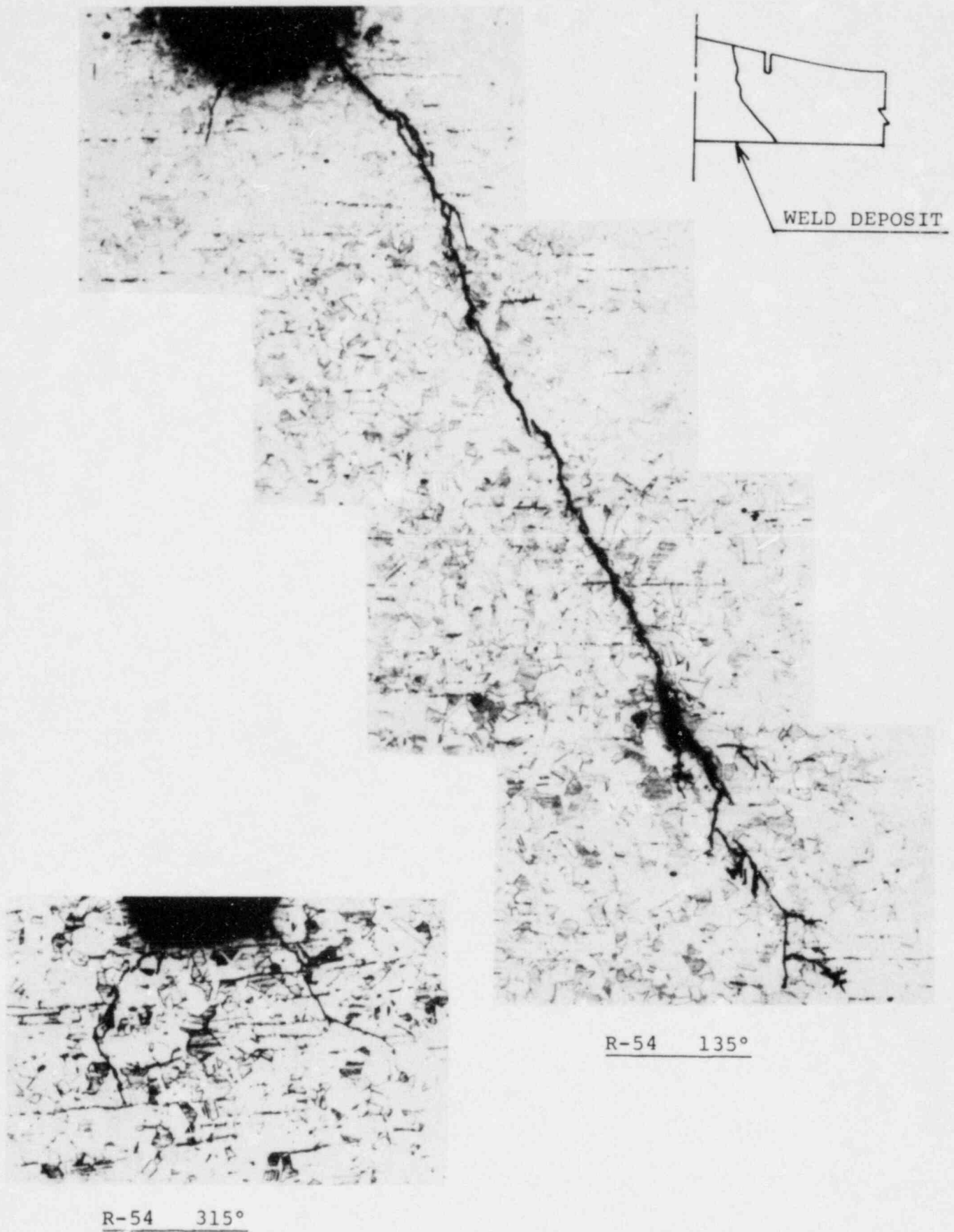


FIG. 5 CRACKING OBSERVATION AT NOTCH TIP (R-54)

A - 5

IMPROVEMENT OF RESIDUAL STRESS PATTERN

IN PIPE WELDMENT

SUMMARY

When IHSI is implemented in an actual plant, some trial heatings become necessary to confirm the heating parameters.

In this investigation, the effect of repeated IHSI treatment was investigated using 12 inch pipes. The residual stresses produced by multiple IHSI heating were compared with a normal single IHSI heat treatment. The results indicated multiple heating produces slightly more compressive residual stresses than a single IHSI heat treatment.

1. Introduction

It has been well documented that the residual stress pattern of a weld joint in pipe can be improved by high frequency induction heating and simultaneous water cooling. This method has been named IHSI (Induction Heating Stress Improvement).

When IHSI is applied to actual pipe weldments, it sometimes becomes necessary to make a trial heating in order to determine the hottest location and to determine the heating power to be used.

This paper describes the results of tests carried out to study the effect of multiple heating cycles on the residual stresses.

2. Experimental

The experimental sequence used in this investigation is shown in Figure 1.

2.1 Material

The chemical composition and mechanical properties of 12B schedule 100 austenitic stainless steel used in the experiment are shown in Table 1.

Table 1 CHEMICAL COMPOSITIONS AND MECHANICAL PROPERTIES

12^B Sch.100 SUS304 TP

Specified Charge No.	C	Si	Mn	P	S	Ni	Cr	Yield Point	Tensile Strength	Elongation
	max. 0.08	max. 1.00	max. 2.00	max. 0.040	max. 0.030	8.00 ~11.00	18.00 ~20.00	21 min. (kg/mm ²)	53 min. (kg/mm ²)	30 min. (%)
TTD 5156	0.06	0.59	1.84	0.020	0.050	9.65	18.70	22	55	74

2.2 IHSI

IHSI was performed in the sequence as shown in Figure 1 and Table 2.

The welding conditions are shown in Table 3.

For R-71, the initial 10 heatings simulated the trial heating to check the hottest point and the electric power to be used, and the last heating simulated the normal IHSI heat treatment. The first four heatings of R-72 simulated imperfect heatings which might result from disconnection of thermocouples or other reasons. A similar heating sequence to that described above is considered unavoidable when IHSI is applied to actual pipe weldments.

2.3 Residual Stress Measurements

Residual stresses on two IHSI'ed pipes were measured by conventional strain gage methods.

3. Results and Discussion

Figure 2 and Figure 3 show the maximum temperature distribution during 10th and 11th heating cycle, respectively for R-71.

For R-72, Figure 4 shows the maximum temperature distribution during 5th heating cycle.

The residual stress measurement results for R-71 and R-72 are shown in Figure 5 and are compared with results for R-21 on which one normal IHSI has

been conducted.

The residual stress at the coil center of R-72 was the maximum, and R-21 was the minimum, among three while the temperature differences were the same.

It is clear, therefore, that repeated heating produced larger compressive residual stress than single heating.

This phenomenon is thought to be caused by cyclic hardening characteristic of 18-8 austenitic stainless steel. A similar effect was also found on R-71.

4. Conclusion

The results obtained in this study lead to the following conclusions.

- (1) Repeating IHSI further improves the residual stress pattern of a welded austenitic stainless steel pipe.
- (2) The preliminary heating process contributes to improved residual stress for an IHSI treated pipe.

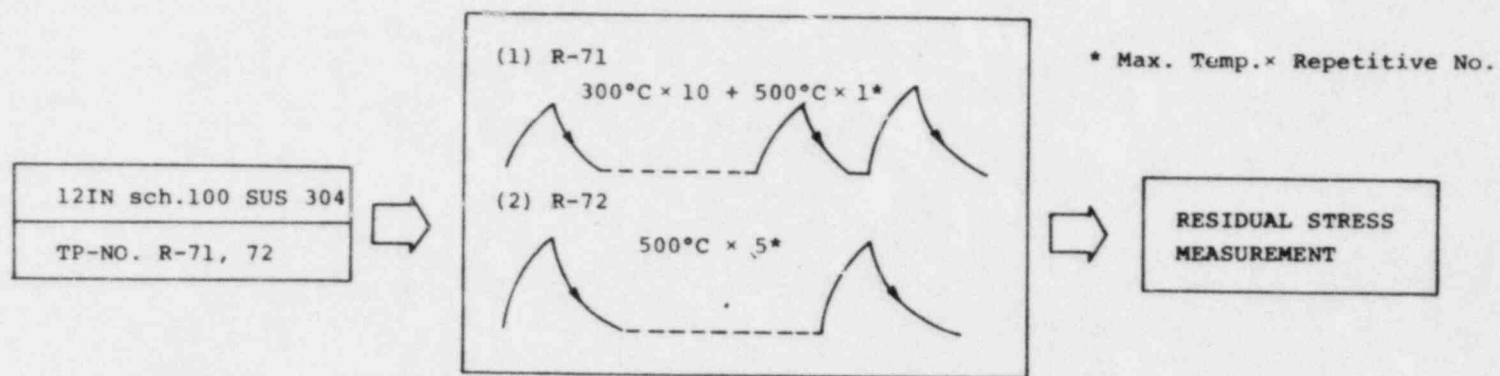
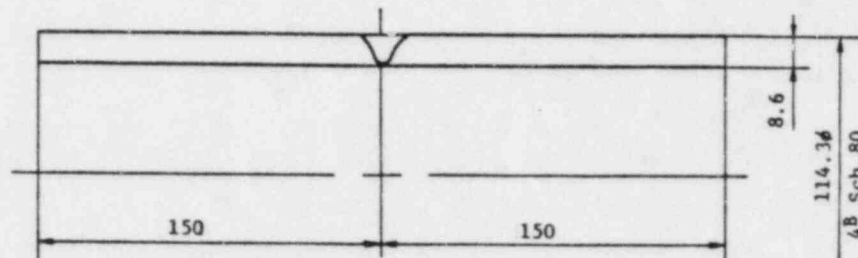


Fig. 1 Test Sequence

9

[illegible]



	Welding Method	Position	Layer	Current (A)	Voltage (V)	Inter Pass Temp. (°C)	Heat Input (KJ/cm)	Welding Rod
R-53	Auto GTAW	1 G	1	60 ~ 150	7 ~ 10	≤ 70	9.9	
			2 ~ 3	60 ~ 170	8 ~ 10	≤ 70	6.1 ~ 9.1	φ1.2 E308
R-54			4 ~ 5	180 ~ 230	10 ~ 11	≤ 70	15.4 ~ 19.9	

- Table 3. Welding Condition

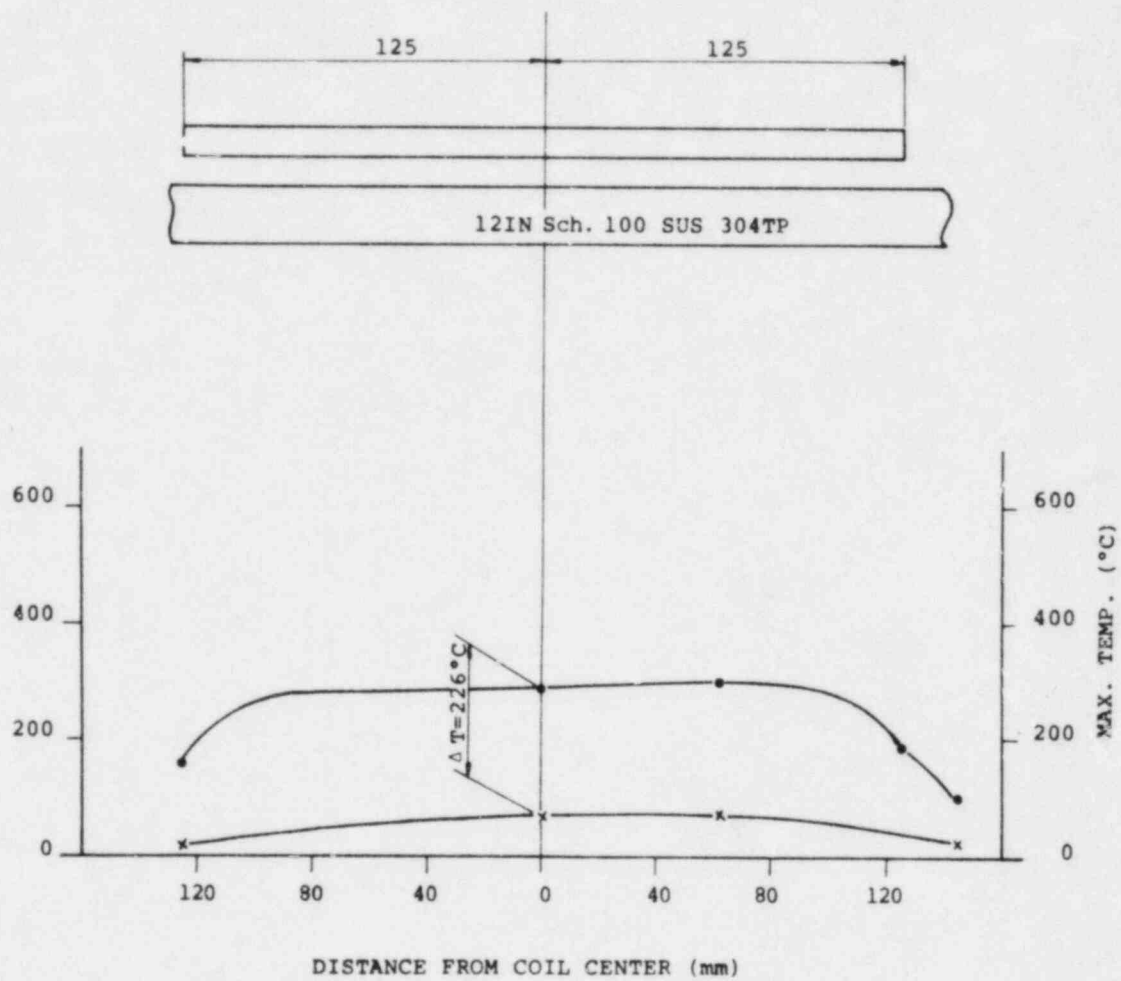


Fig. 2 TEMPERATURE DISTRIBUTION
(R-71, IHSI REPEAT NO.10)

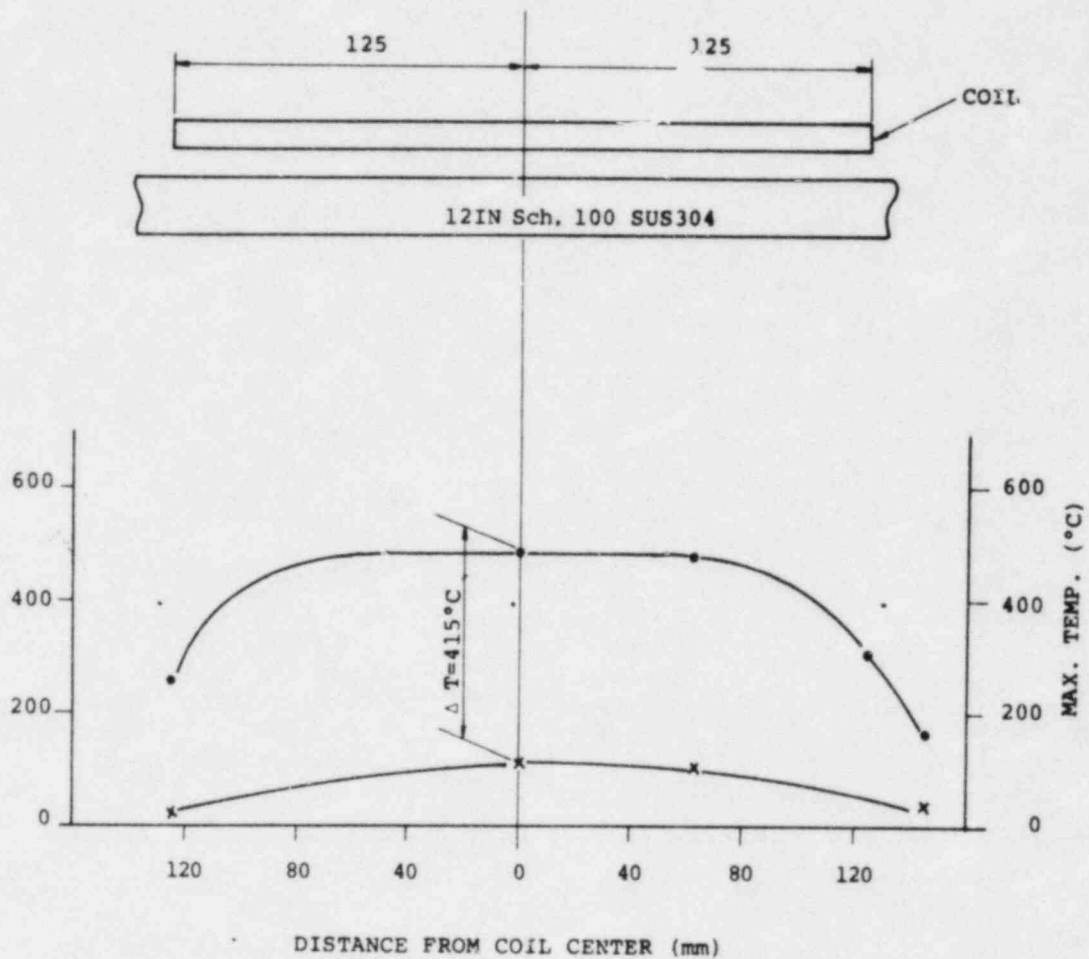


Fig. 3 TEMPERATURE DISTRIBUTION
(R-71, IHSI REPEAT NO.11)

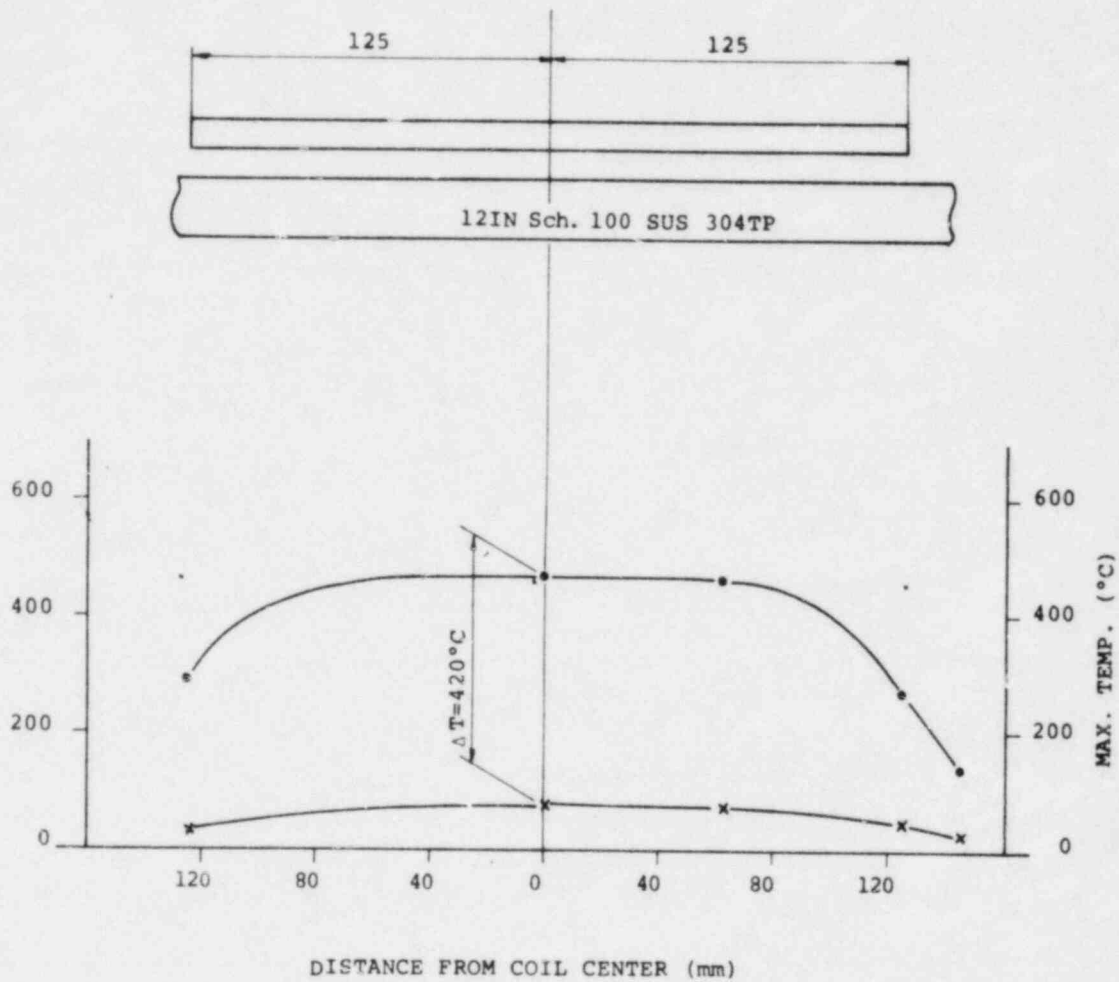


Fig. 4 TEMPERATURE DISTRIBUTION
(R-72, IHSI REPFAT NO.5)

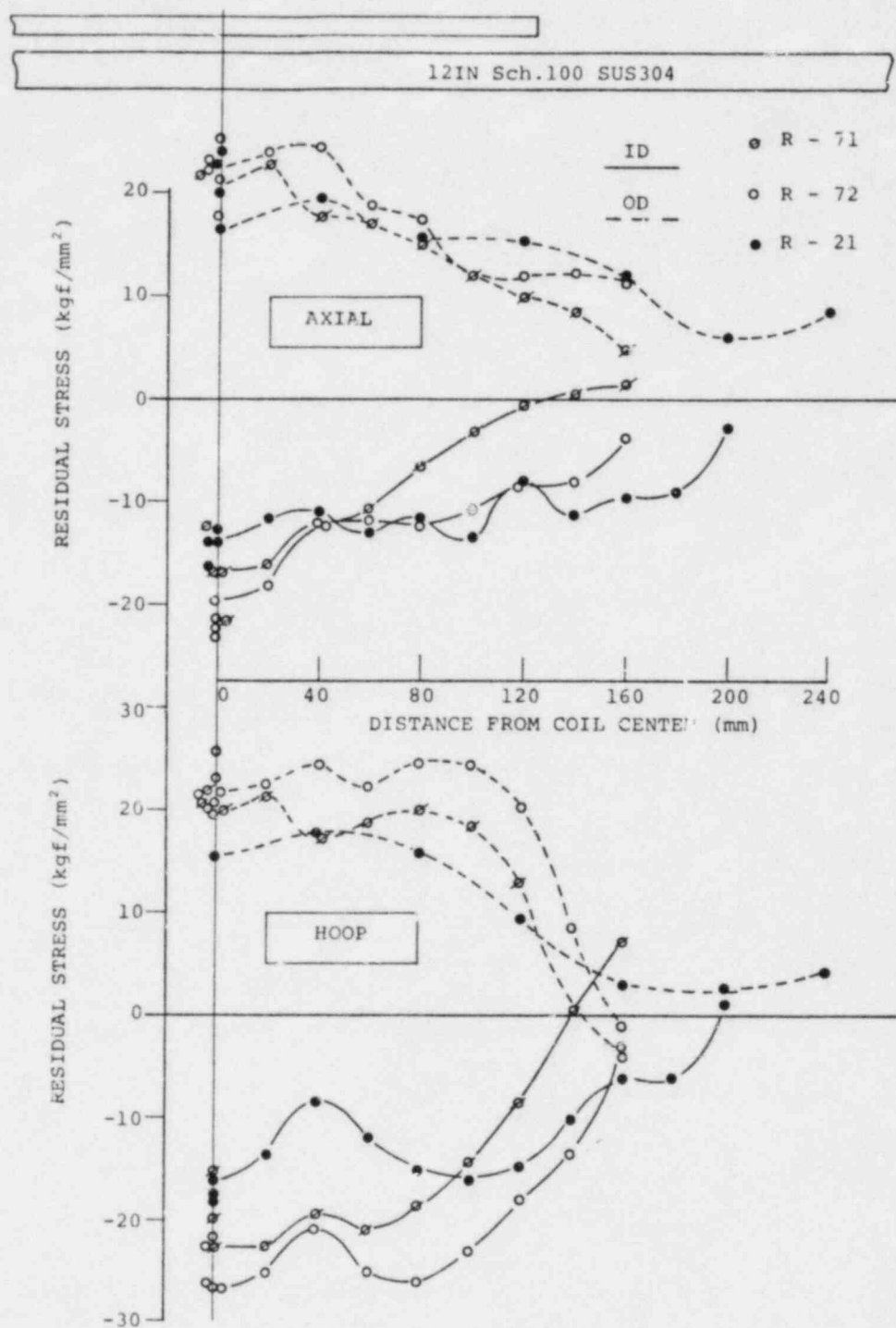


Fig. 5 RESIDUAL STRESS DISTRIBUTION (12IN)

A - 6

RELAXATION STUDY ON IHSI

SUMMARY

Some concern exists that residual stresses produced by IHSI may be relaxed by temperature and/or external stresses during plant operation. The relaxation behavior due to temperature and external load were separately investigated in this study.

Three IHSI treated pipes were subjected to heat treatments of 300°C, 400°C and 500°C for 24 hours respectively and another pipe was stressed by axial load exceeding yield strength. The residual stress measurement after these treatments revealed that the residual stresses were hardly lowered by thermal treatments up to 500°C but were easily relaxed due to axial stresses exceeding the yield strength.

The above mentioned tests were conducted on pipes without circumferencial welds. Weld joints are expected to respond somewhat differently from base metal and an additional test on a weld joint is strongly requested.

1. Introduction

Stress remaining in material is gradually relaxed with increasing temperature rises and/or with time. It is, therefore, of concern that the residual stress induced by IHSI may be relaxed after long service at high temperature. In this study, two kinds of experiments were carried out. They were designed to check the relaxation behavior of IHSI'ed pipe due to elevated temperature and to axial stress.

2. Experimental

2.1 Material

The material used in this experiment was type 304 austenitic stainless steel and its chemical composition and mechanical properties are given in Table 1.

2.2 Preparation of test pipes

Four test pipes, R-73, 74, 75 and 76, were prepared for this experiment. These pipes were 4 inch Schedule 80 and 300 mm in length.

2.3 IHSI

IHSI was performed for these test pipes using the parameters described in Table 2 so that the pipes were subjected to a temperature difference of approximately 300°C . As an example of the temperature distribution during IHSI, R-75 is presented in Fig. 1. The other test pipes were also IHSI'ed in the same manner as R-75.

2.4 Relaxation induced by high temperature

To estimate the relaxation effect of BWR piping in service, (300°C for 40 years), three heat treatment conditions were selected. As shown in Table 3, the test pipes were heat-treated at 300°C , 400°C or 500°C for 24 hours in an electric furnace in air.

2.5 Relaxation induced by axial stress

In order to investigate the residual stress relaxation behavior produced by axial loads, a tensile test was performed on IHSI'ed pipes. The sequence of the tensile test is shown in Fig. 2. The configuration of a test pipe is shown in Fig. 3.

Tensile testing was performed at 290°C by using an Amsler type universal tester. The displacement of a test pipe was measured by high-temperature strain gages fixed on the inside of the test pipe.

2.6 Residual stress measurement

Residual stresses of the IHSI'ed pipes were measured by conventional strain gage methods after heat treatment or tensile tests had been performed.

3. Results and Discussion

The results of the residual stress measurements for pipes, R-73, 74 and 75 are shown in Fig. 4 and are compared with R-15 which had not been subjected to the relaxation heat treatment. R-15 has been similarly IHSI treated with the other pipes as shown in Table 2. No significant difference in residual stress was observed among the pipes tested. In order to estimate the temperature effect for a longer time, for example, the design lifetime, the Larson-Miller equation was used for extrapolation purposes. The calculated service times corresponding to 400 and 500°C for 24 hours are 15 years and 8×10^4 years, respectively as shown in Table 3. These data show that the residual stresses produced by IHSI do not disappear nor vary during 40 years at service temperature only.

Figure 5 shows the load-elongation diagram obtained in the pipe loading test. The test pipe was unloaded to zero axial load after the nominal stress reached $0.5\sigma_y$, σ_y and $1.29\sigma_y$. Using the residual plastic strains, the residual stress after unloading were estimated by a simple two element model as shown below.

Figure 6 (a) illustrates the concept of the two element model. Element A and B correspond to the outer and inner pipe wall. The inner wall has a compressive residual stress and vice versa.

Figure 6 (b) shows the stress-strain relation of elements A and B assuming that the elastic perfectly plastic relationship holds. Curve "C" is composed of curves A and B, and shows the stress-strain relationship of the composed element, A plus B.

The residual stress is maintained at the initial level unless the apparent stress goes beyond point (1) on curve "C" because the stress goes back elastically to point 0 and no plastic strain remains. If the stress goes to point (2) which is beyond point (1), the residual stress is decreased to level (4), because a plastic strain of ϵ_3 remains in the composite element after the axial load is removed. If the axial load reaches the yield strength, the residual stress similarly becomes zero.

The residual stresses corresponding to $0.5 \sigma_y$ and $1.0 \sigma_y$ loading were estimated in the same manner as mentioned above but in this case the stress-strain relations obtained by the pipe loading test and small tensile test were used as those producing the composite element (A + B) and element B respectively. The initial residual stress (at zero axial load) was assumed to be $-\sigma_y$, which is nearly equal to R-15.

The residual stresses on the pipe after $1.29 \sigma_y$ loading were measured and are plotted in Fig. 7 with the estimated values.

Figures 7 and 8 suggest that the axial external load exceeding σ_y lowers the residual stress to approximately zero but it never shifts to tensile stress.

The previous discussion is based on data for a pipe without a weldment. The stress-strain relation at a weld joint is considered to be much different from that of base metal because of strain hardening and deformation during welding.⁽¹⁾ Therefore, the relaxation behavior of a welded joint will be different from that described above and experimental studies on a IHSI treated joint is recommended.

4. Conclusion

The results obtained in this study lead to the following conclusion.

- (1) The effect of IHSI is reduced insignificantly by BWR service temperature.
- (2) The effect of IHSI on a pipe without a weldment nearly disappears due to an external load exceeding σ_y .
- (3) The effect of external loading can be qualitatively explained by a two element model.
- (4) It is recommended that a tensile test be performed on an IHSI treated pipe weldment because the stress-strain behavior of the weldment may be substantially different from that of base metal.

Reference (1) Y. Ando et al, Local Structural Behavior and Safety Analysis in Nuclear Piping (Vol. 3), Japan Welding Engineering Society, 1979.

Table 1 CHEMICAL COMPOSITION AND MECHANICAL PROPERTIES

SPECIFIED	C	Si	Mn	P	S	Ni	Cr
	max. 0.08	max. 1.00	max. 2.00	max. 0.030	max. 0.030	8.00 - 11.00	18.00 - 20.00
TTC-3750	0.05	0.48	1.65	0.026	0.005	9.20	18.20

SPECIFIED CHART NO.	Room Temperature			290°C		
	YIELD POINT 21 (kg/mm ²)	TENSILE STRENGTH 53 (kg/mm ²)	ELONGATION 35 (%)	YIELD POINT (kg/mm ²)	TENSILE STRENGTH (kg/mm ²)	ELONGATION (%)
TTC-3750	29	59	66	17.7	45.1	46

Table 2. ISHI CONDITION

NO.	FREQUENCY (kHz)	POWER (kW)	HEATING DURATION (sec.)	FLOW RATE (m/sec.)	TEMPERATURE (°C)			REMARKS
					OUTSIDE	INSIDE	TEMP. DIFFERENCE	
R-73	3	130	30	2.5	487	240	247	HTGE-451-I-033
R-74		130	30		496	185	311	
R-75		130	28		516	230	286	
R-76		130	30		483	231	252	
R-15	2		21		562	240	322	

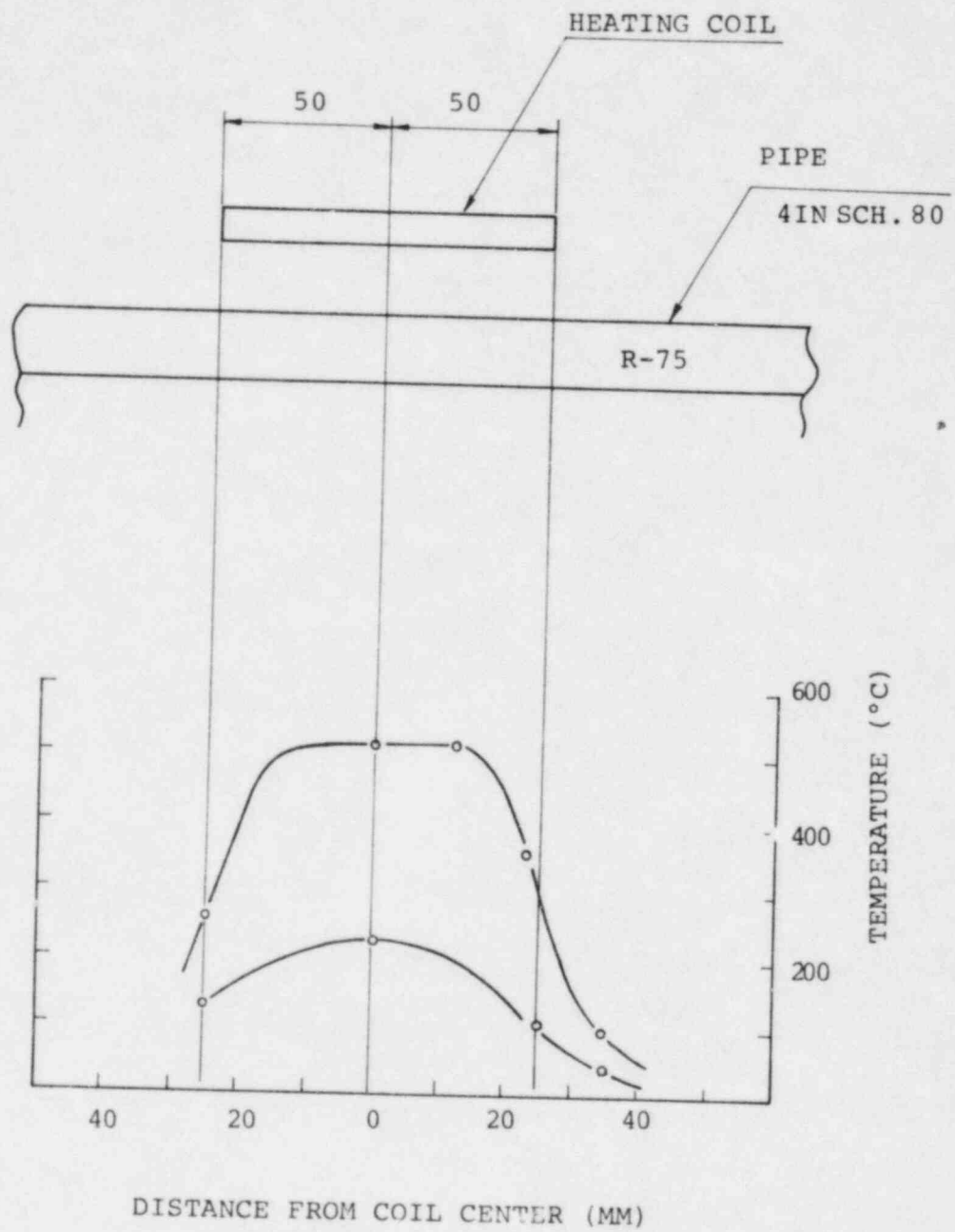


Fig. 1 TEMPERATURE DISTRIBUTION DURING IHCI

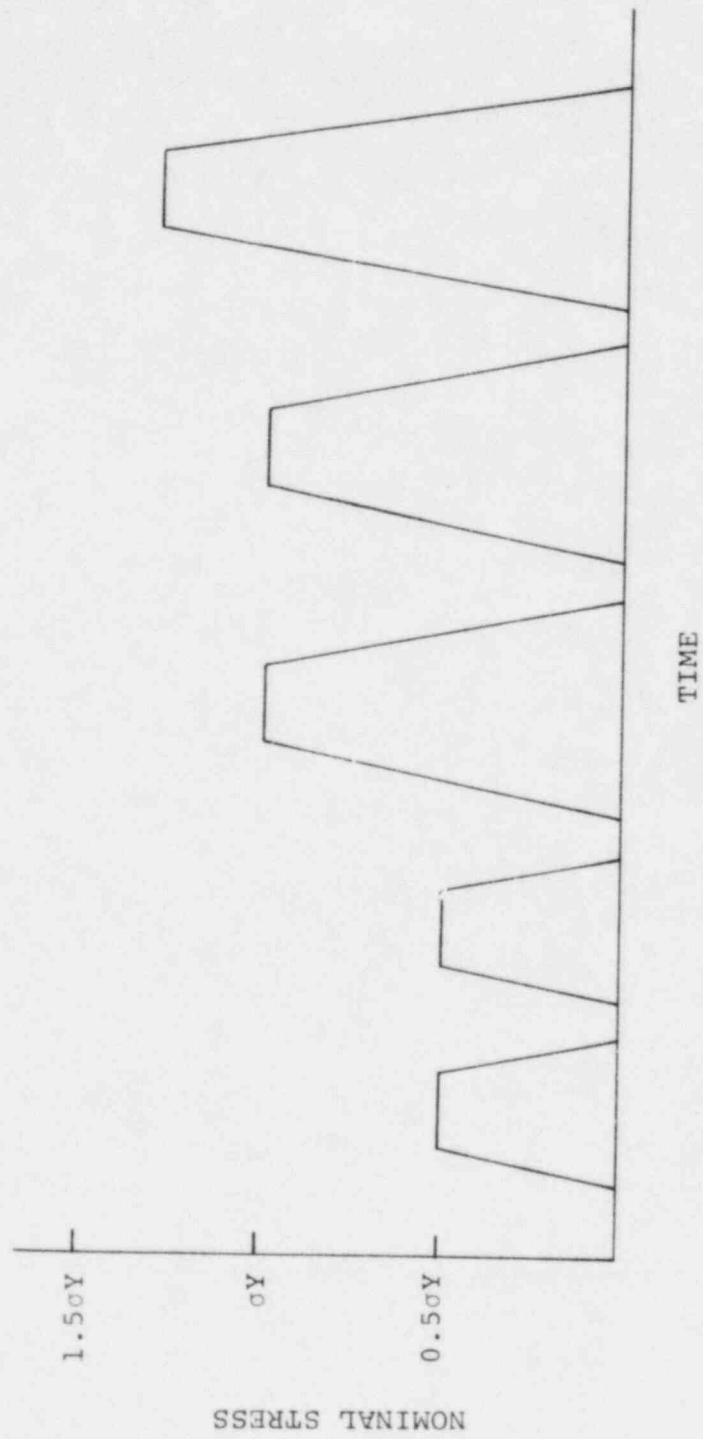


Fig. 2 LOADING SEQUENCE

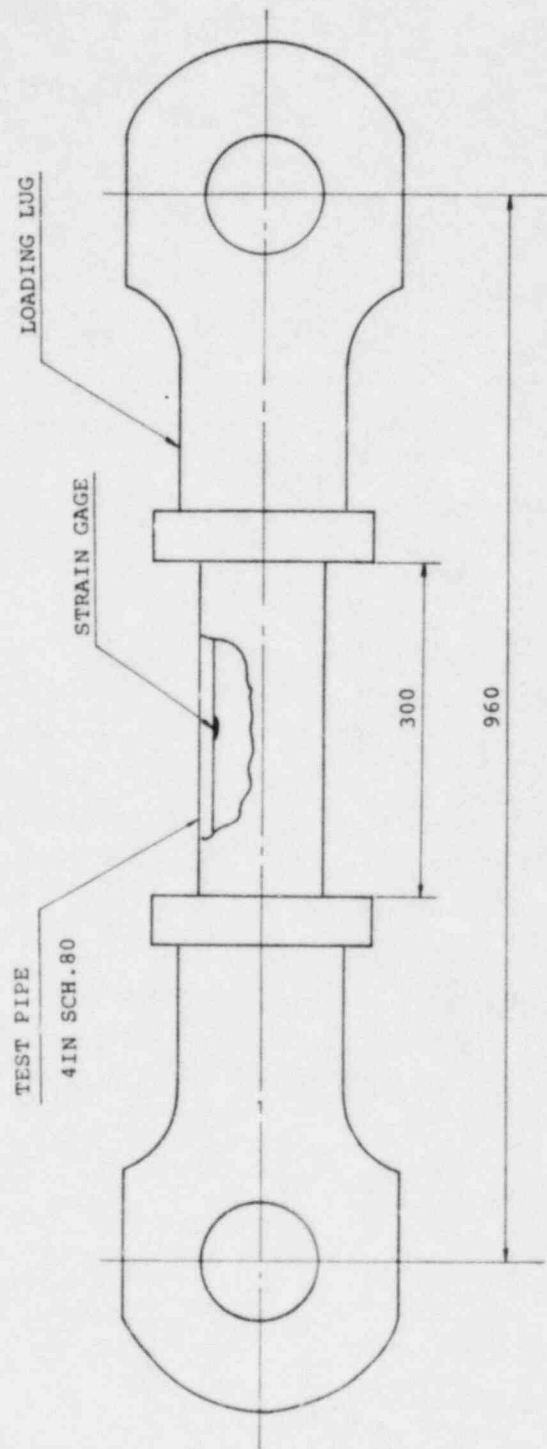


Fig. 3 TEST PIPE FOR LOADING TEST

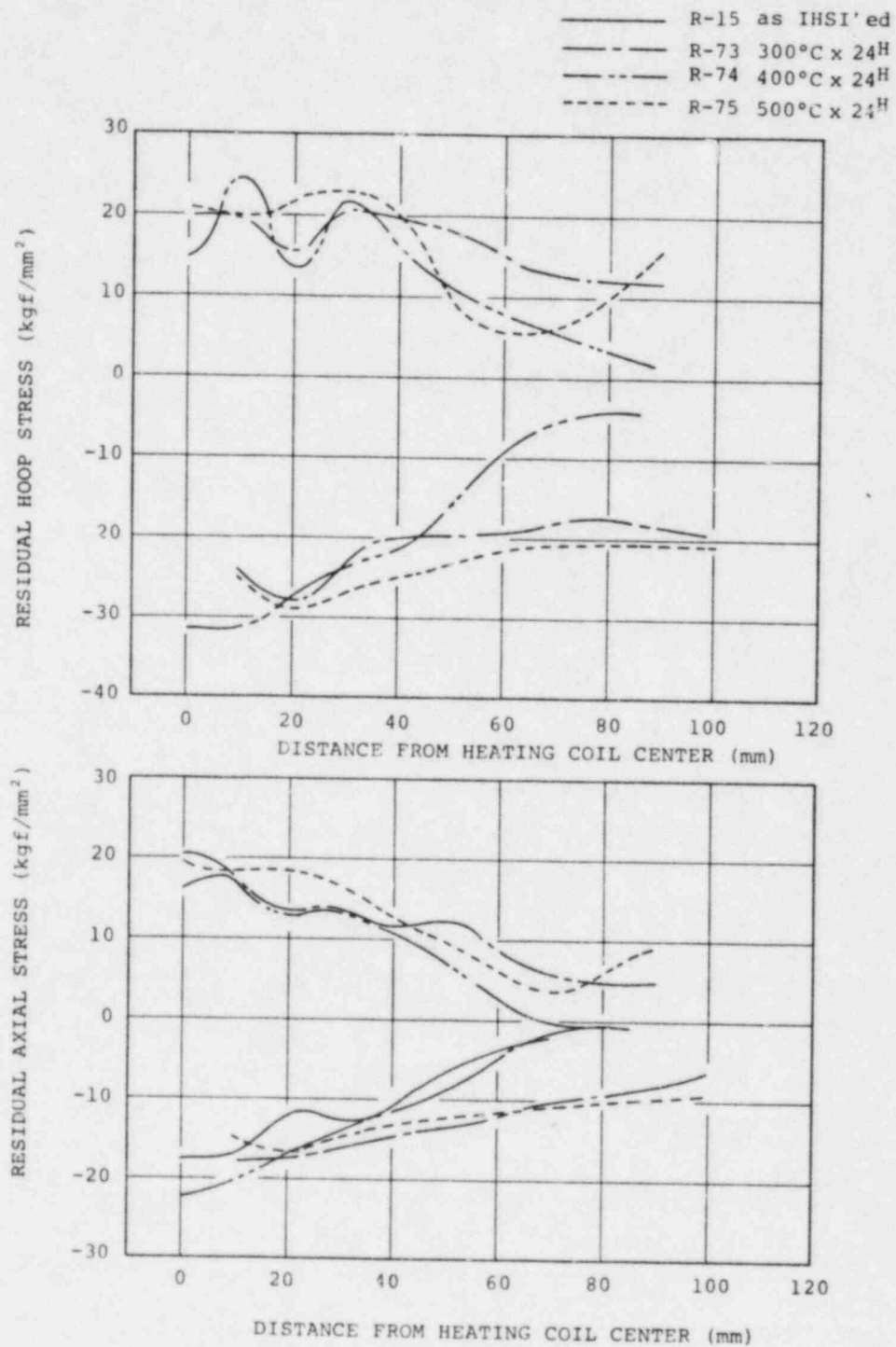


Fig. 4 RESIDUAL STRESS DESTRIIBUTION

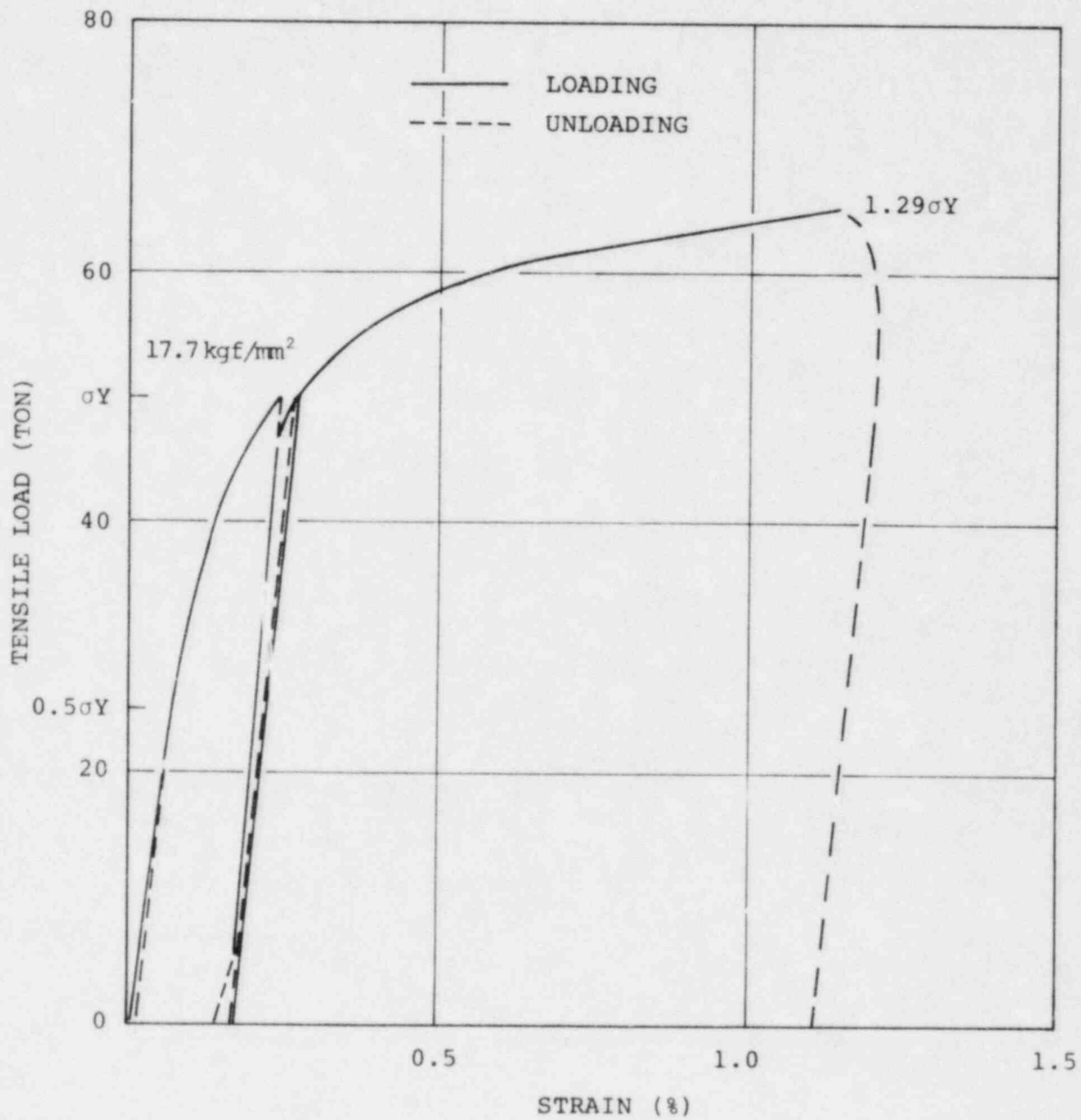
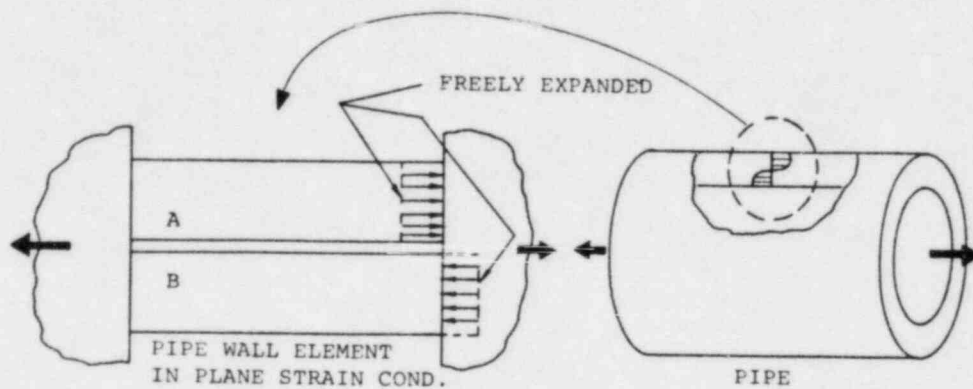
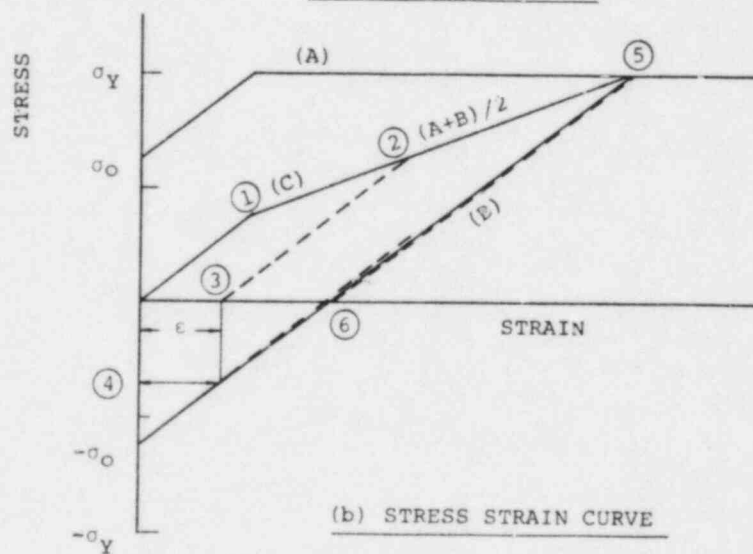


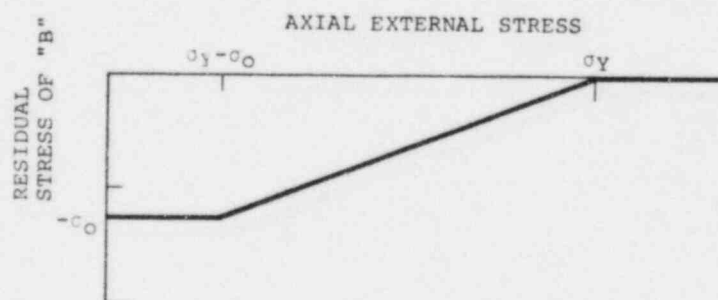
Fig. 5 LOAD-STRAIN CURVE OF PIPE WITH IHSI



(a) TWO ELEMENT MODEL



(b) STRESS STRAIN CURVE



(c) RESIDUAL STRESS

Fig. 6 RESIDUAL STRESS ANALYSIS BY TWO ELEMENT MODEL

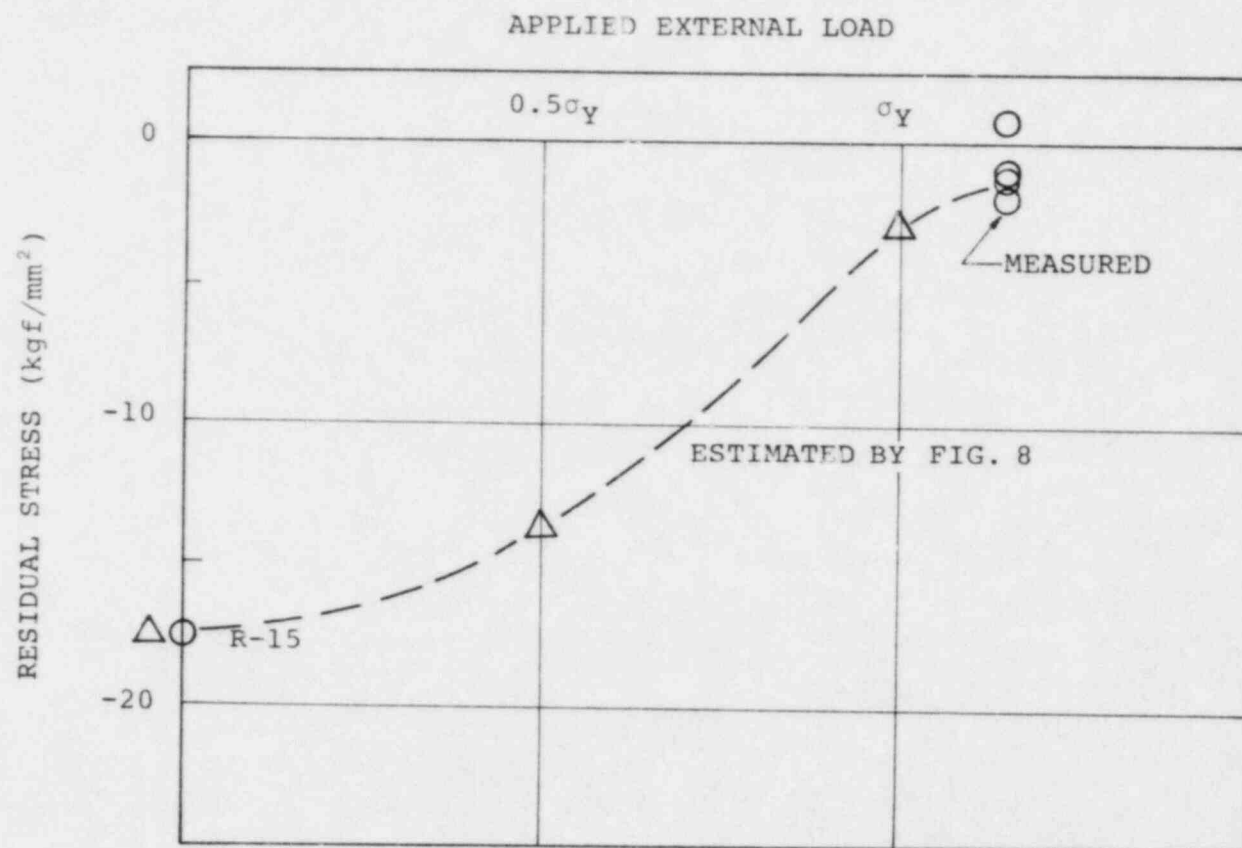


Fig. 7 RESIDUAL STRESS AFTER UNLOADING

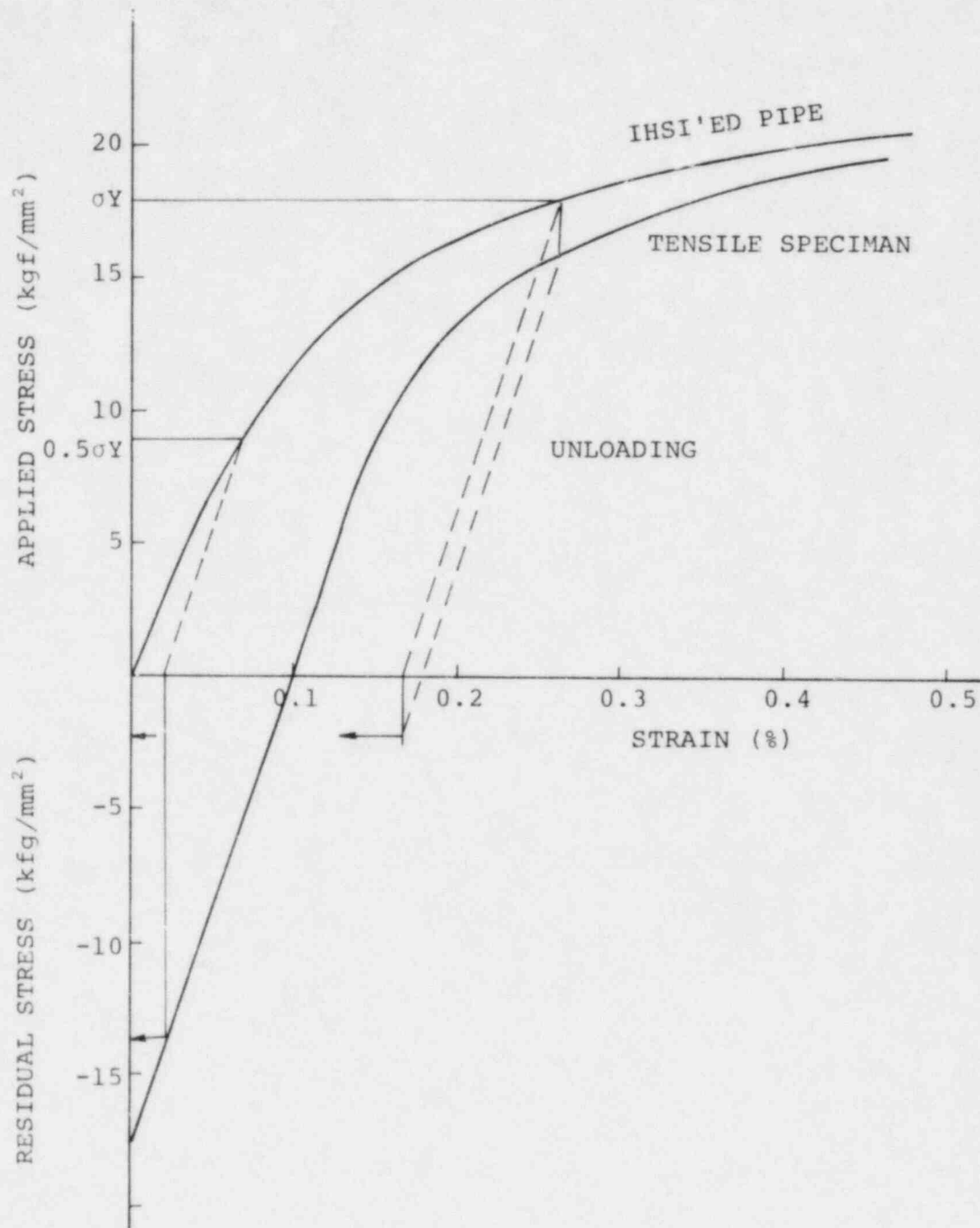


Fig. 8 ESTIMATION OF RESIDUAL STRESS AFTER UNLOADING

Table 3. HEAT TREATMENT CONDITION

LARSON-MILLER PARAMETER

$$P = T (A + \log t), A = 20$$

NO.	TEMPERATURE (°C)	TIME (HRS.)	CALCULATED TIME (YEARS)
R-73	300	24	-
R-74	400		15
R-75	500		80000

A - 7

EFFECT OF PLASTIC DEFORMATION BY IHSI
AND SUBSEQUENT HEAT TREATMENT UPON IGSCC
SUSCEPTIBILITY OF TYPE 304 STAINLESS STEEL

SUMMARY

The effect of plastic strain induced by IHSI on the level of sensitization was studied on 4 inch Schedule 80 stainless steel pipes. Two artificial cracks were prepared in the heat affected zone of three welded joints. One joint was subjected to IHSI and a sensitization treatment while the other two were not subjected to IHSI.

The degree of sensitization was determined by micro and macro-etch tests, and creviced bent beam tests (IGSCC Test). No difference in level of sensitization among the three joints was observed.

1. Introduction

It is well known that plastic deformation generally accelerates sensitization produced during subsequent heat treatment and makes stainless steel more susceptible to IGSCC. IHSI, which is a remedy for IGSCC, is a method to introduce a compressive stress caused by plastic strain on the inside pipe surface, and therefore produces concern that it might make stainless steel more susceptible to IGSCC. The effect of plastic strain induced by IHSI on the subsequent low temperature sensitization characteristics was studied for pipes with and without small artificial cracks.

Corrosion tests and hardness tests were performed so as to examine the above described superimposed effect.

2. Experimental

2.1 Material

Type 304 stainless steel with 0.07 percent carbon content was used in this experiment to provide the worst material condition. The chemical composition and mechanical properties are given in Table 1.

2.2 Preparation of test coupons

Three test coupons were prepared for this experiment. All these coupons were 4 inch Schedule 80 pipe of nominal size and 300 millimeters in length. They were butt-welded by shielded metal arc welding following automatic gas tungsten arc welding (GTAW + SMAW). High weld heat input (20 KJ/cm) was selected to provide a heavily sensitized condition. Four notches were produced by electric discharge machining at a point which was nearly 3.5 millimeters away from the weld fusion line on the inside surface of each test coupon. The notch size was 2 mm in depth and 8 mm in width as shown in Figure 1; this size defect is expected to be easily detected by the usual ultrasonic techniques.

2.3 Heat treatment and IHSI

The sequence of the heat treatment and IHSI is shown in Table 2. The first heat treatment simulated the in-service thermal condition before IHSI. The second heat treatment was intended to investigate whether the plastic deformation produced by IHSI accelerates the subsequent low temperature sensitization or not. The low temperature sensitization heat treatment was conducted for 72 hours at 450°C. This corresponds to about 30 years at 288°C assuming an activation energy of 46 kcal/mol. This IHSI condition is the usual one as shown in Table 3.

2.4 Specimen removal and tests

The specimens were removed as shown in Figure 2. In order to survey the superimposed effect of plastic deformation and sensitizing heat treatment, the following four kinds of tests were conducted;

- (1) Micro-Vickers hardness test
- (2) Chromic acid etch test

(3) Copper sulfate-sulfuric acid etch test

(4) Creviced Bent Beam test

3. Results

The result of chromic acid macro etch tests is shown in Figure 3. There is no significant difference among the three pieces as concern the sensitization zone as shown by the schematic hatching zone in Figure 3(d). Figures 4, 5, and 6 show the results of the chromic acid micro etch tests on 8 points near the notch as illustrated in Figure 7. Figures 4, 5 and 6 correspond to the structure of coupon 1 (AW + 1st LTS), coupon 2 (AW + 1st LTS + 2nd LTS) and coupon 3 (AW + 1st LTS + IHSI + 2nd LTS), respectively. There was little difference in degree of sensitization among each examination.

The result of the copper sulfate-sulfuric acid etch tests is shown in Table 4 and Figure 8. Although a slight difference in extent of sensitization was found among the test pipes, the apparent effect of plastic deformation or low temperature sensitization was not observed.

Micro-vickers hardness distribution is shown in Figure 9. Open circles show the hardness number measured along the line 2.5 mm away from the pipe inside surface without a notch, and solid circles show the one with a notch as shown in Figure 10. Comparing coupon 2 (without IHSI) with coupon 3 (with IHSI), the hardness near the fusion line of coupon 3 was found to be a little higher than for coupon 2. The hardness increased rapidly near the tip of the notch. The result of the creviced bent beam test is shown in Table 5 and Figure 11. The difference in history for each coupon does not correspond to the variation of the maximum crack depth presented in Table 5. The crack

distribution was practically the same for each specimen. A typical crack depth distribution (coupon No. 3) for a test piece with cracks is presented in Figure 11. No deep cracking (SCC) was observed near the notch.

4. Discussion

Plastic strain followed by heating is generally known to accelerate sensitization. As IHSI induces plastic strain through thermal strain, stainless steel pipe may become heavily sensitized as a result of subsequent LTS. In this investigation there was, however, no remarkable difference among each test pipe in condition (1), (2) and (3). This reveals that the additional treatments following welding plus the 1st LTS have little effect on sensitization, that is, IHSI and the 2nd LTS did not change the sensitization state. This may be the result of the fact that thermo-mechanical effects of welding and the 1st LTS were dominant for seeding and subsequent sensitization of the test pipes.

It was observed that hardness near the weld metal increased for the test pipe with IHSI compared to the other. This result showed that IHSI could effectively produce plastic deformation on the pipe. Figure 9 shows that the hardness after IHSI increased rapidly at the notch tip. This observation corresponds well with the calculated strain concentration phenomena presented in Figure 12. This calculation was conducted on a notched 12 inches schedule 100 pipe using a finite element method (IECT-II; an IHI computer code). The maximum strain at the notch tip is approximately 3 percent. It has been reported in reference (2) that a plastic strain of 6% significantly enhances sensitization.

It should be expected, therefore, that severe IGSCC at the notch tip would be observed in the CBB test. No crack, however, was observed in this region and the maximum IGSCC was observed at a distance 8 mm from the notch

as shown in Figure 11. The following can be considered as the reason for this discrepancy:

The plastic strain in the weld HAZ was calculated by FEM^{(1) (2)} to be more than 4 percent. On the other hand the additional strain at the notch tip produced by IHSI was considered to be smaller than 3 percent because the artificial crack had a finite width (= 0.3 mm) while the calculation was based upon zero width.

5. Conclusion

The above discussion leads to the following conclusions.

- (1) Neither IHSI nor the 2nd LTS were effective in accelerating sensitization for stainless steel pipe, namely, the welding and 1st LTS were dominant.
- (2) The plastic strain at the notch tip after IHSI would be less than 3 percent and had little additional effect on the sensitization produced by welding and subsequent LTS.

-
- References: (1) E. Friedman: ASME Paper 75-PVP-27
(2) Y. Ando et al, Localized Structural Behavior and Safety Evaluation of Nuclear Power Plant (No. 3), Japan Welding Engineering Society, Nov. 1978, pp. 38-40.

TABLE 1 CHEMICAL COMPOSITION AND MECHANICAL PROPERTIES

C	Si	Mn	P	S	Ni	Cr	YIELD POINT 21	TENSILE STRENGTH 53	ELONGATION
max. 0.08	max. 1.00	max. 2.00	max. 0.040	max. 0.030	8.00 - 11.00	18.00 - 20.00	(kg/mm ²)	(kg/mm ²)	35 (%)
0.07	0.48	1.52	0.027	0.001	9.65	18.65	30	60	64

TABLE 2 THERMAL HISTORY

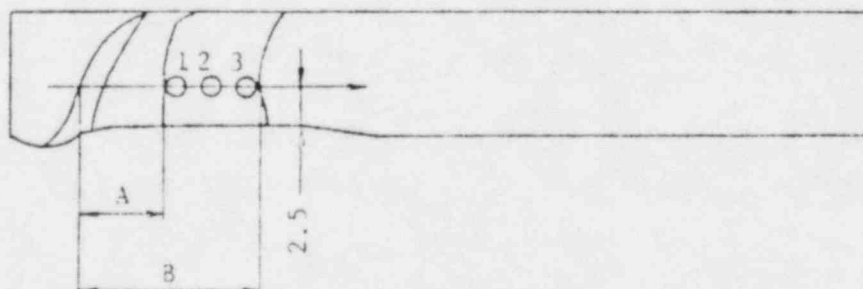
COUPON NO.	HISTORY
1	AS WELDED + 1st LTS
2	AS WELDED + 1st LTS + 2nd LTS
3	AS WELDED + 1st LTS + IHISI + 2nd LTS

TABLE 3 IHSI CONDITION

FREQUENCY (kHz)	POWER (kW)	HEATING DURATION (sec.)	FLOW RATE (m/sec.)	TEMPERATURE (°C)		
				OUTSIDE	INSIDE	TEMP. DIFFERENCE
3	150	35	2.5	513	130	383

TABLE 4 SENSITIZATION REGION (STRAUSS ETCH)

COUPON NO.	DISTANCE FROM FUSION LINE		
	A	B	A - B
1	5.0	11.0	6.0
2	3.5	10.5	7.0
3	6.0	11.5	5.5



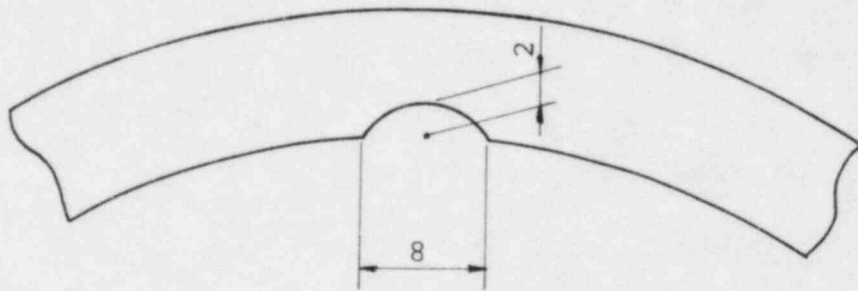
NUMBER IN ABOVE FIGURE
CORRESPONDS TO NUMBER IN FIGURE 3.

A: DISTANCE TO STRAUSS ETCH BEGINNING FROM FUSION LINE
B: DISTANCE TO TERMINAL FROM

TABLE 5 MAXIMUM CRACK DEPTH (CBB TEST)

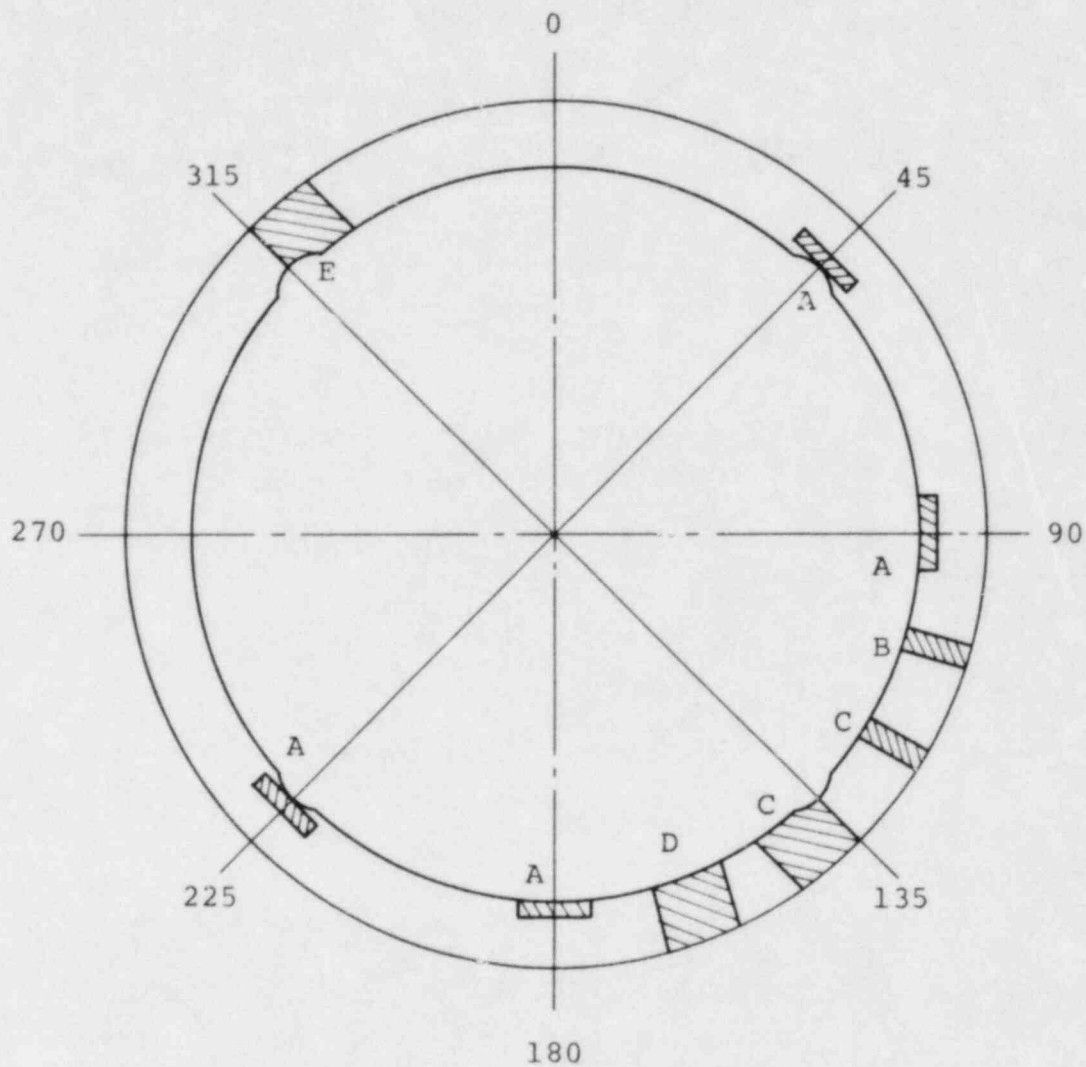
COUPON NO.	NOTCH	MAXIMUM CRACK DEPTH ($\times 10^{-6}\text{m}$)
1	YES	83
	YES	1039
	NO	991
	NO	1589
2	YES	1097
	YES	-
	NO	-
	NO	982
3	YES	153
	YES*	999
	NO	1800
	NO	1779

*: CRACK DEPTH DISTRIBUTION IS SHOWN IN FIGURE 11



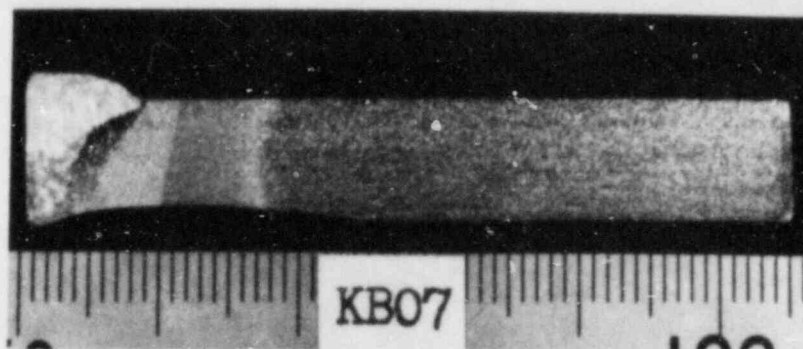
SLIT WIDTH = 0.3

FIGURE 1 EDM NOTCH CONFIGURATION

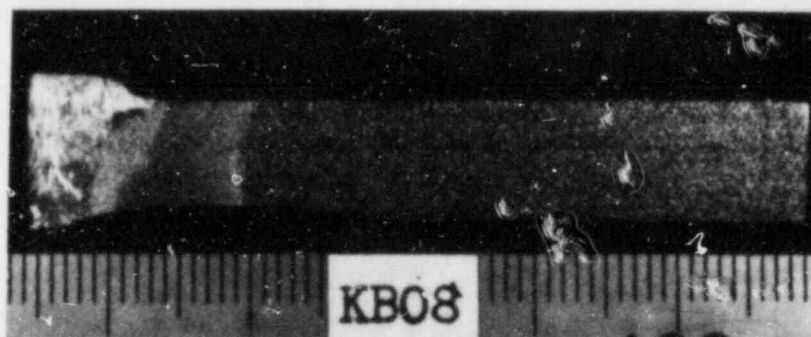


POSITION	TEST ITEM
A	CBB
B	STRAUSS ETCH
C	HARDNESS
D	MACRO
E	MICRO

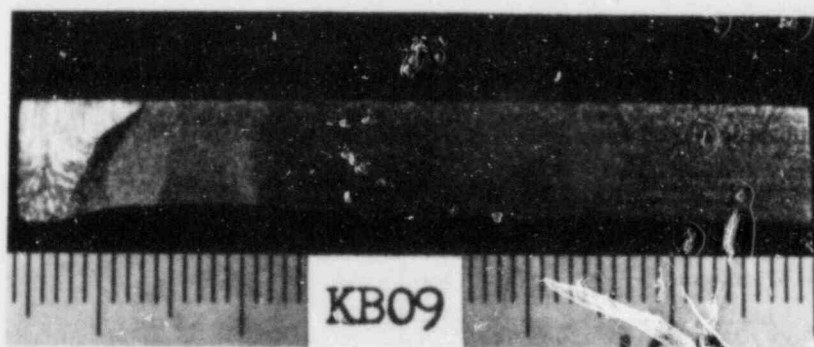
FIGURE 2 SPECIMEN REMOVAL



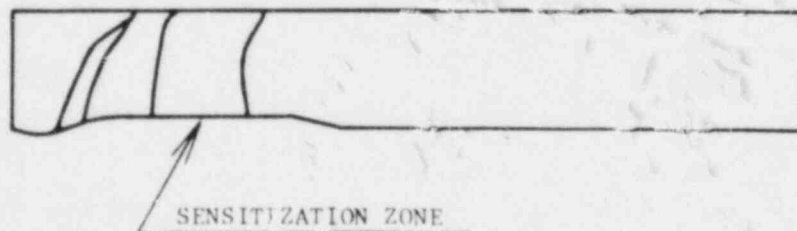
(a) AS WELDED + 1st LTS



(b) AS WELDED + 1st LTS + 2nd LTS



(c) AS WELDED + 1st LTS + HSI + 2nd LTS



(d) SCHEMATIC FIGURE

FIGURE 3 CHROMIC ACID MACRO ETCH TEST RESULTS

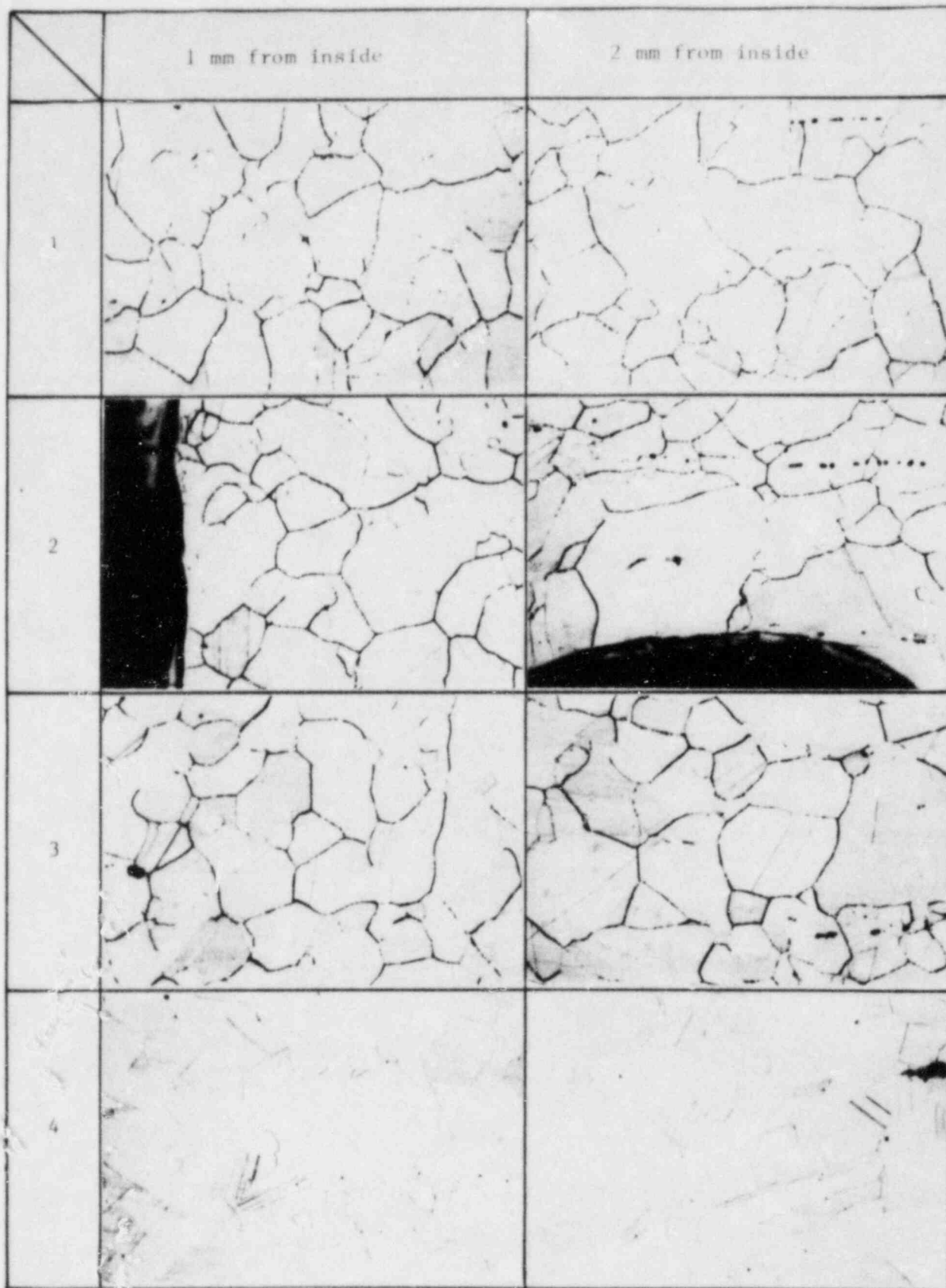


FIGURE 4 CHROMIC ACID MICRO ETCH TEST RESULTS



FIGURE 5 CHROMIC ACID MICRO ETCH TEST RESULTS



FIGURE 6 CHROMIC ACID MICRO ETCH TEST RESULTS

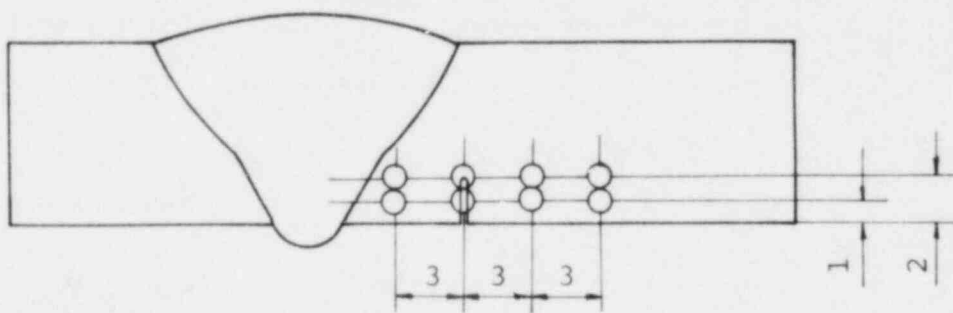


FIGURE 7 MICRO INVESTIGATED POINTS

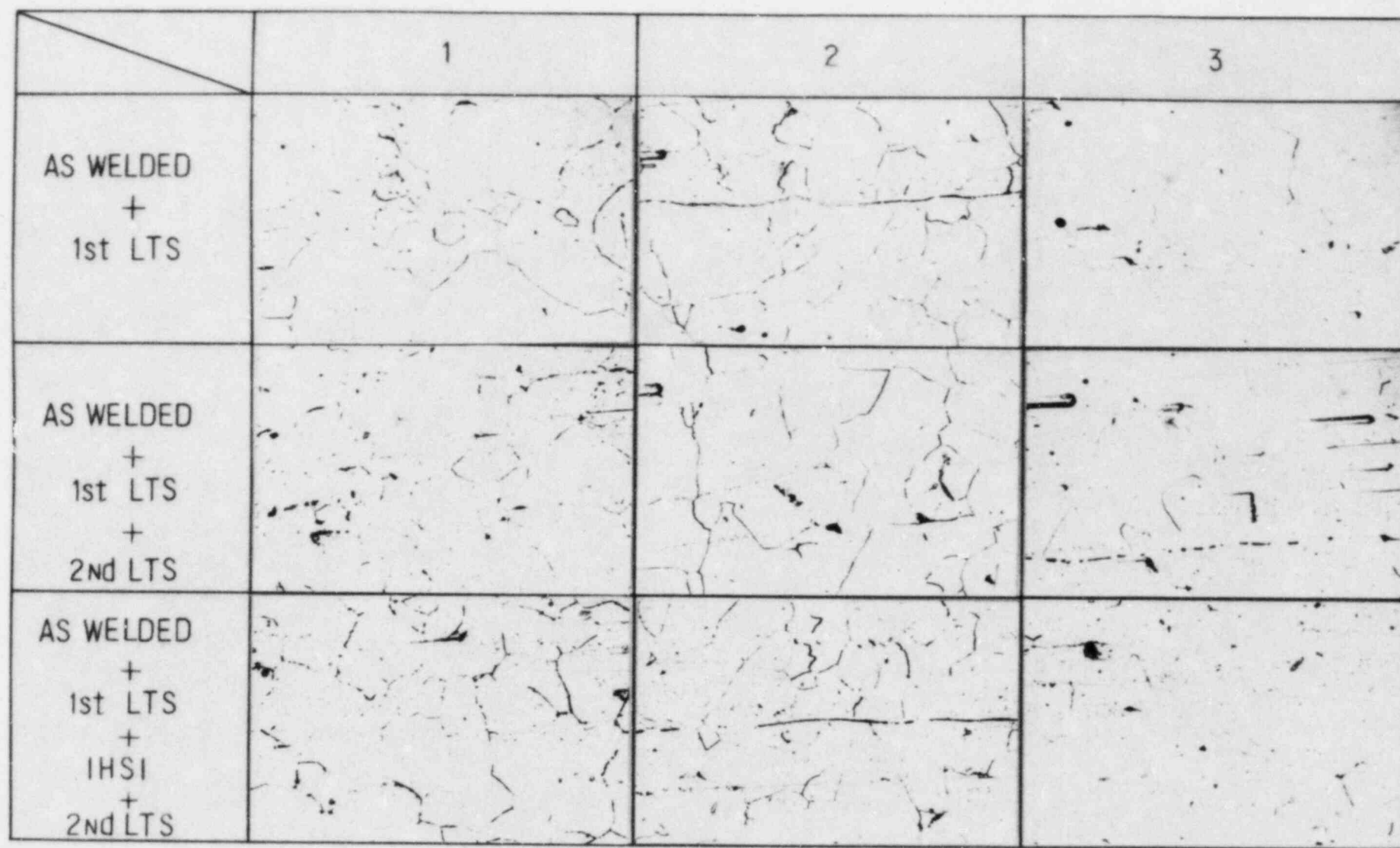


FIGURE 8 SURFACE INVESTIGATION FOR STRAUSS ETCHING

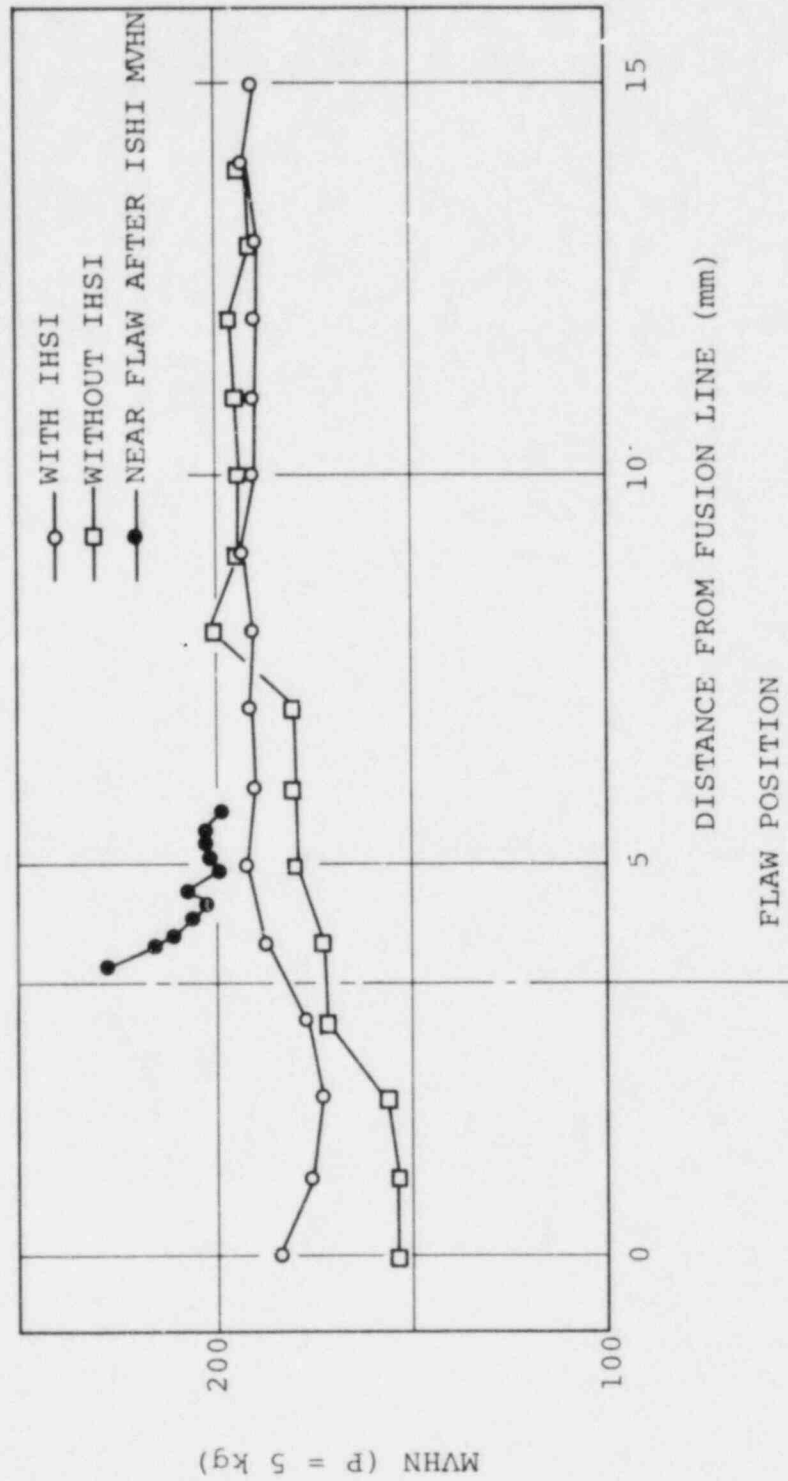


Fig. 9 HARDNESS DISTRIBUTION CHANGE DUE TO IHSI

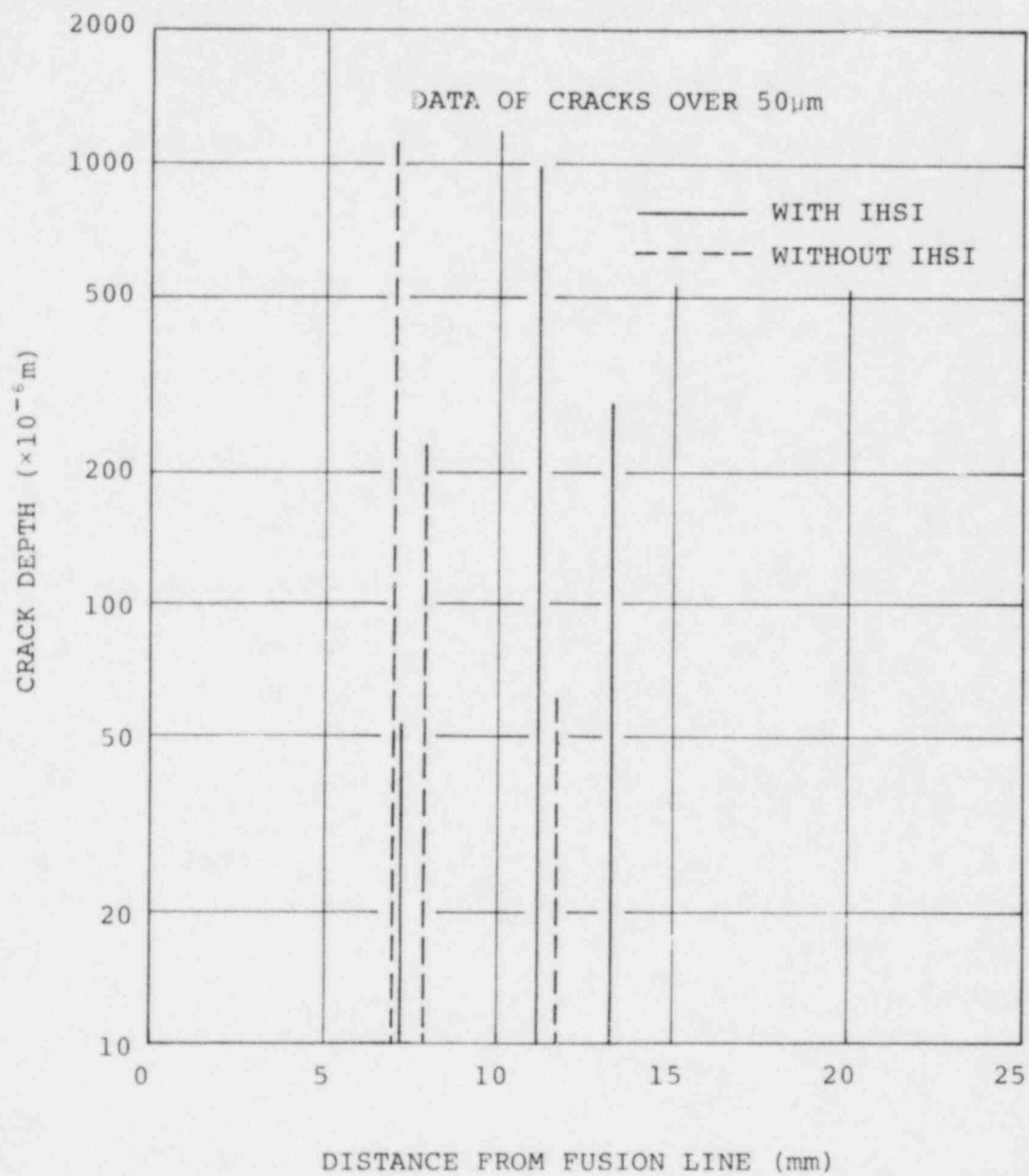


FIG. 10 SCC DISTRIBUTION CHANGE DUE TO IHSI (CBB TEST)

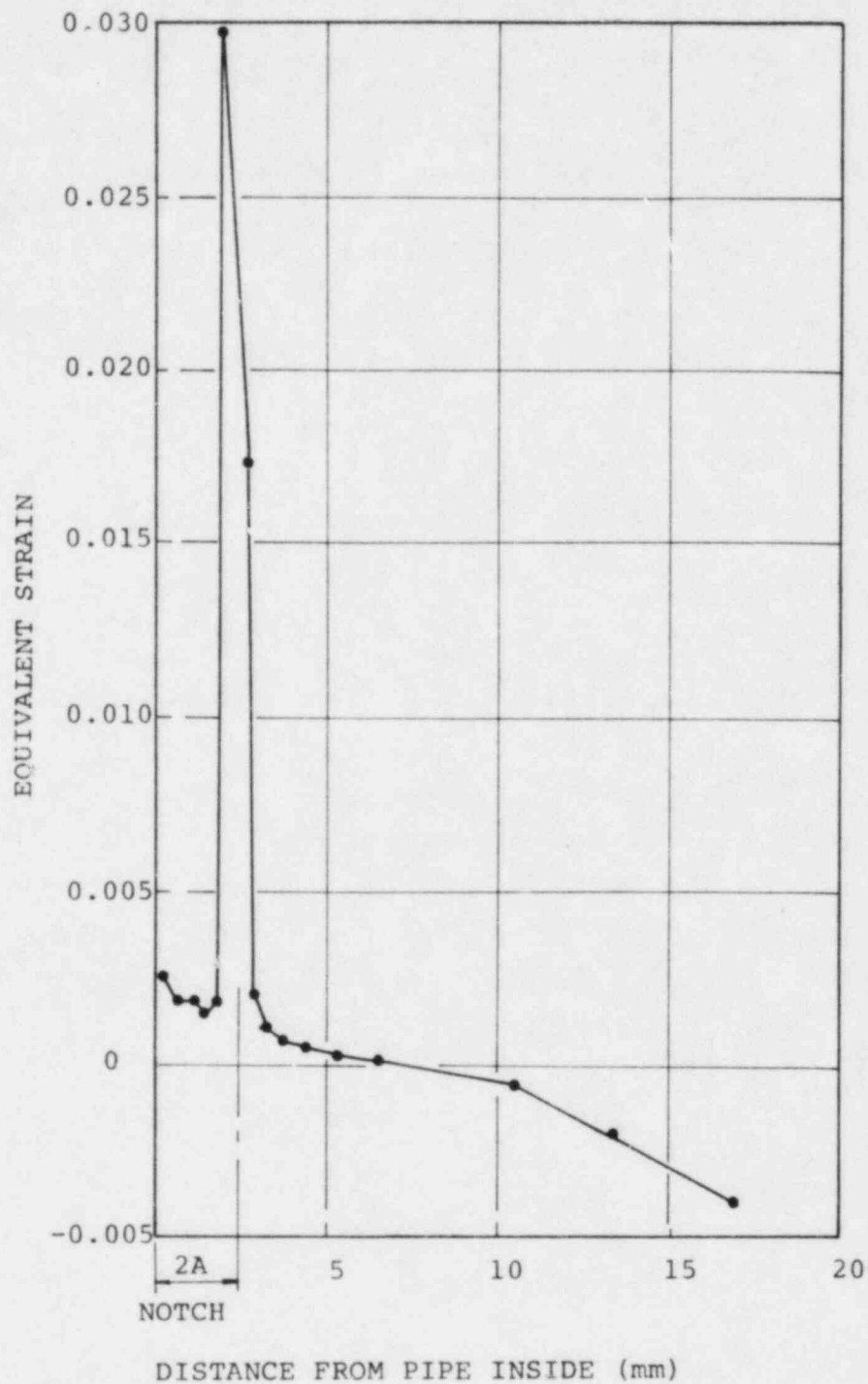


FIGURE 11 MAXIMUM EQUIVALENT STRAIN DISTRIBUTION
BY IHSI (CALCULATED BY FEM)
12 INCHES SCHEDULE 100. NOTCH DEPTH=24 mm

A - 8

SOME ANALYTICAL CASE STUDIES

OF IHSI

SUMMARY

In order to verify the validity of IHSI for various cases, the effect of some geometrical transitions and also of welding residual stresses were analytically studied using a thermo elastic-plastic finite element method.

All of the mechanical and physical properties inputted were temperature dependent. The analytical results reveal that the following geometrical transitions; (1) thickness transition produced by weld edge preparation, (2) large thickness transition such as nozzle to pipe, (3) transition in diameter such as reducer, and (4) pipe to end cap transition have no significant effect on residual stresses and sufficient IHSI effect is expected. Further simulated welding residual stress also have little effect on the final residual stress.

TABLE 0.1 MECHANICAL AND PHYSICAL PROPERTIES

TEMPERATURE (°C)	THERMAL CONDUCTIVITY (Kcal/cm-s-°C)	SPECIFIC HEAT (Kcal/kg-°C)	THERMAL DIFFUSIVITY (cm ² /s)
20	34.7x10 ⁻⁶	0.107	
50	35.7	0.112	0.0390
100	37.2	0.117	0.0399
150	38.9	0.122	0.0409
200	40.5	0.125	0.0420
250	42.1	0.127	0.0432
300	43.7	0.130	0.0439
350	45.4	0.131	0.0447
400	47.0	0.132	0.0453
450	48.6	0.134	0.0462
500	50.3	0.135	0.0470
550	51.8	0.137	0.0478
600	53.5	0.139	0.0487
650	55.1	0.141	0.0497
700	56.7	0.143	0.0506
750	58.3	0.145	0.0514
800	59.9	0.148	0.0523

TEMPERATURE (°C)	YOUNG'S MODULUS (Kg/cm ²)	POISON'S RATIO	DENSITY (kg/cm ²)
20	1.98x10 ⁶	0.260	8.03x10 ⁻³
50	1.97	0.264	8.02
100	1.95	0.270	8.00
150	1.91	0.274	7.97
200	1.88	0.278	7.95
250	1.84	0.281	7.93
300	1.79	0.284	7.90
350	1.76	0.288	7.88
400	1.72	0.292	7.86
450	1.67	0.296	7.83
500	1.63	0.300	7.81
550	1.58	0.304	7.79
600	1.53	0.308	7.77
650	1.47	0.314	7.74
700	1.41	0.318	7.72
750	1.36	0.320	7.70
800	1.31	0.324	7.67

TEMPERATURE (°C)	THERMAL EXPANSION (INSTANTANEOUS) (1/°C)	THERMAL EXPANSION (MEAN FROM R.T.) (1/°C)
20	16.4×10^{-6}	16.4×10^{-6}
50	16.7	16.6
100	17.1	16.8
150	17.5	17.1
200	17.9	17.3
250	18.3	17.4
300	18.6	17.6
350	19.0	17.8
400	19.3	18.0
450	19.8	18.2
500	20.2	18.4
550	20.5	18.6
600	20.9	18.7
650	21.3	18.9
700	21.6	19.0
750	22.0	19.1
800	22.4	19.2

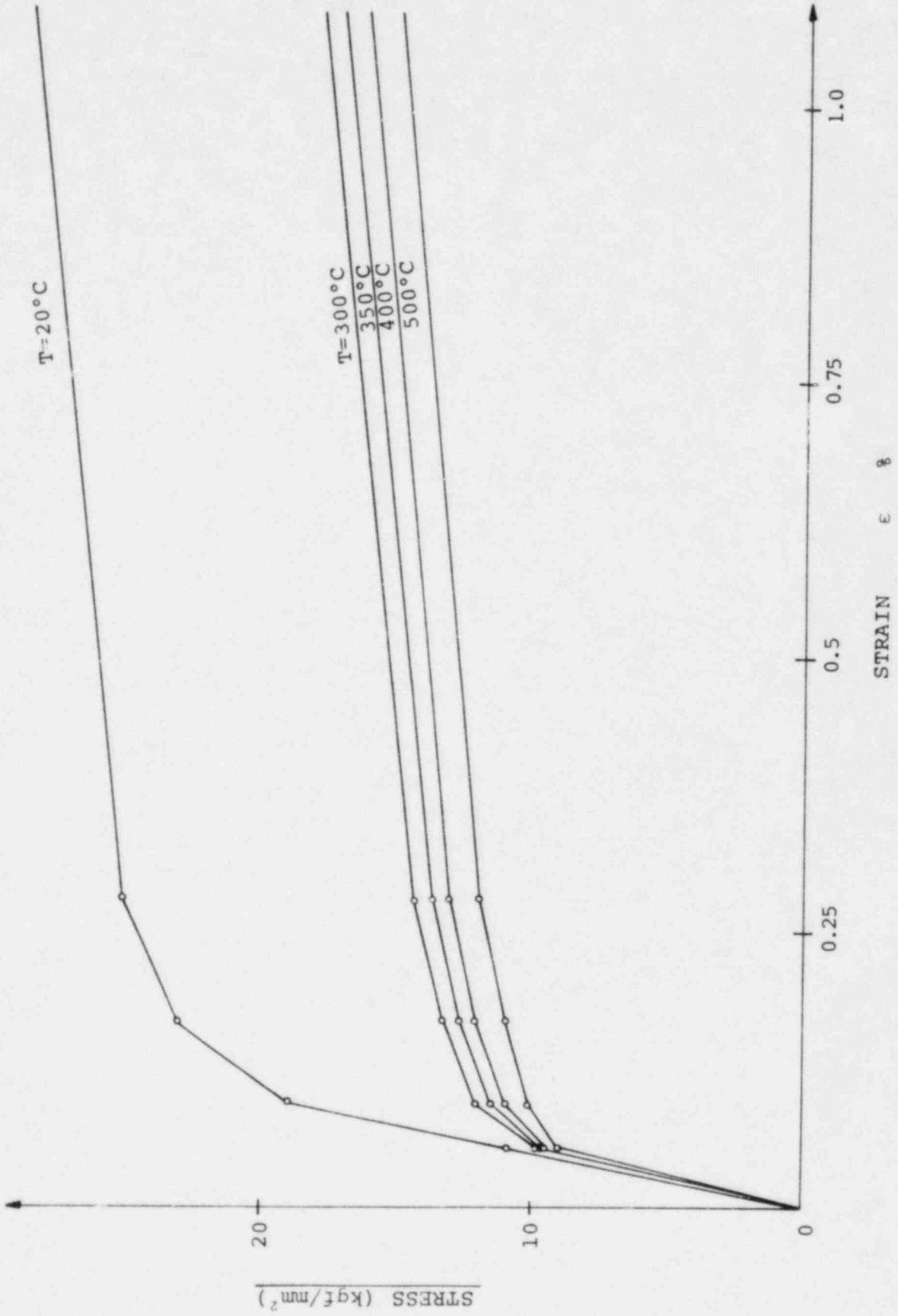


Fig.-01 MECHANICAL PROPERTIES

O. General

In this case study, the following conditions were assumed.

a) Mechanical Properties

- Stress-Strain Curve Fig. 0.1
- Young's Modulus Table 0.1
- Poisson's Ratio Table 0.1

b) Physical Properties

- Thermal Conductivity Table 0.1
- Specific Heat Table 0.1
- Thermal Diffusivity Table 0.1
- Heat Transfer Coefficient : h_m

$$h_m = 0.023 \cdot \frac{\lambda_w}{d \cdot 0.2 \cdot 0.8} Pr^{0.4} \mu_{\infty}^{0.8}$$

λ_w : Thermal conductivity of water

d : Inside diameter of pipe

ν : Coefficient of kinematic viscosity

Pr : Prandtl's number

μ_{∞} : Water flow rate

c) Heating Density : W

$$W = W_0 e^{-2x/s}$$

W_0 : Heating density on outer surface

S : Heating depth (9.6 mm)

x : Distance from outer surface

d) Boundary Condition

As shown in Fig. 2 unless otherwise specified.

e) Work Hardening

Isotropic-work hardening law

f) Computer Program

Temperature distribution.....ITEMP II (Developed by IHI)

Elastic plastic stress.....IEPCT II (Developed by IHI)
analysis

CASE 1 THICKNESS TRANSITION PRODUCED BY WELD EDGE
PREPARATION

MODEL

12 B Sch.100

Thickness

28.15 to 19.25 mm

COIL LENGTH

250 mm

HEATING DENSITY

0.0583 Kcal/mm³h (AT.OD)

HEATING DURATION

180 Sec.

RESULTS

- IMPROVEMENT EQUIVALENT TO SMOOTH PIPE IS EXPECTED.

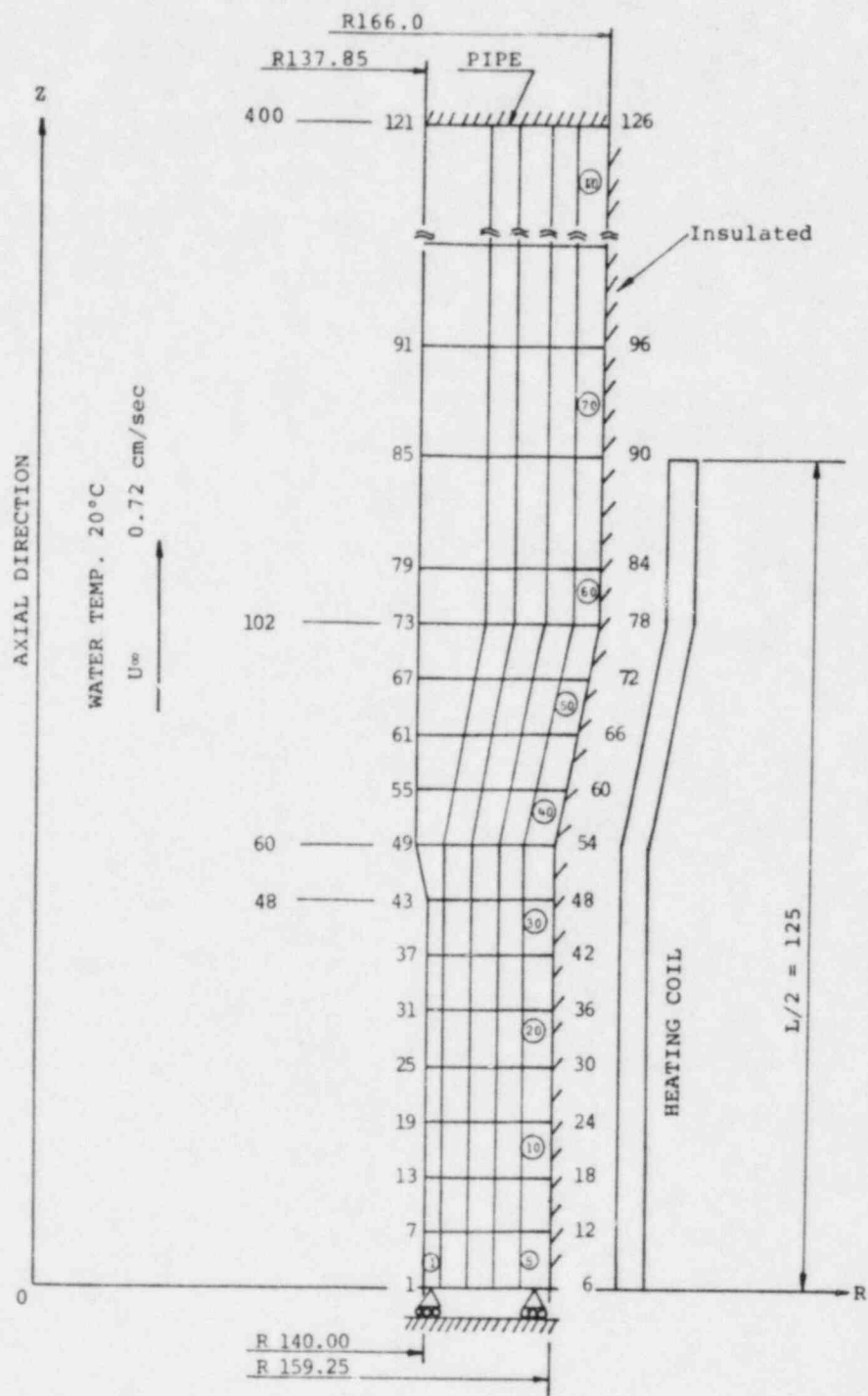


Fig. 1.1 ANALYTICAL MODEL

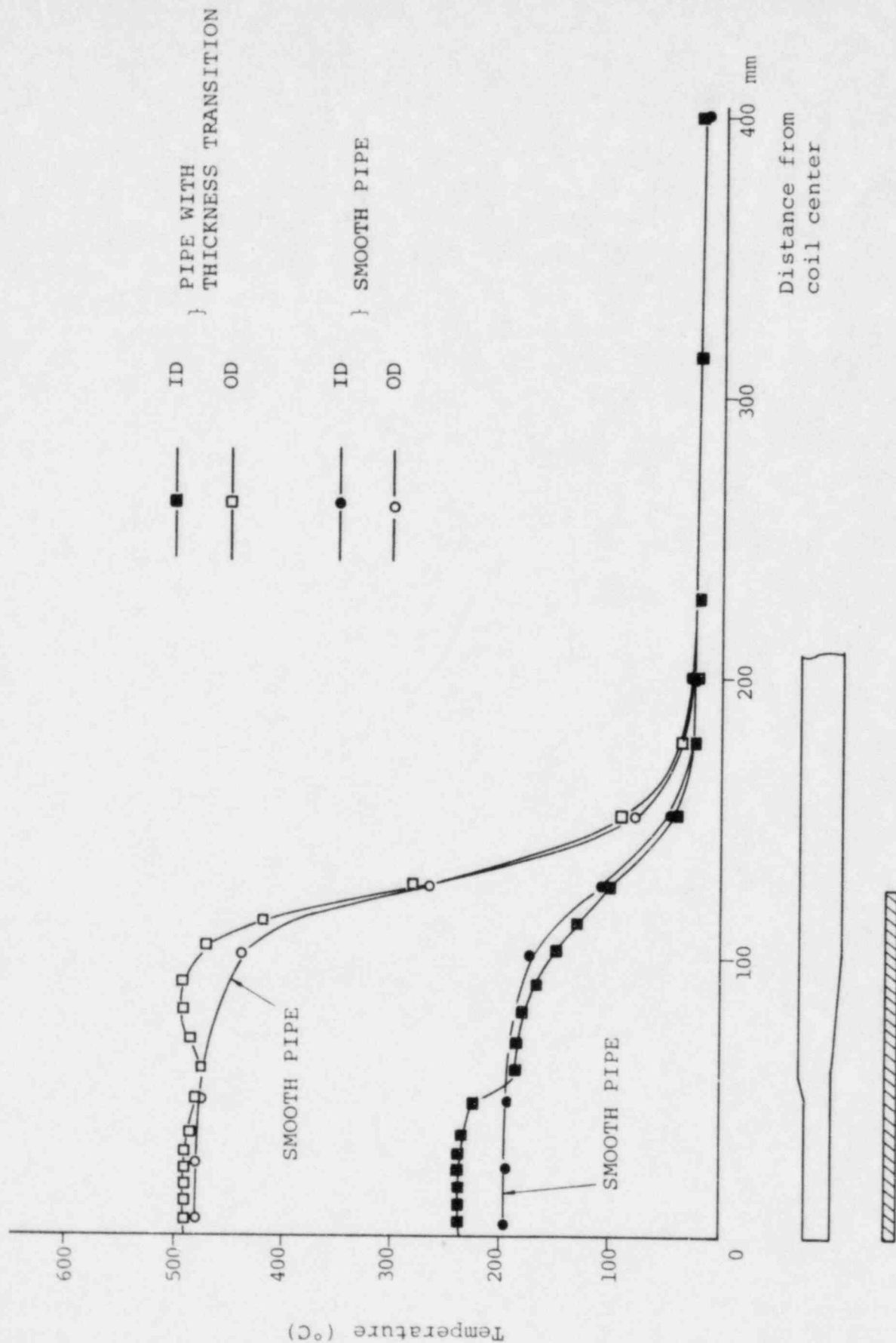


Fig. 1.2 TEMPERATURE DISTRIBUTION

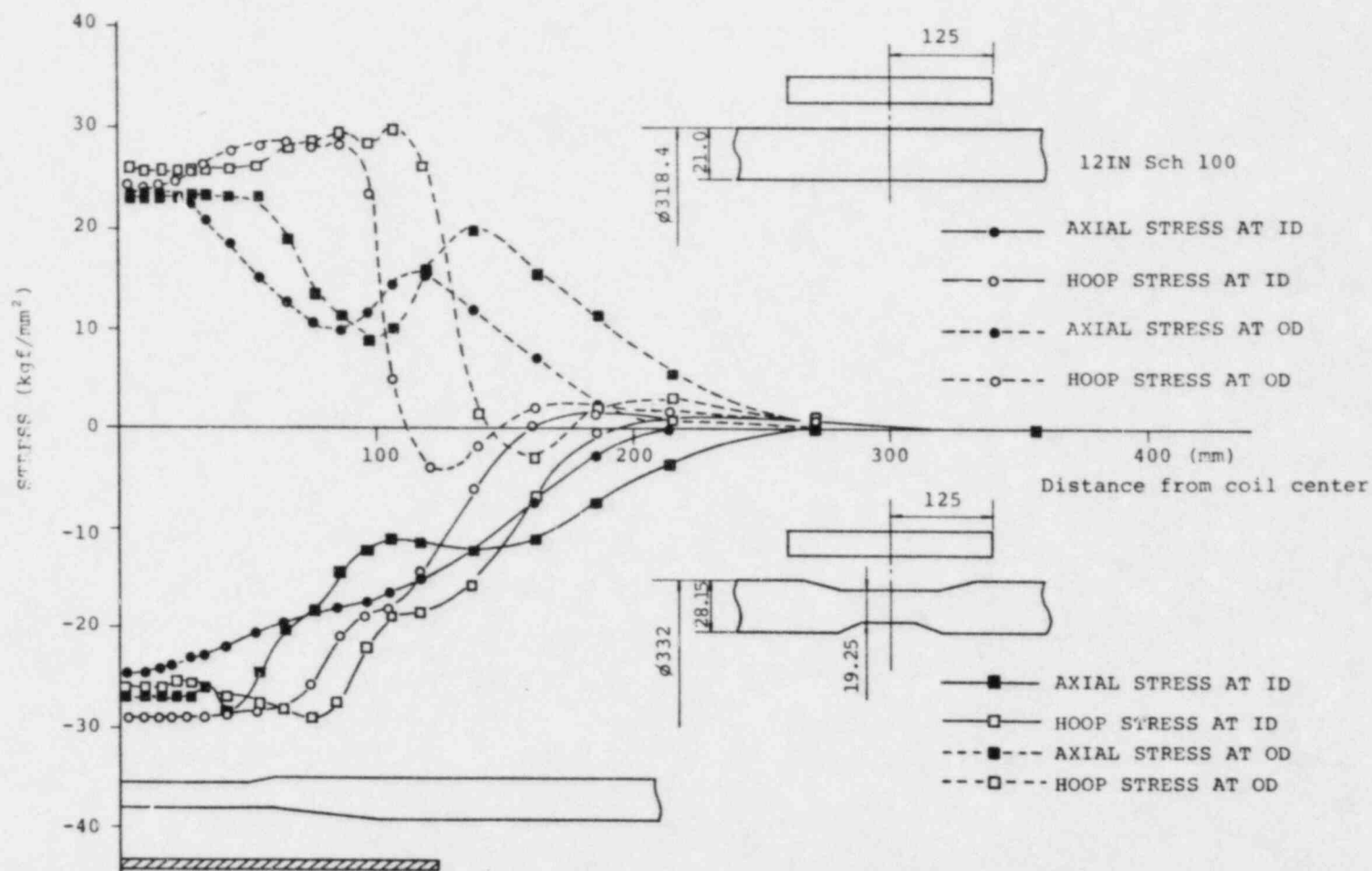


Fig. 1.3 RESIDUAL STRESS DISTRIBUTION

CASE 2 LARGE THICKNESS TRANSITION
(NOZZLE TO PIPE)

MODEL

24B

Thickness	44 mm
COIL LENGTH	400 mm
HEATING DENSITY	0.038 Kcal/mm ³ h (AT. O.D)
HEATING DURATION	240 Sec.
COOLING WATER	
TEMPERATURE	20°C
FLOW RATE	2 m/sec.

RESULTS

- SIGNIFICANT EFFECT OF LARGE THICKNESS TRANSITION
AT COIL END WAS NOT OBSERVED.

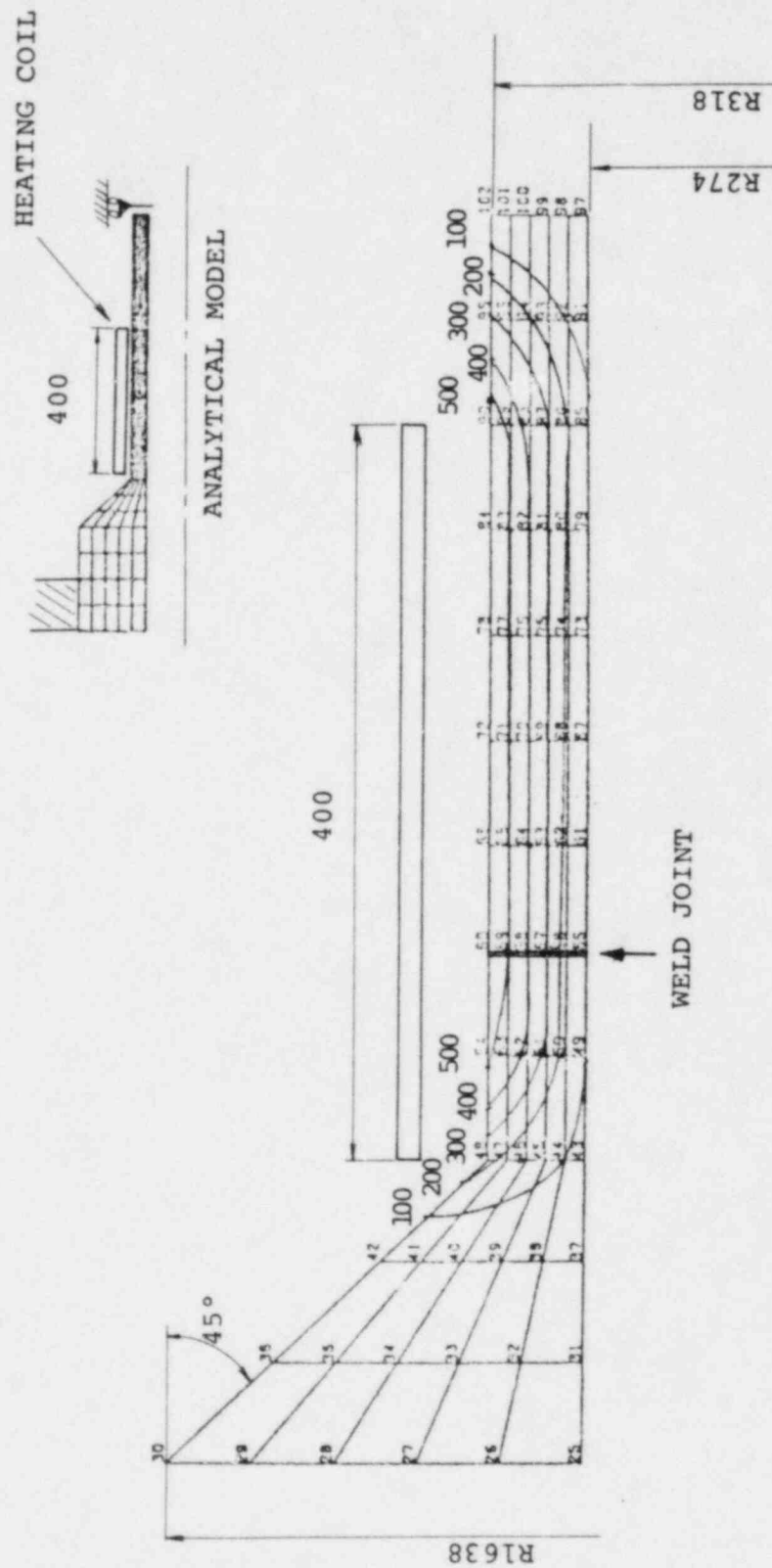


Fig. 2.1 TEMPERATURE DISTRIBUTION

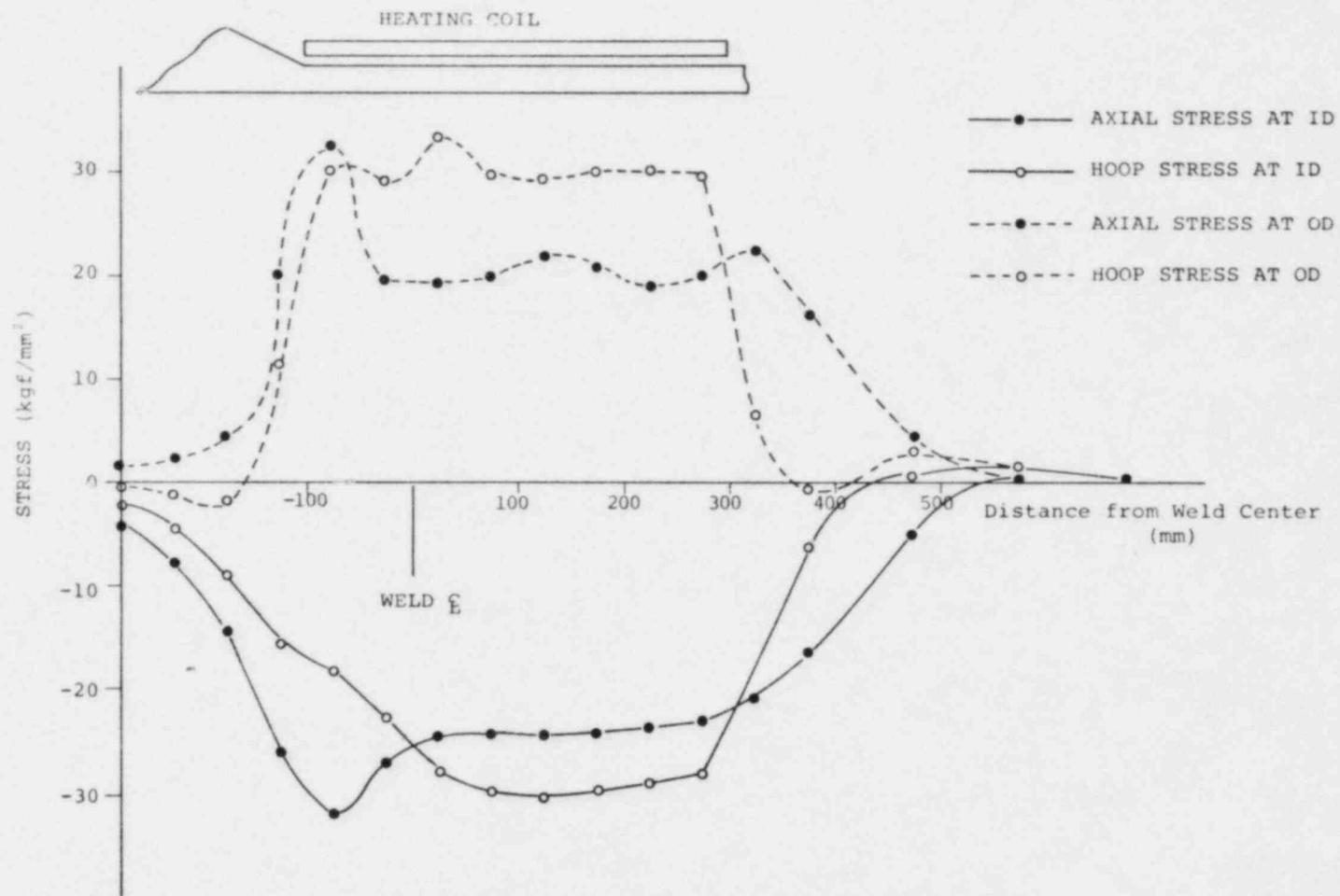


Fig. 2.2 RESIDUAL STRESS DISTRIBUTION

CASE 3 TRANSITION IN DIAMETER
(REDUCER: 24B TO 12B)

MODEL

REDUCER

24B to 12B (FIG. 3.1)

COIL DIMENSION

SEE FIG. 3.1

HEATING DENSITY

0.026 Kcal/mm³h (AT O.D.)

HEATING DURATION

360 Sec.

RESULTS

- COMPLICATED DISTRIBUTION OF RESIDUAL STRESS WAS OBSERVED
AT BOTH IN AND OD.
- COMPRESSIVE RESIDUAL STRESSES WERE INDUCED ON ALL ID
SURFACES UNDER COIL

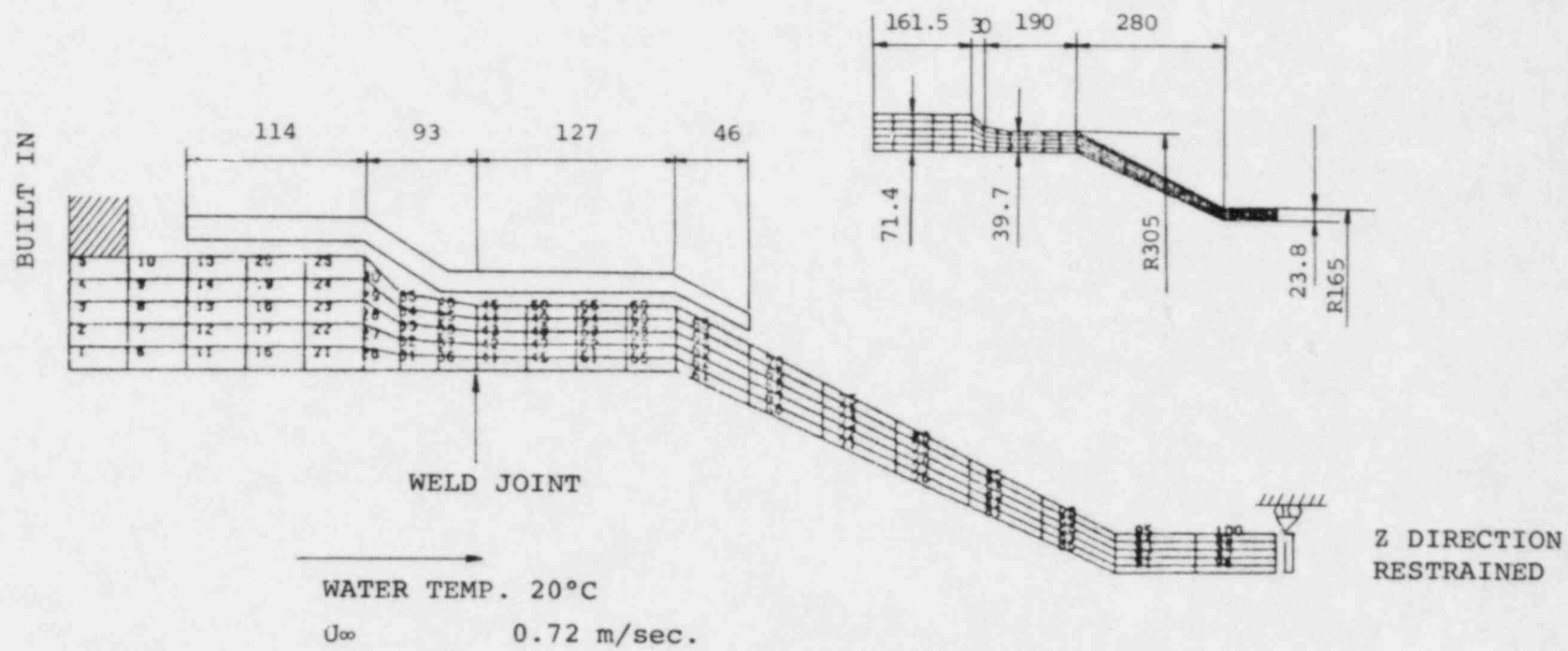


Fig. 3.1 ANALYTICAL MODEL

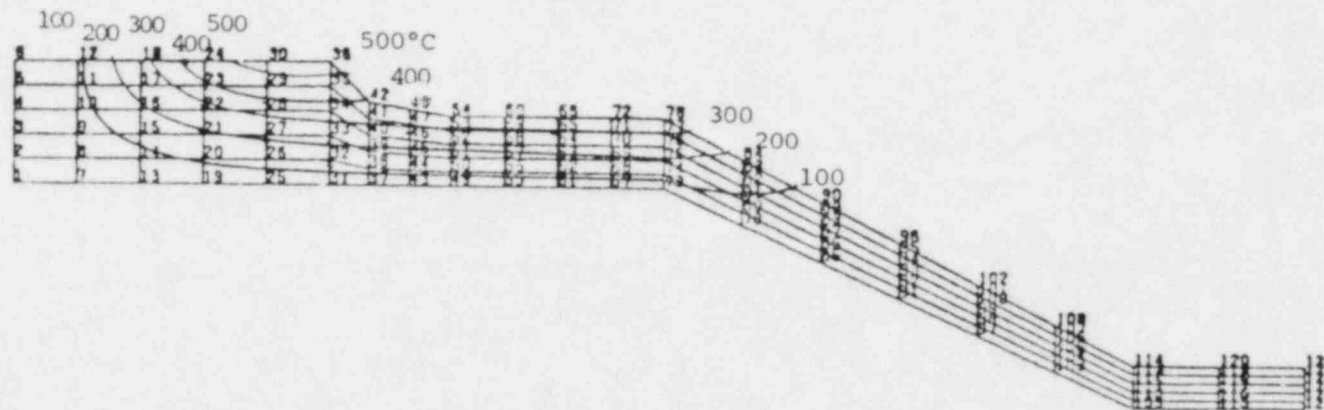


Fig. 3.2 TEMPERATURE DISTRIBUTION

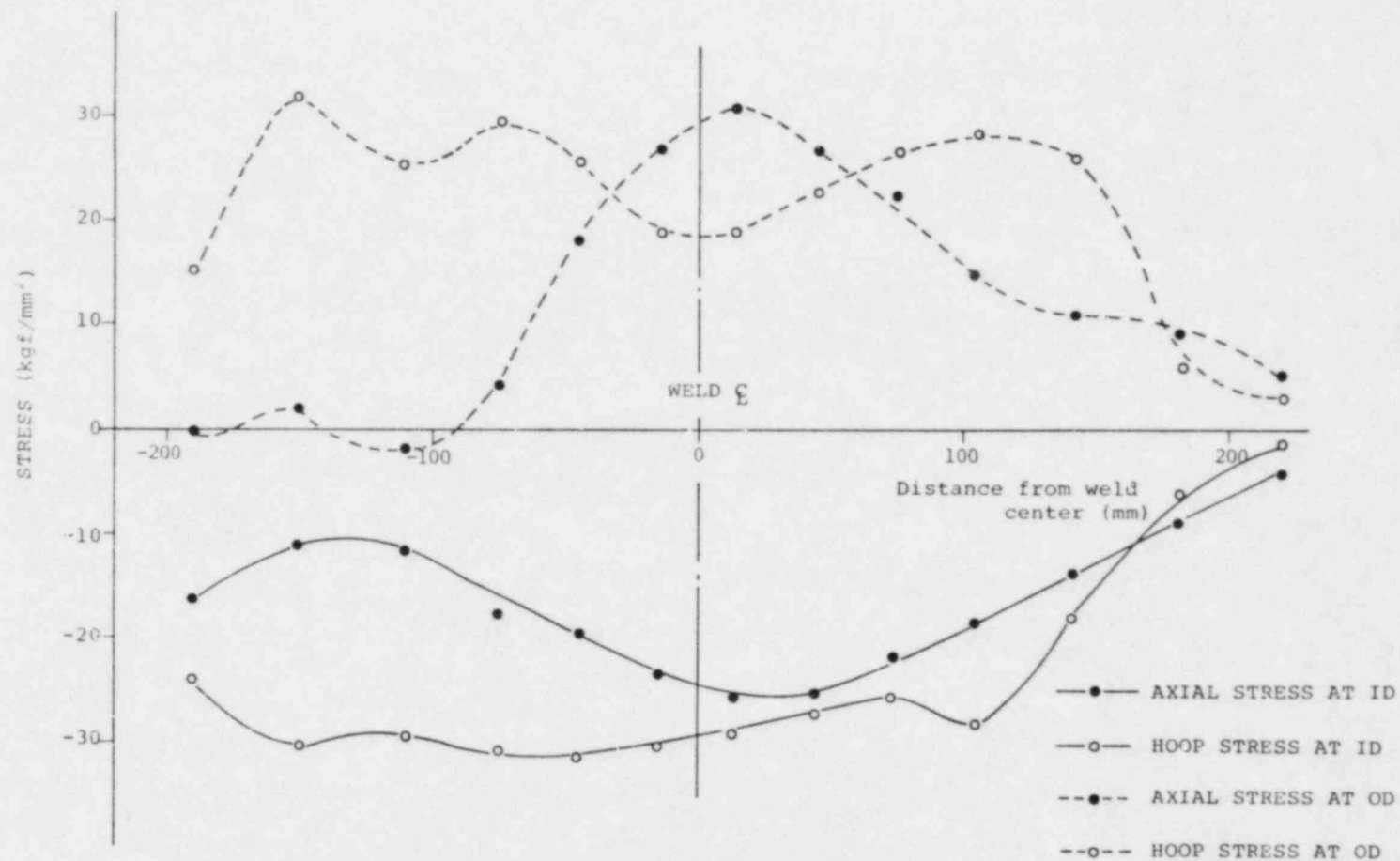


Fig. 3.3 RESIDUAL STRESS DISTRIBUTION

CASE 4 PIPE TO END CAP

MODEL	16B PIPE TO END CAP (SEE FIG. 4.1)
COIL LENGTH	330 mm
HEATING DENSITY	0.0515 Kcal/mm ³ h
HEATING DURATION	150 Sec.

RESULTS

- COMPLICATED DISTRIBUTION OF RESIDUAL STRESS WAS OBSERVED NEAR THE END CAP
- COMPRESSIVE RESIDUAL STRESSES WERE INDUCED ON ALL ID SURFACES UNDER THE COIL

Fig. 4.1 ANALYTICAL MODEL

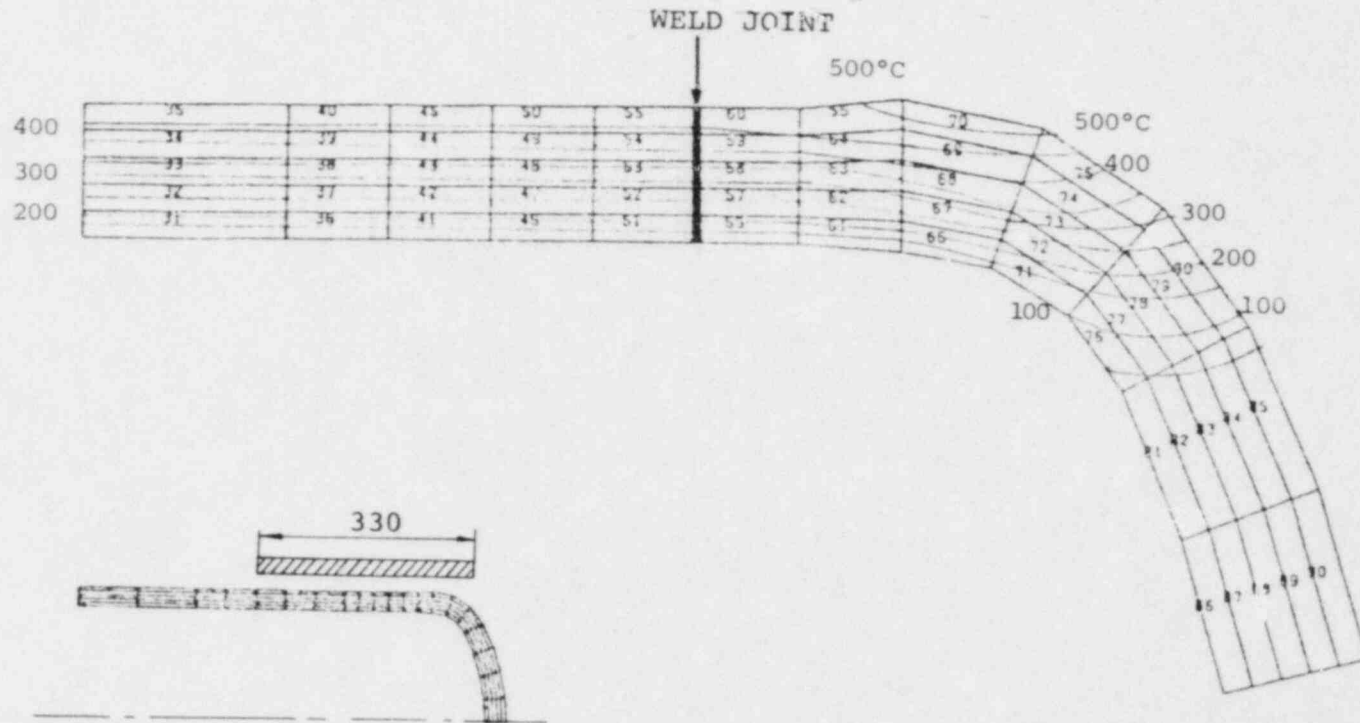


Fig. 4.2 THERMAL DISTRIBUTION

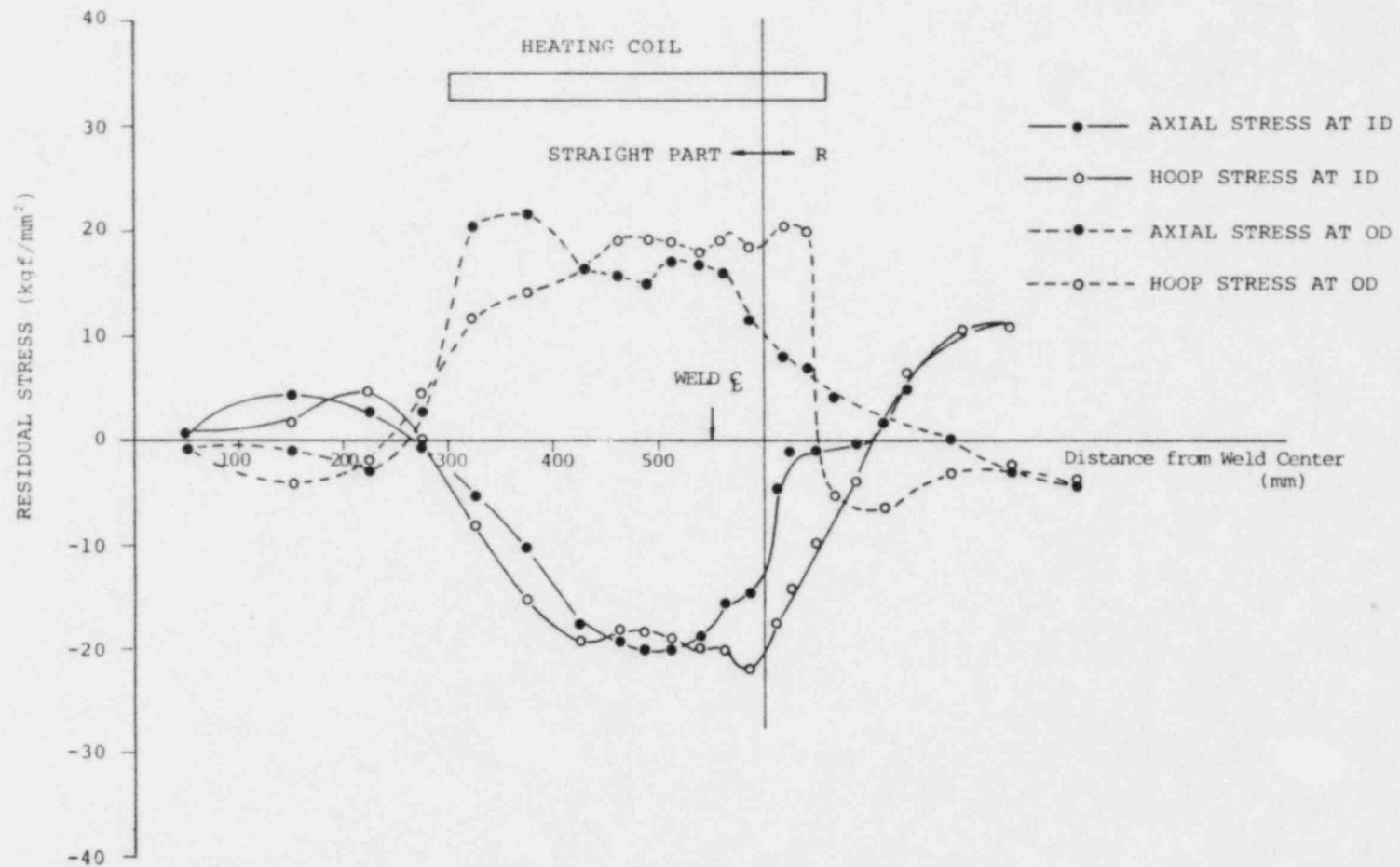


Fig. 4.2 RESIDUAL STRESS DISTRIBUTION

CASE 5 EFFECT OF INITIAL RESIDUAL STRESS

MODEL 12B PIPE (318.5^{mm}O.D, 21.4^{mm} THICK)

ANALYTICAL SEQUENCE

- STEP 1 GENERATING INITIAL STRESS BY
 SIMULATING A SINGLE PASS WELD
- STEP 2 IHSI TREATMENT

INITIAL RESIDUAL STRESS

- TEMPERATURE HISTORY FIG. 5.1
- RESIDUAL STRESS FIG. 5.2

RESULTS

- INITIAL RESIDUAL STRESSES HAVE NO SIGNIFICANT
EFFECT ON THE RESIDUAL STRESS LEVEL AFTER IHSI

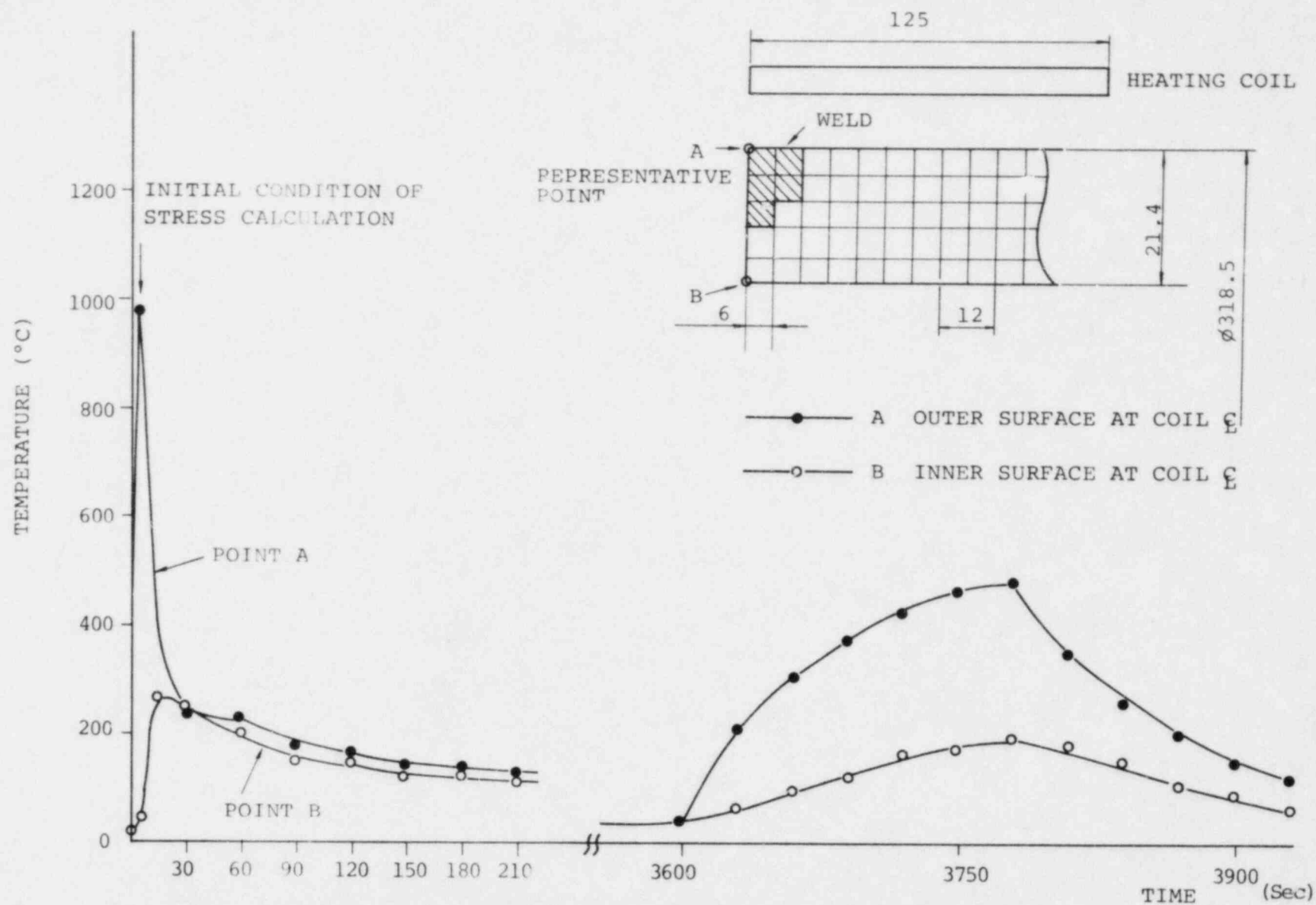


Fig. 5.1 THERMAL CYCLE OF WELDING AND IHSI

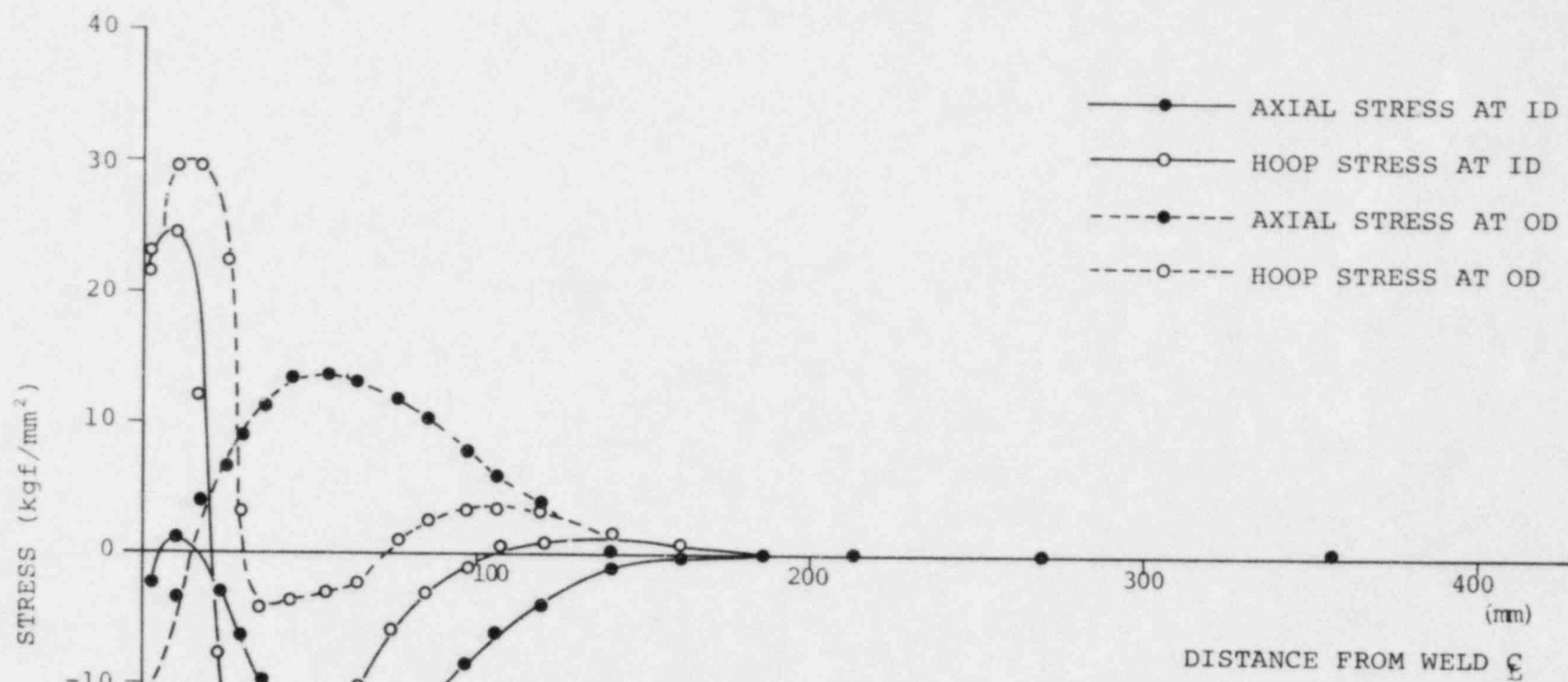


Fig. 5.2 RESIDUAL STRESS DISTRIBUTION AFTER WELDING

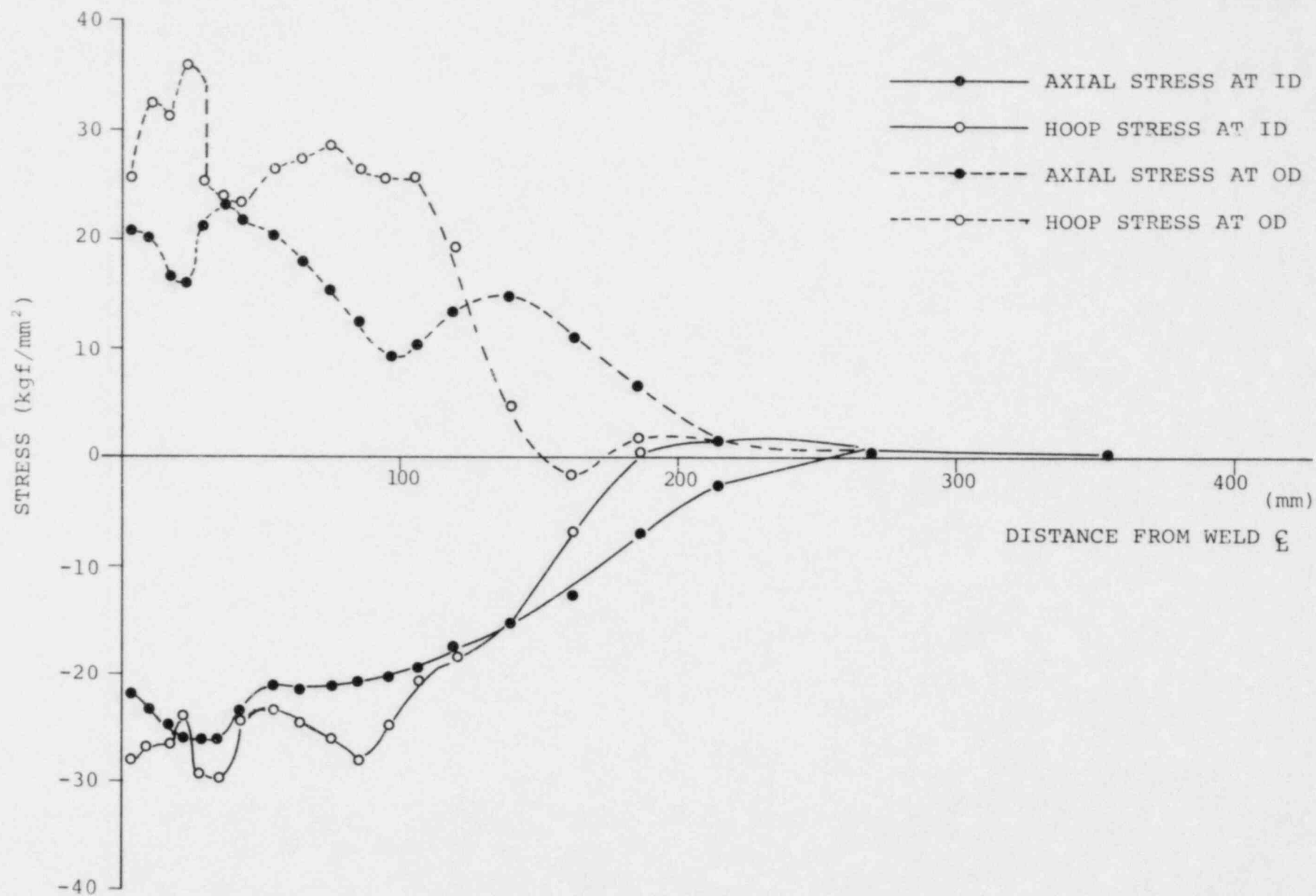


Fig. 5.3 RESIDUAL STRESS DISTRIBUTION AFTER IHSI

A - 9

ANALYTICAL STUDIES OF SOME IHSI PARAMETERS

- Temperature Difference
- Coil Width
- Current Frequency

1. Introduction

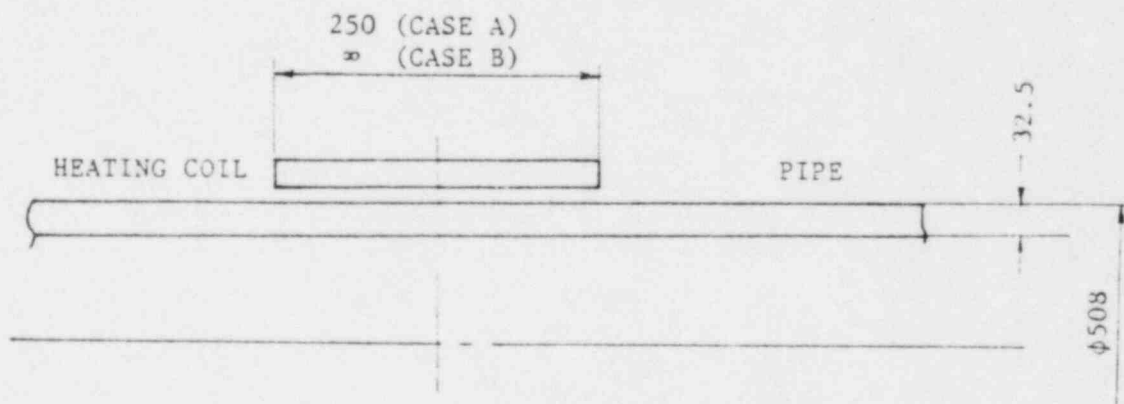
This appendix presents analytical studies of three parameters, temperature difference, heating depth and coil width for IHSI. In Chapter 5, evaluation of these parameters and brief explanations are provided. In this appendix, the analytical results are explained in detail.

2. Temperature Difference

In Chapter 5, the required temperature difference is calculated using an elastic perfectly plastic model. Some analyses were performed to determine the amount of temperature difference which was required to improve the residual stresses.

2.1 Pipe Model

The pipe model was a 20 in. Schedule 100 pipe. Two coil widths were selected. One was 250 mm ($2.8\sqrt{Rt}$), the other was infinity.



Coil length of 250 mm represents the lower limit of the coil length. On the other hand, a coil length of infinite length was selected as the ideal case.

2.2 Analytical model

The analytical models are shown in Fig. 2.1 and Fig. 2.2. Fig. 2.1 represents CASE A and Fig. 2.2 represents CASE B.

2.3 Analytical condition

(a) Cooling condition

Cooling water flows inside pipe. Water temperature is 20°C and water velocity is 0.72m/sec. The hatched regions of Fig. 2.1 and Fig. 2.2 show insulating boundaries. The heat transfer coefficient for the pipe inside was determined as 1500 kcal/m²h°C.

Calculations are shown below.

$$Pr = 7.11$$

$$Re = \frac{Wd}{\nu} = \frac{0.72 \times 0.443}{1.01 \times 10^{-6}} = 3.16 \times 10^5$$

$$Nu = 0.023 Re^{0.8} Pr^{0.4} = 0.023 \times (3.16 \times 10^5)^{0.8} \times 7.11^{0.4} = 1265$$

$$h_m = \frac{Nu \cdot \lambda}{d} = \frac{1265 \times 0.511}{0.443} = 1459 \text{ kcal/m}^2\text{h}^\circ\text{C}$$

Nu : Nusselt number

Re : Reynolds number

Pr : Prandtl number

W : Average water velocity

d : Pipe inside diameter

ν : Coefficient of kinematic viscosity

λ : Thermal conductivity

h_m : Average heat transfer coefficient

(b) Heating condition

As shown in Fig. 2.1, the elements located beneath the heating coil were induction heated. The heating density distribution in the thickness direction is shown below.

$$w = w_0 e^{-2x/S} \text{ (kcal/mm}^3 \text{ sec)}$$

$$s = \frac{1}{2\pi} \sqrt{\frac{\rho}{\mu f}} = 9.6 \text{ (mm)}$$

s : Heating depth

ρ : Specific resistance

μ : Specific magnetic permeability

f : Frequency

x : Depth from outside diameter

w_0 : Heating density at outside surface

w_0 was selected so that the temperature difference between the outside and inside diameter would be in the range $100^\circ\text{C} \sim 400^\circ\text{C}$.

(c) Boundary condition

The calculation is performed for one half of the length because the analytical model is symmetrical.

Nodal points 1 ~ 6 in Fig. 2.1 and Fig. 2.2 are restricted in the axial direction. Nodal points 121 ~ 126 in Fig. 2.1 and 13 ~ 18 in Fig. 2.2 are tied in the axial direction.

(d) Physical properties

The temperature dependency of physical properties from $20^\circ\text{C} \sim 600^\circ\text{C}$ were used.

- 1) The thermal expansion coefficient, Young's modulus and Poisson's ratio are shown in Table 2.1 and Table 2.2.
- 2) The temperature dependency of yield point is shown in Fig. 2.3.

(3) Calculating condition

The calculating conditions are summarized in Table 2.3.

2.4 Calculated results

Calculated results are shown in Table 2.4 and these results are summarized graphically in Fig. 2.4 and Fig. 2.5.

From Fig. 2.4 for short coil case and Fig. 2.5 for infinite coil case, the following items are considered.

- (1) While residual stress for the short coil case saturates at about 350°C , that for the infinite coil case saturates at about 300°C .
- (2) Saturated residual stress for the infinite coil case is lower than that for short coil case.
- (3) The temperature difference calculated by elastic perfectly plastic theory does not correspond to the saturated residual stress but gives satisfactory residual stress results.

Some typical results for CASE A1 are attached.

Fig. 2.6 is the temperature transition curve.

Fig. 2.7 is the temperature distribution in the thickness direction.

Fig. 2.8 is the temperature distribution in the axial direction.

Fig. 2.9 is the residual stress distribution in the thickness direction.

Fig. 2.10 is the residual stress distribution in the axial direction.

2.5 Conclusion

Whether the coil width is of full length or not, the residual stress becomes satisfactorily compressive.

Simply calculating temperature difference corresponding to perfect elastic perfectly plastic theory gives satisfactory large compressive stress results.

3. Coil Width

In Chapter 5 the effects of coil width are graphically illustrated using the data obtained experimentally and analytically.

If the coil width is not of full length, the coil end effects due to the bending moment which is produced by temperature difference in the axial direction are significant so that the residual stress benefit will be reduced.

Some elastic-plastic calculations were performed to determine how much width would be required for the coil.

3.1 Objects for analysis

The objects for analysis were 12 inch Schedule 100 pipe and 20 inch Schedule 100 pipe.

3.2 Analytical model

The analytical model is shown in Fig. 3.1

3.3 Analytical condition

The analytical condition is the same as presented in article 2 of this appendix.

3.4 Calculated results

The calculated results are summarized in Table 3.1 and Fig. 3.2. These results are the same as in Chapter 5 in the text.

From Fig. 3.2, the following is observed. Residual stresses saturate at about $3\sqrt{Rt}$ coil width. Hoop stress is lower than axial stress but is equal to axial stress at about $5\sqrt{Rt}$ coil width.

The residual stresses are shown in Fig. 3.3 ~3.11.

Some typical results are shown in Fig. 3.12 ~3.15 for case No. 5.

Fig. 3.12 shows the time-temperature diagram.

Fig. 3.13 shows the temperature distribution in the axial direction at maximum temperature.

Fig. 3.14 shows the temperature distribution in the thickness direction at maximum temperature.

Fig. 3.15 shows the residual stress distribution in the thickness direction.

3.5 Conclusion

As shown in Fig. 3.2, the residual stress becomes saturated and sufficiently compressive when the coil width is about $3\sqrt{Rt}$ or greater. Therefore, a coil width of $3\sqrt{Rt}$ is enough to improve the residual stress.

4. Current Frequency

Current frequency effects on the heating depth, namely the temperature distribution will depend on current frequency. Heating depth(s) is given by the following equation.

$$s = \frac{1}{2\pi} \sqrt{\frac{\rho}{\mu f \times 10^{-9}}} \quad (\text{cm})$$

μ : Specific magnetic permeability

f : Frequency (cycle/s)

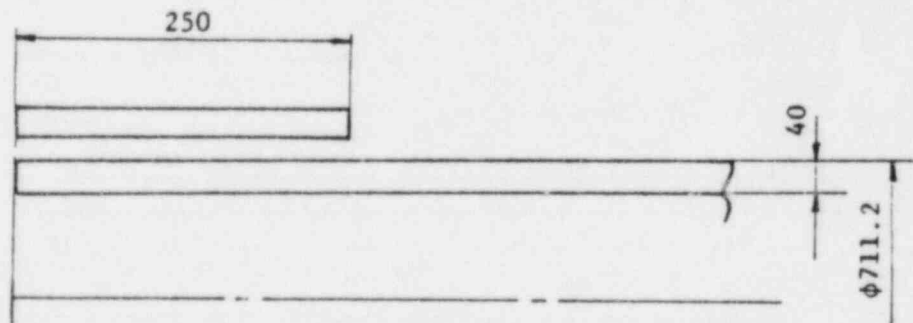
ρ : Specific resistance ($\Omega \cdot \text{cm}$)

Some elastic-plastic and elastic calculations were performed to evaluate current frequency,

4.1 Elastic-plastic calculation

4.1.1 Object of analysis

Object of analysis was 28 inch Schedule 100 pipe.



The modelled coil width was 500 mm. 500 mm corresponds to about $4.3\sqrt{Rt}$.

4.1.2 Analytical condition

Three current frequencies were considered. Analytical conditions are summarized in Table 4.1. Heating power P is calculated by the following equations. The heating power was selected so that the temperature difference between the outside surface and inside surface is the same value when the heating depth is different.

For a current frequency of 0.3 and 3 kHz

$$P = \int_{\text{volume}} w_o e^{-2x/s} dV$$

For a current frequency of ∞ kHz

$$P = \int_{\text{surface}} Q dS$$

Where w_o : Heating density at the outside surface
 Q : Heat flux at the outside surface

4.1.3 Calculated results

The calculated results are shown in Fig. 4.1 & Fig. 4.2

Fig. 4.1 shows the temperature distribution in the thickness direction.

Fig. 4.2 shows the residual distribution in the thickness direction for different heating depths.

4.3 Conclusion

The calculation using an elastic-plastic analysis shows that the residual stresses are not affected by the current frequency. The reason why the current frequency gives no effect is that when sufficient temperature difference exists, the residual stress will saturate and the current frequency barely produces an effect.

TABLE 2.1

TEMPERATURE (°C)	THERMAL EXPANSION (INSTANTANEOUS) (1/°C)	THERMAL EXPANSION (MEAN FROM R.T.) (1/°C)
20	16.4×10^{-6}	16.4×10^{-6}
50	16.7	16.6
100	17.1	16.8
150	17.5	17.1
200	17.9	17.3
250	18.3	17.4
300	18.6	17.6
350	19.0	17.8
400	19.3	18.0
450	19.8	18.2
500	20.2	18.4
550	20.5	18.6
600	20.9	18.7
650	21.3	18.9
700	21.6	19.0
750	22.0	19.1
800	22.4	19.2

TABLE 2.2

TEMPERATURE (°C)	THERMAL CONDUCTIVITY (Kcal/cm-s-°C)	SPECIFIC HEAT (Kcal/kg-°C)	THERMAL DIFFUSIVITY (cm ² /s)
20	34.7×10 ⁻⁶	0.107	
50	35.7	0.112	0.0390
100	37.2	0.117	0.0399
150	38.9	0.122	0.0409
200	40.5	0.125	0.0420
250	42.1	0.127	0.0432
300	43.7	0.130	0.0439
350	45.4	0.131	0.0447
400	47.0	0.132	0.0453
450	48.6	0.134	0.0462
500	50.3	0.135	0.0470
550	51.8	0.137	0.0478
600	53.5	0.139	0.0487
650	55.1	0.141	0.0497
700	56.7	0.143	0.0506
750	58.3	0.145	0.0514
800	59.9	0.148	0.0523

TEMPERATURE (°C)	YOUNG'S MODULUS (kg/cm ²)	POISSON'S RATIO	DENSITY (kg/cm ³)
20	1.98×10 ⁻⁶	0.260	8.03×10 ⁻³
50	1.97	0.264	8.02
100	1.95	0.270	8.00
150	1.91	0.274	7.97
200	1.88	0.278	7.95
250	1.84	0.281	7.93
300	1.79	0.284	7.90
350	1.76	0.288	7.88
400	1.72	0.292	7.86
450	1.67	0.296	7.83
500	1.63	0.300	7.81
550	1.58	0.304	7.79
600	1.53	0.308	7.77
650	1.47	0.314	7.74
700	1.41	0.318	7.72
750	1.36	0.320	7.70
800	1.31	0.324	7.67

TABLE 2.3 CALCULATING CONDITION (PROGRAM I TEMP II I EPTC II)

CASE	ANALYTICAL MODEL	BOUNDARY TEMPERATURE (°C)	HEATING DENSITY (Kcal/mm ² h)	HEAT TRANSFER COEFFICIENT (Kcal/m ² h°C)	COIL WIDTH (mm)
A1	Fig. 2.1	20°	0.055	1500	125
A2			0.0452		
A3			0.0357		
A4			0.0238		
A5	↓		0.0119		↓
B1	Fig. 2.2		0.055		∞
B2			0.0452		
B3			0.0357		
B4			0.0238		
B5	↓	↓	0.0119	↓	↓

TABLE 2.4 CALCULATED RESULTS

CASE	TEMPERATURE DIFFERENCE BETWEEN OUTSIDE AND INSIDE SURFACES (°C)	RESIDUAL STRESS AT INSIDE SURFACE
A1	366.715	-23.3
A2	313.904	-22.8
A3	258.874	-20.9
A4	183.359	-14.2
A5	98.100	-3.05
B1	367.267	-28.0
B2	314.346	-27.8
B3	259.211	-26.6
B4	183.578	-24.6
B5	98.214	-6.14

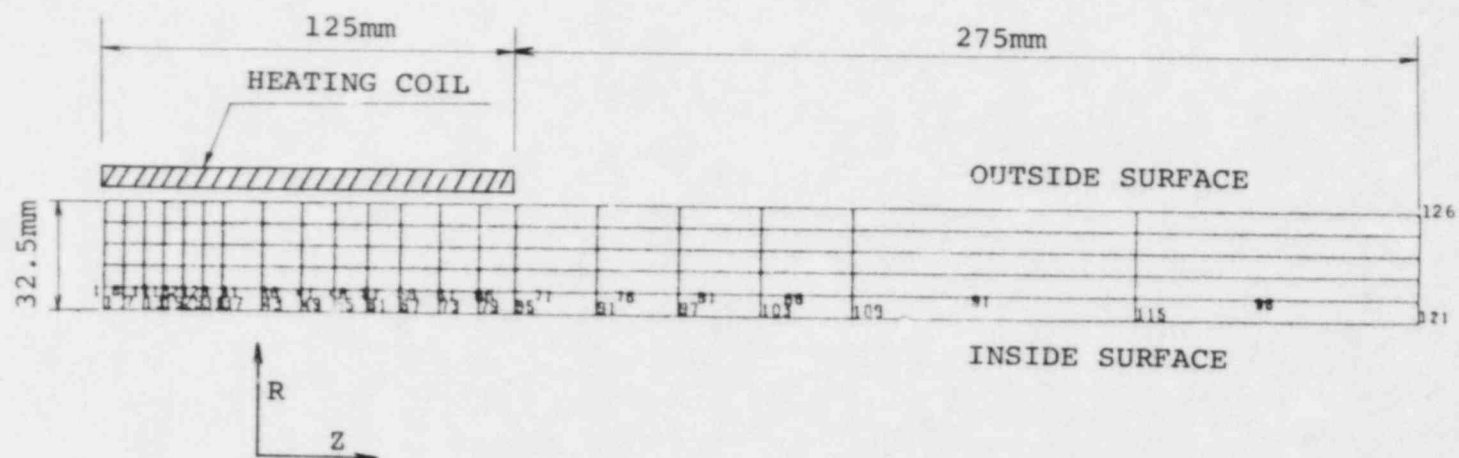


Fig. 2.1 ANALYTICAL MODEL (CASE A1 ~ A5)

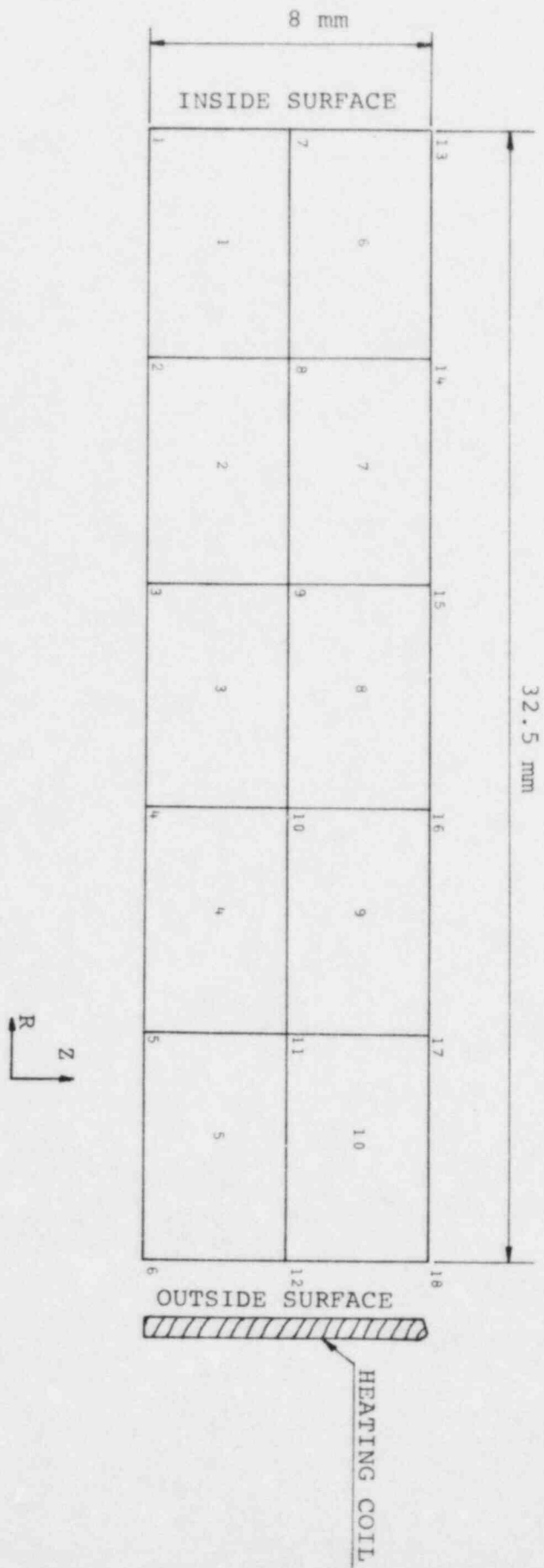


Fig. 2.2 ANALYTICAL MODEL (CASE B1 ~ B5)

* Japan Society of Mechanical Engineer

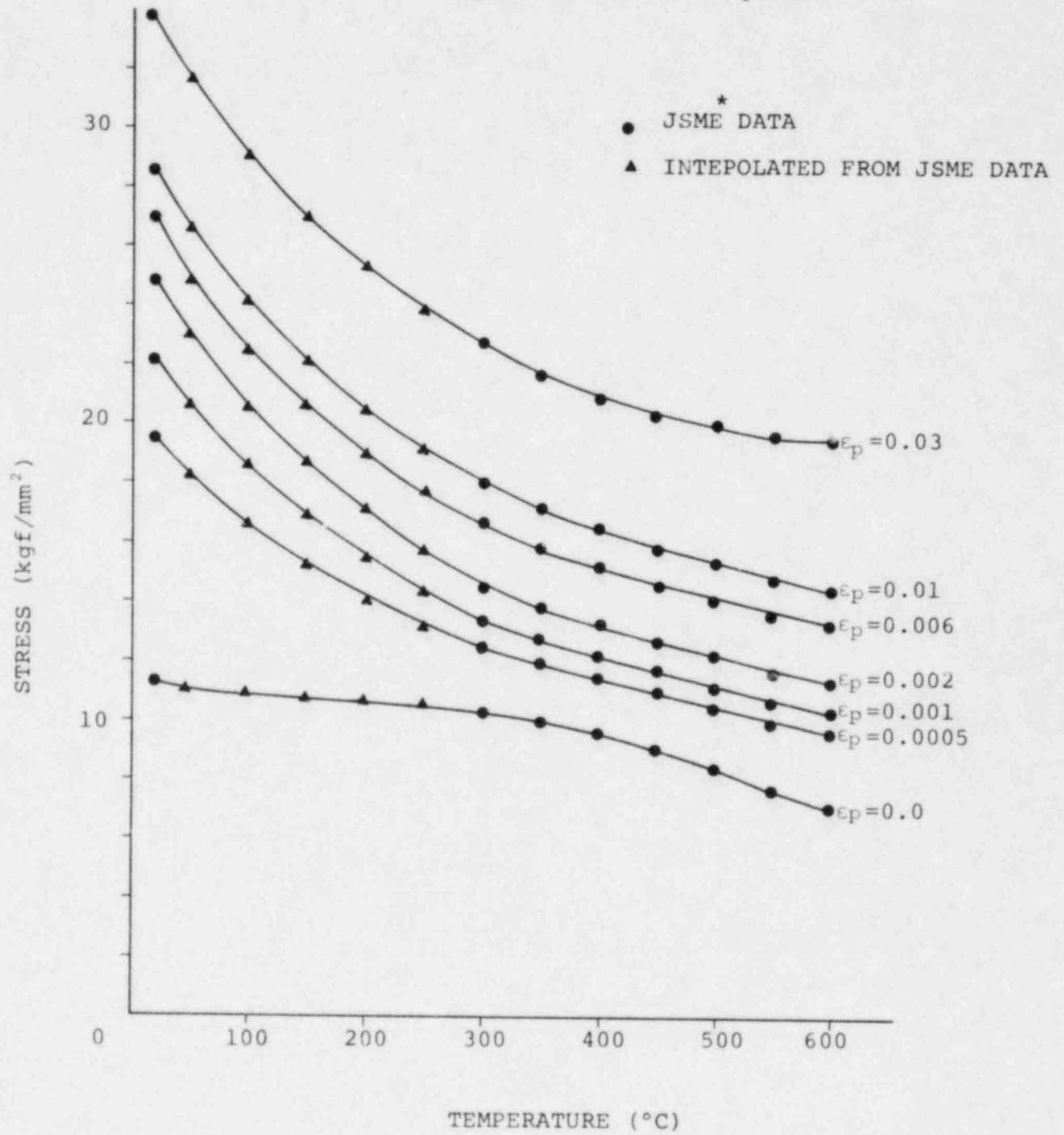


Fig. 2.3 STRESS-TEMPERATURE RELATION

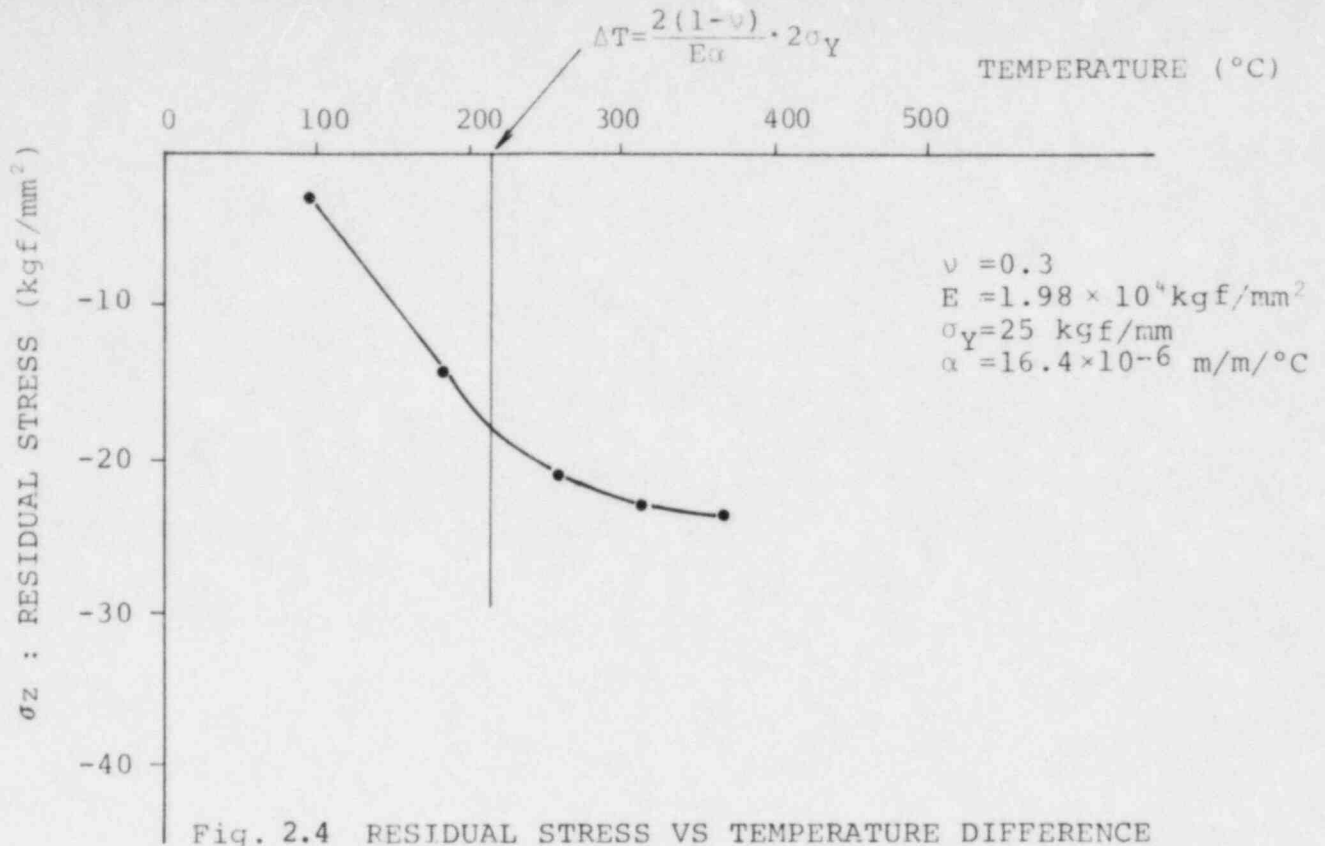


Fig. 2.4 RESIDUAL STRESS VS TEMPERATURE DIFFERENCE
(COIL LENGTH : $2.8\sqrt{Rt}$)

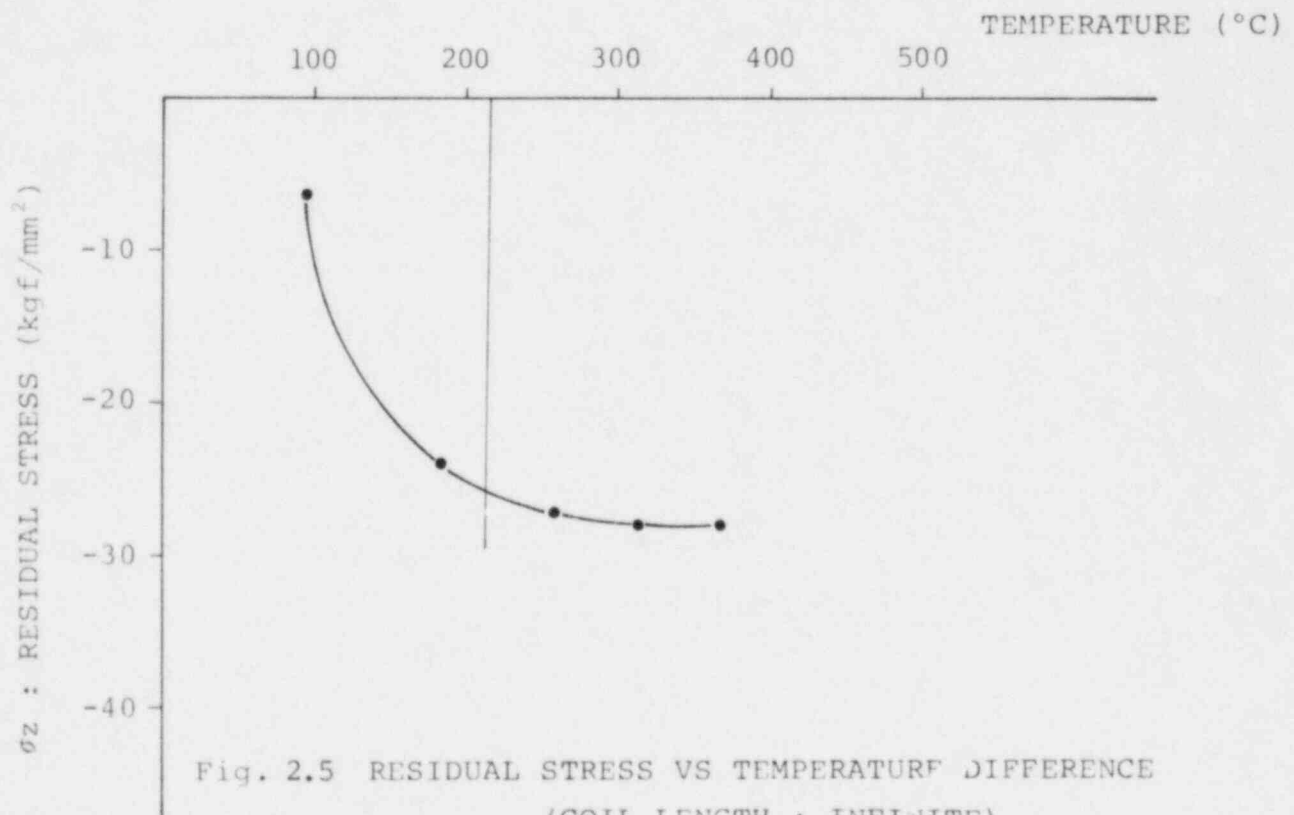


Fig. 2.5 RESIDUAL STRESS VS TEMPERATURE DIFFERENCE
(COIL LENGTH : INFINITE)

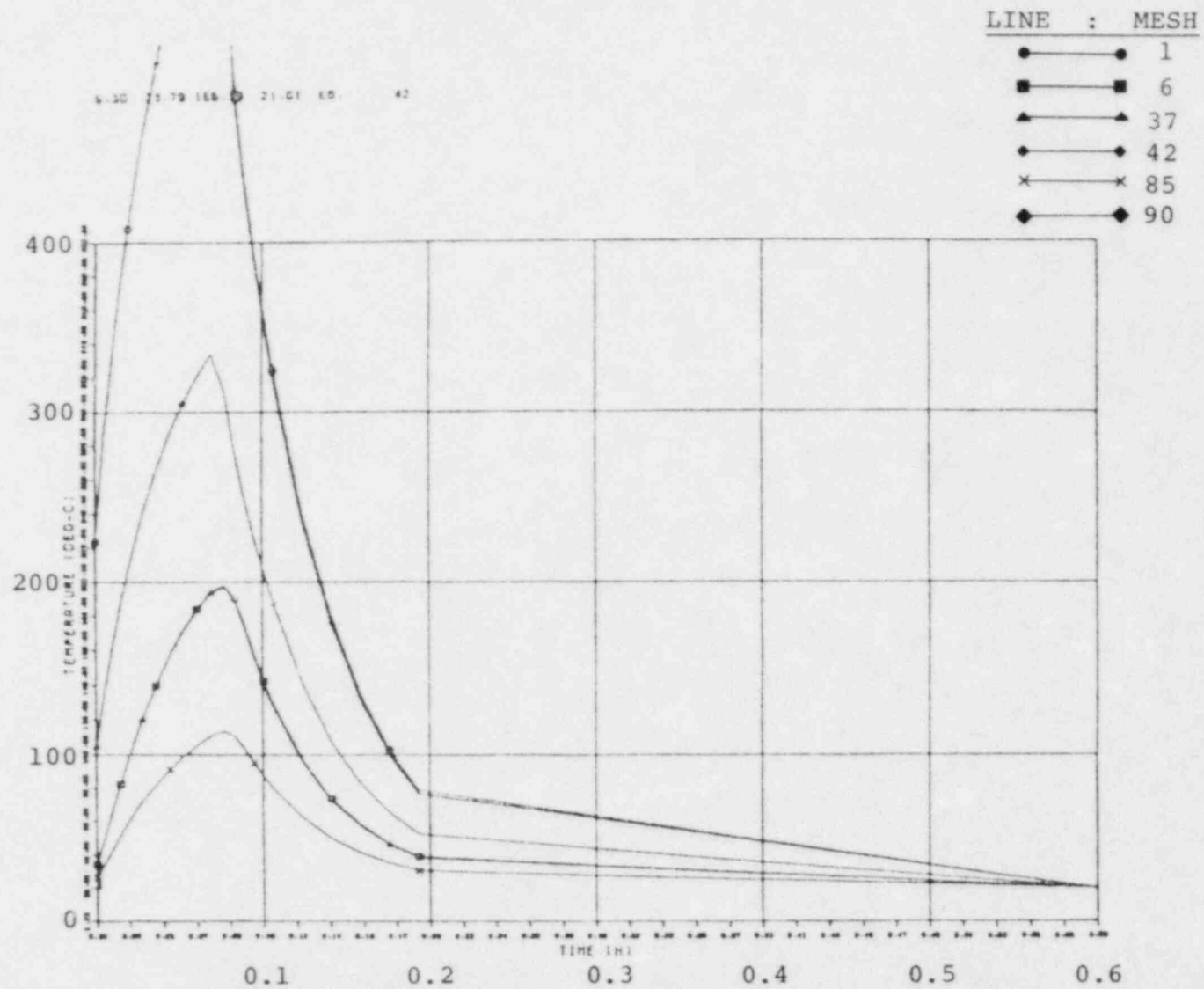


Fig. 2.6 CASE A1 TEMPERATURE TRANSITION

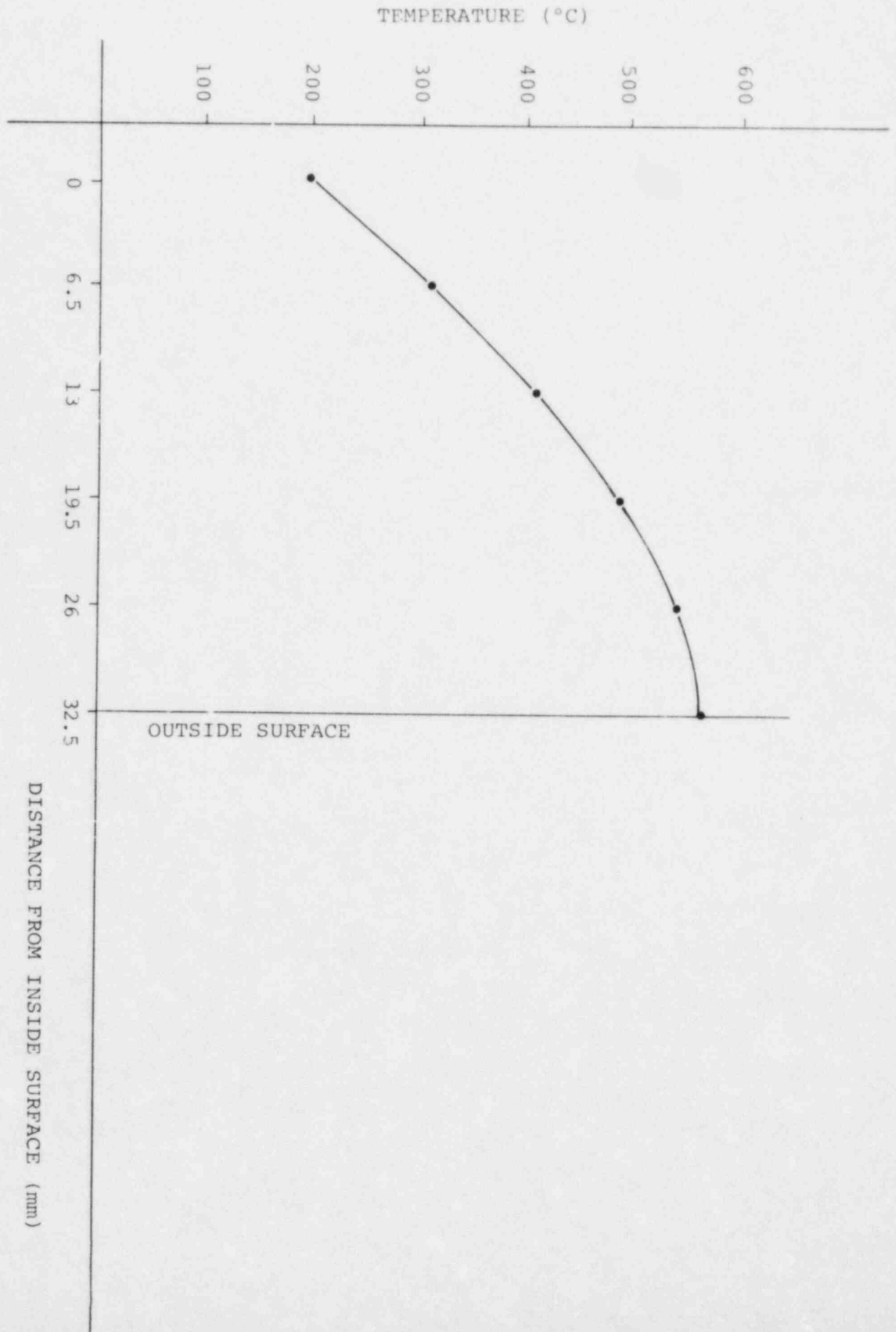


Fig. 2.7 CASE A1 TEMPERATURE DISTRIBUTION THROUGH THICKNESS

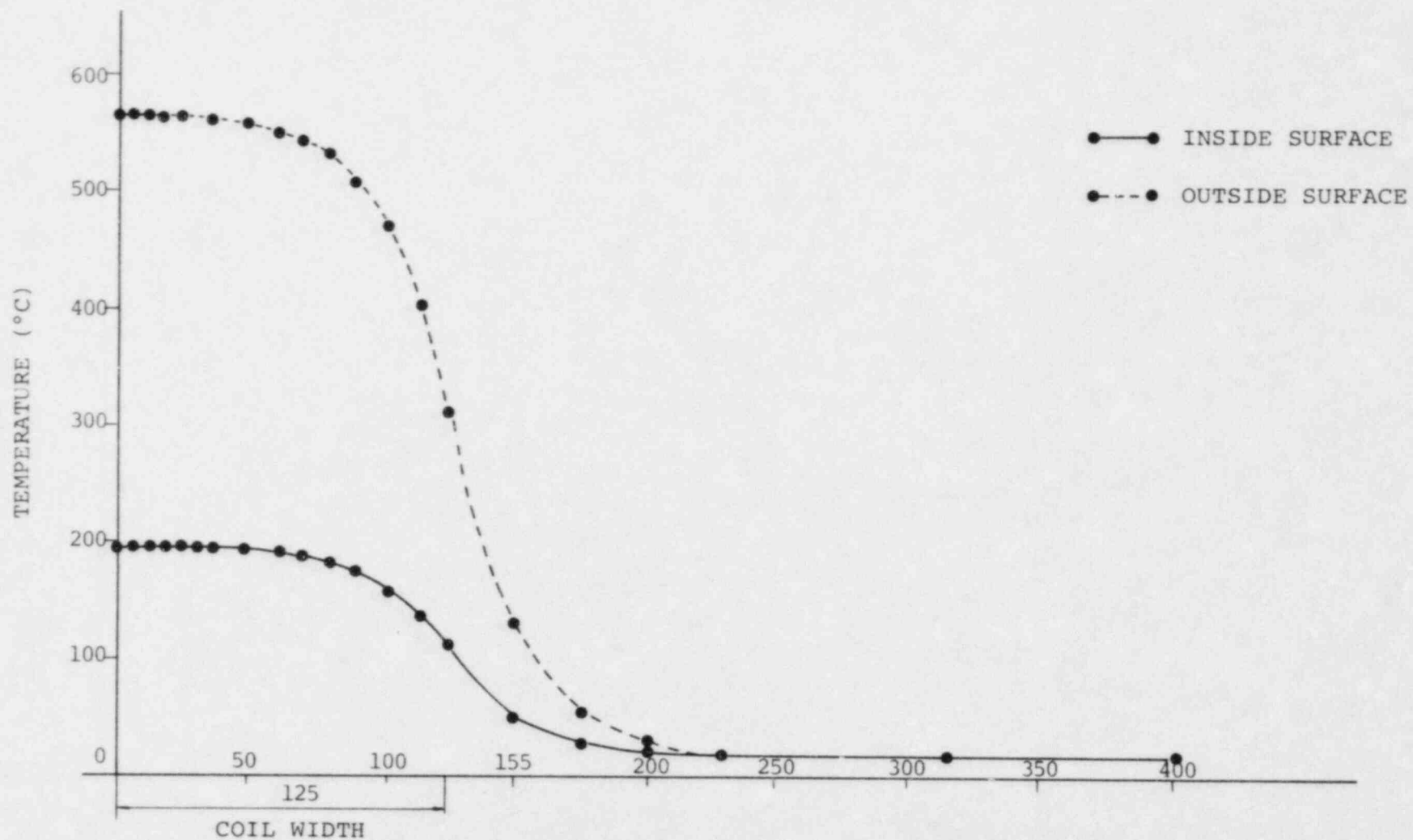


Fig. 2.8 CASE A1 TEMPERATURE DISTRIBUTION IN AXIAL DIRECTION

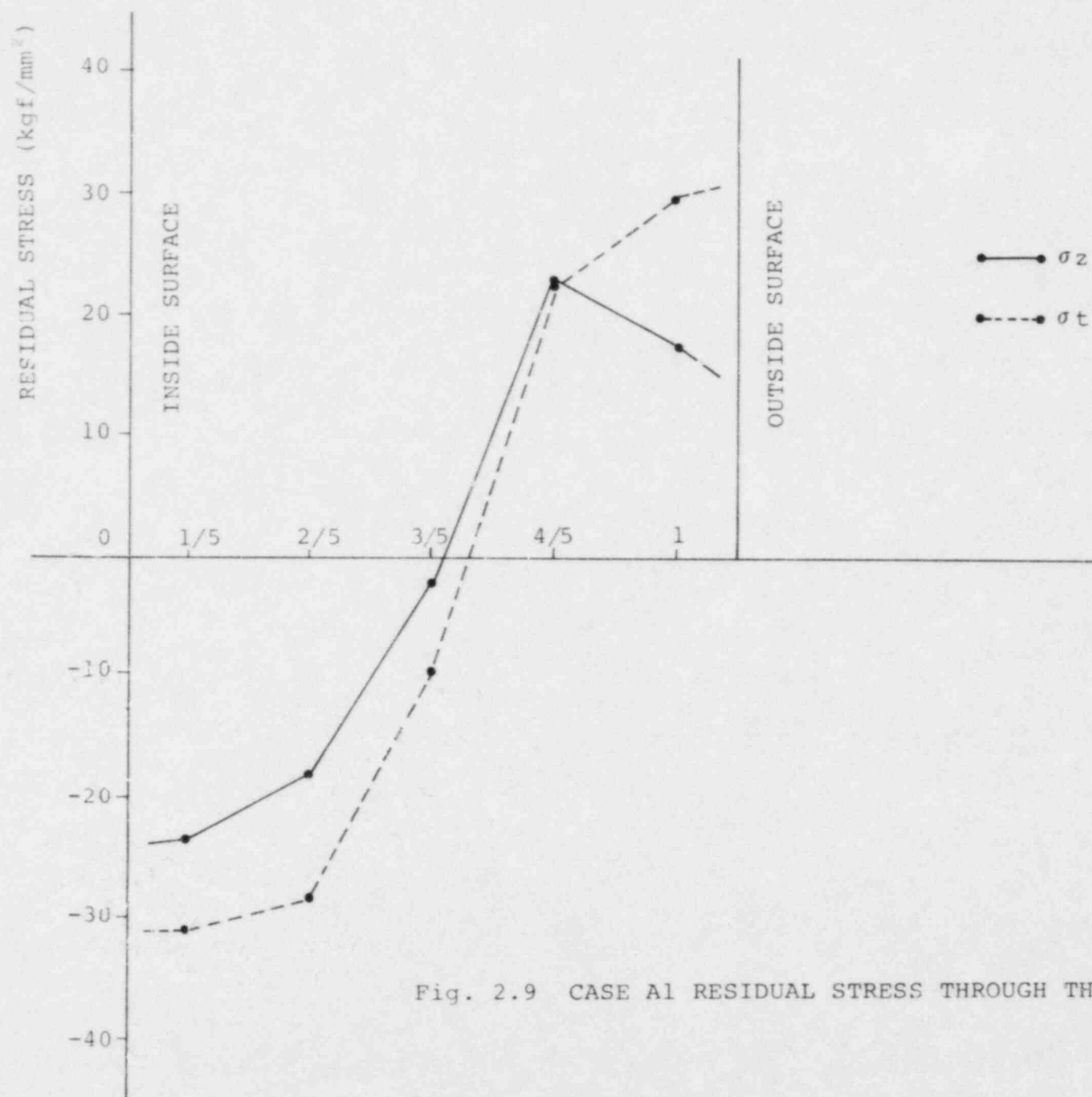


Fig. 2.9 CASE A1 RESIDUAL STRESS THROUGH THICKNESS DIRECTION

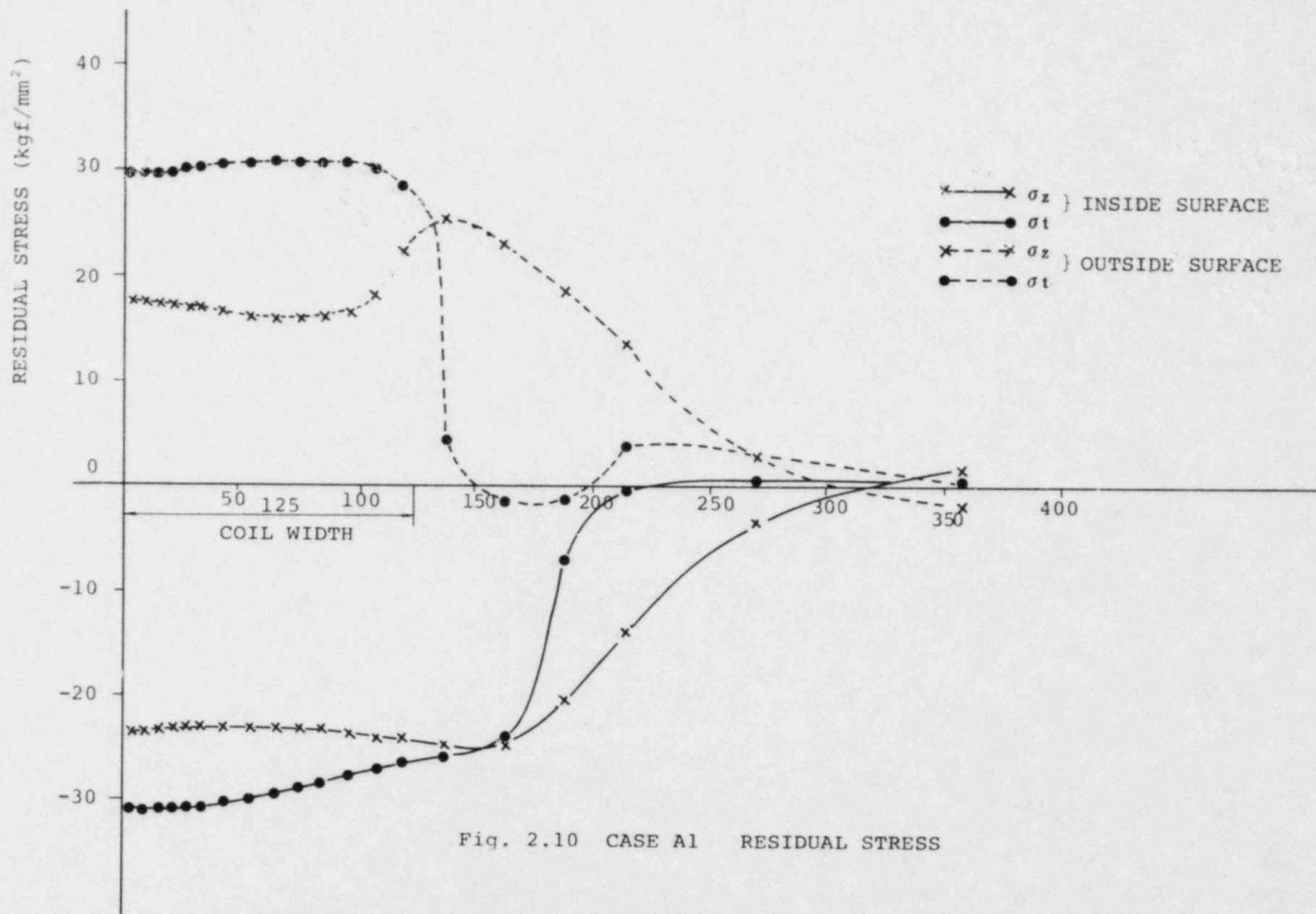


Fig. 2.10 CASE A1 RESIDUAL STRESS

TABLE 3.1 CALCULATION RESULTS

CASE NO.	PIPE SIZE	COIL WIDTH () (mm)	HEATING TIME (sec)	HEATING DENSITY (kcal/mm ³ h)	RESIDUAL STRESS			
					AXIAL		CIRCUMFERENCE	
					OUTSIDE	INSIDE	OUTSIDE	INSIDE
1	12 IN SCH100	30 (0.53)	180	0.0583	-7.8	6.8	21.0	- 5.6
2		96 (1.70)	180	0.0583	-0.6	-2.0	20.6	-22.0
3		160 (2.84)	180	0.0583	17.0	-20.0	23.0	-30.0
4		250 (4.43)	180	0.0583	24.5	-24.5	23.5	-29.0
5		350 (6.21)	180	0.0583	25.5	-27.7	25.5	-27.7
6	20 IN SCH100	204 (2.32)	300	0.0452	13.5	-19.5	29.7	-30.0
7		250 (2.84)	300	0.0452	19.5	-23.0	28.5	-30.3
8		350 (3.98)	300	0.0452	26.0	-27.0	26.0	-27.7
9		456 (5.19)	300	0.0452	27.0	-27.0	26.0	-27.0

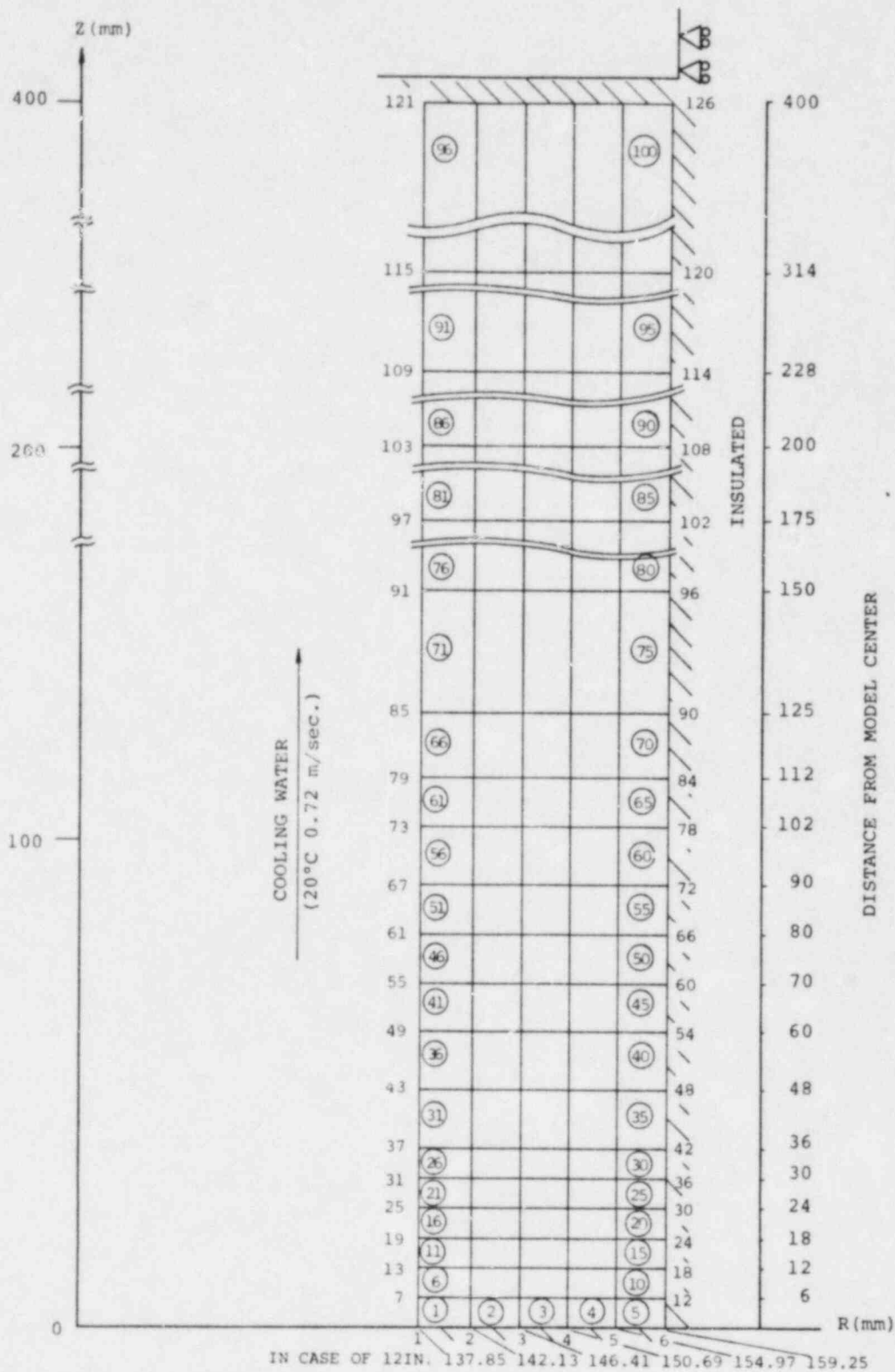


Fig. 3.1 ANALYTICAL MODEL

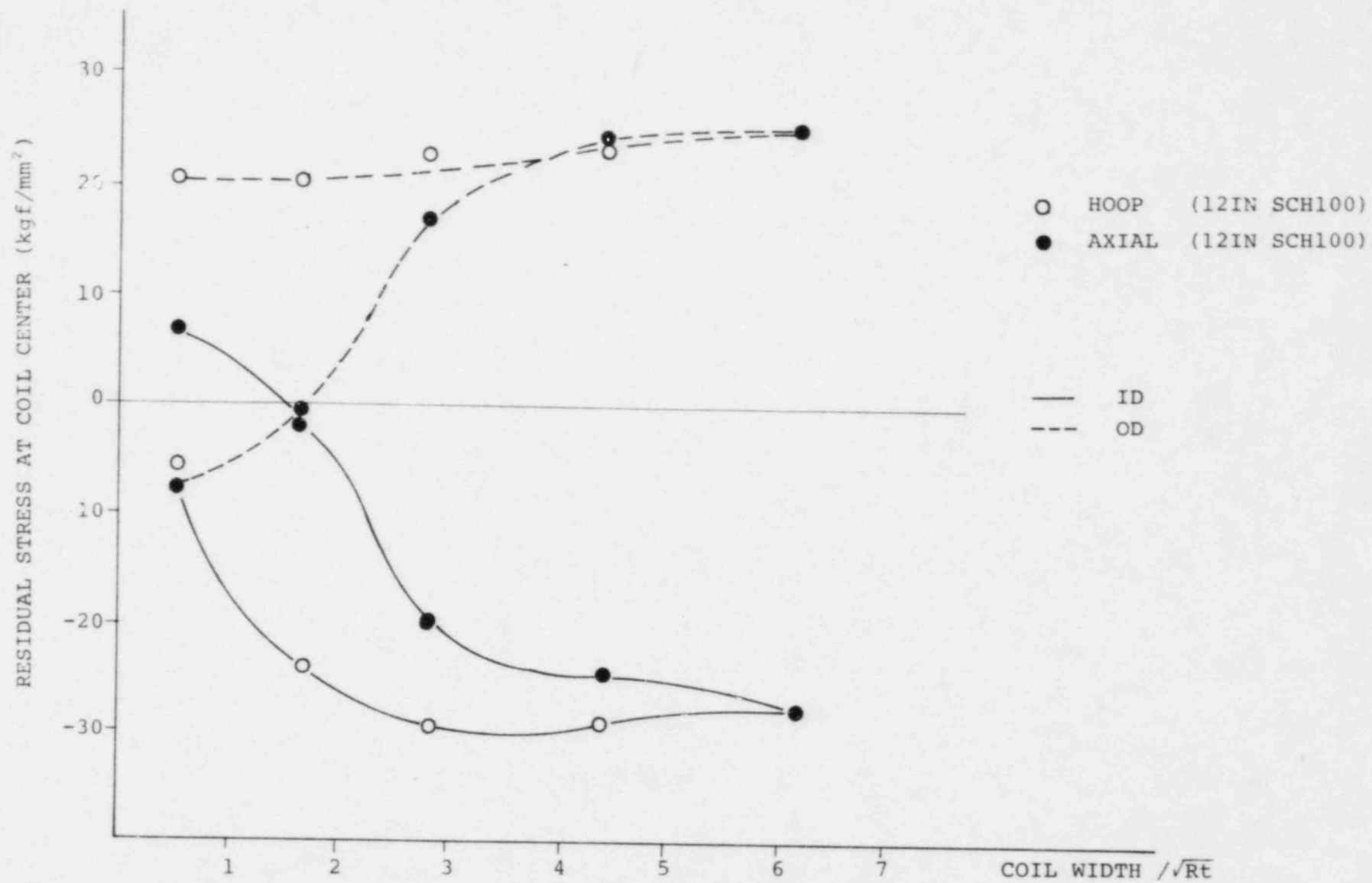


Fig. 3.2 EFFECT OF COIL WIDTH

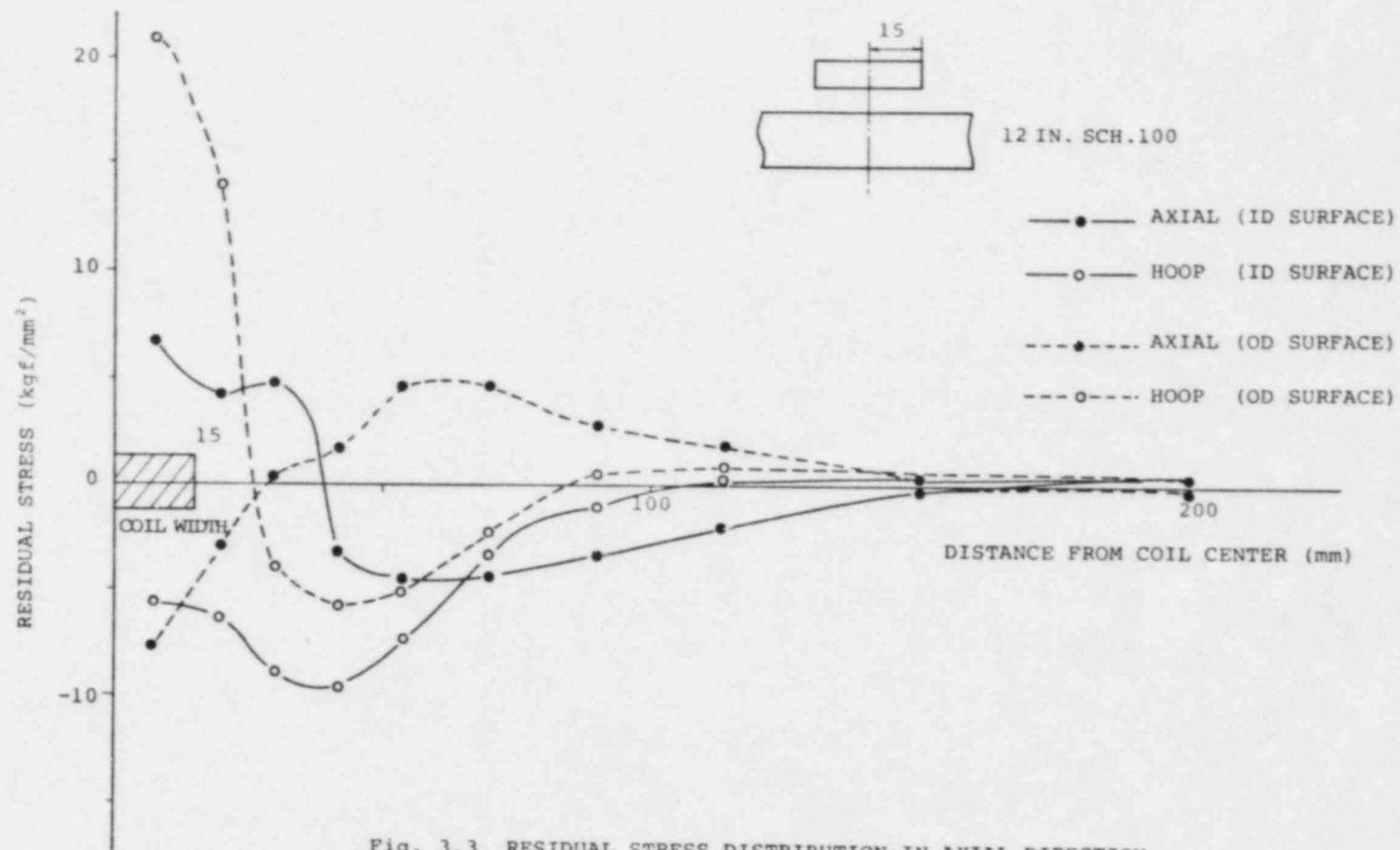
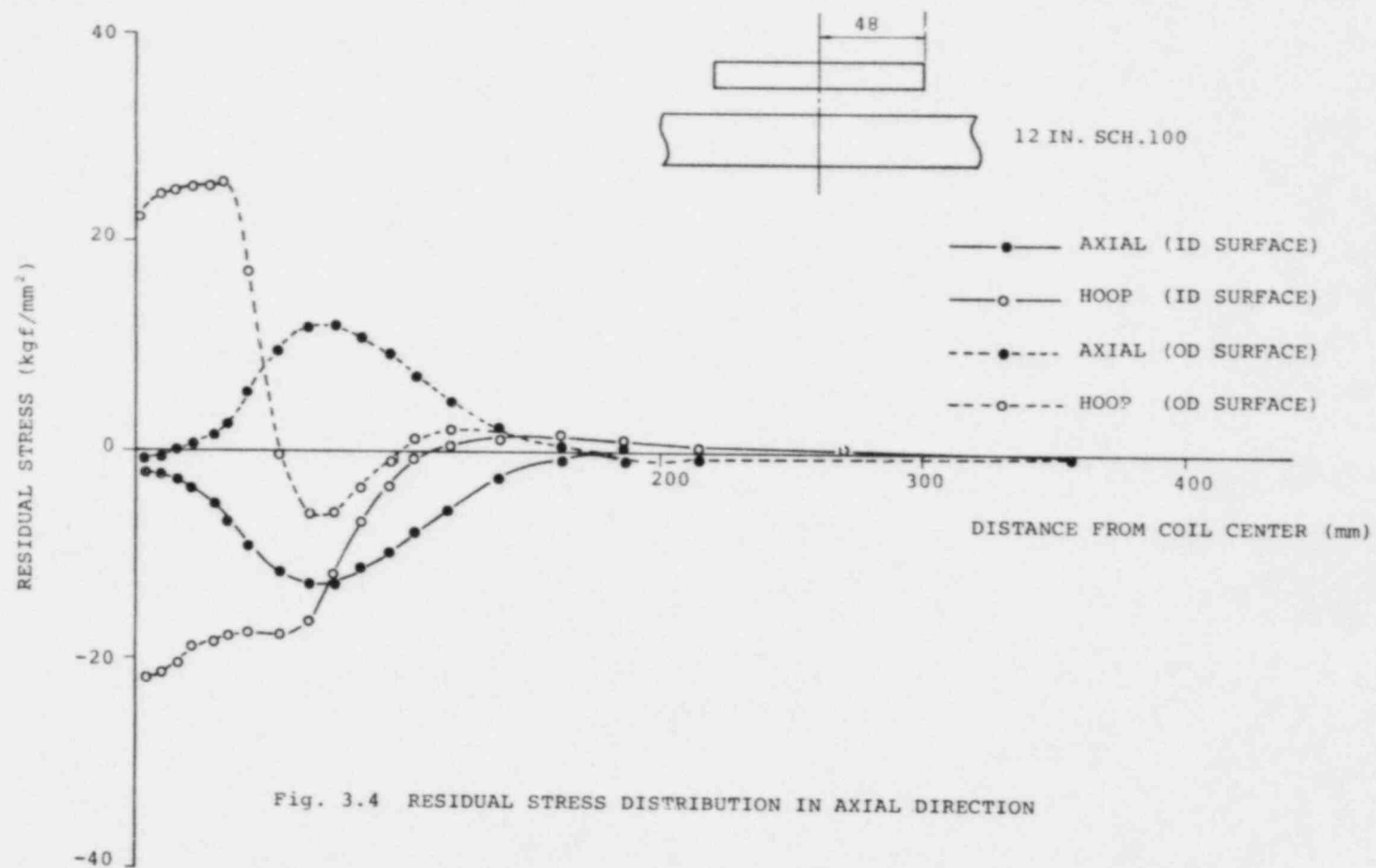


Fig. 3.3 RESIDUAL STRESS DISTRIBUTION IN AXIAL DIRECTION



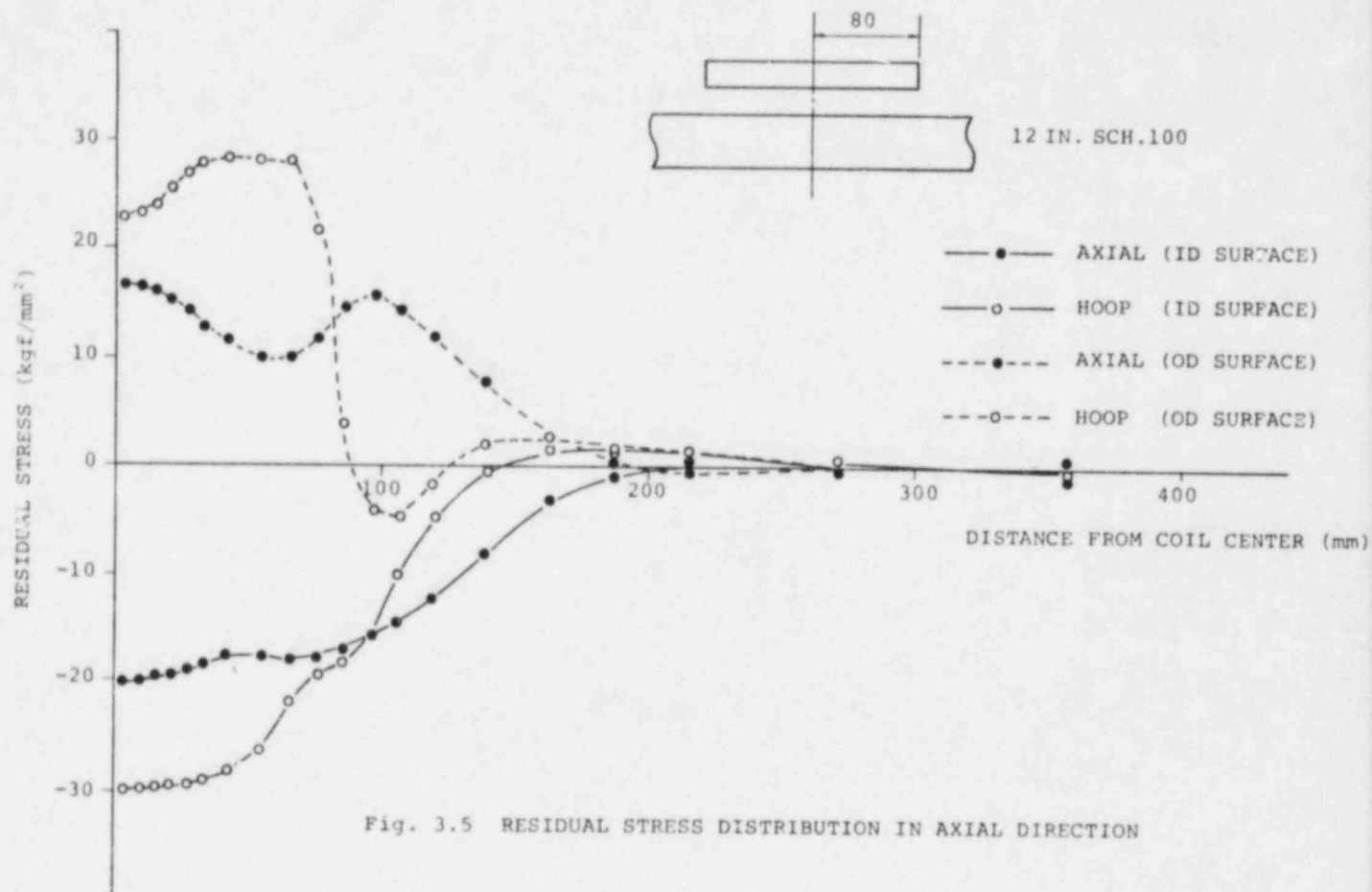
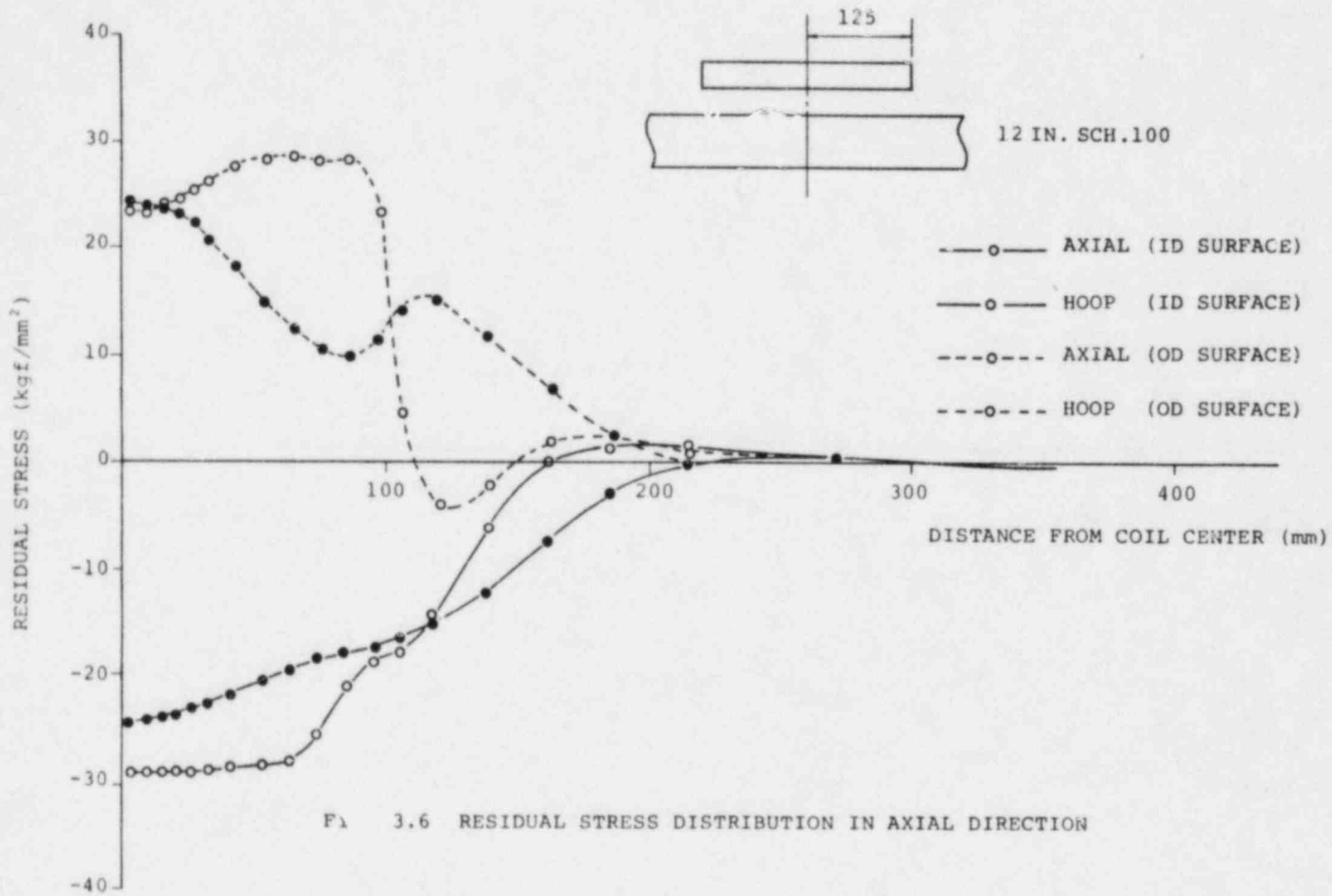
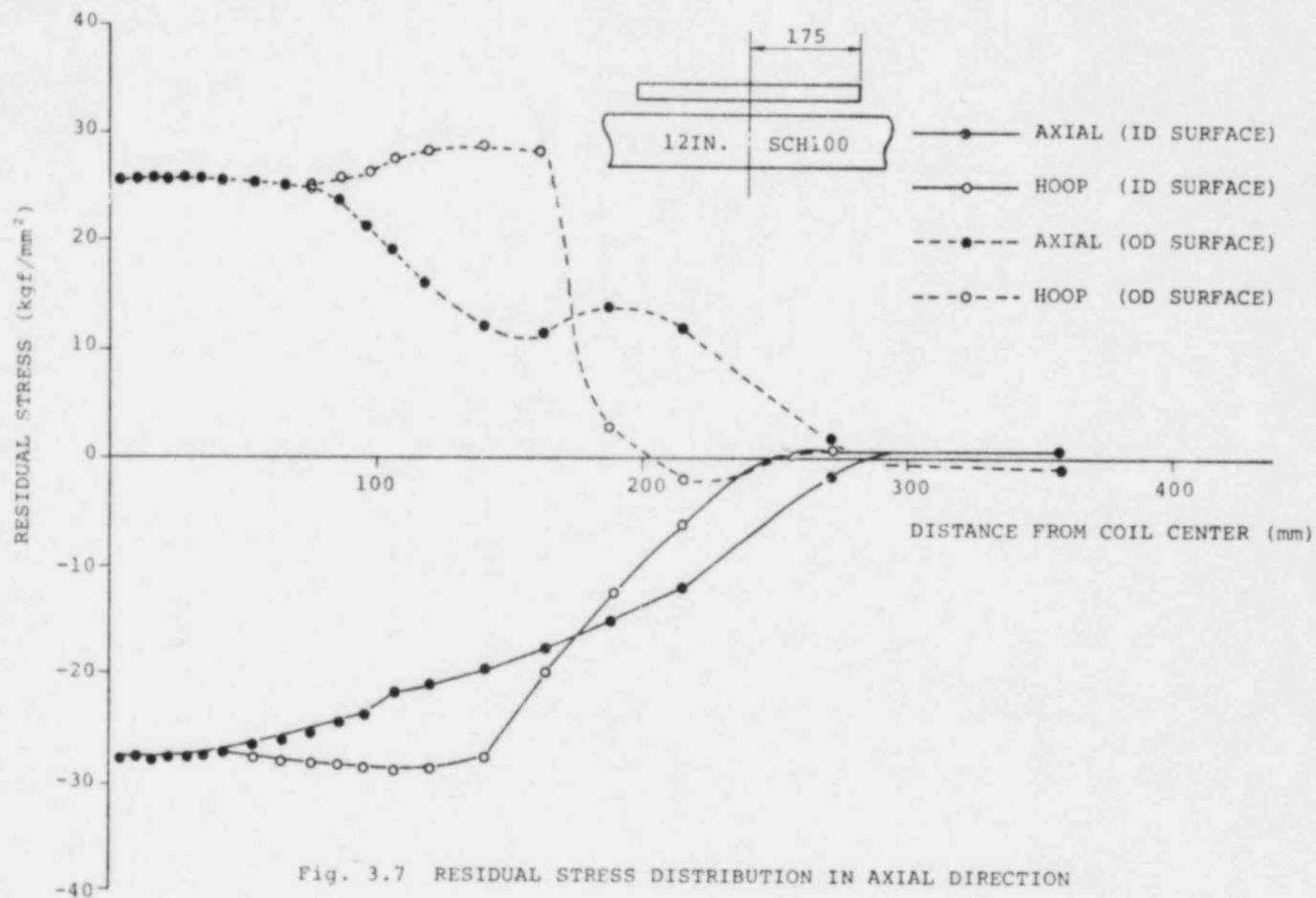


Fig. 3.5 RESIDUAL STRESS DISTRIBUTION IN AXIAL DIRECTION





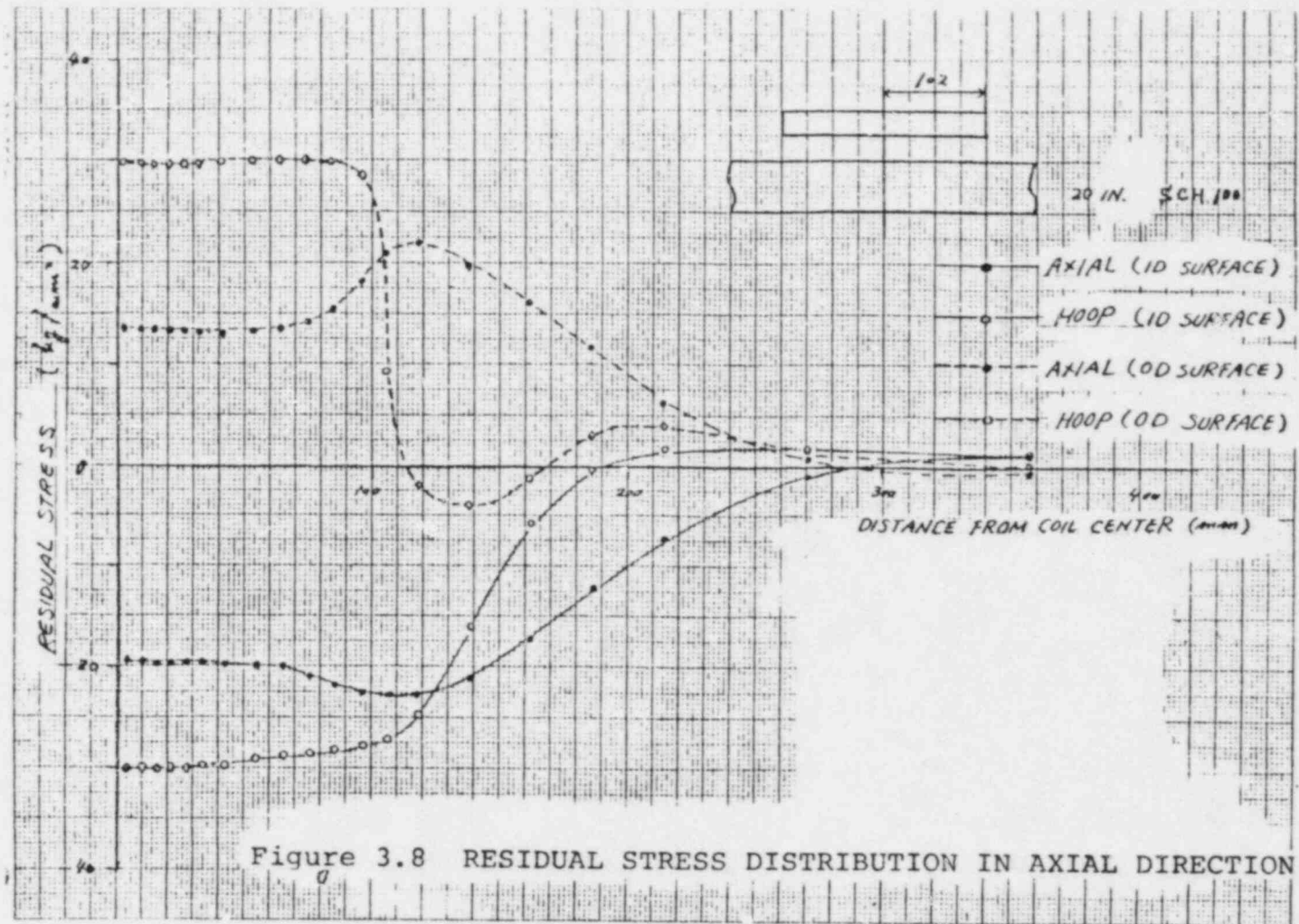
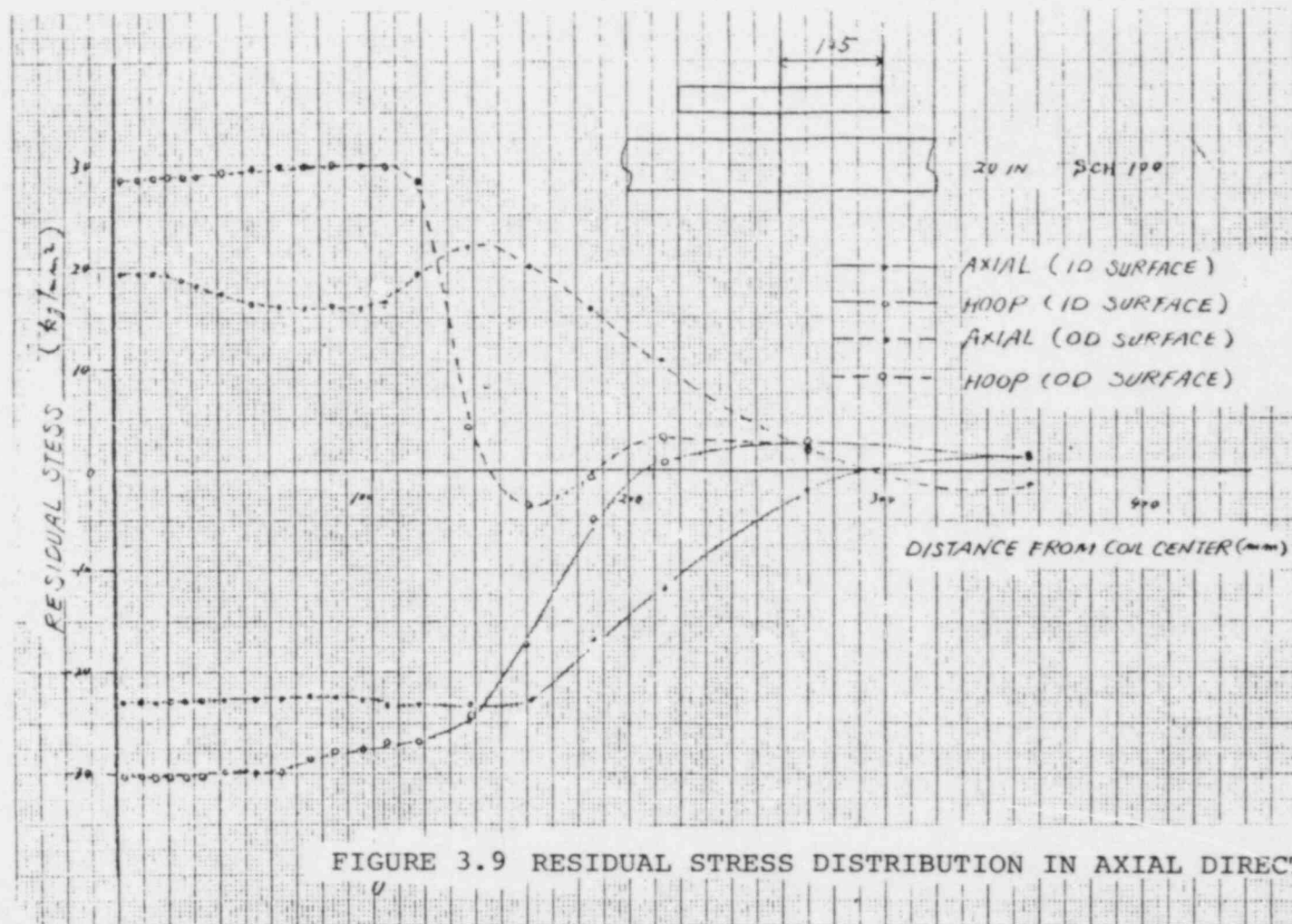


Figure 3.8 RESIDUAL STRESS DISTRIBUTION IN AXIAL DIRECTION



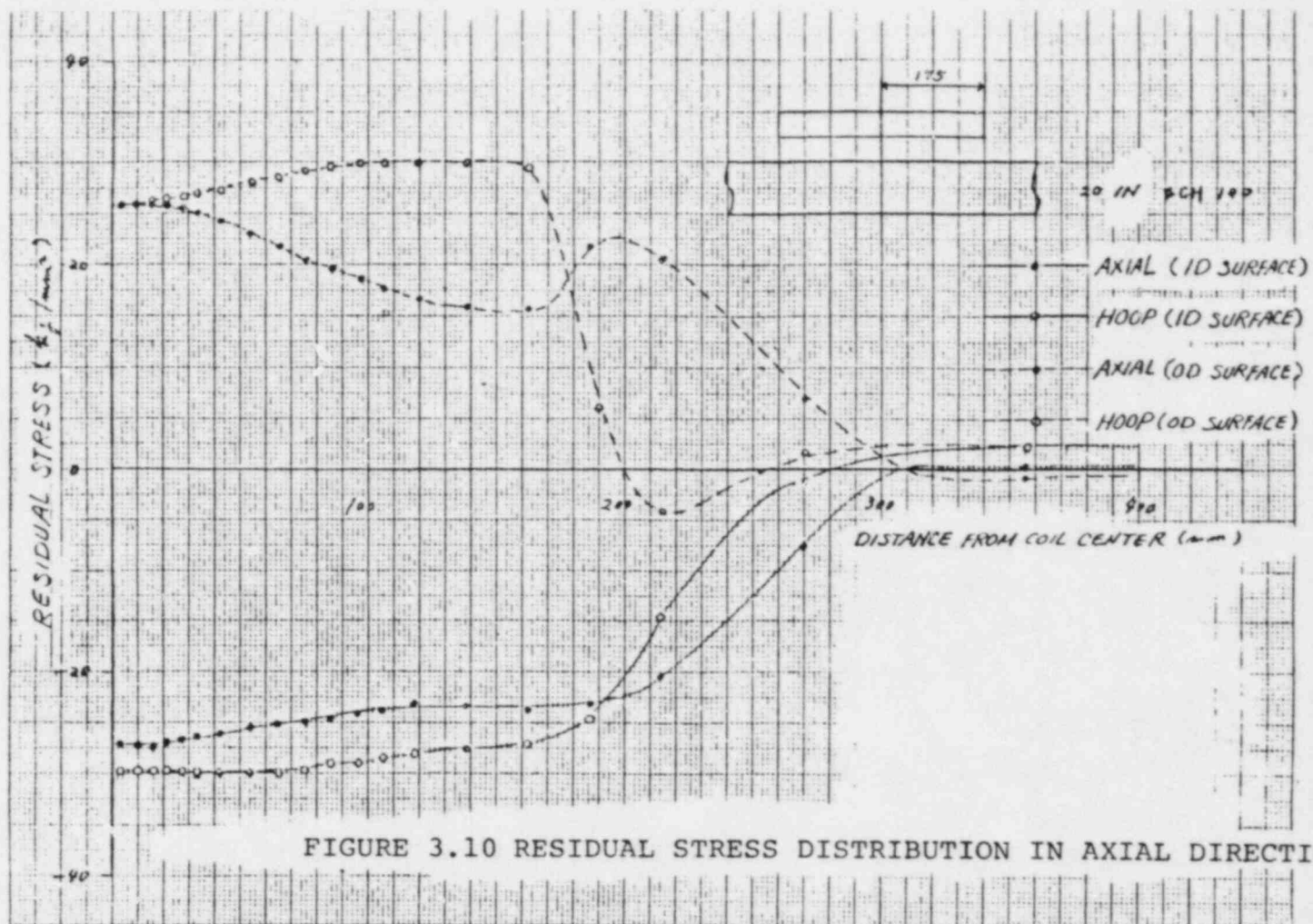
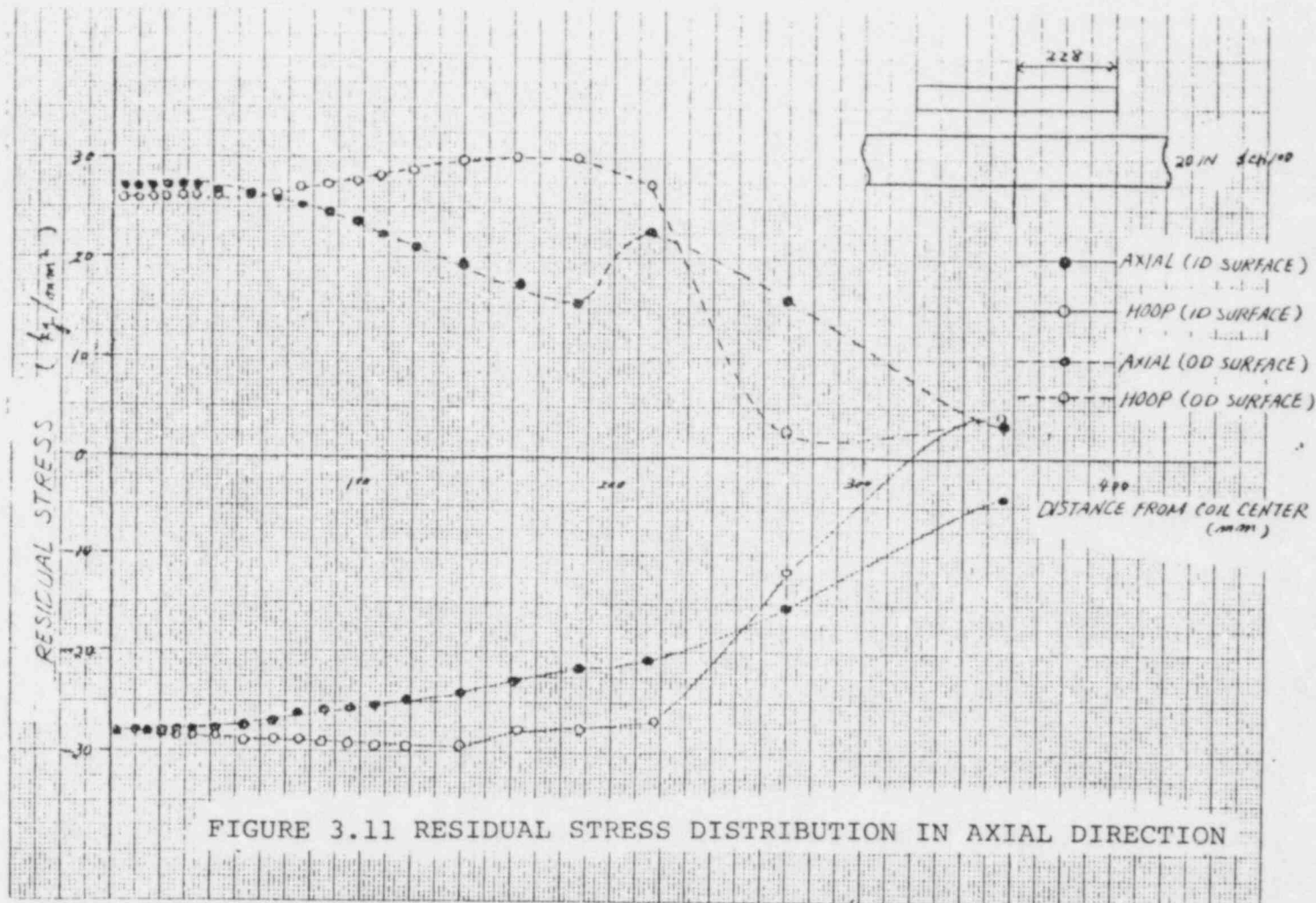


FIGURE 3.10 RESIDUAL STRESS DISTRIBUTION IN AXIAL DIRECTION



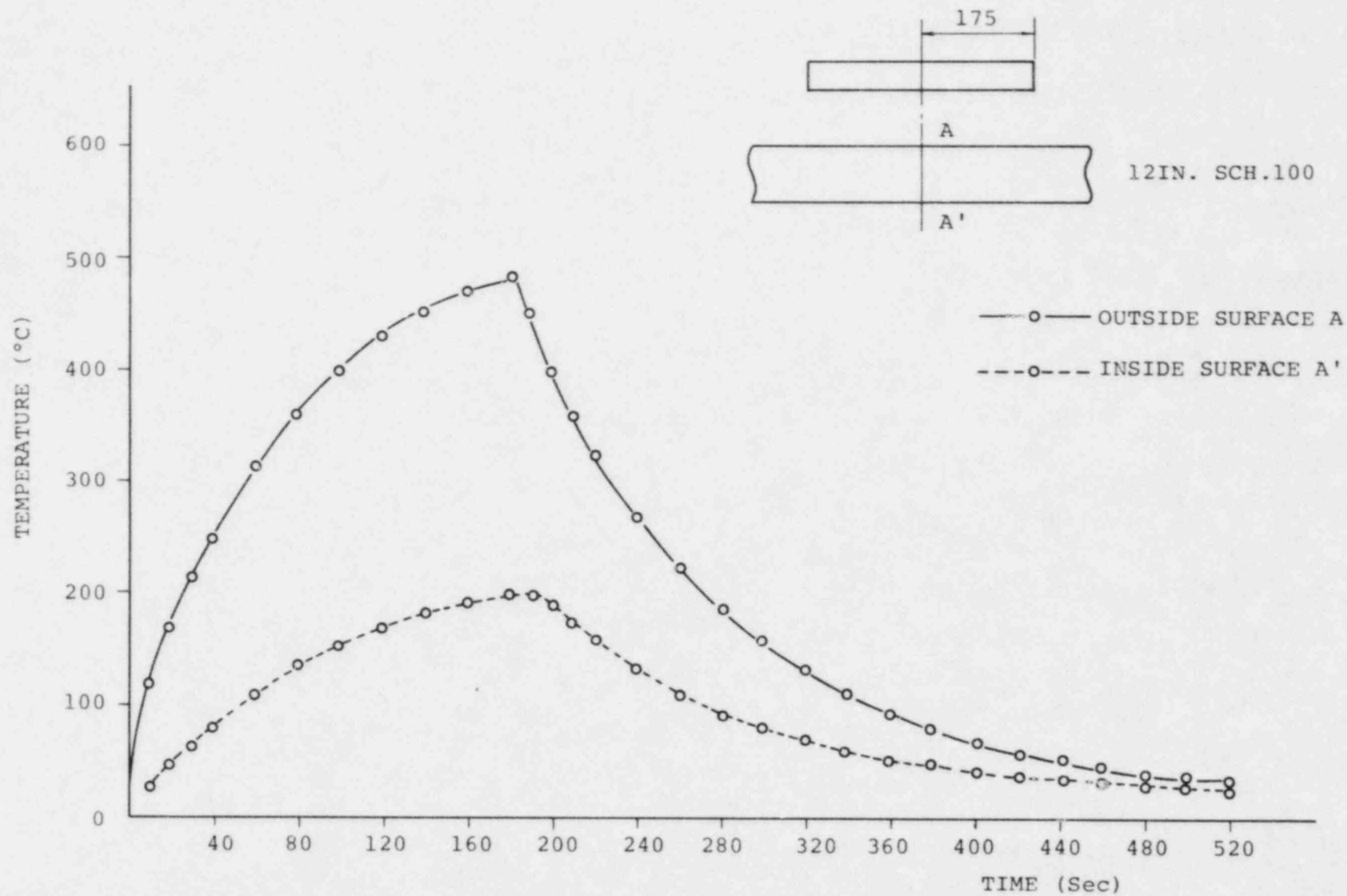


Fig. 3.12 TEMPERATURE TRANSITION

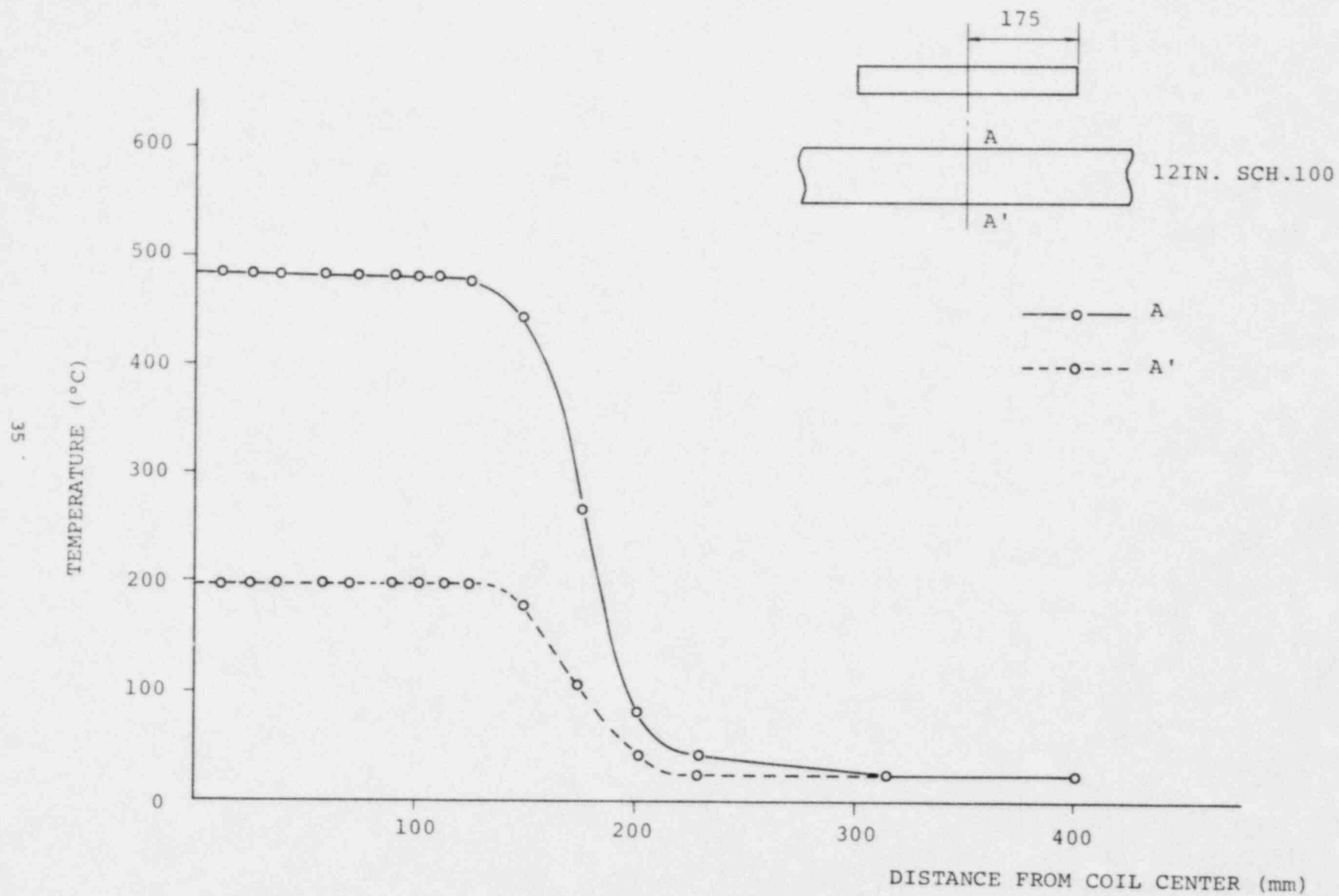


Fig. 3.13 TEMPERATURE DISTRIBUTION IN AXIAL DIRECTION

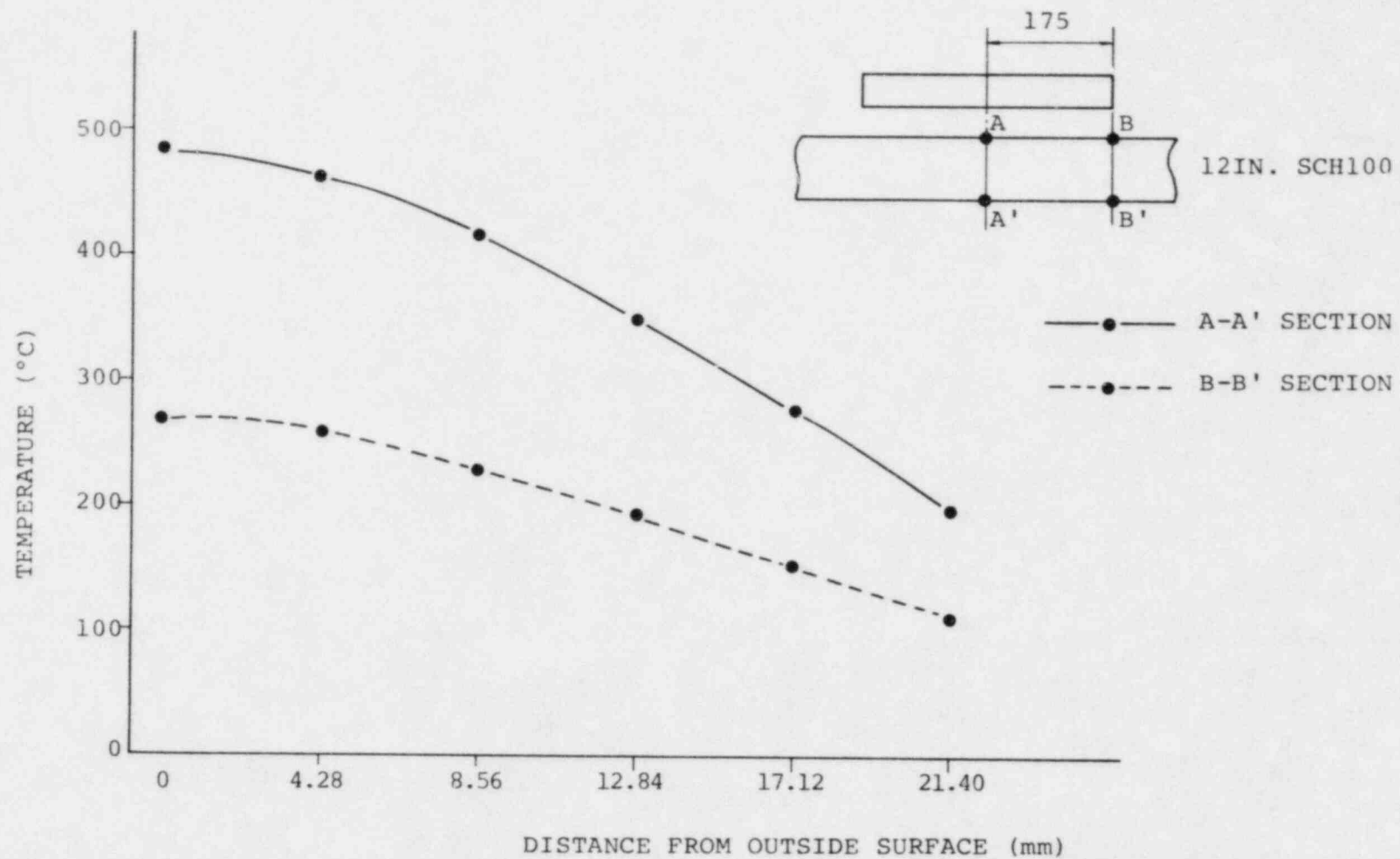


Fig. 3.14 TEMPERATURE DISTRIBUTION THROUGH THICKNESS
(AFTER START UP 180 sec.)

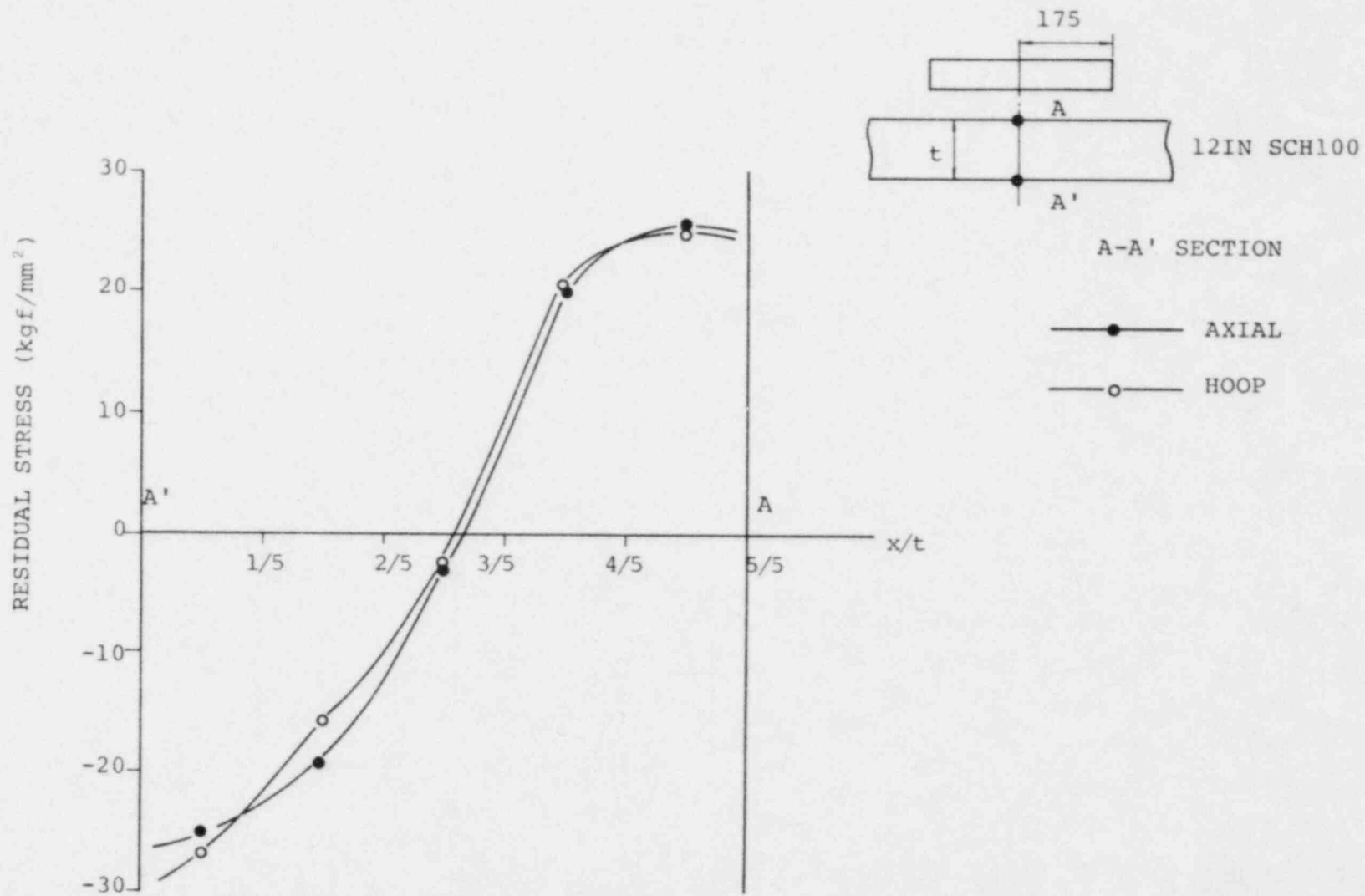


Fig. 3.15 RESIDUAL STRESS OF A-A' SECTION

TABLE 4.1 CALCULATED RESULTS

CURRENT FREQUENCY	HEATING DEPTH	W_0 or Q	HEATING TIME	COIL WIDTH	COOLING WATER	TOTAL HEATING POWER
0.3 kHz	30.4 mm	$W_0 = 0.016$ kcal/cm ² h	420 sec	500 mm	20°C 0.72 m/sec	315 kW
3	9.6	$W_0 = 0.032$	420	"	"	200 kW
∞	0	$Q = 0.136$ kcal/cm ² h	360	"	"	175 kW

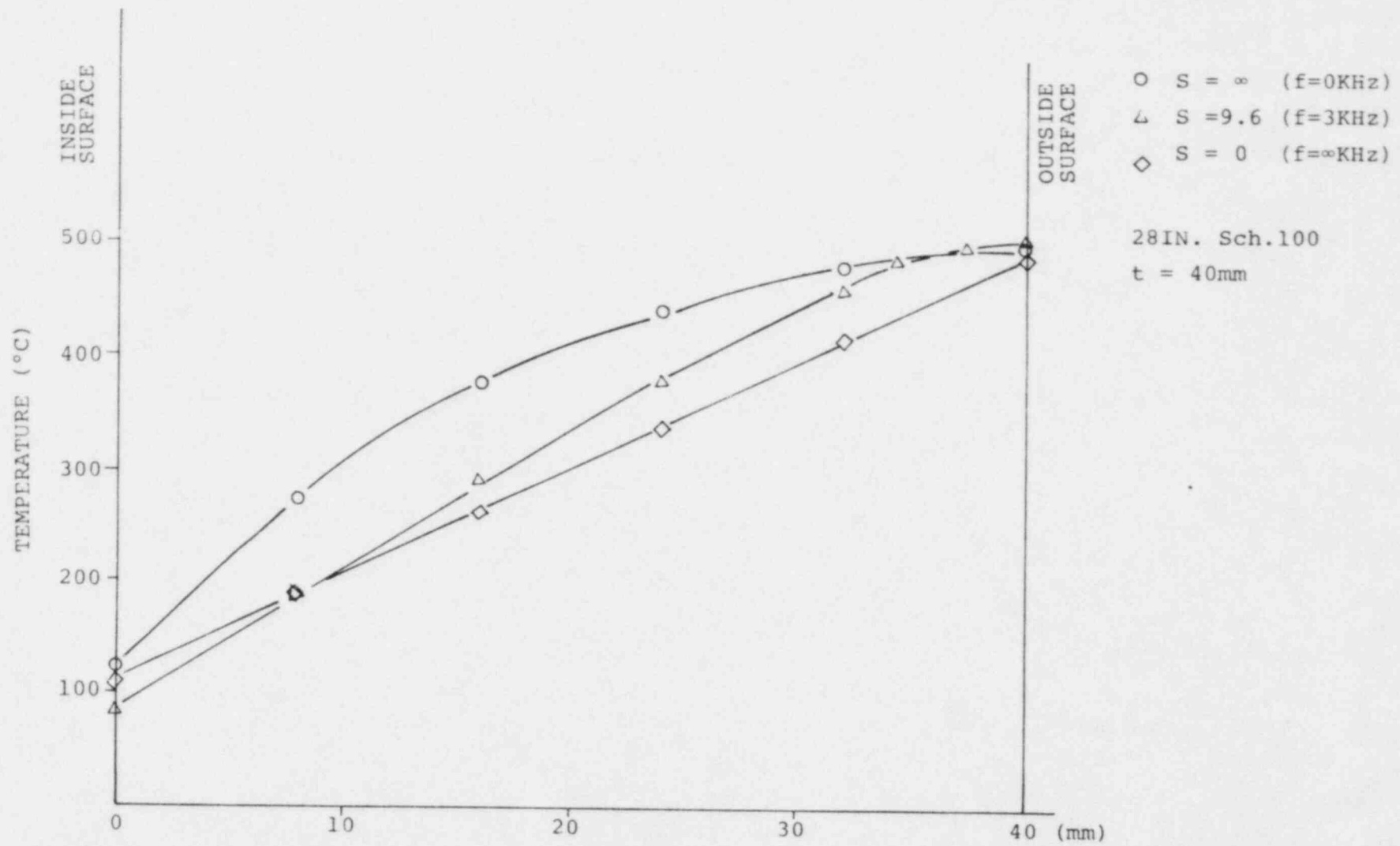


Fig. 4.1 TEMPERATURE DISTRIBUTION THROUGH THICKNESS

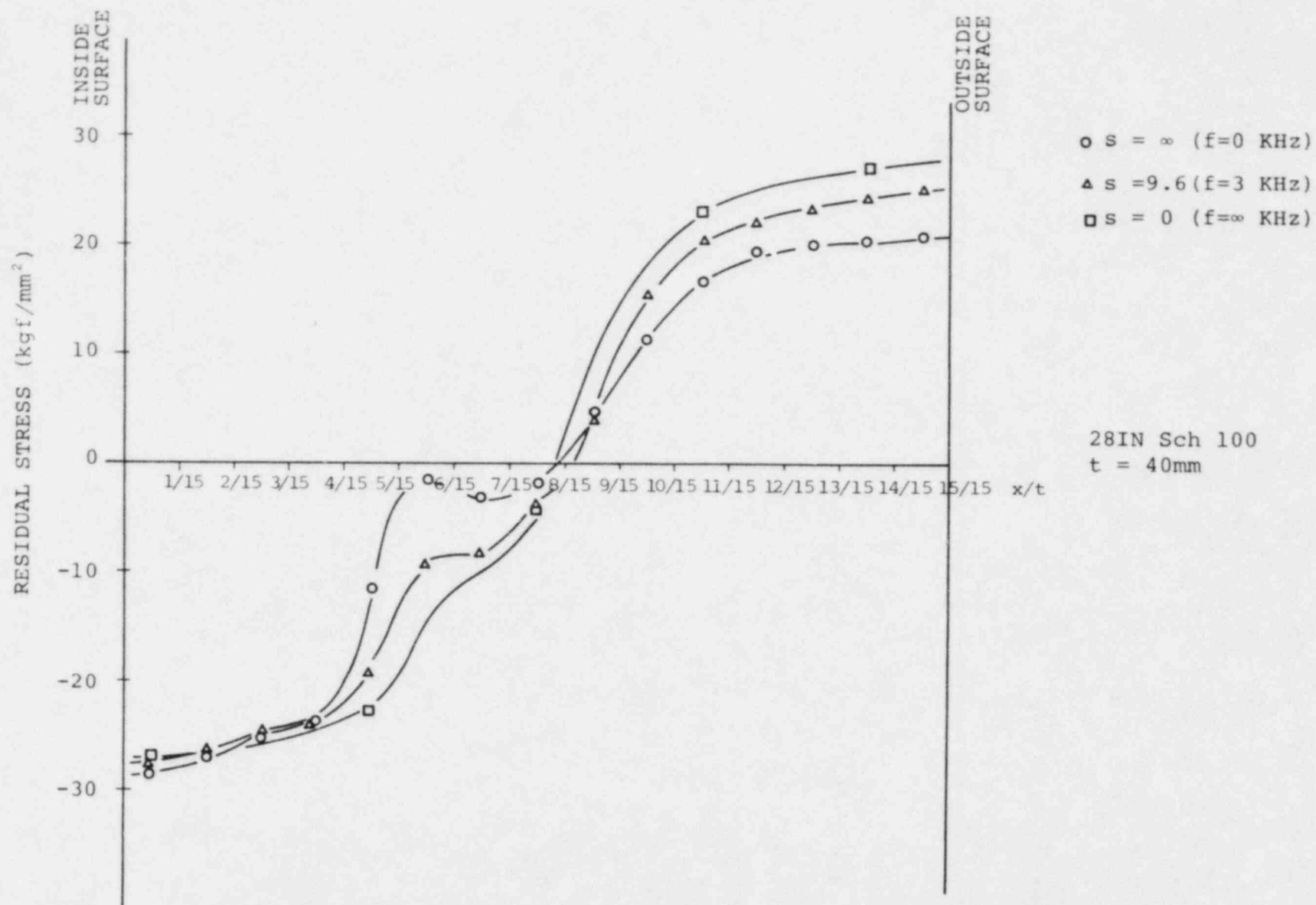


Fig. 4.2 AXIAL STRESS DISTRIBUTION THROUGH THICKNESS

A - 10

RESIDUAL STRESS IMPROVEMENT FOR

24 INCH PIPES

1. INTRODUCTION

In a BWR power station, PLR (Primary loop recirculation) piping is among the most important piping. It is intended that the IHSI technique be qualified for large diameter piping. To evaluate this process on large diameter components, mock-up testing was conducted on a pipe to forging joint.

2. Mock-up

The mock-up is composed of a 24 inch forging and pipe. Fig. 2.1 shows the configuration of the mock-up. The fabrication method and welding condition are the same as for a fabricated plant. The piping was fabricated by rolling and welding the plate.

Welding was performed using standard TIG and SMAW welding techniques.

3. IHSI

The IHSI was performed using the parameters in Table 3.1. These essential variables satisfy the values in Table 5.1 in this text. Fig. 3.1 shows the heating cycle for IHSI application.

4. Test Results

(1) Temperature distribution

The temperature was measured using chromel-almel thermocouples which were attached to the pipe outside surfaces. Since thermocouples were not attached to the pipe inside, the temperature of pipe inside surface was estimated using the method of App. A-13 ESTIMATION OF PIPE ID TEMPERATURE DURING IHSI and the temperature difference between the pipe outside and inside surfaces was obtained.

Fig. 4.1 shows the temperature distribution through the thickness which was obtained by measurement and calculation.

The temperature distribution in axial direction during IHSI is shown in Fig. 4.2. Fig. 4.2 indicates that a fairly uniform temperature distribution was obtained at the induction coil center while comparatively abrupt cooling was noted at the coil ends.

(2) Residual stress

Fig. 4.2 shows the residual stress distribution in the axial direction after IHSI. From the figure it appears that the residual stresses became compressive.

5. Conclusion

This mock-up test was performed using the conditions of Table 3.1. The temperature distribution was well controlled so that the temperature difference was sufficiently large to satisfy the required value. The residual stresses on the ID became compressive. This result indicates that IHSI can be applied to large pipe such as 24 inch PLR piping.

TABLE 3.1 ESSENTIAL VARIABLE FOR J-1

VARIABLE	COIL WIDTH L (mm)	HEATING TIME T (SEC)	TEMPERATURE DIFFERENCE ΔT ($^{\circ}\text{C}$)	COIL LOCATION l (mm)
REQUIRED VALUE	$\frac{L}{\sqrt{RT}} \geq K$	$a \frac{T}{t^2} \geq A$	$\Delta T \geq \frac{2(1-\nu)}{E\alpha} \sigma_y$	$l \geq \text{MAX}(\frac{1}{2}t, 15)$
DESIGNED VALUE	370	150 ~ 300	≥ 220	≥ 15
ACTUAL VALUE	369 ^{*1} (4.1)	228 ^{*2} (1.10)	328	40

NOTE : *1 The value in parentheses indicates the value of L/\sqrt{Rt} .

*2 The value in parentheses indicates the value of $a T/t^2$.

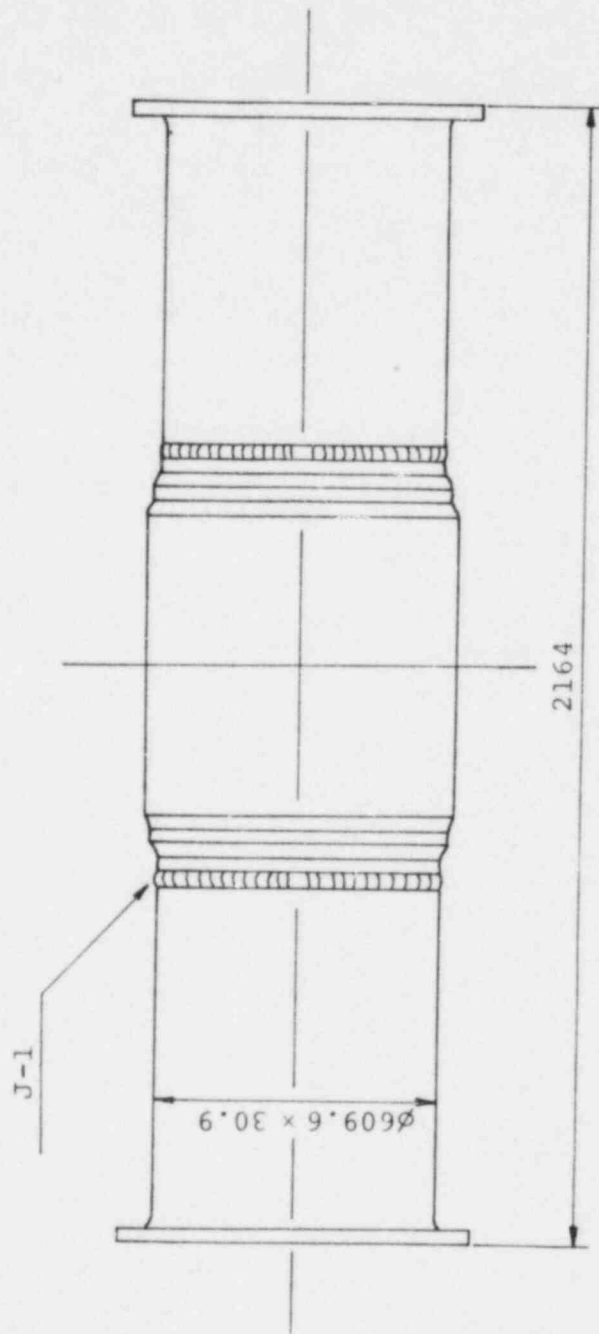


Fig. 2.1 MOCK UP CONFIGURATION

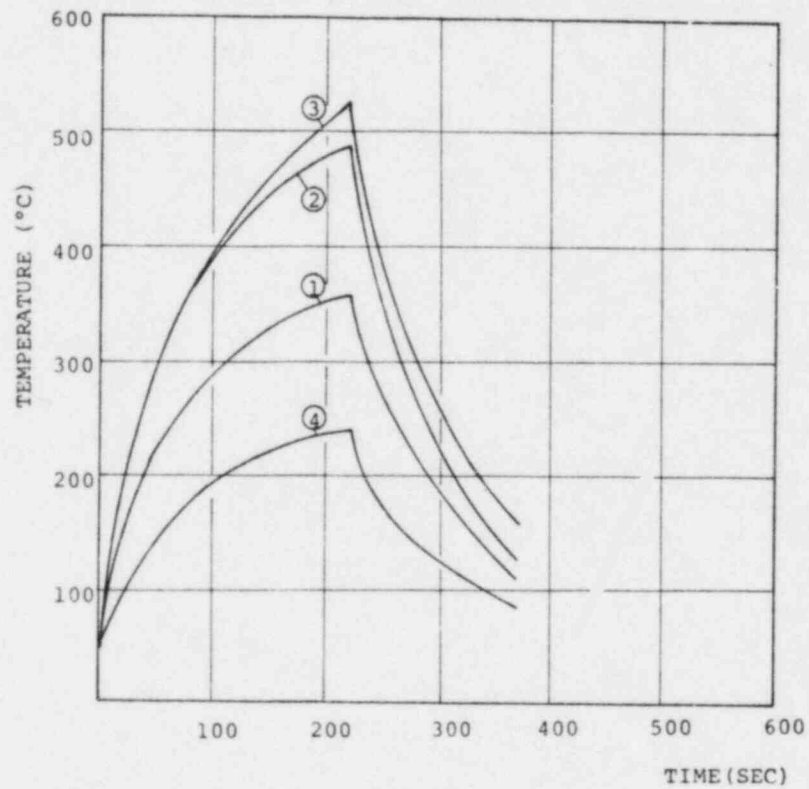
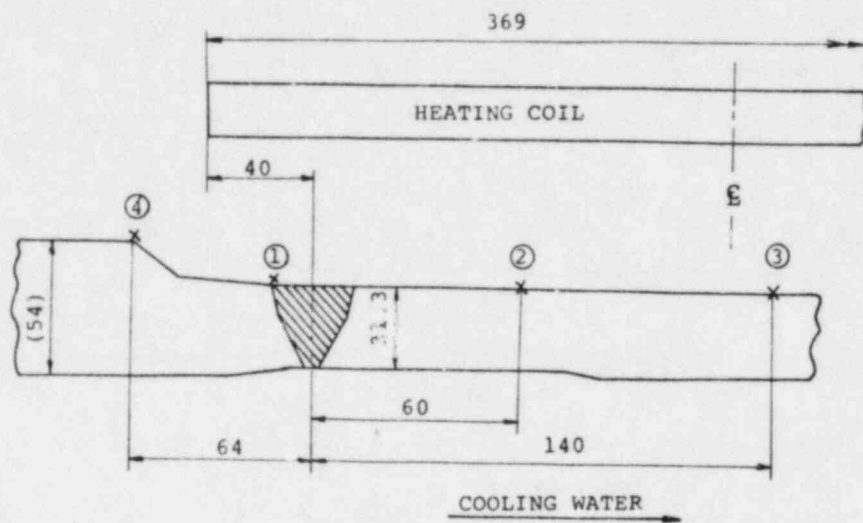


Fig. 3.1 J-1 TEMPERATURE TRANSITION

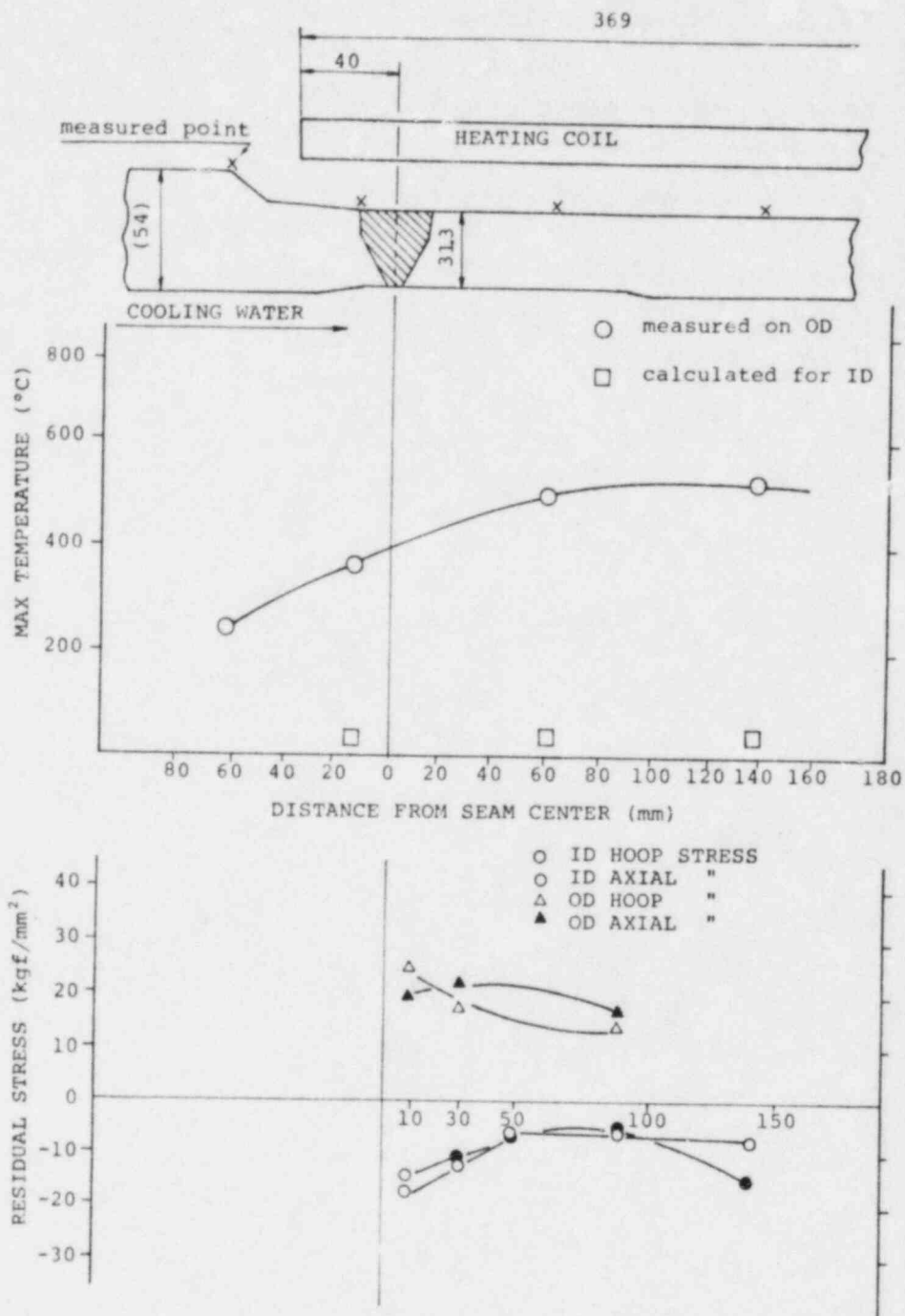


Fig. 4.2 J-1 RESIDUAL STRESS DISTRIBUTION

A - 11

ESTIMATE OF INPUT POWER

FOR IHSI

1. INTRODUCTION

As mentioned in Chapter 7, Field Application; suitable input power produces good results. We have developed a method which estimates input power by using an experimentally obtained equation.

2. EXPERIMENTAL RESULTS

Coil input power P_c is given by the following equation.

$$P_c = \eta \frac{\Delta T \cdot D \cdot L}{t} \quad (1)$$

Where, P_c : Coil input Power
 ΔT : Temperature difference
 D : Pipe Diameter
 L : Coil width
 t : Pipe thickness
 η : Efficiency (Experimentally determined)

The experimental results are summarized in Table 2.1, (CASE NO. 1 ~ 4) and these data are graphically shown in Fig. 2.1 using the parameters shown in equation (1). These results show that there is a linear relationship between P_c and $\Delta T \cdot D \cdot L / t$

3. ANALYTICAL RESULTS

In article 4. current frequency of App. A-9, the input power is calculated. The calculation is performed for a 28 inch schedule 100 pipe. The calculated total heat generation is 200 kw. Coil input is calculated as follows:

$$P_c = 200/0.75 = 267 \text{ kw}$$

0.75 : Efficiency

The data are summarized in Table 2.1 CASE NO. 5. And data points are plotted in Fig. 2.1.

4. CONCLUSION

The required coil input power P_c is proportioned to $\Delta T.D.L/t$ and that value can be obtained by using Fig. 2.1.

Table 2.1 COIL INPUT POWER

CASE NO.	PIPE SIZE (IN)	DIAMETER D (M)	THICKNESS t (M)	COIL WIDTH L (M)	TEMPERATURE DIFFERENCE ΔT ($^{\circ}C$)	COIL POWER	$\frac{\Delta T \cdot D \cdot L}{t}$ $\times 10^3$	HEATING TIME (SEC)
1	12	0.3185	0.0214	0.25	345	117	1.45	180
2	20	0.508	0.0325	0.24	418	126	1.48	300
3	24	0.6096	0.0389	0.369	470	230	2.88	288
4	16	0.418	0.032	0.273	437	153	1.56	200
5 *	28	0.7112	0.040	0.500	360	267	3.20	420

* calculated data by FEM.

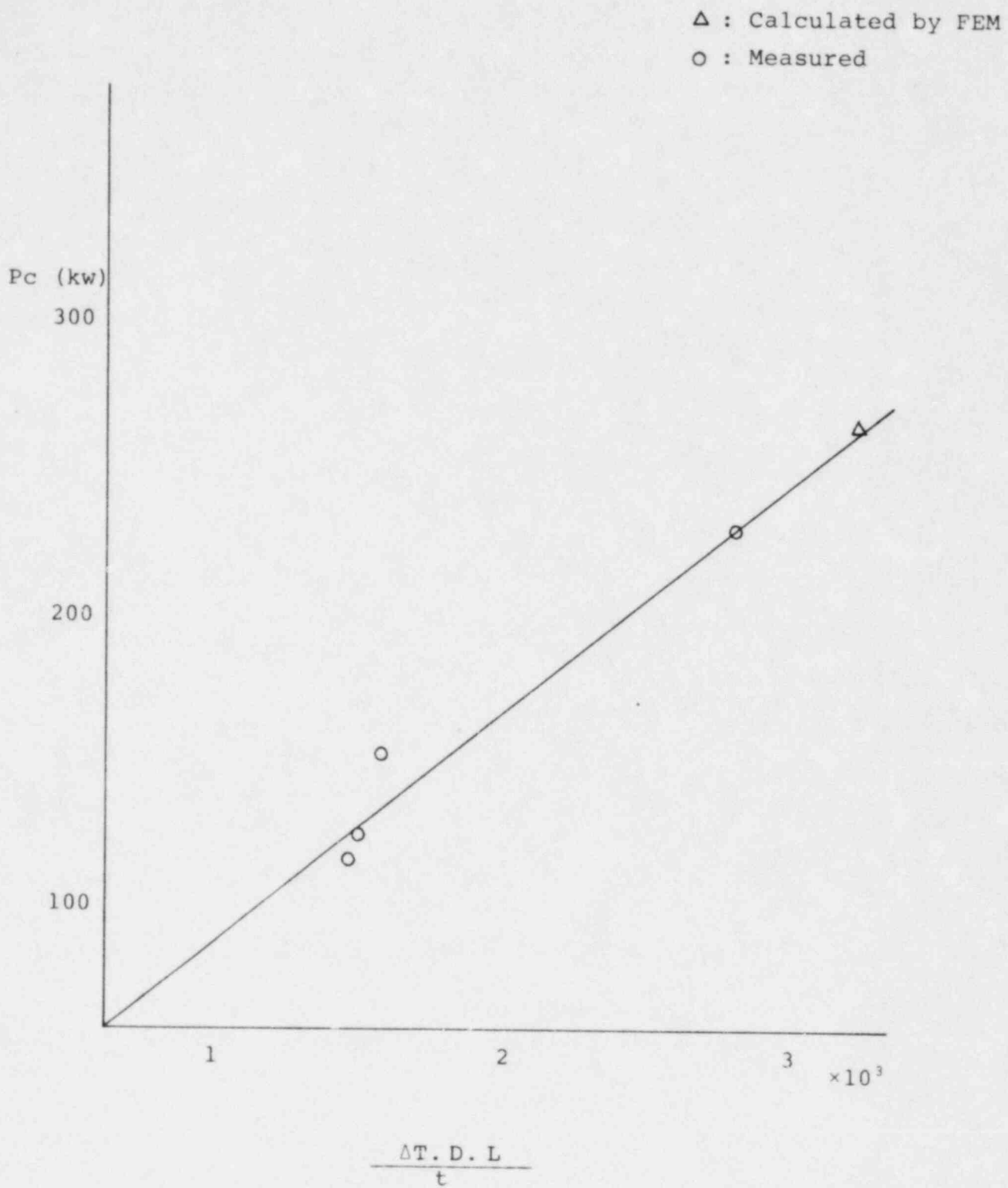


Fig. 2.1 COIL INPUT POWER

A - 12

TRIAL HEATING TECHNIQUE OF IHSI

1. Introduction

It is desirable to standardize the IHSI performance. Suitable heating conditions are developed to satisfy the essential variables.

- (1) The temperature difference ΔT of the outer and inner surface of an IHSI'ed weld joint shall be greater than the required value. The required value is explained in this chapter of the test.
- (2) The heating duration shall be larger than the required value which is determined so that Fourier No. is greater than or equal to 0.7.
- (3) The maximum temperature of the outer surface shall be lower than 550°C .

The temperature distribution depends on the coil performance for the most part. The desirable coil produces a good temperature distribution which is uniform in the heating range and does not produce small hot spots.

After the coil design is fixed, we must determine the input power which is suitable to satisfy the above mentioned conditions. The input power can adjust the following items.

- (1) Raise or lower the maximum temperature.
- (2) Make the heating duration longer or shorter.

2. Trial Heating

Trial heating is performed by heating the pipe until the maximum temperature is 280°C so as to confirm that the required ΔT will be obtained and to adjust the power.

Since the heating is under 280°C , repeated heating produces no side effects. Fig. 2.1 was developed for the trail heating.

(1) The following data should be measured from the trial heating.

1-1 Heating time T_{280} which is necessary to raise the maximum temperature to 280°C .

1-2 Weld joint temperature at the time when the maximum temperature rises to 280°C .

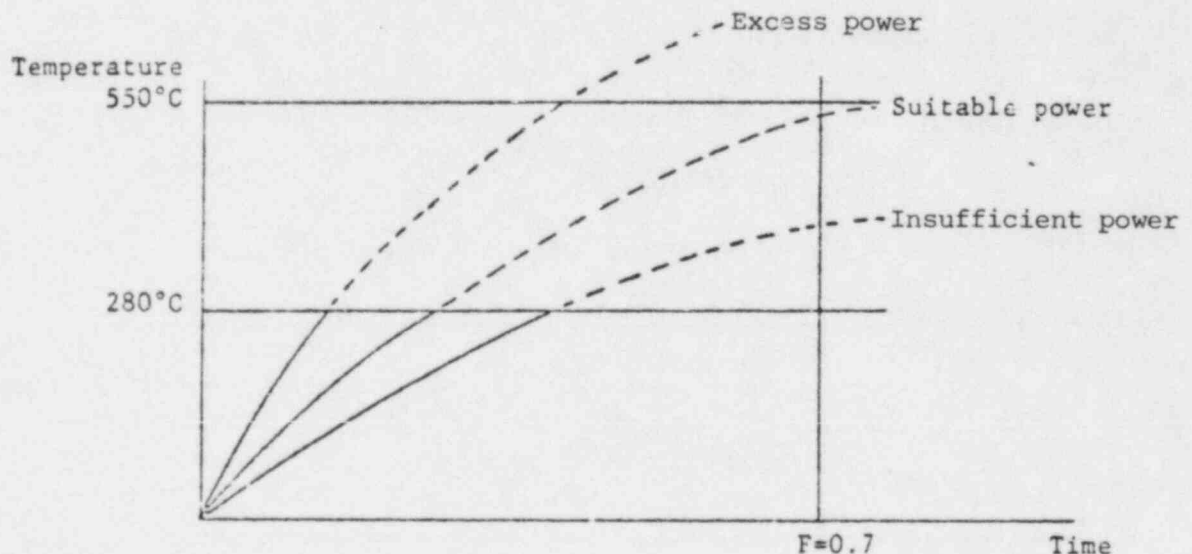
1-3 Cooling water temperature t_w , cooling water velocity U_w .

1-4 Pipe thickness at the location where the maximum temperature occurs.

(2) The following items can be estimated.

2-1 ΔT value at the weld joint when the maximum temperature is 550°C .

2-2 Whether the input power is suitable.



(3) Items estimated from trial heating.

The trial heating is performed to estimate the following items.

3-1 ΔT

From Fig. 2.1, "Estimating ΔT by trial heating," if one uses the obtained data τ , to t_w and plate thickness L , then ΔT_E , the temperature difference in this tested state condition, can be estimated. In this case the steady state condition is considered that condition where the Fourier No. is greater than 0.7.

From Table 2.1, one observes that Fig. 2.1 shows $^{\circ}\text{C} \sim 60^{\circ}\text{C}$ lower than the actual temperature difference.

3-2 Suitability of power level

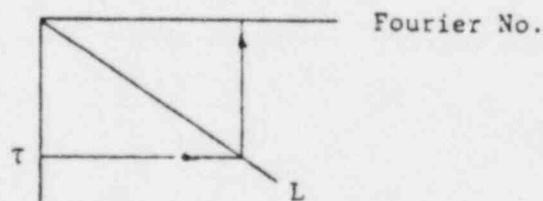
If the estimated ΔT is smaller than the required ΔT , the power shall be raised.

3. Using the approach of Fig. 2.1 (estimating ΔT by trial heating), Fig. 2.1 is used as follows:

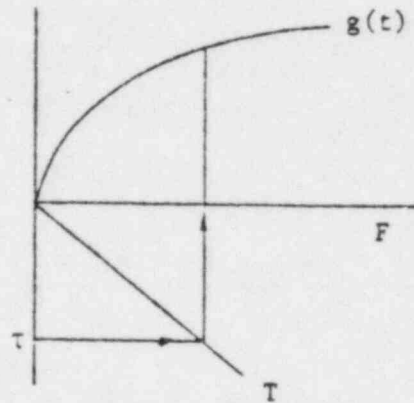
Step 1. Obtain the following parameters from trial heating data.

- (a) Plate thickness L
- (b) Heating duration τ
- (c) Measured temperature T_o - Water temperature T_w

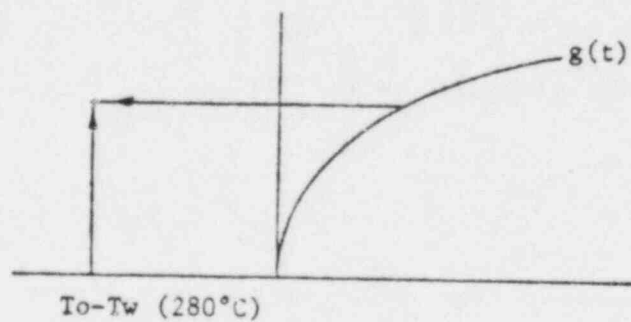
Step 2. From fourth quadrant of Fig. 2.1, Fourier No. is obtained using t and τ as shown below.



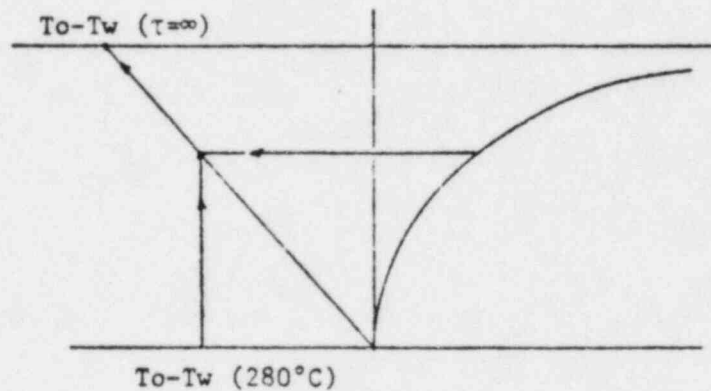
Step 3. From first quadrant of Fig. 2.1, the $g(t)$ value is obtained. Where the $g(t)$ value denotes a nondimensional temperature. This process is presented in the sketch below.



Step 4. From this intersection point move horizontally left, intersecting the measured value of $(T_o - T_w)$ of the lower abscissa of the second quadrant, move vertically upwards to the intersection point of the above mentioned horizontal line as shown in the sketch below.



Step 5. Connect the intersection point and the origin of the coordinates and extend to obtain the intersection point with the upper abscissa of the second quadrant. This value is the predicted maximum temperature of outer surface - water temperature, and the predicted maximum temperature of the outer surface is obtained from this value as shown in the sketch below.



4. Derivation of $g(t)$

Begin with an infinitely wide plate whose temperature is 0°C uniformly as the initial condition. When heat is generated at one surface which is insulated and the other surface is maintained at 0°C , the Green function $G_0(t)$ of the heat generated side is given by the following equation.

$$G_0(t) = \frac{2}{L} \sum_{n=1}^{\infty} e^{-\left(\frac{2n-1}{2}\right)^2 \pi^2 \frac{at}{L^2}} \dots\dots\dots (1)$$

Where, L : Thickness (m)
 τ : Time (h)
a : Thermal diffusivity
n : Natural number

The Green function means that when the instant heating source which generates heat and disappears instantly occurs in the substance which is uniformly at 0°C as the initial condition. The Green function gives the temperature distribution in the substance.

The Green function after a heating of τ hour is obtained by integrating equation (1) from $\tau=0$ to $\tau=t$.

$$G_1(t) = \int_0^t G_0(t) dt = \frac{2}{T} \sum_{n=1}^{\infty} \frac{1}{\left(\frac{2n-1}{2}\right)^2 \pi^2 \frac{a}{T^2}} \left(1 - e^{-\left(\frac{2n-1}{2}\right)^2 \pi^2 \frac{a\tau}{T^2}}\right) \dots (2)$$

If the heat generation is q kcal/hm², then

$$\theta = \frac{qa}{\lambda} \cdot \frac{2}{T} \sum_{n=1}^{\infty} \frac{1}{\left(\frac{2n-1}{2}\right)^2 \pi^2 \frac{a}{T^2}} \left(1 - e^{-\left(\frac{2n-1}{2}\right)^2 \pi^2 \frac{a\tau}{T^2}}\right) \dots (3)$$

In order to obtain a dimensionless temp., divide eq. (3) by the steady state temp. $t=\infty$ which is obtained from equation (3) after an infinite heating time following the heating application.

$$g(\tau) = \frac{\theta \tau^2 t}{\theta \tau^2 \infty} \\ = \frac{2}{\pi^2} \sum_{n=1}^{\infty} \frac{1}{\left(\frac{2n-1}{2}\right)^2} \times \left(1 - e^{-\left(\frac{2n-1}{2}\right)^2 \pi^2 \frac{a\tau}{T^2}}\right) \dots (4)$$

The value $g(t)$ in equation (4) means (Measured temperature of outer surface - Water temperature), because the assumption is that the inside surface and water temperature are at 0°C as the initial condition.

TABLE 2.1 TRIAL HEATING RESULTS

JOINT NO.	THICKNESS (mm)	Temperature difference $\Delta T (^{\circ}\text{C})$	Estimated ΔT ($^{\circ}\text{C}$)	ΔT - Estimated ΔT ($^{\circ}\text{C}$)	T_{280} (sec)	T_0 $T=280$ ($^{\circ}\text{C}$)	T_0 ($^{\circ}\text{C}$)	T_{max} ($^{\circ}\text{C}$)
1	35.0	384	339	45	57	255	505	540
2	33.5	286	254	32	50	184	353	540
3	28	428	370	58	47	280	510	510
4	36.4	356	338	18	97	280	423	460
5	36	354	349	5	89	280	419	438
6	34	314	290	24	45	195	384	505

NOTE: T Max : Maximum temperature

T_0 : Temperature at outside surface of welding joint

T_{280} : Heating time at which T max becomes 280°C

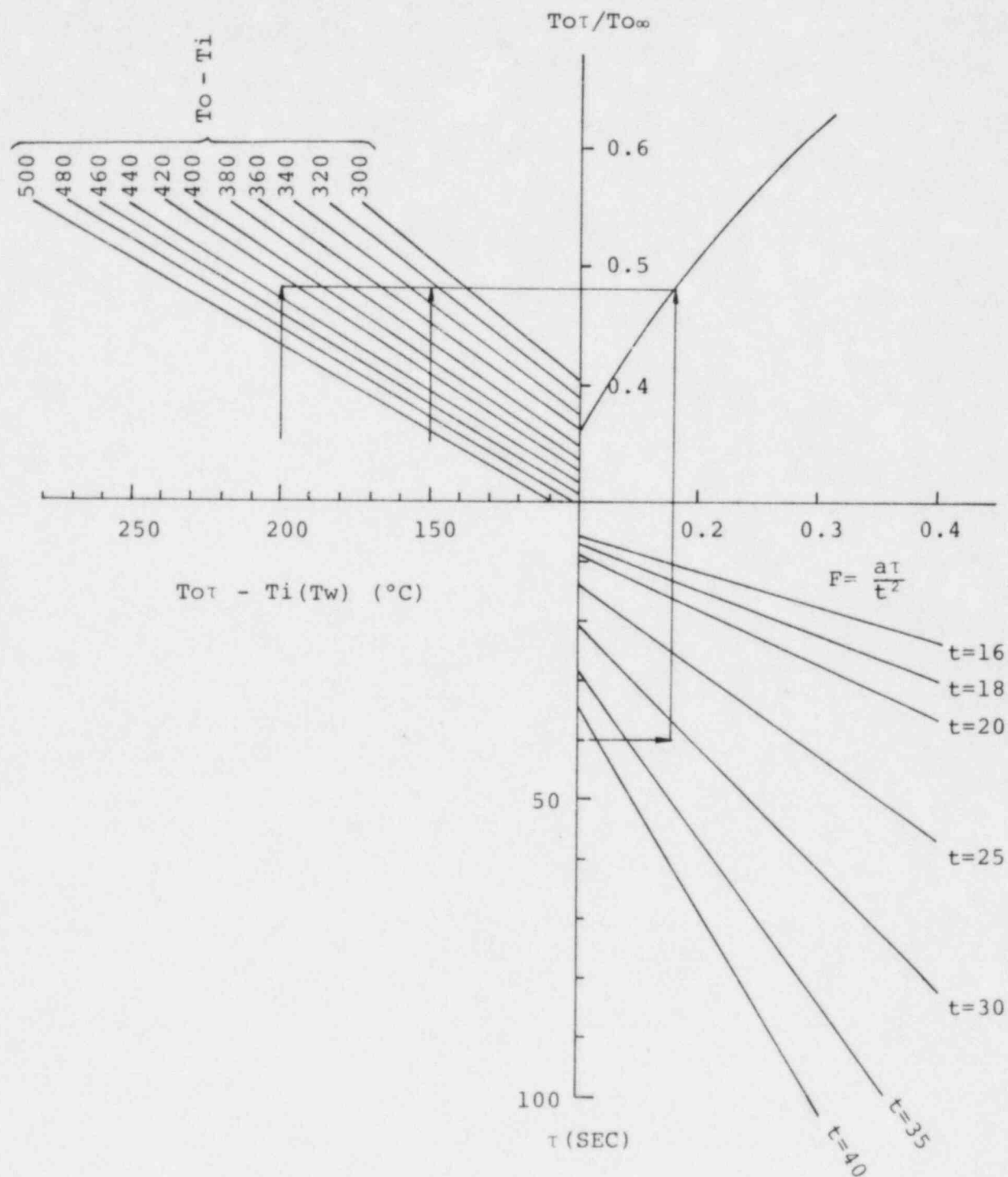


Fig. 2.1 ESTIMATION OF STEADY STATE CONDITION BY TRIAL HEATING

A - 13

ESTIMATE OF PIPE ID TEMPERATURE

DURING IHSI

1. Introduction

The effect of IHSI strongly depends on the temperature difference between the outer and inner pipe surfaces. The temperature on the outer surface is easily measured by thermocouples, as to the inner surface of the installed pipe, however, the temperature cannot be measured generally unless some special device is provided. Therefore, temperature estimate for the pipe inner surface is an important issue.

Generally, the heating duration of IHSI is sufficient so that heat conduction can be regarded as steady state, and the coil width is very large with respect to the pipe thickness, consequently, this condition is reduced to a one dimensional steady state heat transfer problem.

2. Theoretical considerations

(1) Fundamental Equation

Under the steady state condition induced by a long coil, heat transfer in the radial direction is dominant near the coil centre. This reduces to a 1-D steady heat transfer problem for which the fundamental equation is given as follows:

$$\frac{\partial^2 \theta}{\partial x^2} + \frac{1}{\lambda_p} \omega = 0 \dots (1)$$

θ : Temperature at point x

λ_p : Heat conductivity of a pipe

ω : Heat generation density

x : Distance from the outer pipe surface

Heat generation density (ω) in induction heating is given as follows:

$$\omega = \omega_0 e^{-2x/S} \quad \dots (2) \quad \omega_0: \text{Heating density at the surface}$$

where,

$$S = \frac{1}{2\pi} \sqrt{\frac{\rho}{\mu f \times 10^{-9}}} \quad \begin{array}{l} \mu : \text{Specific permeability} \\ f : \text{Frequency} \\ \rho : \text{Specific resistance} \end{array}$$

(2) Solution

Assuming that the outer surface is thermally insulated and its temperature is T_0 , Eq. (1) is solved as follows:

$$\theta = T_0 - \frac{\omega_0 S^2}{4\lambda p} \left(-1 + \frac{2}{S}x + e^{-2x/S}\right) \quad \dots (3)$$

As the temperature at the inner surface is obtained substituting $x = L$ into Eq. (3). The temperature difference between the outer and inner surface in a pipe ($\Delta T = T_0 - T_i$) is given as follows:

$$\Delta T = T_0 - T_i = \frac{\omega_0 S^2}{4\lambda p} \left(-1 + \frac{2}{S}L + e^{-2L/S}\right) \quad \dots (4)$$

(3) CALCULATING THE TEMPERATURE DIFFERENCE OF OUTER AND INNER SURFACE IN A PIPE

As shown in Eq. (4), ω_0 is the only unknown. ω_0 is determined from the following calculation.

The heat flux at the inner surface: q_i is given by Fourier's law as follows:

$$q_i = -\lambda p \frac{d\theta}{dx} \quad \dots \dots \dots (5)$$

Heat flux in the water at the pipe inner surface: q_2 is given as follows:

$$q_2 = h_m \Delta T_2 \dots\dots\dots (6)$$

h_m : Average Heat transfer coefficient

ΔT_2 : Temperature difference between the inner surface and fluid (bulk)

The differential coefficient of Eq. (3) at $x=L$ is given as follows:

$$\frac{d\theta}{dx} \bigg|_{x=L} = - \frac{\omega_o S}{2\lambda_p} (1 - e^{-2L/S}) \dots\dots\dots (7)$$

Under $q_1 = q_2$, Eq. (5) through Eq. (7) are reduced to the following:

$$\Delta T_2 = T_i - T_w = \frac{\omega_o}{2h_m} (1 - e^{-2L/S}) \dots\dots\dots (8)$$

T_w : Temperature of Fluid

From Eq. (4) and Eq. (8).

$$\Delta T + \Delta T_2 = T_o - T_w = \frac{\omega_o S}{2} \left\{ \frac{S}{2\lambda_p} \left(-1 + \frac{2L}{S} + e^{-2L/S} \right) + \frac{1}{h_m} (1 - e^{-2L/S}) \right\}$$

From Dittus - Boelter's equation. (9)

$$Nu = \frac{h_m d}{\lambda_w} = 0.023 Re^{0.8} Pr^{0.4}$$

$$h_m = 0.023 \frac{\lambda_w}{d^{0.2} \nu^{0.8}} Pr^{0.4} U_\infty^{0.8} \dots\dots\dots (10)$$

λ_w : Thermal Conductivity of Fluid

d : Inner Diameter of a Pipe

ν : Kinematic coefficient of viscosity

Pr : Prandtle Number

U_∞ : Fluid Flow Rate

From Eq. (9) and Eq. (10), ω_0 is given as follows:

$$\omega_0 = (T_0 - T_w) \times \frac{2}{S} \frac{1}{\frac{S}{2\lambda_p} \left(-1 + \frac{2L}{S} + e^{-2L/S}\right) + \frac{d^{0.2} \nu^{0.8}}{0.023 \lambda_w \text{Pr}^{0.4} U_\infty^{0.8}} (1 - e^{-2L/S})}$$

..... (11)

The temperature difference of the outer and inner surface of a pipe is obtained by substituting Eq. (11) into Eq. (4).

It is complicated, especially at a reactor site, to make the calculation described above for each heating and therefore a monograph to calculate the temperature difference is useful. One example of such a monograph is shown in Fig. 1.

The temperature difference $\Delta T = T_0 - T_i$ is obtained as follows.

Step. 1 Locate in Fig. 1 the measured $T_0 - T_w$

Step. 2 Move horizontally to the line for the value of the pipe thickness. Interpolation may be made for intermediate value of the pipe thickness.

Step. 3 From this intersection, move vertically upwards to the horizontal axis.
(This point shows ω_0 , the heating density at the pipe outer surface.)

Move vertically upwards from this point to the line for the pipe thickness.

Step. 4 From the intersection obtained in step 3, move horizontally left to the ordinate and read the value of ΔT .

Notes: It is noteworthy that ω_0 , and consequently ΔT , are not sensitive to the pipe diameter, the water flow rate and the physical properties of water as shown below, and therefore one monograph will be sufficient for the determination of ΔT at a site.

The reasons for the above mentioned statement follow.

(1) Effect of pipe inside diameter: d

It is clear from eq. (11) that the inside diameter contributes in the form of $d^{0.2}$ to ω_0 and the variation of ω_0 owing to the change of d is very small.

Consequently, ω_0 can be considered to be almost independent from d .

(2) Effect of water flow rate: U_∞

The effect of U_∞ on ΔT (the temperature difference through thickness) is shown in Fig. 2 and becomes very small if $U_\infty \geq 2$ m/s. (generally, U_∞ at site is greater than 3 m/s)

(3) Effect of water temperature: T_w

The physical constants of the water affect ω_0 in the form of $\nu^{0.8}/(\lambda_w \times Pr^{0.4})$. This term decreases slowly as temperature rises. Therefore if the constants corresponding to a lower temperature are used, ω_0 , and consequently ΔT , can be estimated conservatively.

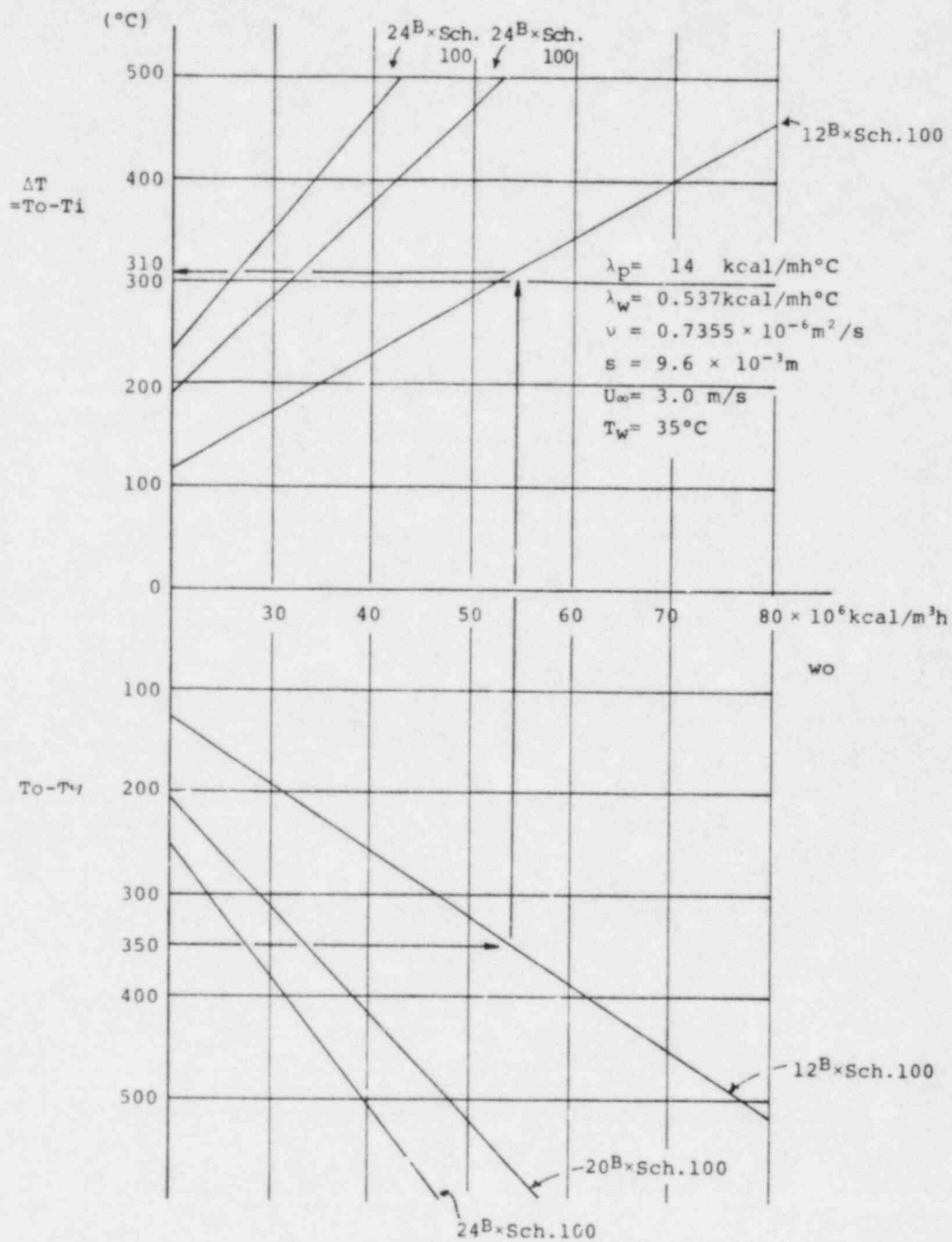


Fig. 1 TEMPERATURE DIFFERENCE BETWEEN OUTER AND INNER SURFACE OF A PIPE

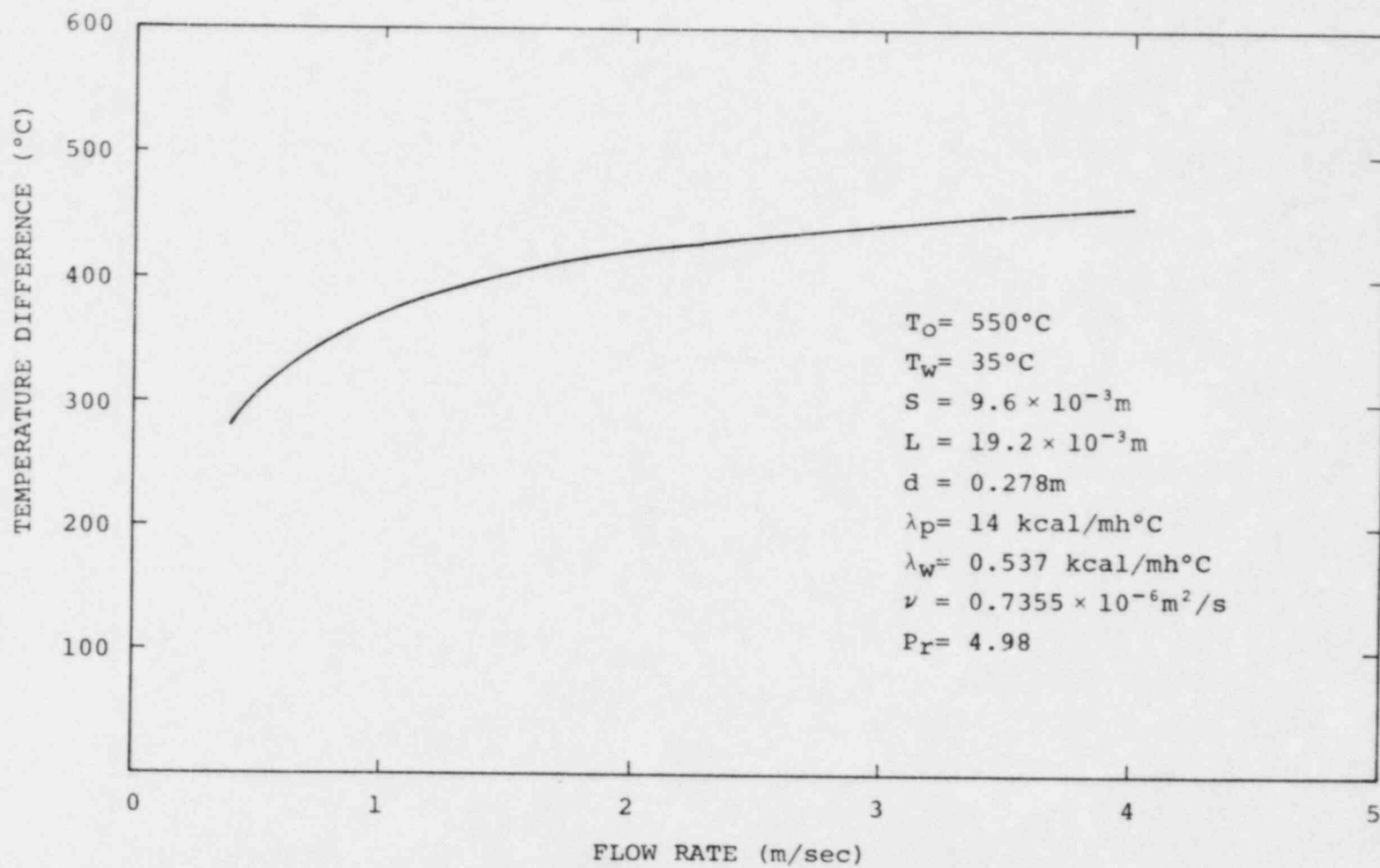


Fig. 2 EFFECT OF FLOW RATE ON ΔT

A - 14

ANALYTICAL STUDIES OF IHSI

FOR

A PIPE WITH A SMALL PRE-FLAW

1. Introduction

When applying IHSI to a pipe with small preflaw which is undetectable using ultrasonic technique, one must confirm that IHSI is effective for stress improvement and that the small preflaw can never propagate during the IHSI treatment.

In order to evaluate the behavior of a preflaw during IHSI, Finite Element Calculations were conducted as follows.

2. Analytical Models and Programs

The analytical study of IHSI was conducted for a 12 inch Schedule 100 stainless steel pipe. It was assumed that only the inside surface of the pipe was the heat-transfer surface, and that the others were insulated. The analytical IHSI condition was assumed to be as shown in Table 2.1.

An analytical model for calculating the temperature distribution through the pipe wall and an analytical model for calculating the residual stress distribution through the pipe wall are shown in Fig. 2.1 and 2.1 respectively. In the former analytical model, the pipe wall is divided into nineteen equal parts. In the latter analytical model, the analytical mesh as shown in Fig. 2.2 is offset since the constraint condition is changed due to the preflaw and the history of stress-strain near the preflaw is affected by the preflaw.

The finite element calculations consisted of transient temperature and elastic-plastic stress analysis. The programs utilized are ITEMP II and IEPTC II which are developed by IHI. The ITEMP II analytical code was developed for the purpose of solving the steady state and transient temperature distribution in an axisymmetric thick cylindrical body and in a two dimensional structure.

The IEPTC II analytical code was developed for the purpose of solving the thermal elastic-plastic creep problem in an axisymmetric thick cylindrical body and in a two dimensional structure.

3. FEM calculation results for the temperature analysis

The analytical result of the temperature distribution through the pipe wall at maximum heating was obtained as shown in Fig. 3.1. The temperature inside the pipe and the temperature outside the pipe were determined to be 91°C and 368°C , respectively. The temperature-pipe wall curve was nearly exponential, and the temperature distribution through the pipe wall was likely to be steady. The thermal history was obtained as shown in Fig. 3.2. The highest temperature curve, the medium curve and the lowest temperature curve present the thermal history of the pipe outside, the pipe intermediate position and the pipe inside, respectively. The temperature history was calculated 500 seconds after the heating initiation.

4. FEM calculation result for the stress analysis

The result of the elastic-plastic stress analysis was obtained as follows:

The temperature profile calculated by ITFMP II was the input source for the temperature-load data program. The temperature-load data were input to IEPTC II program, the stress analysis data were calculated.

The COD (crack opening displacement) at the maximum heating condition was calculated as shown in Fig. 4.1. As shown in the figure, the COD increases as the initial flaw depth increases.

Fig. 4.2 shows the distribution of the axial residual stress on the extension of each flaw after IHSI. The residual stress showed the maximum compressive value at the flaw tip, and became gradually more compressive as the flaw depth increased. The obtained residual stress is larger than the residual stress that was obtained for IHSI of a pipe without a small flaw.

The distribution of the axial residual stress through the remaining pipe wall is shown in Fig. 4.3. The stress distribution for the position at a distance of 2.4 mm from the small flaw was unstable as compared with that for the ordinary IHSI. The stress distribution at a distance of 17 mm from the small flaw ignores the presence of the small flaw.

PIPE LENGTH (m)	PIPE THICKNESS (mm)	CRACK DEPTH (mm)	RATIO OF CRACK DEPTH (%)	BOUNDARY TEMPERATURE (°C)	HEAT TRANSFER COEFFICIENT (kcal/m ² ·°C)	HEATING DENSITY (kcal/m ² ·h)	HEATING TIME (sec)
50	19	2.4	12.5	20	4.050×10^{-3}	0.0583	180

TABLE 2.1 ANALYTICAL CONDITION

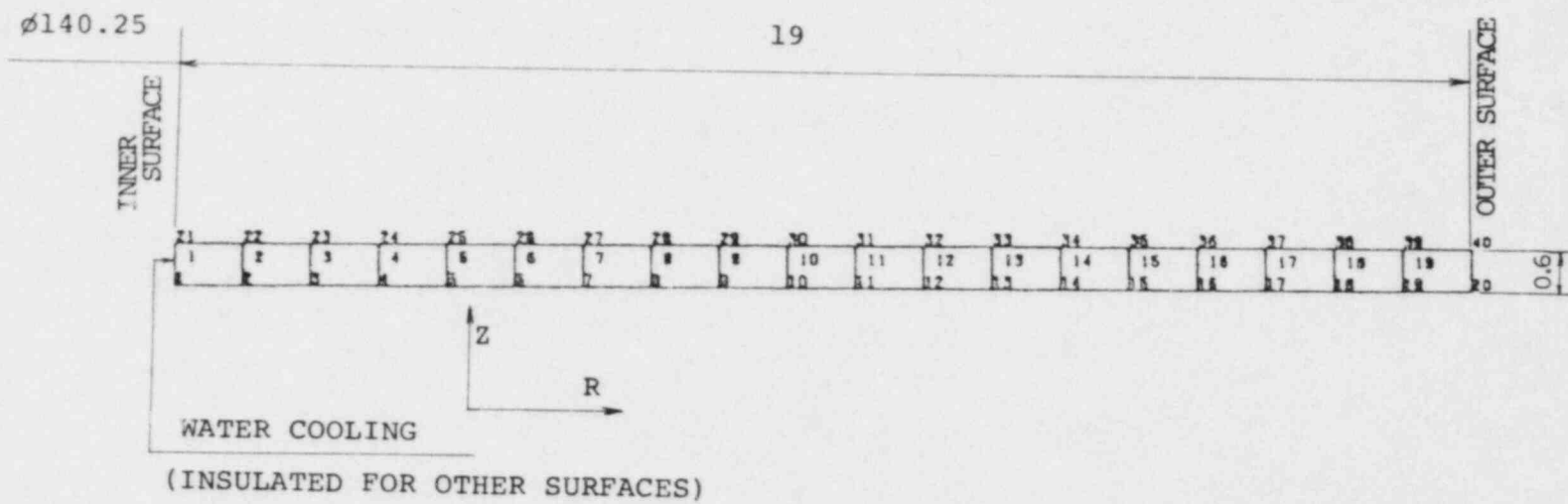


Fig. 2.1 ANALYTICAL MODEL FOR THERMAL ANALYSIS

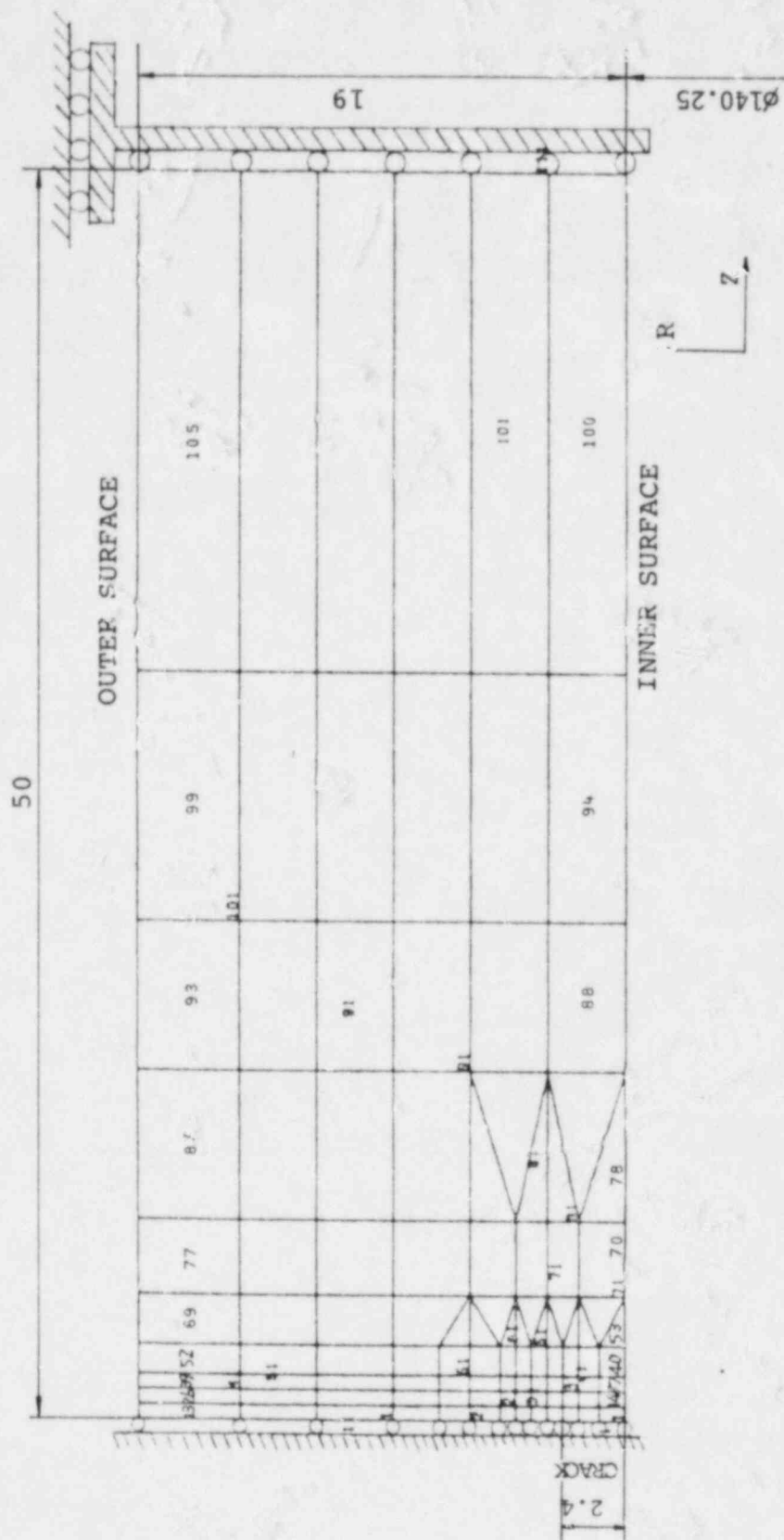


Fig. 2.2 ANALYTICAL MODEL FOR RESIDUAL STRESS (FIGURE OF ELEMENTS)

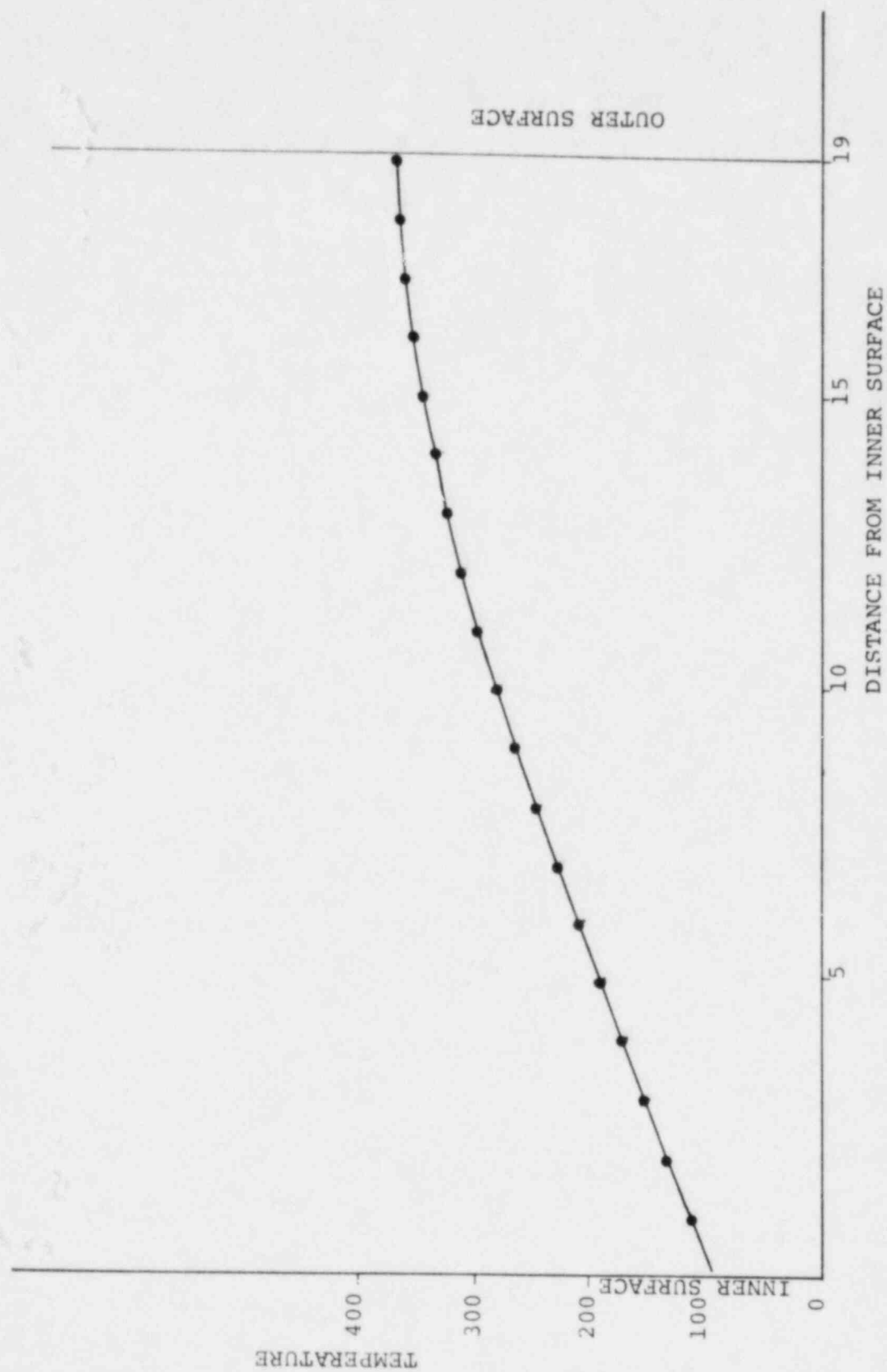


Fig. 3.1 TEMPERATURE DISTRIBUTION (THROUGH THICKNESS DIRECTION)

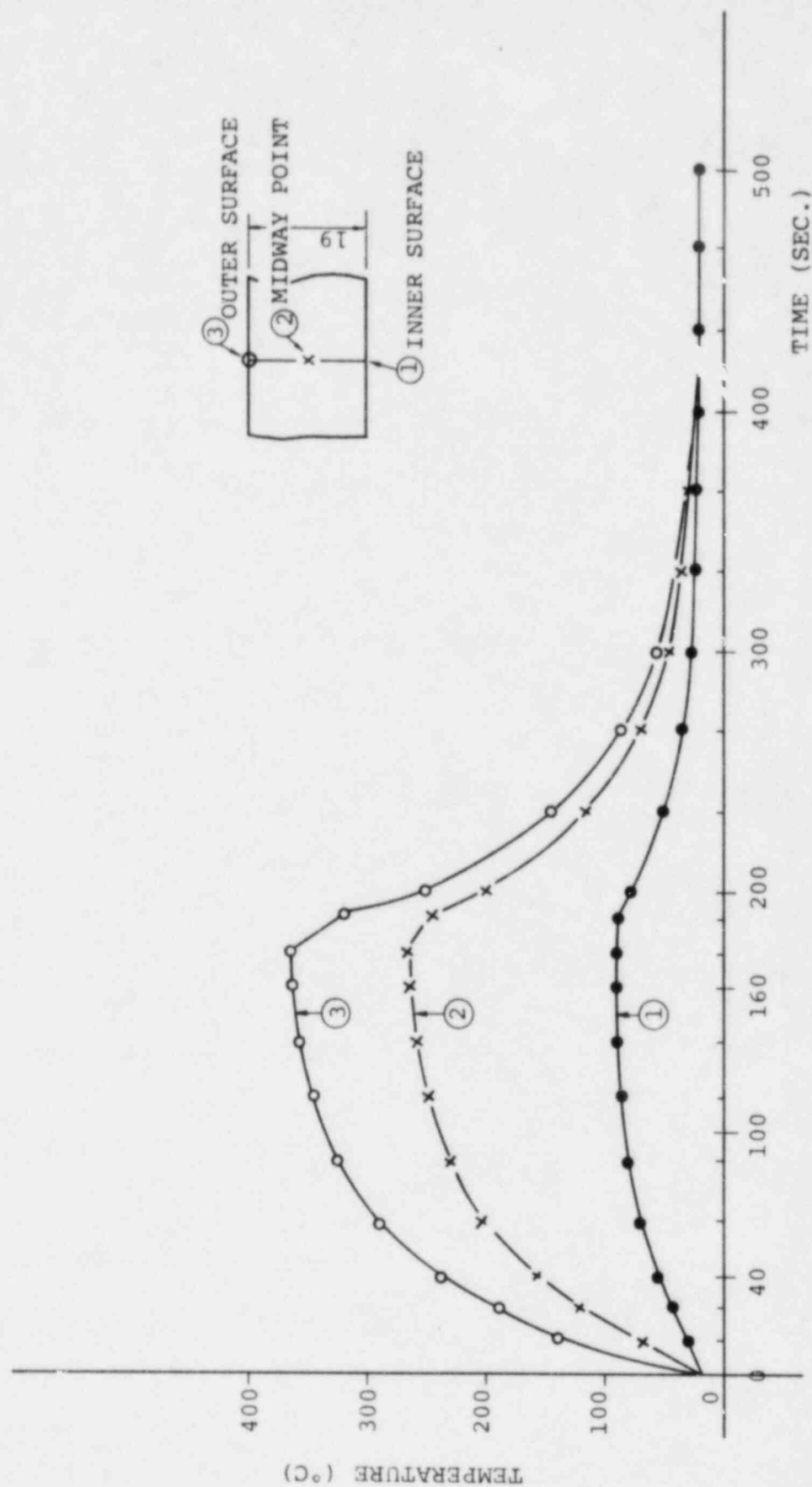


Fig. 3.2 TEMPERATURE TRANSITION CURVE

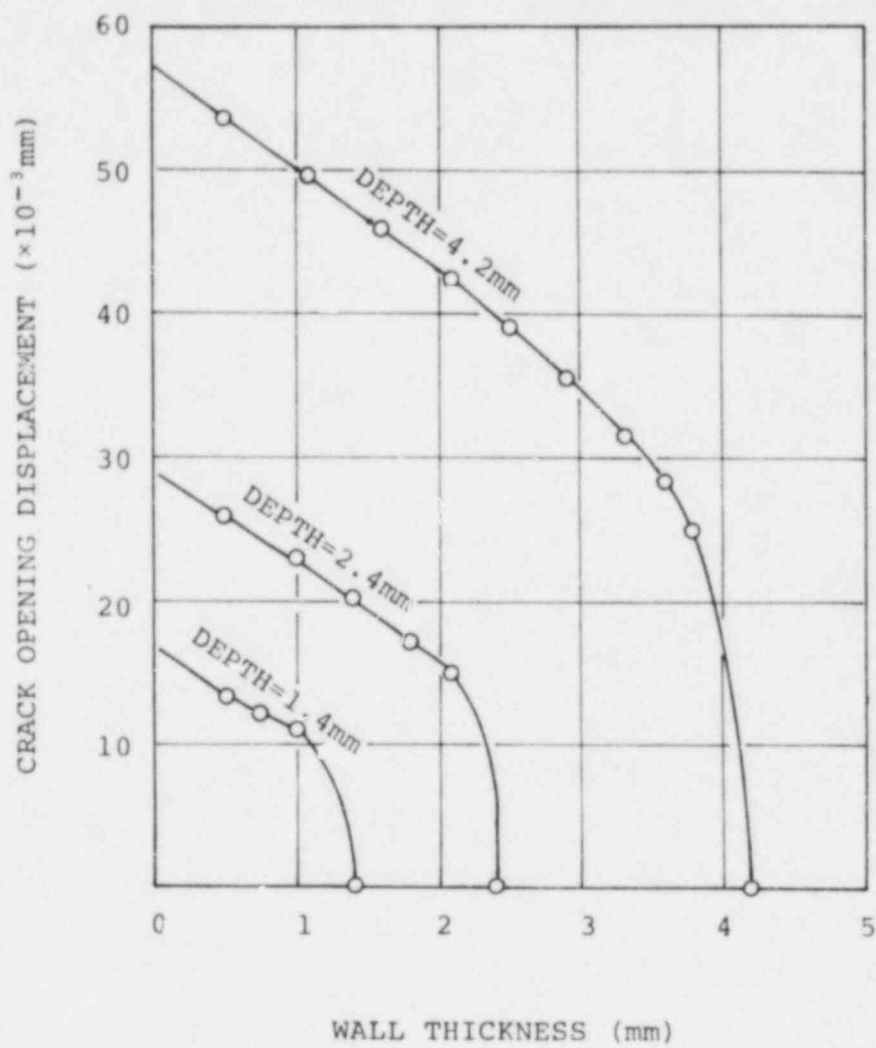


Fig. 4.1 CALCULATED COD AT MAXIMUM HEATING

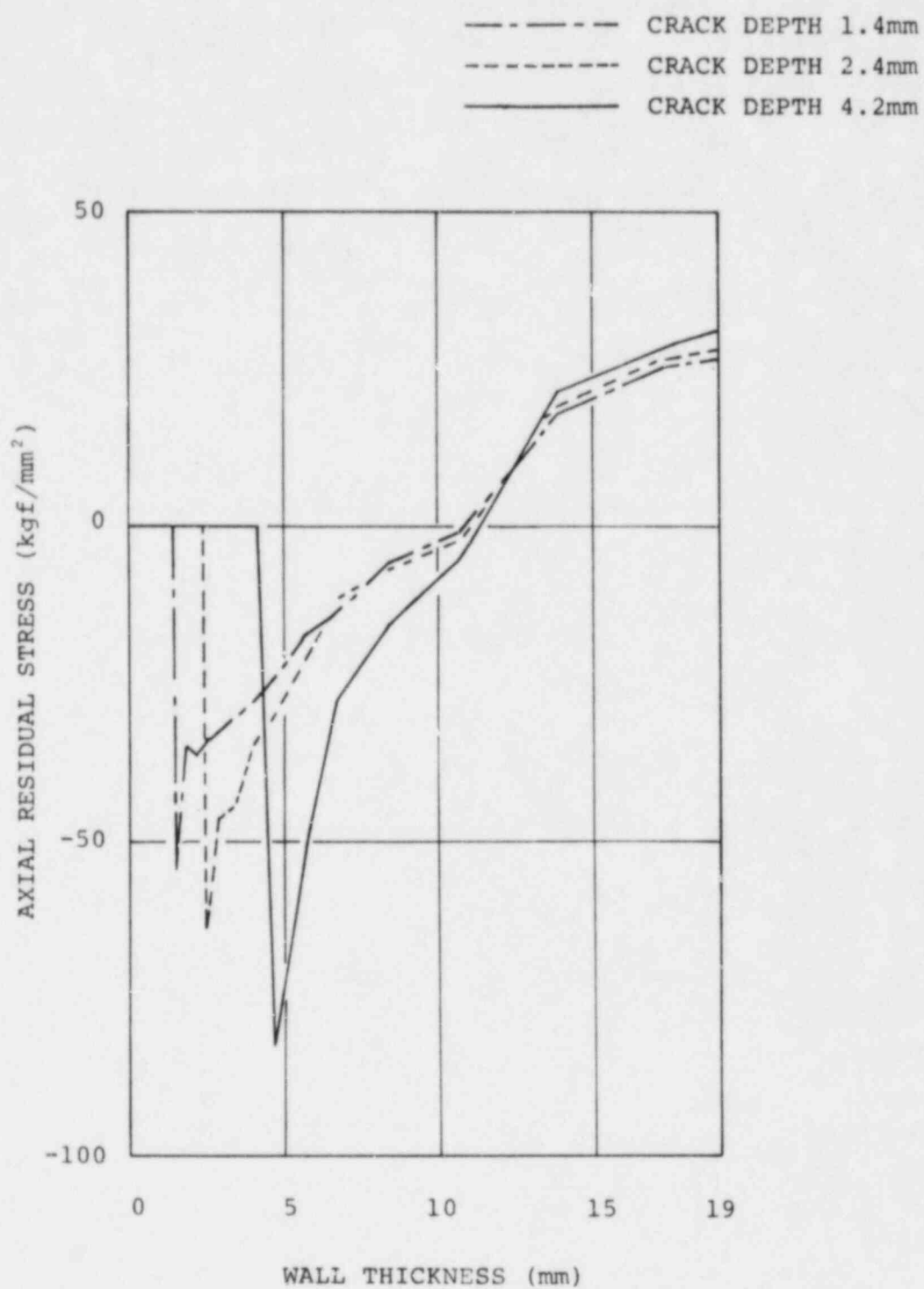


Fig. 4.2 CALCULATED RESIDUAL STRESS ON THE
EXTENSION OF FLAW OF 12 IN. PIPE

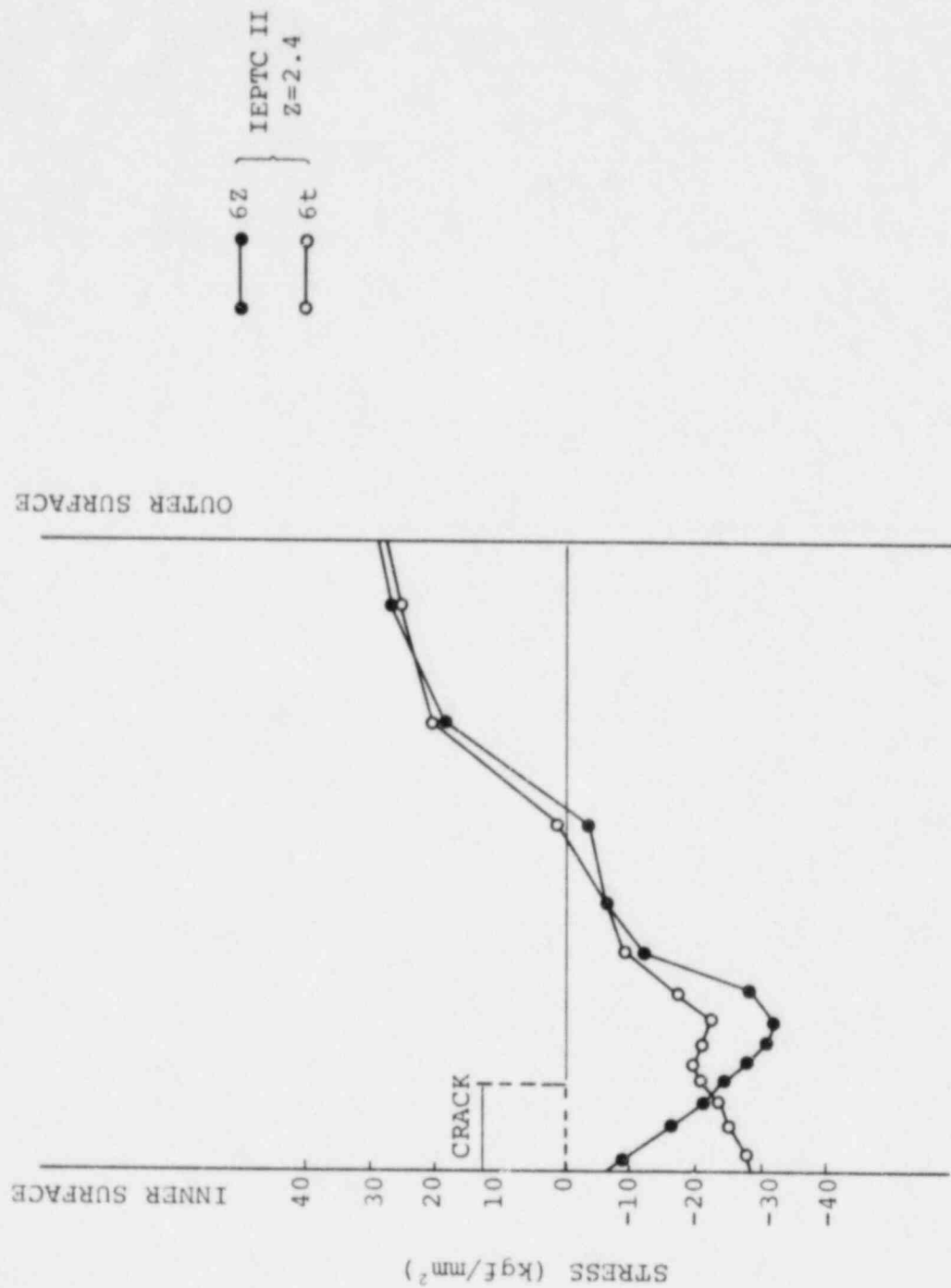


Fig. 4.3 RESIDUAL STRESS DISTRIBUTION (THROUGH THICKNESS DIRECTION)
(2.4mm FROM CRACK)

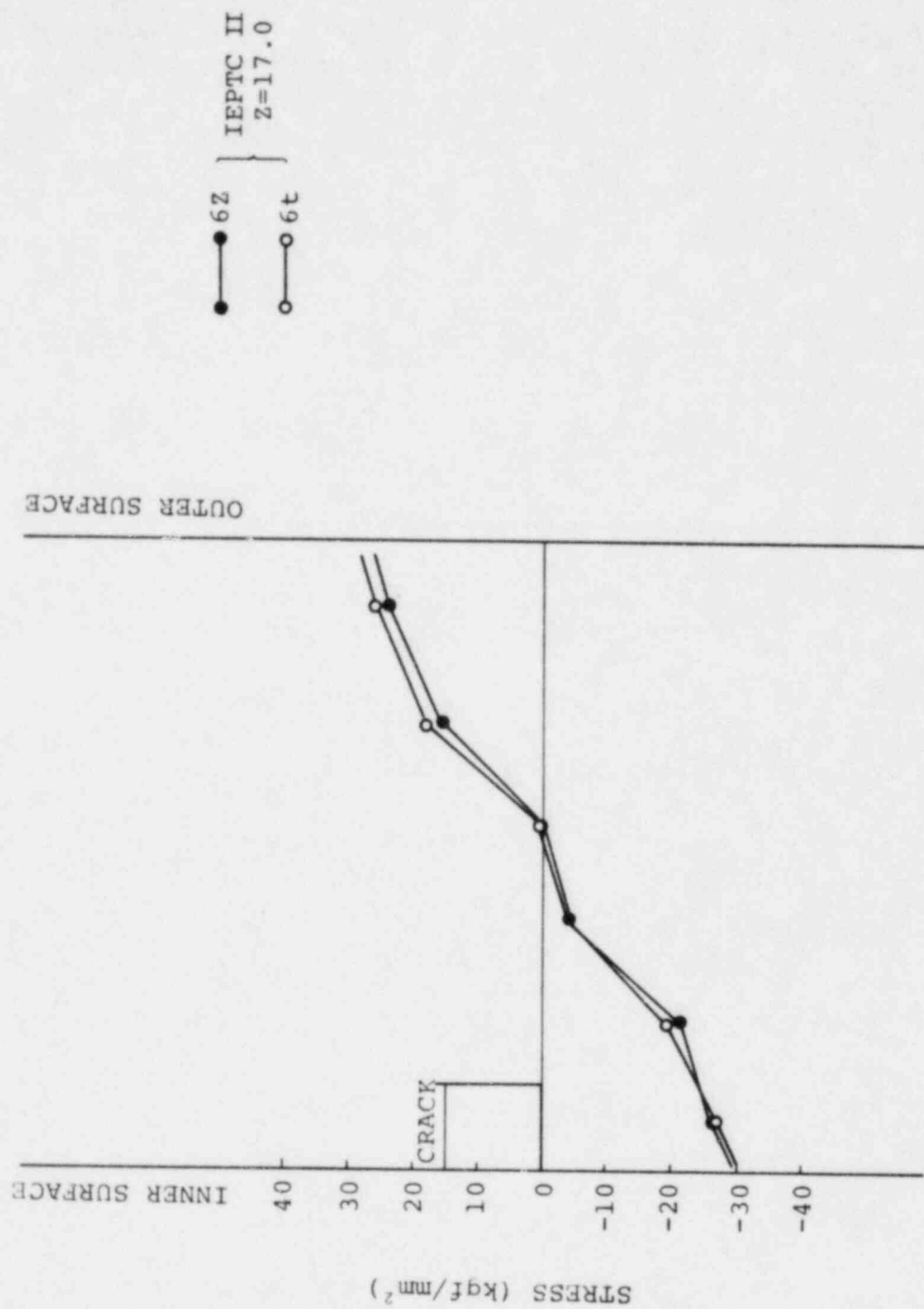


Fig. 4 RESIDUAL STRESS DISTRIBUTION (THROUGH THICKNESS DIRECTION)
(17mm FROM CRACK)

**Residual Stress Improvement by Means of
Induction Heating**

IHI

Ishikawajima-Harima Heavy Industries Co., Ltd.

Residual Stress Improvement by Means of Induction Heating

Tadahiro Umemoto*
Shinji Tanaka*

A new method for improving residual stresses in pipe weldment has been proposed. This method, named IHSI (Induction Heating Stress Improvement), has been developed to improve residual stresses by creating local plastic flows through the application of high thermal stresses induced when a pipe is heated from the outside by an induction coil and cooled simultaneously from the inside by water. To obtain a better heating condition and to make a demonstration test, some basic studies were conducted on 304 type austenitic stainless steel pipes. The residual stresses with and without IHSI were measured by the conventional strain gage method. A cracking test was also conducted for demonstration by boiling 42% MgCl₂ solution. The following experimental results were obtained, showing that IHSI is capable of satisfactory improvement of the residual stresses in pipe weldment.

1. High tensile residual stresses were lowered or shifted to the compressive side
2. No cracks were observed on the inside surface near the pipe weldment after the application of IHSI
3. Little variation was observed on microstructure and mechanical properties.

1. Introduction

It has been noted that intergranular stress corrosion cracking (IGSCC) does damage to weld heat affected zones of 304 type austenitic stainless steel pipes in boiling water reactors reducing reactor availability. IGSCC is known to occur by interactions of three factors: stress (residual stress due to welding, operating stress, etc.), material (sensitization by welding, alloy element content, etc.), and environment (dissolved oxygen in reactor water, corrosion products, foreign material on inside pipe walls, etc.). Various measures have been taken to solve these problems. As to the problem of material sensitization, for instance, reduction in carbon content, and battering process of covering inner pipe surfaces with SCC-resisting weld metal, or resolid solution treatment, have been attempted. To improve environmental factors, deaeration operation is being performed in plants.

The induction heating stress improvement (IHSI) is a method developed to improve stress factors, especially residual stresses in pipe joint weld affected zones. In this method a pipe is heated from the outside by an induction coil and cooled from the inside with water simultaneously so as to produce an appropriate differential temperature between inner and outer pipe surfaces for the resultant thermal stresses to improve residual stresses.

The authors conducted a parametric survey to determine better treatment parameters (such as, frequency, heating time, coil width, etc.) and a test to demonstrate the effectiveness of the treatment. Test pipes 4B, 10B,

and 12B were used for the former experiment, and 4B and 12B were used for the latter. Elastoplastic calculations by the finite element method were also made to verify the experimental results. Results of these efforts to improve residual stress by IHSI and a discussion of the applicability of the method to actual plants will be presented in this paper.

2. Principle

It is known universally that thermal stress occurs when a difference in temperature is introduced in a substance. If a temperature difference is introduced between the inner and outer surfaces of a long pipe with linear temperature gradient, then the thermal stress produced between the two points can be expressed by the following equation⁽¹⁾:

$$\sigma = E\alpha \Delta T / (1 - \nu) \quad \dots\dots\dots(1)$$

where

E : Young's modulus

α : Linear expansion coefficient

ν : Poisson's ratio

ΔT : Temperature difference between inner and outer surfaces

As long as this thermal stress is within an elastic region, or below the yield point (point ① in Fig. 1) of material, the stress is relieved when the temperature difference is removed, and no residual stress remains behind. However, if the thermal stress goes beyond the yield point (point ② in Fig. 1), the subsequent removal of the temperature difference will cause thermal strain to occur linearly from point ② to point ③ on the stress-strain curve (at an angle equal to Young's modulus) and then return to the zero point. In this instance, a residual

* Plant Engineering Department, Nuclear Power Engineering Division

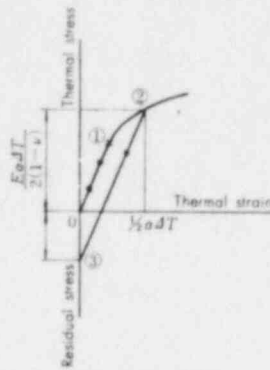


Fig. 1 Stress-strain diagram

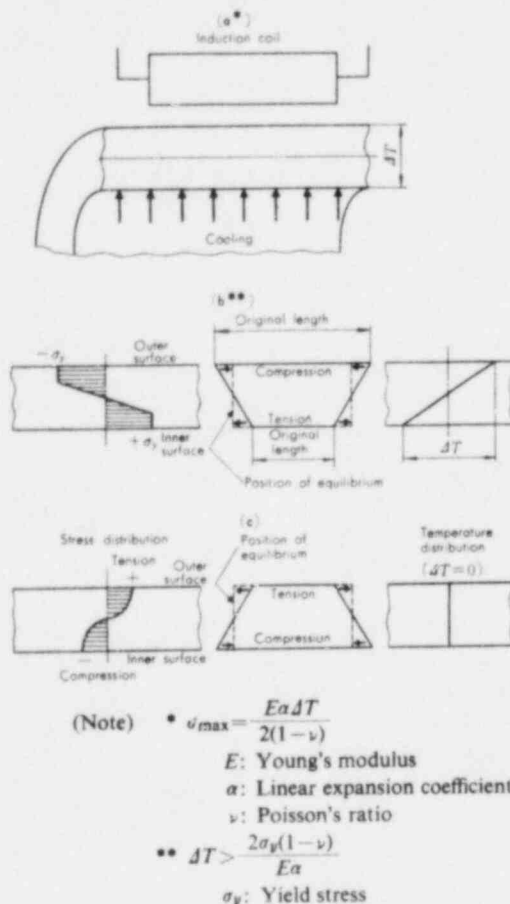


Fig. 2 Principle of IHSI

stress with a reverse sign with respect to the thermal stress that has occurred during the heating remains behind.

The treatment to be discussed here is a method for introducing a large temperature difference between inner and outer pipe surfaces by heating the pipe from the outside with an induction coil attached thereto by a high frequency induction technique while supplying cooling water to the inside pipe face concurrently (Fig. 2-(a)). The thermal stress obtained as a result of the temperature difference is expressed by equation (1). Under a proper temperature difference condition ($\Delta T \geq 2\sigma_y(1-\nu)/E\alpha$), the pipe length becomes shorter at the outside than it originally is due to its yield to compressive force, while at the inside it becomes longer than the original length, because it yields to tensile force (Fig. 2-(b)). The difference between the inside and outside pipe temperatures will disappear as the heating is stopped, and the outside pipe area where compressive yield has taken place will be stretched back to the original length. The inside pipe area where tensile yield has taken place, on the other hand, will be compressed to the original length (Fig. 2-(c)). In other words, tensile and compressive residual stresses will be produced in the outside and inside pipe surfaces, respectively. This principle is applied to pipe weldments with the objective of reducing tensile residual stresses in inside surfaces of pipe joint weldments, or otherwise shifting them into the compressive side.

3. Experiment

3.1 Test samples

304 type stainless steel pipes of sizes 4B, 10B and 12B, and stainless forgings of 12B were used as test samples, the mechanical properties of which were as shown in Table 1. Test pipes for a parametric survey were all subjected to stress relief heat treatment ($900^\circ\text{C} \times 2$ hours), and those for demonstration testing were joint welded in or by the same way as normally used for actual plants. The demonstration test pipes were combinations of [a straight pipe + an elbow] and [a straight pipe + a nozzle safe end] so as to conform to pipe configurations in an actual plant. An example of the test pipe used is illustrated in Fig. 3.

3.2 Experimental methods

Table 1 Mechanical properties

Pipe parts	Pipe diameter	Mechanical properties			Remarks*
		Yield point (kgf/mm ²)	Tensile strength (kgf/mm ²)	Elongation (%)	
Pipe	4B	21	62	65	R-12~R-17
		24	57	70	R-1B, R-2, R-4A
	10B	22	55	70	R18
	12B	24	58	70	R21~R23
Elbow	12B	22	56	72	R-25, 26, 28, 29
Nozzle safe end	—	26.1	54.5	67.5	R-24, 27, 30, 33

(Note) *Refers to the test sample No. or joint No.

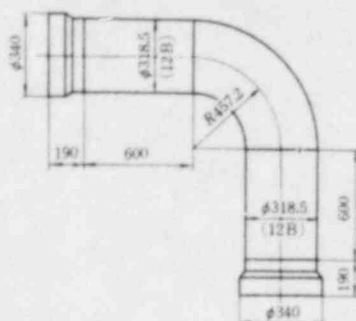


Fig. 3 Configuration of test pipe

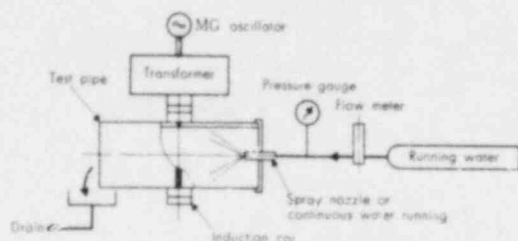


Fig. 4 Assembly of IHSI

Shown in Fig. 4 is the setup of IHSI used in the experiment. With an induction coil placed on the outside of a test pipe, the inside of the pipe was cooled by continuously running or spraying water. The coil was powered for a predetermined time. The test matrix used is shown in Table 2. Table 2-(a) gives the test matrix for a parametric survey which was made with various frequencies, heating durations, and coil widths to determine induction heating conditions. Table 2-(b) lists the data of a demonstration test on test pipe joints similar to those of actual plant pipes.

After induction heating, residual stresses on the joint weldments were measured by the commonly used strain gage method. In addition, the test pipes were submerged in 42% magnesium chloride solvent and then inspected for cracking by dye penetrant technique in order to

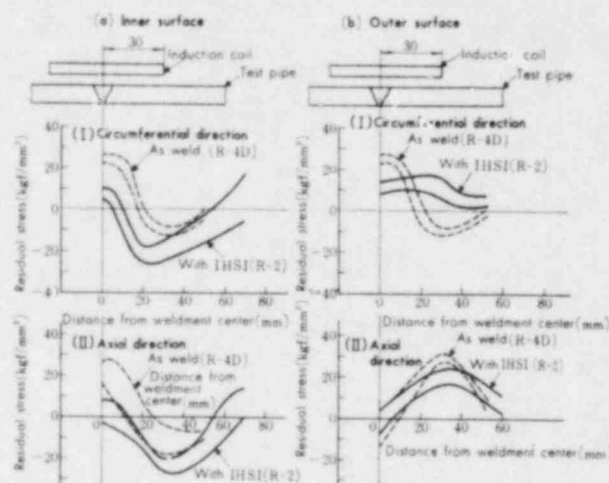


Fig. 6 Stress distribution after application of IHSI (4B demonstration test)

grasp stress patterns throughout the pipe inside surfaces.

4. Results

4.1 Temperature distribution

Some examples of temperature distribution in the axial direction during induction heating are given in Fig. 5 and Fig. 7-(a). Each sample tested indicated almost the same temperature rise at the induction coil center while comparatively abrupt down curves were noted at coil ends.

The effect of heating depth was examined by changing frequency, the results of which are given in Table 2-(a). A comparison between R-12 and R-15 indicated a higher frequency could produce a larger difference between inner and outer pipe surface temperatures. Another comparison between R-21 and R-22 for the effect of cooling water flow rate on pipe temperature indicated that a higher velocity could reduce the temperature at inner and outer pipe surface more greatly.

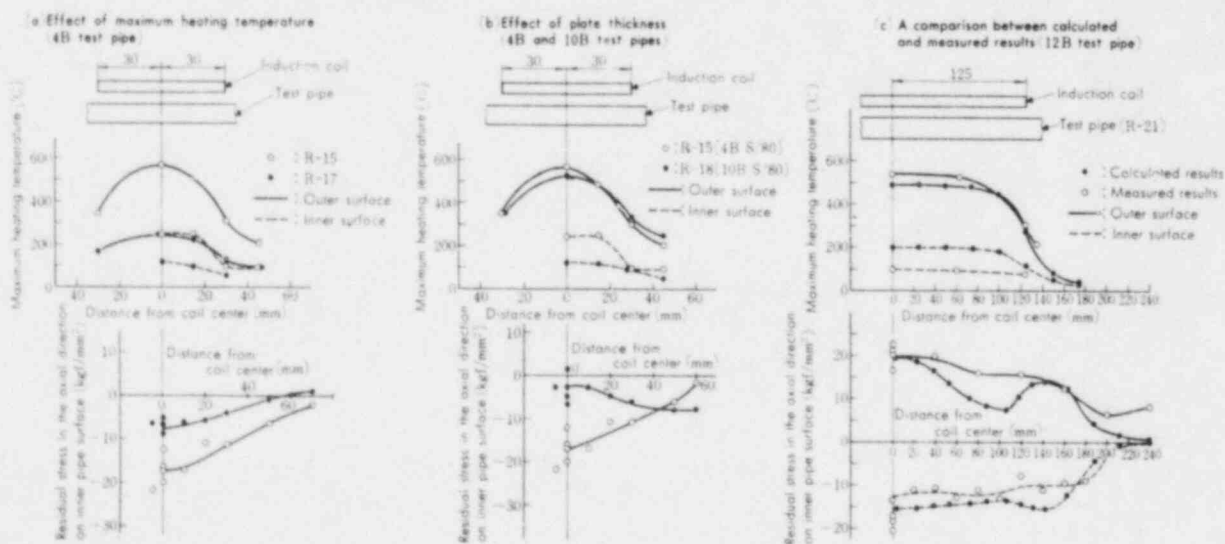


Fig. 5 TTD and stress distributions after application of IHSI (parametric survey)

Table 2 Test matrix

(a) Parametric survey

Test pipe	Item	Pipe size	IHSI conditions				Temperature (°C)*			Residual stress** (kgf/mm ²)
			Frequency (kHz)	Coil width (mm)	Heating time (s)	Cooling method	Outside surface (T _o)	Inner surface (T _i)	ΔT (T _o - T _i)	
R-12		4B S/80	8.4	60	19	Spray method	530	105	425	-12.3
-13		do.	2	do.	16	do.	676	250	426	-12.9
-14		do.	do.	do.	102	do.	520	192	328	-12.3
-15		do.	do.	do.	21	do.	562	240	322	-16.6
-16		do.	do.	do.	23	do.	322	167	155	-7.6
-17		do.	do.	do.	25	do.	247	115	132	-7.6
-18		10B S/80	do.	do.	29	do.	519	118	401	-3.5
-21		12B S/100	3	250	180	Running through method (0.72 m/s)	537	102	435	-17.3
-22		do.	3	250	157	Running through method (0.43 m/s)	548	126	422	-17.5
-23		do.	3	200	125	do.	558	122	436	-14.7

(b) Demonstration test

Test pipe	Item	Pipe size	IHSI conditions				Temperature (°C)*		
			Frequency (kHz)	Coil width (mm)	Heating time (s)	Cooling method	Outside surface (T _o)	Inner surface (T _i)	ΔT (T _o - T _i)
R-1B***		4B S/80	8.4	60	60	Spray method	540	168	372
-2****		do.	8.4	60	60	do.	536	170	366
-4A***		do.	—	—	—	—	—	—	—
-25****		12B S/100	—	—	—	—	—	—	—
-26***		do.	—	—	—	—	—	—	—
-28****		do.	3	250	177	Running through method (0.5 m/s)	514	119	395
-29***		do.	3	250	178	do.	514	128	386
-30****		do.	3	250	116	do.	556	79	477
-33****		do.	—	—	—	—	—	—	—

(Note) * Temperature measurements taken at induction coil center

** Average measurements of stress in the axial direction on inner pipe surface taken at coil center

*** Test pipes for crack testing

**** Test pipes for residual stress measurements

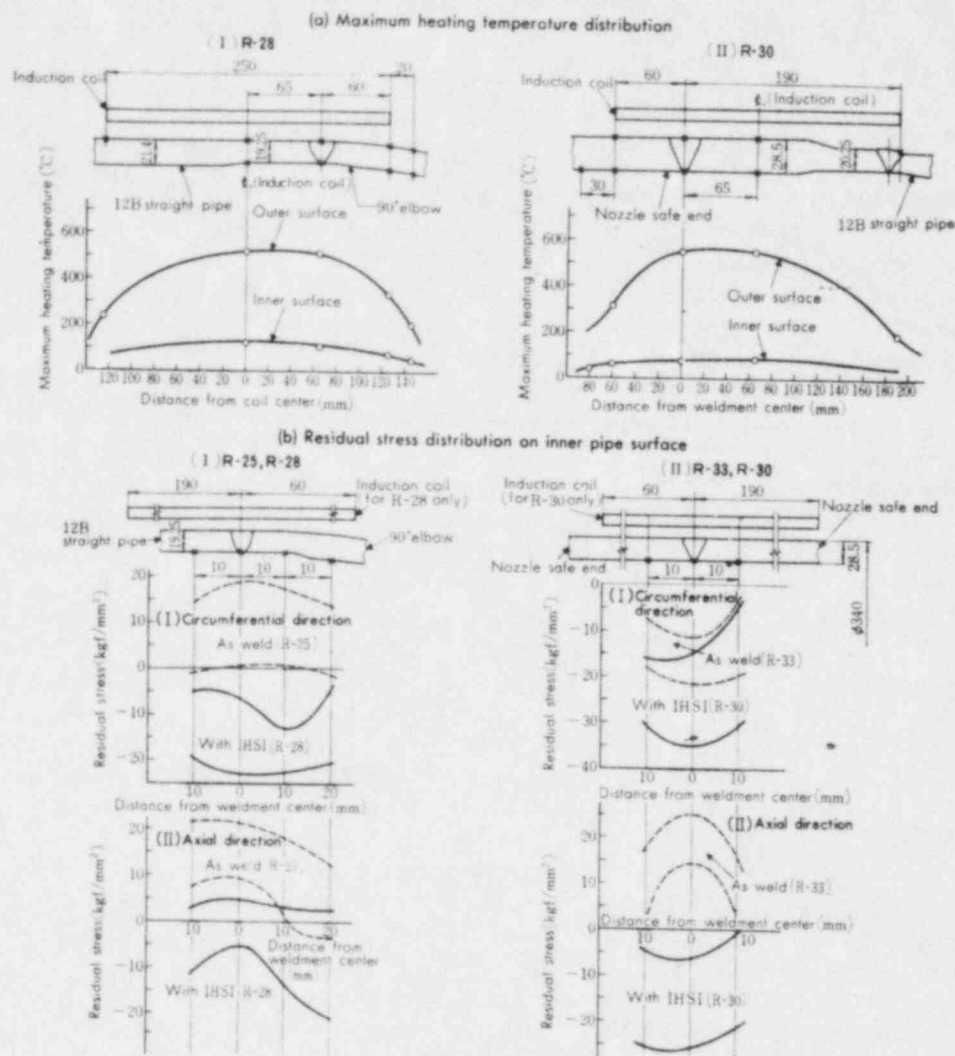
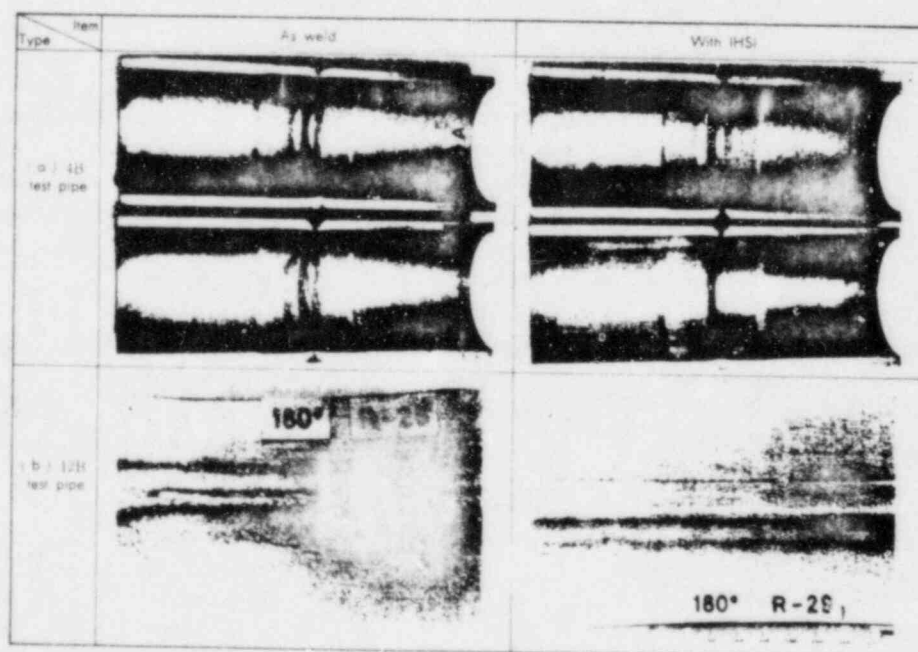


Fig. 7 TTD and stress distributions after application of IHSI (12B demonstration test)

Fig. 8 Crack pattern of inner surface of pipe joint after 42% $MgCl_2$ test (demonstration test)

4.2 Residual stress

4.2.1 Residual stress measurement with strain gage

Shown in Fig. 5 are examples of the distribution of residual stresses in the axial direction on pipes 4B, 10B and 12B after induction heating (parametric survey). From the figure it will be seen that in each case residual stresses on the inner surface, down to the coil end, are mostly in the compressive side.

Some examples of the results of a demonstration test on pipes 4B and 12B which were provided with welded joints are given in Fig. 6 and Fig. 7-(b), respectively. In both cases, residual stresses on the inner pipe surface were shifted toward the compressive side when induction heat treatment was performed, in comparison with as weld.

4.2.2 $MgCl_2$ cracking test

Fig. 8 shows the results of the observation of inner pipe surface cracking induced by $MgCl_2$. Fig. 8-(a) compares crack patterns of two 4B pipes; one was induction heat treated and the other was not, and Fig. 8-(b) compares the crack patterns of 12B pipes. Induction heat treating was proved, in both cases, to be effective in preventing such cracks.

5. Discussion

5.1 Comparison with calculated results by finite element method

Thermal elastoplastic calculations by the finite element method were conducted using R-21 as a model. The results of the calculations are compared with the experimental results in Fig. 5-(c). The calculated results of temperature distribution in the axial direction agreed quite well qualitatively with the experimental results, whereas some quantitative difference was observed between the inner and outer surfaces. One possible reason for the difference is that the calculations regarded heating intensity at each mesh in the pipe thickness direction as constant. But, in the experimental induction heating, heating intensity was reduced from outer to inner surfaces forming a curve like an exponential function (equation (2)). As a result, a milder-than-actual temperature curve between the outer and inner surfaces was obtained for the model calculations. In addition, slightly lower measurements are anticipated in the experiment because the thermocouple acted as a cooling fin.

As to residual stress distribution, the calculated results agreed very well for this type of model calculation with the experimental results, especially on inner pipe surfaces where complete agreement was noted. This indicates that this calculative method will provide a good means of predicting residual stresses on inner pipe surfaces with acceptably high accuracy in the future. The residual stresses on the inner pipe surfaces were found to be almost the same in the range from the coil center to 25 mm outside the coil ends. This implies that the residual stress improvement is effective even at weldments slightly

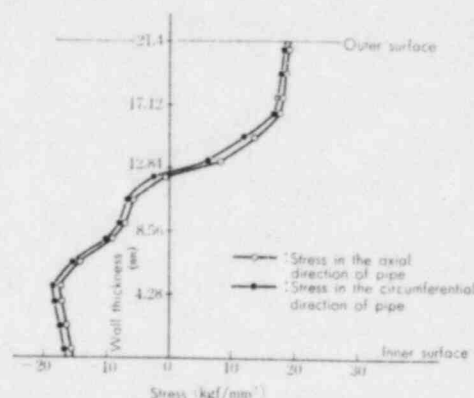


Fig. 9 Residual stress distribution in the plate thickness direction (calculated results)

away from an induction coil.

Fig. 9 shows the calculated results of residual stresses in the plate thickness direction. The residual stresses in the compressive side amounted to about 60% of the plate thickness. This property illustrates the superiority of IHSI to other stress improvement methods, for instance, shot peening, by which only at most several hundred microns of a surface become residual stresses of the compressive side^{(2),(3)}.

5.2 Heating factors and residual stress

Heating factors, which are considered comparatively important, and their effects on residual stress will be discussed here.

5.2.1 Effect of heating temperature

Thermal stress produced during heating is proportional to temperature difference (ΔT) between inner and outer pipe surfaces (equation (1)). Accordingly, it is assumed that as ΔT increases, plastic strain produced during heating and resulting residual stress will be increased. The effect of ΔT was experimentally examined, some results of which are shown in Fig. 5-(a). R-15 showed a residual stress (σ_R) of -17 kgf/mm^2 at $\Delta T = 322^\circ\text{C}$ and R-17 showed -8 kgf/mm^2 at $\Delta T = 132^\circ\text{C}$, which agreed well with the above assumption. This residual stress $-\Delta T$ relationship, however, holds true only when residual stress (σ_R) is equal to, or less than the yield stress of material (σ_y). Under $\sigma_R > \sigma_y$, work hardening is the only factor to increase σ_R . The effect of the heating temperature, therefore, cannot be fully relied on to increase residual stress beyond σ_y .

5.2.2 Effect of heating depth

The depth of heating by induction heating is inversely proportional to the square root of current frequency. At extremely high frequencies, therefore, only an outer surface is, in effect, heated, and in an equilibrium condition, a linear pattern of temperature distribution as illustrated in Fig. 10-(a) is obtained. When an extremely short heating period is used, a temperature distribution pattern will be as shown in Fig. 10-(b). In contrast, at lower frequencies, the heating best penetrates deeply, and in an equilibrium condition, a temperature distribution forms a pattern like a parabola, as seen in Fig. 10-(c). In

Type	Item	a) Linear temperature distribution	b) Exponential function like temperature distribution	c) Parabolic temperature distribution
Temperature distribution				
Heating depth		Small	Small	Large
Heating time		Large	Small	Large

Fig. 10 Three patterns of temperature distribution in the plate thickness direction

such temperature distribution conditions as stated above, thermal stresses (σ_{th}) on inner pipe surfaces can be expressed by elastic calculations as follows⁽¹⁾:

- (1) In the case of Fig. 10-(a):

$$\sigma_{th} = E\alpha \Delta T / 2(1 - \nu)$$

- (2) In the case of Fig. 10-(b):

Assuming that the temperature distribution takes a pattern of a symmetric parabola with respect to an inner pipe surface,

$$\sigma_{th} = E\alpha \Delta T / 3(1 - \nu)$$

- (3) In the case of Fig. 10-(c):

Assuming that the temperature distribution takes a pattern of a symmetric parabola with respect to an outer pipe surface,

$$\sigma_{th} = 2E\alpha \Delta T / 3(1 - \nu)$$

Thus, σ_{th} of condition (3) is assumed to be the largest and capable of producing the largest plastic strain for the same ΔT value. Hence, the resultant residual stress will be the largest. In contrast, the resultant residual stress of condition (2) is assumed to be the smallest. The above assumption can be verified by comparing R-12 with R-15 again. The latter having a larger heating depth produced a slightly larger residual stress than the former which was subjected to a greater ΔT value but had a smaller heating depth. This agrees well with the assumption.

5.2.3 Effect of heating time

When heating is applied for a very short period, the temperature distribution takes a pattern (Fig. 10-(b))

very similar to that of induction heating intensity distribution. This type of temperature distribution is undesirable, in terms of residual stress, for the reasons stated above. It is not wise to use an extremely limited heating time.

The relations between heating time and temperature distribution in the plate thickness direction obtained by IHSI are shown in Figs. 11-(a) and (b). The calculated results showed that a temperature distribution pattern similar to equilibrium condition was obtained in about 80 seconds on a 21.4 mm thick pipe. A similar pattern was experimentally measured in about 180 seconds for a pipe with 34.5 mm plate thickness. This exemplifies that heating time depends on plate thickness. Simplifying the relationship by using Fourier's number⁽⁴⁾ as

$$F = at/L^2$$

where, a : Thermal conductivity (m^2/h)
 t : Heating time (h)
 L : Plate thickness (m)

gives 0.78 for the 21.4 mm thick plate and 0.66 for the 34.5 mm thick plate. In addition, it is known that a $2L$ thick plate with a uniform temperature of ϕ_0 at $t < 0$, when cooled quickly at $t = 0$, till its surface temperature becomes $0^\circ C$, is cooled down to about 20% of the initial temperature ϕ_0 as measured at its core, providing that $F \approx 0.7$. The above data lead to the conclusion that a temperature distribution pattern similar to the equilibrium condition can be obtained by selecting an appropriate heating time for making Fourier's number 0.7 or higher.

5.2.4 Effect of plate thickness

The effect of plate thickness on temperature distribution is discussed here first. Assuming that a coil with a large width in relation to a plate thickness is heated till an equilibrium temperature distribution is obtained; then, in the neighborhood of the coil center, the problem is reduced only to that of heat conduction in the radial direction, which can be expressed by a simple equation. A basic equation for the problem is:

$$\frac{\partial^2 \theta}{\partial x^2} + \frac{1}{\lambda_p} w = 0$$

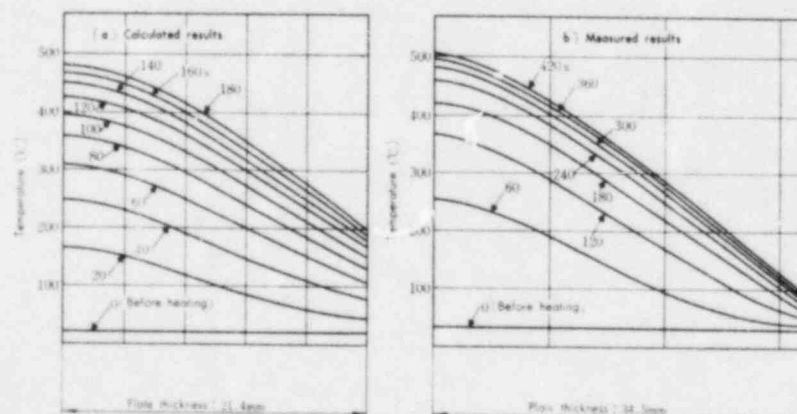


Fig. 11 Temperature distribution in the plate thickness direction

where, θ : Temperature at position x
 λ_p : Thermal conductivity of a pipe
 w : Heating density
 x : Distance from outer surface

Heating density (w) by induction heating can be given by the following equation⁽⁵⁾:

$$w = w_o e^{-2x/S} \quad \dots\dots(2)$$

where, w_o : Heating density on outer surface

$$S = \frac{1}{2\pi} \sqrt{\frac{\rho}{\mu f \times 10^{-9}}} \quad (\text{cm})$$

μ : Specific magnetic permeability

f : Frequency (cycle/s)

ρ : Specific resistance ($\Omega \cdot \text{cm}$)

When the outer surface is insulated and temperature is T_o , equation (2) leads to

$$\theta = T_o - \frac{w_o S^2}{4\lambda_p} \left(-1 + \frac{2}{S} x + e^{-2x/S} \right) \quad \dots\dots(3)$$

Substituting $x=L$ in equation (3) yields the value of temperature (T_i) on the inner pipe surface. Hence, temperature difference ($\Delta T = T_o - T_i$) between the outer and inner pipe surfaces is derived from

$$\Delta T = T_o - T_i = \frac{w_o S^2}{4\lambda_p} \left(-1 + \frac{2}{S} L + e^{-2L/S} \right) \quad \dots\dots(4)$$

When two plates of different thickness are heated with the same heat input under the conditions of $L \gg S$ and ΔT is proportional to L , the plate with a larger thickness will produce a larger ΔT . In addition, the resultant thermal stress is proportional to ΔT . Therefore, it is generally assumed that the thicker plate gives the better results. Fig. 5-(b), when reviewed from the above standpoint, indicated pipe 10B having a larger temperature difference than pipe 4B but the resultant residual stress was smaller compared with that of 4B which had a smaller plate thickness. This implies a considerable effect of coil width,

which is to be discussed later.

On the other hand, in the case of R-28 and R-30, where a coil of sufficient width was used, a greater differential temperature between the outer and inner surfaces and a better improvement in residual stress were obtained for the latter sample which had the larger plate thickness (Fig. 7). These results agreed well with the above assumption.

5.2.5 Effect of cooling water flow rate

As seen from equation (4), the temperature difference in the plate thickness direction increases proportionally with heating intensity and plate thickness regardless of cooling conditions on the inner surface. However, in heating pipes, it is generally suggested that pipe temperature be held within the safe limits to prevent pipe material deterioration. For this reason cooling conditions come into the picture. An equation for heat flux q_1 on inner pipe surface is derived from Fourier's law as

$$q_1 = -\lambda_p \frac{d\theta}{dx} \quad \dots\dots(5)$$

Another heat flux q_2 from inner pipe surface to a liquid can be expressed by

$$q_2 = h_m \Delta T_2 \quad \dots\dots(6)$$

where, h_m : Average heat conduction ratio of liquid

ΔT_2 : Temperature difference between inside pipe wall and liquid

Differentiating equation (3) and putting $x=L$ gives

$$\left[\frac{d\theta}{dx} \right]_{x=L} = -\frac{w_o S}{2\lambda_p} (1 - e^{-2L/S}) \quad \dots\dots(7)$$

As $q_1 = q_2$ equations (5) to (7) give

$$\Delta T_2 = T_i - T_w = \frac{w_o}{2h_m} (1 - e^{-2L/S}) \quad \dots\dots(8)$$

where T_w is the temperature of the liquid.

From equations (8) and (4) it follows

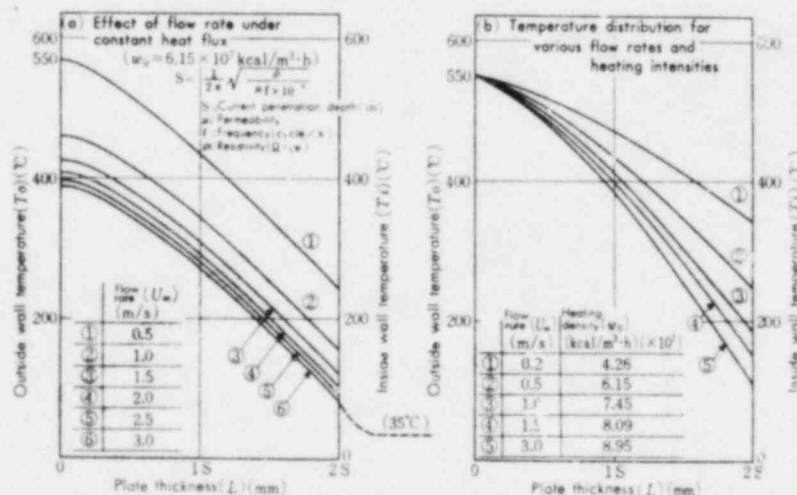


Fig. 12 Effect of flow rate on temperature distribution

$$\Delta T_1 + \Delta T_2 = T_o - T_w = \frac{w_o S}{2} \left\{ \frac{S}{2\lambda_p} \left(-1 + \frac{2L}{S} + e^{-2L/S} \right) + \frac{1}{h_m} (1 - e^{-2L/S}) \right\} \dots (9)$$

h_m is given by Dittus-Boelter equation⁽⁵⁾

$$Nu = \frac{h_m d}{\lambda_w} = 0.023 Re^{0.8} Pr^{0.4}$$

$$h_m = 0.023 \cdot \frac{\lambda_w}{d^{0.2} \nu^{0.8}} \cdot Pr^{0.4} U_w^{0.8} \dots (10)$$

where, λ_w : Thermal conductivity of liquid
 d : Inside diameter of pipe
 ν : Coefficient of kinematic viscosity
 Pr : Prandtl number
 U_w : Flow rate of liquid

In Figs. 12-(a) and (b) are shown the results of calculations using equations (9) and (10) for the effect of flow rate at constant heating intensity and at constant outside pipe wall temperature, respectively. In the former case, the temperature of both the inside and outside pipe walls dropped as the cooling water flow rate was increased, but the temperature difference was maintained constant (Fig. 12-(a)). In other words, the flow rate, when increased, did not change the resultant residual stress but did decrease the outer surface temperature, giving a margin of safety, within which the temperature will not cause the material deterioration. In the latter case, a greater temperature difference between the inside and outside pipe walls was obtained as the flow rate was increased (Fig. 12-(b)), under such conditions a great residual stress could be expected. In summary, the higher the flow rate the better residual stress improvement is anticipated.

The experiment on R-21 and R-22 was made by changing the flow rate at a constant heating intensity. The results indicated almost the same tendency as shown in Fig. 12-(a). The fact that R-22 was subjected to thermal exposure for a period shorter by more than 10% than R-21 was presumably the cause for the small difference in the outside wall temperatures of the two samples. Naturally, almost the same residual stress resulted because the differential temperature on both samples was nearly the same.

5.2.6 Effect of coil width

A difference in temperature occurs in the axial direction of pipe, as well, because a pipe is heated by a coil with a finite width. The stress on the inner pipe surface, just below the coil end, is compressed by this temperature change and, as a result, acts to cancel the tensile stress produced by the temperature difference between the inner and outer pipe surfaces. Therefore, the areas intended for stress improvement should preferably be a sufficient distance from the areas where drastic axial direction temperature changes take place. To precisely compute this distance, thermal elastoplastic calculations by the finite element method must be performed.

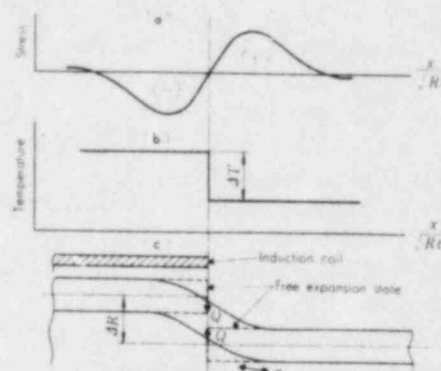


Fig. 13 Stress distribution of pipe subjected to step temperature change in axial direction

But elastic calculations can be substituted as a simple way to obtain a guide value; the effect of step temperature change in the axial direction, as shown in Fig. 13-(b), can be expressed as the effect obtained when circular pipes with different radii by ΔR are connected together by applying shearing force (Q) as shown in Fig. 13-(c). The effect of shearing force (Q) increases to a maximum at a certain distance from the pipe end, and then diminishes as illustrated in Fig. 13-(a)⁽⁶⁾. The force exhibits a relatively large effect within the range from the pipe end of $1.5\sqrt{Rt}$ where R is the radius from pipe wall thickness center, and t is plate thickness. Therefore the effect at coil ends can reduce when a coil width is $2 \times 1.5\sqrt{Rt}$ or larger. R-22 and R-23 were tested using different coil widths, more than $3.0\sqrt{Rt}$ in both cases, and showed little difference. But R-18, which was heated by a coil of about $1.4\sqrt{Rt}$ width, produced small compressive residual stresses.

5.3 Comparison with other stress improvement methods

5.3.1 Stress relief annealing treatment

To relieve residual stress by this method generally requires heating up to about the temperature at which the heated material starts recrystallization. When applied to 304 type stainless steel this method induces material sensitization during heating, sustaining, and cooling cycles, making the materials less IGSCC resistant. To remove such sensitization and relieve residual stresses the material must be heat treated in a solution treatment at a higher temperature. It is quite difficult to apply this treatment to an installed plant with the present technology.

5.3.2 Tensile load method

A tensile correcting machine is one application of this method. But this type of machine is inapplicable to large diameter pipe because an extraordinarily large mechanical load is required. Another possible approach is to provide tensile load by pressurizing an inner pipe surface. This method, however, can cause plastic deformation of the whole piping system, and in an already installed plant, residual stress can occur unexpectedly at other than the piping being corrected. Furthermore, this method cannot shift positively the residual stress on the inner pipe surface to the compressive side.

5.3.3 Residual stress relief by vibration

This method can reduce peak stress, but is incapable of effecting complete stress relieving or positive introduction of compressed residual stress on an inner pipe surface. It cannot be applied to a large-scale construction, because of the limitation of capacity of a vibrating machine. Neither it is suitable for installed piping systems.

5.3.4 Shot peening

This method can impart a large compressed residual stress, but depth of improvement is small and the material is subjected to a high degree of plastic deformation. As a result, surfaces of some materials are embrittled. The inner pipe surface must be cleaned after treatment to eliminate foreign material that has been inserted into the pipe. The difficulty of shotting small diameter pipes from inside is one other incidental drawback of shot peening.

5.3.5 Advantages of IHSI

IHSI has the following advantages:

1. Improvements in resistance to SCC and corrosion fatigue strength are achieved through positive shifting of residual stresses on inner pipe surface to the compressive side.
2. The treatment is readily applicable even to installed pipings as local heating of pipe exerts little influence on other members.
3. Residual stresses of any desired level can be obtained by selecting proper temperature difference between inner and outer pipe surfaces without fear of material deterioration.
4. The depth of compressive residual stresses is large.
5. The treatment can be applied to large diameter pipes without much difficulty.
6. The treatment is simple to perform as there is no need to insert equipment into the pipe interior.

6. Conclusion

Stress corrosion cracking occurs as a result of interactions of three factors—stress, environment, and material. An experimental study was made of residual stress improvement by induction heating with the objective of improving SCC resistance of a plant through reducing the stress factor. The following is a summary of the findings of the study.

1. The capability of IHSI to change residual stresses

on pipe weldments into compressive ones or into very small tensile stresses was confirmed by strain measurements with strain gages and by a cracking test in a $MgCl_2$ solvent.

2. The above was also confirmed by calculations by the finite element method. In addition, it was found that compressive residual stresses covered about 60% of a pipe wall thickness.
3. The authors suggest the following as factors that can improve IHSI efficiencies:
 1. A large temperature difference between inner and outer pipe surfaces is preferable.
 2. A large heating depth is preferable.
 3. The heating time should not be too short.
 4. A pipe with a thick wall can obtain a larger temperature difference between inner and outer surfaces than a thin-wall pipe, if heating intensity is constant.
 5. A larger temperature difference can be obtained between inner and outer pipe surfaces with a high flow rate of cooling water running on the inner surface than with a low flow rate, providing that the heating temperature of inner pipe face is constant.
 6. Heating width (coil width) should preferably be $3\sqrt{Rt}$ or more.

REFERENCES

- (1) S. Timoshenko et al.: Theory of Elasticity (2nd edition) McGraw-Hill (1951)
- (2) A. Takaku and M. Tokiwai: Basic Study on Some Metallurgical Factors and Surface Treatment Effects of Stainless Steels for BWR Cooling Pipes, Central Research Institute of Electric Power Industry, Japan, Reports No. 275038 (1976)
- (3) S. Yonetani: Occurrence and Countermeasures of Residual Stress, Yokendo, Japan (1975) p. 192
- (4) Y. Katsuto: Outline of Heat Transfer, Yokendo, Japan (1964) p. 34
- (5) The Japan Society of Mechanical Engineers: A Handbook of Mechanical Engineering (4th edition) (1960)
- (6) S. Timoshenko et al.: Theory of Plates and Shells, McGraw-Hill (1959) pp. 469-471